ISSN 0030-5987. Orthopaedics, traumatology and prosthetics. 2026. № 1

Зміст

Contents

ISSN 0030-5987. Orthopaedics, traumatology and prosthetics. 2026. № 1

ORIGINAL ARTICLES

УДК 616.717/.718-001.5-089.843Masquelet:303.442.3](045)

DOI: http://dx.doi.org/10.15674/0030-5987202615-11

Application of surgical technologies for the treatment of victims with long bone defects due to modern combat trauma. Message 2. Induced membrane technology (Masquelet technique)

S. Guryev [1], S. Hariyan [2], V. Kushnir [1], O. Tsybulsky [2]

[1] SI «Ukrainian Scientific and Practical Center for Emergency Care and Disaster Medicine of the Ministry of Health of Ukraine», Kyiv
[2] Ternopil Regional Clinical Hospital. Ukraine

Combat trauma, which, unfortunately, is now widespread in Ukraine as a result of the Ukrainian-Russian war, causes severe traumatic injuries to both military personnel and civilians. Objective. To provide a complete description of the indications for the use of induced membrane technology (Masquelet technology) in victims with long bone defects resulting from combat trauma. Methods. This study is based on an analysis of 51 cases of the use of the Masquelet technique in victims with long bone defects due to combat injuries. Connection criteria: the use of this particular technology is effective according to absolute or conditionally absolute indications, it was effective Masquelet.Results. It was established that the Masquelet technology was mainly used in victims with long bone defects aged 31–40 years (52.94 %). In addition, the Masquelet technology was most often used on the lower limb 64.70 %. There is a pattern in the use of the Masquelet technology depending on the localization of the long bone defect: in the proximal part of both the upper and lower limbs, this technology was used more often. The Masquelet technology was mainly used in victims with long bone defects measuring 5.0–9.99 cm (45.10 %). At the same time, the Masquelet technology was not used for long bone defects larger than 15 cm. Conclusions. The use of Masquelet technology is appropriate in victims with defects of long bones due to combat trauma in young and middle age, which is due to the age-dependent nature of bone tissue repair processes. There is an obvious dependence of the effectiveness and feasibility of using the induced membrane technology on the size of the defect. The most appropriate application is with a defect size of 5.0–9.99 cm and cavitary defects, regardless of the localization of the defect. It is also necessary to take into account the results of a comprehensive analysis of clinical-epidemiological and clinical-anatomical features.

Бойова травма, яка, на жаль, зараз є поширеною в Україні внаслідок російсько-української війни, призводить до тяжких травматичних уражень. Мета. Навести повноцінну характеристику показів щодо застосування технології індукованої мембрани (технологія Masquelet) у постраждалих із дефектами довгих кісток унаслідок бойової травми. Методи. Дослідження ґрунтується на аналізі 51 випадку застосування технології Masquelet у пацієнтів із дефектами довгих кісток унаслідок бойових уражень. Критерії включення: використання саме цієї технології здійснене за абсолютними або умовно абсолютними показами, було ефективним. Результати. Виявлено, що технологія індукованої мембрани переважно використовувалася в постраждалих із дефектами довгих кісток віком 31–40 років (52,94 %), найчастіше на нижніх кінцівках — 64,70 %. Існує закономірність її застосування залежно від локалізації дефекту довгої кістки, а саме в проксимальному відділі як верхньої, так і нижньої кінцівки. Здебільшого Masquelet застосовано в постраждалих із дефектами розмірами 5,0–9,99 см (45,10 %) і не використовувалася за дефектів довгих кісток більше 15 см. Висновки. Застосування технології Masquelet доречне в постраждалих із дефектами довгих кісток унаслідок бойової травми в молодому та середньому віці, що обумовлено віковою залежністю репараційних процесів кісткової тканини. Існує вірогідна залежність ефективності та необхідності застосування технології індукованої мембрани від розміру дефекту. Найбільш доцільне використання — за розміру дефекту 5,0–9,99 см і кавітарних дефектах незалежно від локалізації. Також необхідно враховувати результати комплексного аналізу клініко-епідеміологічних і клініко-анатомічних ознак. Ключові слова. Довгі кістки, дефекти, хірургічне лікування, технологія Masquelet, бойові ушкодження.

Key words. Long bones, defects, sizes, surgical treatment, technology Masquelet, combat injuries

Introduction

Combat injuries, unfortunately, have become widespread in Ukraine due to the Russian-Ukrainian war, causing severe traumatic injuries among both military personnel and civilians. These injuries include damage to long bones and the resulting defects in these bones [1]. Treating individuals with such injuries requires the use of medical technologies that were not frequently used in the past [2–5]. In our previous study we demonstrated that one of the most common treatment methods for these injuries is the induced membrane technology (Masquelet) [6]. Unfortunately, there is a lack of data in open and accessible scientific sources regarding the characteristics of applying this technology depending on the clinical-epidemiological and clinical-nosological characteristics of the injured individuals, which is why this aspect is analyzed in the current study.

Purpose: To deliver an in-depth analysis of the clinical indications for utilizing induced membrane technology (Masquelet) in patients presenting with long bone defects due to combat-related injuries.

Materials and Methods

The study is based on a retrospective analysis of 51 cases where the Masquelet technology was used to treat individuals with long bone defects due to combat injuries. Inclusion criteria: This technology was implemented according to absolute or conditionally absolute indications and demonstrated efficacy. All patients received treatment at civilian healthcare institutions. The study examined and analyzed the use of the Masquelet technology depending on the clinical-epidemiological characteristic "age" and the clinical-anatomical characteristic "injury" (location and size of the defect). This was due to the influence of these factors on the regenerative and reparative abilities of bones and soft tissues. The analysis was carried out in both descriptive and integrative aspects. Parametric (rank) and non-parametric (polychoric analysis) statistical methods were used, applying formal logic laws and fractal analysis.

The software and methodological support of the research meets the requirements and criteria of evidence-based medicine.

The study was conducted in accordance with the requirements and criteria of evidence-based medicine, following the conditions of the Helsinki Declaration and was approved by the Bioethics Committee of the State Institution "Ukrainian Scientific-Practical Center of Emergency Medical Care and Disaster Medicine of the Ministry of Health of Ukraine" (Protocol No. 1 dated 12.01.2026).

Results

To achieve the purpose of our study, we analyzed the data of the injured based on age, using a decadal age grading principle (Fig. 1).

More than half of the patients who received Masquelet technology treatment for injuries were aged 31–40 years. A rank analysis revealed data presented in Table 1.

The analysis identified that the Masquelet technique was not implemented for injured individuals in the under-20 and over-60 age groups. It is known that there is a significant variation in the distribution across age groups, with the ratio of the maximum to minimum values being 6.8. This suggests, albeit indirectly, a potential correlation between the use of Masquelet technology and age.

We also conducted a distribution analysis based on the localization of the defect, with the results shown in Table 2.

The lower limb was the most common site for the use of Masquelet, accounting for 64.70 %. Furthermore, a pattern emerged in the use of this technology depending on the location of the long bone defect: in the proximal part of both the upper and lower

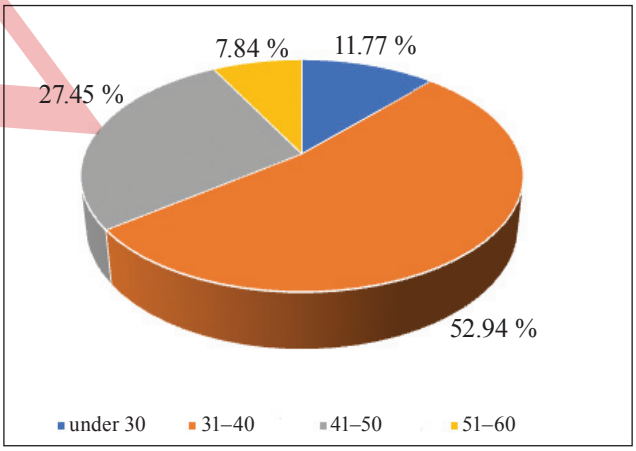

Fig. 1. Age distribution of the patient sample: Under 30 years old

Table 1

Rank analysis of the distribution of the patient sample by age characteristic

Age (years)	Proportion (%)	Rank
Under 20	0	5
21–30	11.77	3
31–40	52.94	1
41–50	27.45	2
51–60	7.84	4
Over 60	0	5
Total	100.00	—

limbs, the technology was used more frequently. On the forearm Masquelet was used 1.3 times more often than on the shoulder, and on the lower leg, it was used 1.8 times more often than on the thigh. The technology was predominantly used on the lower leg, namely 41.17 % (first rank), and the least on the shoulder (15.69 %). The coefficient of the ratio of the maximum to minimum values was 2.6, indicating moderate dissipation in the distribution of the sample and indirectly suggesting a sufficient degree of reliability and objectivity in this distribution.

Another important clinical-anatomical characteristic of the sample of injured individuals treated with the Masquelet technology for long bone defects is the "size of the defect" characteristic (Table 3).

In the group of patients with long bone defects who were treated using the Masquelet technology, most defects ranged from 5.0 to 9.99 cm in size, making up 45.10 % (the highest rank). It is noteworthy that this technology was not used for defects smaller than 15 cm, and only 7.84 % were applied to defects smaller than 10 cm.

A significant proportion of patients who underwent the procedure had cavitary defects and injuries up to 5 cm in size, with each group comprising 23.53 %. Given this, it can be stated that the Masquelet technology is most commonly used for long bone defects up to 10 cm.

To establish the relationship between the age factor and defect size in patients with long bone defects treated with Masquelet technology, we performed a distribution analysis within age groups based on the "defect size" characteristic and conducted a rank analysis, the results of which are presented in Table 4.

Table 2

Rank analysis of the distribution of the patient sample by the characteristic "injury localization"

Injury localization	Proportion (%)	Rank
Shoulder	15.69	1
Forearm	19.61	2
Thigh	23.53	3
Lower leg	41.17	4
Total	100.00	—

Table 3

Rank analysis of the distribution of the patient sample by the characteristic "injury size"

Injury size (cm)	Proportion (%)	Rank
2.5–4.99	23.53	2
5.0–9.99	45.10	1
10.0–14.99	7.84	3
More than 15.00	0	4
Cavitary	23.53	2
Total	100.00	—

Table 4 data show a mismatch in the ranking positions across age groups for the "defect size" characteristic. It is also noteworthy that the highest ranks are occupied by patients aged under 30 and over 51 years, with bone defects ranging from 2.5 to 4.99 cm. For patients aged 31 to 50 years, defects were primarily between 5.0 and 9.99 cm.

In the age group of patients under 30 years, most defects treated this way were up to 5 cm (66.67 %), with cavitary defects comprising 33.33 %. In the 31–40 age group, defects between 5.0 and 9.99 cm were predominant (55.56 %), with fewer cases of defects smaller than 5 cm.

In the 41–50 age group, the majority of defects were also 5.0–9.99 cm in size, followed by cavitary defects (28.57%), with the least frequency for defects smaller than 5 cm (14.29 %).

Among combat trauma patients treated with Masquelet, defects most frequently ranged from 2.5 to 4.99 cm, with other defect sizes not appearing in statistically significant volumes. This distribution is primarily driven by age-related activity.

The coefficient of the ratio of maximum to minimum values in the age group under 30 years was 2.0, indicating moderate dissipation in the distribution. For the 31–40 age group, the ratio was 7.5, reflecting a very high level of dissipation, while in the 41–50 age group, the ratio was 4.0, indicating a high level. Thus, the strongest probable correlation is found in the 31–40 and 41–50 age groups.

On the other hand, to achieve the objective of the study, we performed a distribution analysis of the patients in the "defect size" groups by age. The results are presented in Table 5.

Analyzing the data from Table 5, we found that only defect sizes from 2.5 to 4.99 cm were observed in all age groups of patients, with the highest frequencies being in those under 30 and over 51 years (33.33 % each).

Defect sizes of 5.0–9.99 cm were found only in patients from the 31–40 and 41–50 age groups, with the 31–40 age group having nearly twice as many cases. Masquelet technology was applied to patients with long bone defects of 10–14.99 cm only in the 31–40 age group. For cavitary long bone defects, treatment with this method was most commonly performed in the 31–40 age group (50.00 %), and less frequently in those under 30 years (16.67 %).

Polychoric analysis of the data from Table 5 confirmed a positive (φ^2 = 0.5628), very strong (C = 0.6001), and statistically significant relationship (χ^2 = 28.71) between the "age" and "defect size" characteristics in patients treated with Masquelet for long bone defects due to combat trauma. Thus, these findings lie within the field of statistical reliability.

To determine the clinical-anatomical structure of long bone defects for which Masquelet technology was applied, we conducted an integrated analysis based on defect size and location, the results of which are shown in Tables 6–7.

During the rank analysis of the data from Table 6, we found that there was a match in ranking positions only in the upper limb segments, while no match was found in the lower limb.

In the group of patients with shoulder defects, Masquelet technology was predominantly applied to

Table 4

Rank analysis of the distribution of the patient sample by injury size within age groups

Injury size (cm)	Age of the patients, years							
	under 30		31–40		41–50		51–60	
	proportion (%)	rank	proportion (%)	rank	proportion (%)	rank	proportion (%)	rank
2.5–4.99	66.67	1	7.41	4	14.29	3	100	1
5.0–9.99	0	3	55.56	1	57.14	1	0	2
10.0–14.99	0	3	14.81	3	0	4	0	2
Cavitary	33.33	2	22.22	2	28.57	2	0	2
Total	100	—	100	—	100	—	100	—

Table 5

Rank analysis of the distribution of the patient sample by age within injury size groups

Injury size (cm)	Age of the patients, years				Total
	under 30	31–40	41–50	51–60	
2.5–4.99	33.33	16.67	16.67	33.33	100
5.0–9.99	0	65.22	34.78	0	100
10.0–14.99	0	100	0	0	100
Total	16.67	50	33.33	0	100

Table 6

Integral analysis within the groups "injury localization" by injury size

Injury size (cm)	Localization							
	shoulder		forearm		thigh		lower leg	
	proportion (%)	rank	proportion (%)	rank	proportion (%)	rank	proportion (%)	rank
2.5–4.99	25.00	2	40.00	2	16.67	2	19.05	3
5.0–9.99	75.00	1	60.00	1	49.99	1	23.81	2
10.0–14.99	0	3	0	3	16.67	2	9.52	4
Cavitary	0	3	0	3	16.67	2	47.62	1
Total	100	—	100	—	100	—	100	—

Table 7

Integral analysis within the groups "injury size" by injury localization

Injury size (cm)	Injury localization				Total
	shoulder	forearm	thigh	lower leg	
2.5–4.99	16.67	33.33	16.67	33.33	100
5.0–9.99	26.09	26.09	26.09	21.73	100
10.0–14.99	0	0	50.00	50.00	100
Cavitary	0	0	16.67	83.33	100

defects ranging from 5.0 to 9.99 cm in size (75.00 %), with 25.00 % having defects between 2.5 and 4.99 cm. Cavitary defects and defects smaller than 10 cm were not observed in statistically significant numbers in our study.

In patients with forearm defects, a similar distribution was observed, but the majority of cases (60.00%) were for defects between 5.0 and 9.99 cm.

In the group of patients with femoral bone defects, the most common defect size was 5.0–9.99 cm (49.99 %), with other sizes each having the same percentage (16.67 %). On the lower leg, the highest proportion was for cavitary defects (47.62 %), and the smallest proportion was for defects between 10–14.99 cm.

The results of the distribution of the patient sample by defect size and defect localization are shown in Table 7.

When reviewing the data from Table 7, it was found that the Masquelet technology was most frequently used in patients with long bone defects between 2.5–4.99 cm in size on the distal segments of the forearm and lower leg (33.33 % each), and on the shoulder and femur (16.67 % each).

The largest proportion of long bone defects measuring 5.0–9.99 cm was almost evenly distributed across all segments, each segment accounting for 26.09 %, except for the lower leg (21.73 %).

Cavitary defects and defects between 10.0–14.99 cm in size were not encountered in statistically significant numbers on the upper limbs in our study. For defects of this size on the lower limb, they were evenly distributed (50.00%), with cavitary defects being five times more common on the lower leg.

To assess the reliability of the data in Table 7, we conducted a polychoric analysis, which revealed a positive (φ^2 = 0.4353), strong (C = 0.5507), and statistically significant relationship (χ^2 = 22.20) between the “defect size” and “defect localization” characteristics. These results are within the field of statistical reliability.

From a didactic perspective, we present a clinical case study example of the use of Masquelet technology in patients with long bone defects resulting from combat injuries.

Case study

A 38-year-old male patient sustained a mine-blast injury with an open fracture of the lower leg, including bone and soft tissue defects (Fig. 2).

On the 7th day post-injury, debridement and correction of the bone defect were performed, with a cement spacer inserted and the wound closed with a flap (Fig. 3).

Two weeks later, at the second stage of treatment, the Masquelet technique was applied. A plate fixation and bone grafting were performed (Fig. 4).

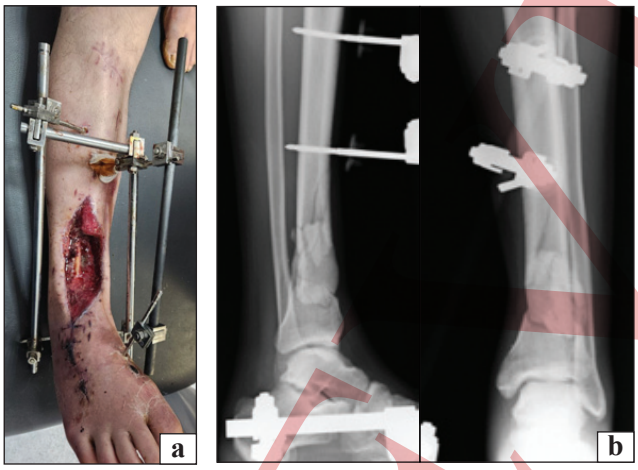

Fig. 2. Photo of the injury upon hospitalization (a); radiographic image of the patient at the time of hospitalization (b)

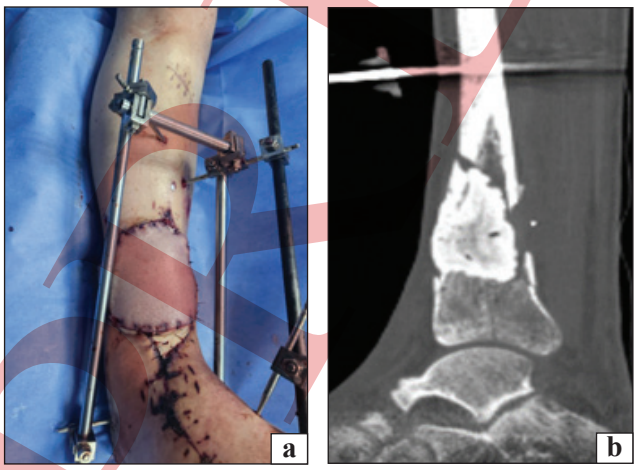

Fig. 3. Soft tissue defect closure (a); radiographic images after cement spacer insertion (b)

Discussion

The study found that the effective use of induced membrane technology (Masquelet) depends on the results of a comprehensive evaluation of patients based on clinical-epidemiological features (age) and the clinical-anatomical characteristics of the bone defect (size and localization).

This dependence has been indirectly suggested by some foreign researchers, but it mainly concerns defect size in cases of peacetime injuries [7–9]. We established a significant advantage for the use of the induced membrane method in individuals under 40 years old, which, in our view, is linked to the power and intensity of the reparative processes in bone tissue. In open and accessible scientific sources, we found no data specifically studying the use

of the Masquelet technology in patients with long bone defects due to modern combat injuries.

Research indicates that Masquelet technology is primarily utilized for the management of long bone defects measuring between 5.0 and 9.99 cm, as well as those ranging from 2.5 to 4.99 cm. This technology is rarely used for defects between 10–14.99 cm and is not used at all for defects larger than 15 cm. These results generally correlate with data from global scientific sources concerning peacetime injuries [10–12], but it should be noted that there is almost no information on combat injuries. Recent domestic research has addressed this topic; however, most studies primarily provide descriptive accounts of the phenomenon [5, 13].

In our opinion, the advantage of this study lies in its comprehensive analysis of the use of Masquelet technology based on age and defect size, which allowed us to establish a clear relationship between its use and these factors. The results indicate that Masquelet technology is most effective for large and cavitary defects in individuals aged 31–50 years. It was also proven that the effective use of Masquelet depends on the clinical-anatomical characteristics of the defect. The technology was most commonly required for defects between 5.0–9.99 cm in size, regardless of location (except for the lower leg), while cavitary defects were most prevalent on the lower leg. Such data in global scientific sources in statistically significant volumes were not found by us [14, 15]. We believe this is objectively related to the limitations of the method due to the determined power of reparative processes in bone tissue.

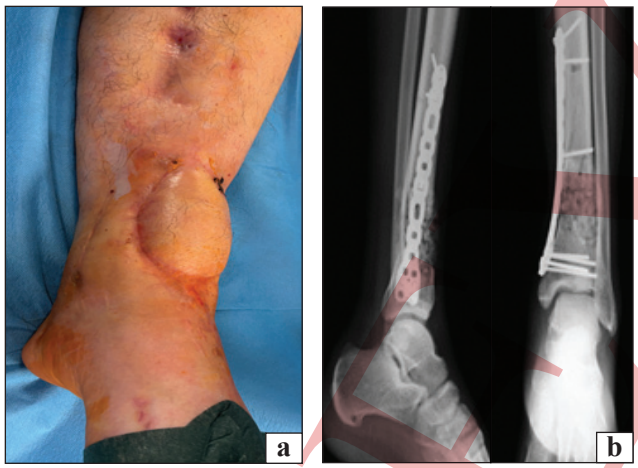

Fig. 4. External appearance of the injured limb (a); radiographic images after SCT bone grafting (b)

Fig. 5. Radiographic images of the patient. In 3 months, the patient was able to perform full, painless axial loading. Bone graft integration was observed

In conclusion, it is essential to note that for the effective use of Masquelet technology in patients with long bone defects resulting from combat trauma, it is necessary and advisable to take into account the results of an integrated analysis of clinical-epidemiological and clinical-anatomical characteristics of the injury.

Conclusions

The use of Masquelet technology is most effective for patients with long bone defects resulting from combat trauma, particularly in young and middle-aged individuals. This is due to the age-related dependency of reparative processes in bone tissue.

There is a significant correlation between the effectiveness and appropriateness of using induced membrane technology and the size of the defect. The technology is most necessary for defects ranging from 5.0–9.99 cm in size, as well as for cavitary defects, regardless of the defect's location.

For the effective and appropriate use of Masquelet technology, it is essential to consider the results of a comprehensive analysis of both clinical-epidemiological and clinical-anatomical characteristics.

Conflict of Interest. The authors declare that there is no conflict of interest.

Prospects for Further Research. Further research will focus on analyzing the application of other surgical technologies for the treatment of bone defects resulting from modern combat injuries.

Funding Information. No financial gain in any form has been received or will be received.

Authors' Contributions. Huryev S. O. — Justification of the research direction and objective, overall leadership; Kushnir V. A. — Analysis of research materials, literature review; Harian S. V. — Drafting the main text of the article, conclusions; Tsybulskyi O. S. — Collection of research materials.

References

1. Khomenko, I. P., Korol, S. O., Khalik, S. V., Shapovalov, V. Y., Yenin, R. V., Herasimenko, O. S., & Tertyshnyi, S. V. (2021). Clinical and epidemiological analysis of the structure of combat surgical injury during antiterrorist operation / Joint forces operation. *Ukrainian journal of military medicine, 2*(2), 5–13. https://doi.org/10.46847/ujmm.2021.2(2)-005
2. Trutyak, I., Los, D., Medzyn, V., Trunkvalter, V., & Zukovsky, V. (2022). Treatment of combat surgical trauma of the limbs

in the conditions of modern war. Proceeding of the Shevchenko Scientific Society. *Medical sciences, 69*(2). https://doi.org/10.25040/ntsh2022.02.16
3. Yang, N., Ma, T., Liu, L., Xu, Y., Li, Z., Zhang, K., Wang, Q., & Huang, Q. (2023). Shortening/re-lengthening and nailing versus bone transport for the treatment of segmental femoral bone defects. *Scientific reports, 13*(1). https://doi.org/10.1038/s41598-023-40588-6
4. Fu, J., Wang, X., Wang, S., Chen, Z., Shen, J., Li, Z., & Xie, Z. (2023). Induced membrane technique combined with a retrograde intramedullary nail for the treatment of infected bone defects of the ankle. *Scientific reports, 13*(1). https://doi.org/10.1038/s41598-023-34014-0
5. Hrytsai, M., Kolov, H., Sabadosh, V., Vyderko, R., Polovyi, A., & Hutsailiuk, V. (2024). Main surgical methods of critical tibial bone defects replacement (Literature review). *Terra orthopaedica,* (1(120)), 42–49. https://doi.org/10.37647/2786-7595-2024-120-1-42-49
6. Guryev, S., Hariyan, S., Kushnir, V., & Tsybulsky, O. (2025). Application of surgical technologies for the treatment of victims with long bone defects due to modern combat trauma. *Orthopaedics traumatology and prosthetics,* (4), 25–30. https://doi.org/10.15674/0030-59872025425-30.
7. Gindraux, F., Rondot, T., De Billy, B., Zwetyenga, N., Fricain, J., Pagnon, A., & Obert, L. (2017). Similarities between induced membrane and amniotic membrane: Novelty for bone repair. *Placenta,* 59, 116–123. https://doi.org/10.1016/j.placenta.2017.06.340
8. Hsu, C., Chen, S., Chan, S., & Yu, Y. (2020). The induced membrane technique for the management of segmental tibial defect or Nonunion: A systematic review and meta-analysis. *BioMed research international, 2020*(1). https://doi.org/10.1155/2020/5893642
9. Alford, A. I., Nicolaou, D., Hake, M., & McBride-Gagyi, S. (2021). Masquelet's induced membrane technique: Review of current concepts and future directions. *Journal of orthopaedic research, 39*(4), 707–718. https://doi.org/10.1002/jor.24978
10. Wu, J., Bao, Q., Wang, S., Zhou, P., & Xu, S. (2025). Mechanisms of the Masquelet technique to promote bone defect repair and its influencing factors. *Chinese journal of traumatology, 28*(3), 157–163. https://doi.org/10.1016/j.cjtee.2024.04.003
11. Rohilla, R., Sharma, P. K., Wadhwani, J., Das, J., Singh, R., & Beniwal, D. (2021). Prospective randomized comparison of bone transport versus Masquelet technique in infected gap nonunion of tibia. *Archives of orthopaedic and trauma surgery, 142*(8), 1923–1932. https://doi.org/10.1007/s00402-021-03935-8
12. Musa, R. A., Shah, D. U., Makwana, V. R., Hadiya, A. K., Shah, P. K., & Bhavsar, N. M. (2021). Masquelet's induced membrane technique for the reconstruction of post-traumatic, open-grade distal femur fracture with bone defect. *Journal of orthopaedics, trauma and rehabilitation*. https://doi.org/10.1177/2210491721992525
13. Burianov, O., Kvasha, V., Yarmoliuk, Y., & Pasenko, M. (2025). Modern technologies for replacing bone tissue defects (bone transport, Masquelet): Literature review and meta-analysis. *Trauma, 26*(6), 453–463. https://doi.org/10.22141/1608-1706.6.26.2025.1060.
14. Pederiva, D., De Luca, L., Faldini, C., & Vergano, L. B. (2025). Masquelet's induced membrane technique in the upper limb: A systematic review of the current outcomes. *Journal of orthopaedics and traumatology, 26*(1). https://doi.org/10.1186/s10195-024-00815-w
15. El Farhaoui, A., Benalia, K., Lachkar, A., Abdeljaouad, N., & Yacoubi, H. (2022). The induced membrane technique: A therapeutic option for managing bone defects in the upper extremity: Case series for 7 patients. *Annals of medicine & surgery*, 81. https://doi.org/10.1016/j.amsu.2022.104533

The article has been sent to the editors	Received after review	Accepted for printing
20.01.2026	20.02.2026	22.02.2026

APPLICATION OF SURGICAL TECHNOLOGIES FOR THE TREATMENT OF VICTIMS WITH LONG BONE DEFECTS DUE TO MODERN COMBAT TRAUMA. MESSAGE 2. INDUCED MEMBRANE TECHNOLOGY (MASQUELET TECHNIQUE)

S. Guryev [1], S. Hariyan [2], V. Kushnir [1], O. Tsybulsky [2]

[1] SI «Ukrainian Scientific and Practical Center for Emergency Care and Disaster Medicine of the Ministry of Health of Ukraine», Kyiv
[2] Ternopil Regional Clinical Hospital. Ukraine

✉ Sergiy Guryev, MD, DMedSci, Prof.: gurevsergej1959@gmail.com; https://orcid.org/0000-0003-0191-945X
✉ Serhiy Hariyan, MD, PhD: drhariyan@gmail.com; https://orcid.org/0009-0006-2662-5756
✉ Vitalii Kushnir, MD, DMedSci: kv78@i.ua; https://orcid.org/0000-0003-4569-7246
✉ Oleksandr Tsybulskyi: tsybulsky.oleksandr@gmail.com; https://orcid.org/0009-0009-5310-3621

УДК 616.728.3-089.843-089.48:303.442.3](045)

DOI: http://dx.doi.org/10.15674/0030-59872026112-18

Wound drainage after total knee arthroplasty, comparative analysis

M. L. Golovakha [1], W. Orljanski [2], E. O. Belykh [1], E. Agayev [3]

[1] Zaporizhzhya State Medical and Pharmaceutical University. Zaporizhzhia, Ukraine
[2] Department of Orthopedic Surgery, Vienna Private Clinic, Pelikangasse 15, 1090, Vienna, Austria
[3] Research Centre, Lindenhofgruppe AG, Bern, Switzerland

Diseases and injuries of the knee occupy a significant place in the structure of orthopedic pathology. The main method of knee arthritis of the III–IV degree is total knee arthroplasty (TKA). Purpose. To analyze the postoperative period after TKA without wound drainage. Methods. For the study, a homogeneous group of 140 patients was selected, their age ranged from 45 to 78 years, the diagnosis was knee arthritis of the III–IV degree. Patients were divided into 2 groups: study group — the wound was not drained (73 people), comparison group — the wound was drained (67). Results. Blood loss during surgery was comparable in both groups and ranged from 80 to 340 ml, with an average of (217.59 ± 76.19) ml in the study group and (195.6 ± 67.97) ml in the comparison group. No statistically significant difference was found in both groups (p > 0.05, p = 0.16277). A comparative analysis of the course of the postoperative period revealed a shorter treatment period in the study group. Refusal to drain the postoperative wound under conditions of stable hemostasis contributed to a faster recovery of hemoglobin and erythrocyte indices. ESR and CRP levels showed a tendency towards a faster reduction in inflammation in the study group. The postoperative management used did not show any differences in the healing time of the postoperative wound. The low intensity of postoperative pain according to VAS in the study group allowed to reduce the use of analgesics and shorten the patient's hospital stay by 2 days. Therefore, TKA without drainage of the postoperative wound can be considered as the method of choice. Conclusion. TKA without drainage of the wound after surgery did not cause an increase in postoperative complications in our series of operations. In addition, it reduced pain syndrome and, according to laboratory data, reduced the indicators of the inflammatory process.

Захворювання та травми колінного суглоба займають значне місце в структурі ортопедичної патології. Основним методом лікування гонартрозу III–IV ст. є тотальне ендопротезування колінного суглоба (ТЕКС). Мета. Проаналізувати післяопераційний період після ТЕКС без дренування рани. Методи. Для дослідження провели вибірку однорідної групи із 140 пацієнтів, їхній вік коливався від 45 до 78 років, діагноз — гонартроз III–IV ст. Пацієнтів розподілили на 2 групи: дослідження — рану не дренували (73 особи), порівняння — рану дренували (67). Результати. Крововтрата під час операції була порівняна в обох групах і склала від 80 до 340 мл, у середньому в групі дослідження (217,59 ± 76,19) мл і 195,6 ± 67,97 у групі порівняння. Статистично достовірної різниці в обох групах не виявлено (p > 0,05 p = 0,16277). Порівняльний аналіз перебігу післяопераційного періоду виявив скорочення терміну лікування в групі дослідження. Відмова від дренування післяопераційної рани за умов стабільного гемостазу сприяла швидшому відновленню показників гемоглобіну й еритроцитів. Рівні ШОЕ та СРБ показали тенденцію до швидшого зменшення запалення в групі дослідження. Тактика післяопераційного ведення хворих, яку використовували, не показала відмінностей у термінах загоєння післяопераційної рани. Низька інтенсивність післяопераційного болю за даними ВАШ у групі дослідження дозволила знизити застосування аналгетиків і скоротити термін перебування хворого в стаціонарі на 2 дні. Отже можна розглядати ТЕКС без дренування післяопераційної рани як метод вибору. Висновок. ТЕКС без дренування рани після операції не спричинило збільшення післяопераційних ускладнень у нашій серії операцій. Окрім того зменшило больовий синдром і знизило, за лабораторними даними, показники запального процесу. Ключові слова. Колінний суглоб, дренаж, хірургічне лікування, тотальне ендопротезування колінного суглоба.

Keywords. Knee, drainage, surgical treatment, total knee arthroplasty

Introduction

Knee-related impairments and injuries are prevalent and frequently necessitate surgical intervention for effective management. The main method of treatment for gonarthrosis of grade III–IV is total knee arthroplasty (TKA). With the increasing number of such surgeries, the incidence of postoperative complications inevitably rises, a significant portion of which are infections [1].

Numerous studies indicate that one of the ways infection can enter the wound is through the drainage tube [1, 2, 14], and prolonged hospitalization after surgery can lead to the risk of developing a nosocomial infection.

Active drainage of the postoperative wound is widely used during various interventions and with negative pressure, the drainage activity increases. Theoretically, this leads to a reduction in postoperative hematoma, pain syndrome, and swelling, as well as accelerating wound healing and reducing the risk of infection [4]. Some authors [3–7, 16] argue that the advantages of active drainage are greatly overstated. Discontinuing drainage reduces blood loss and the risk of retrograde infection [8, 10, 12, 15].

Purpose: To analyze the postoperative period after total knee arthroplasty without wound drainage.

Materials and Methods

For the study, a sample was made from a homogeneous group of 140 patients who underwent total knee arthroplasty (TKA) from early 2017 to February 2022. The study was approved by the Ethics Committee of Zaporizhzhia State Medical and Pharmaceutical University (protocol No. 14 dated 26.11.2025) in accordance with ICH GCP, the Helsinki Declaration on Human Rights and Biomedicine of 1977, and current Ukrainian legislation. All involved patients provided written and oral consent.

The age of the patients ranged from 45 to 78 years. Upon hospitalization, primary or secondary grade III–IV gonarthrosis was diagnosed. The following exclusion criteria were applied: history of deep vein thrombosis (DVT); use of any blood-thinning medications on a regular basis due to comorbidities; anemia requiring preoperative correction, including blood transfusions; exacerbation of any comorbidities after surgery; other somatic complications.

The procedures were performed by a single surgeon. The distribution of patients with the clarified diagnosis is presented in Tables 1–3. The patients were divided into two groups based on whether wound drainage was used postoperatively:

Study group: wound without drainage (patients operated on from 2019 to 2022)

Comparison group: wound drainage used (patients operated on in 2017–2018).

In the comparison group, one drainage tube (polyvinyl chloride (PVC) No. 15) was inserted into the operated joint cavity. The drainage was maintained for 1–2 days.

Both groups showed no deviations in general blood tests or coagulation profiles prior to the operation that could suggest issues with the clotting system.

Both groups were similar in terms of gender, age, primary diagnosis, implant type, and antimicrobial prophylaxis (Tables 1–3).

The body mass index (BMI) ranged from 25 to 38 with no significant differences between the patients in both groups ($p > 0.05$). No hemostatic tourniquet was used during surgery. In both groups, tranexamic acid (1,000 ml) was administered 30 minutes before the procedure, as well as antibacterial prophylaxis with amoxicillin-clavulanic acid (1.2 g) 30 minutes before surgery, continuing for 72 hours postoperatively. Thromboprophylaxis was provided with enoxaparin at a dose of 40 mg per day, starting preoperatively and continuing for 35 days post-TKA.

Postoperative pain management: Day 1 — femoral nerve block, dexketoprofen 50 mg IV twice a day, paracetamol 1000 mg intravenously three times a day, diclofenac 75 mg IM once a day; Day 2 — diclofenac 75 mg IM once a day, dexketoprofen 50 mg IV twice a day, paracetamol administered on the patient's demand for pain relief; Day 3 — only dexketoprofen remained.

A comparative analysis was conducted in the postoperative period, evaluating parameters such as general blood test values, body temperature, and pain severity according to the Visual Analog Scale (VAS). Controls were made before the surgical intervention, on the first day postoperatively, and on the day of discharge. Activation of patients in both groups occurred the following morning. Drainage was removed 24–48 hours after the intervention in the comparison group.

After TKA, patients were monitored for the development of early infectious complications in the first 6 months.

Statistical analysis was performed using the licensed package Statistica, version 13. Parametric and non-parametric statistical methods were applied. The significance of results (for data differing from the normal distribution) was assessed using non-parametric tests: Mann-Whitney U test (for two independent groups) and Wilcoxon T test (for several dependent groups).

Table 1

Distribution of patients in both groups by preoperative diagnosis

Group						p
study			comparison			
diagnosis	abs.	%	diagnosis	abs.	%	
Primary gonarthrosis	55	75.34	Primary gonarthrosis	48	71.64	> 0.05
Secondary gonarthrosis	18	24.66	Secondary gonarthrosis	19	28.36	> 0.05
Total	73	100	Total	67	100	—

Table 2

Distribution of patients in both groups by aage

Group						p
study			comparison			
Age, years	abs.	%	Age, years	abs.	%	
30–50	9	12.32	30–50	8	11.94	> 0.05
51–60	17	23.29	51–60	14	20.90	> 0.05
61–71	30	41.10	61–71	30	44.78	> 0.05
71 and over	17	23.29	71 and over	15	22.39	> 0.05
Total	73	100	Total	67	100	—

Table 3

Distribution of patients in both groups by gender

Група						p
study			comparison			
gender	abs.	%	gender	abs.	%	
Female	52	71.23	Female	51	76.12	> 0.05
Male	21	28.77	Male	16	23.88	> 0.05
Total	73	100	Total	67	—	—

Results

Blood loss during surgery was comparable between both groups and ranged from 110 to 320 mL. The average blood loss in the study group was 217.59 ± 76.19 mL, and 195.6 ± 67.97 mL in the comparison group. No statistically significant difference was found between the groups ($p > 0.05$, $p = 0.16277$).

Blood test results on the first postoperative day and the day of discharge showed significant changes. Hemoglobin levels were significantly higher in patients without drainage during the postoperative period (Table 4). Erythrocyte values were significantly different in favor of the study group, indicating less blood loss (Table 5). No cases of early periprosthetic infection were recorded in either group.

Interestingly, the dynamics of inflammatory markers (ESR and CRP) after surgery showed significant differences. Before the intervention, these markers did not differ significantly between the two groups. After surgery and on the day of discharge, inflammation markers were significantly lower in the group that did not have postoperative drainage (Tables 6 and 7).

The decrease in inflammatory markers in the comparison group was associated with blood loss through the drainage. The amount of exudate varied greatly: day 1 from 80 to 230 mL, day 2 – from 50 to 110 mL, with an average range of 130 to 340 mL of postoperative blood loss.

Body temperature in the study group throughout the hospital stay ranged from a minimum of 36.3 °C to a maximum of 37.9 °C. In the second group, it ranged from a minimum of 36.5 °C to a maximum of 39.1 °C. The maximum body temperature in the drainage-free group was significantly lower (Table 8). Moreover, 80 % of patients in the comparison group experienced a single temperature rise to 38–39 °C after drainage removal.

Pain assessment using the VAS showed that in the study group, the maximum pain score was 5, while in the comparison group, it was 8 (controls were

Table 4

Hemoglobin levels (g/L) before and after surgery in patients of both groups

Indicator	Hemoglobin		
	before surgery	one day after surgery	on discharge
Mean ± standard error (M ± m): – Without drainage; – With drainage	 134.38 ± 3.41 137.42 ± 3.58	 121.81 ± 4.19 120.96 ± 4.84	 119.81 ± 3.25 111.62 ± 3.68
Mann-Whitney U test (p)	p > 0.05 (p = 0.658362)	p > 0.05 (p = 0.153830)	p < 0.05 (p = 0.0002458)

Table 5

Erythrocyte levels (×10¹²/L) before and after surgery in patients of both groups

Indicator	Erythrocytes		
	before surgery	one day after surgery	on discharge
Mean ± standard error (M ± m): – Without drainage; – With drainage	 4.35 ± 0.07 4.28 ± 0.06	 4.12 ± 0.05 4.01 ± 0.04	 3.69 ± 0.06 3.56 ± 0.05
Mann-Whitney U test (p)	p > 0.05 (p = 0.0582)	p < 0.05 (p = 0.000299)	p < 0.05 (p = 0.00015727)

Table 6

ESR (mm/h) before and after surgery in patients of both groups

Indicator	Erythrocyte sedimentation rate		
	before surgery	one day after surgery	on discharge
Mean ± standard error (M ± m): – Without drainage; – With drainage	 10.38 ± 1.26 9.89 ± 0.94	 51.83 ± 4.18 67.08 ± 5.61	 48.72 ± 4.11 59.25 ± 3.39
Mann-Whitney U test (p)	p > 0.05 (p = 0.164)	p < 0.05 (p = 0.000076)	p < 0.05 (p = 0.000045)

Table 7

CRP levels (mg/l) before and after surgery in patients of both groups

Indicator	C-reactive protein		
	before surgery	one day after surgery	on discharge
Mean ± standard error (M ± m): – Without drainage; – With drainage	 6.48 ± 3.98 7.65 ± 2.11	 88.25 ± 16.98 97.18 ± 15.43	 48.76 ± 8.37 74.4 ± 9.16
Mann-Whitney U test (p)	p > 0.05 (p = 0.095839)	p > 0.05 (p = 0.000593)	p < 0.05 (p = 0.000279)

made before the surgical intervention, on the first postoperative day, and on the day of discharge).

Patient activation was initiated the morning after surgery. Patients moved with crutches, bearing the maximum load on the operated leg under the supervision of a physical rehabilitation specialist. The activity level in patients without drainage was significantly better (on average, 2 days earlier) (Table 9).

Although the use of drainage during knee joint surgeries is no longer a routine technique, our study revealed other effects associated with active drainage. All patients were verticalized and learned to walk the following day after surgery. However, the extended duration of vertical positioning in the study group and the absence of problems related to the presence of a drainage tube showed a reduction in pain according to the VAS and, accordingly, a lower use of "on-demand" analgesics.

Patients in the study group did not require additional pain relief compared to the control group, where paracetamol 1000 mg was administered additionally (as needed) for 2–3 days. This allowed them to be discharged from the hospital an average of 2 days earlier

(Table 9). During the dressing changes, 12 patients in the study group had small subcutaneous hematomas, which did not affect the healing time of the postoperative wound. During subsequent follow-up in the first year after surgery, no signs of infectious complications were observed in either group.

Thus, the absence of wound drainage after total knee arthroplasty was shown to provide stable hemostasis, without resulting in an increase in complications or delayed healing of the postoperative wound.

Discussion

The use of drains after elective surgical procedures is increasingly becoming a topic of discussion. There are no clear criteria for their application that would allow general recommendations to be made. K. Zhou et al. suggest that in uncomplicated knee arthroplasties, wound drainage can be avoided [16]. H. W. Jones et al. noted the ineffectiveness of reinfusing drainage erythrocytes [8]. The most common argument in favor of drainage is the risk of hematoma formation and the potential for infection. However, most experts today no longer support this concern [1, 2, 11, 13]. All studies and everyday experience indicate an increase in blood loss due to the use of drains. Reinfusion of autologous erythrocytes from drainage blood has not shown high effectiveness [8, 9, 11]. M. Basilico et al. argue that postoperative drainage after TKA is a routine procedure for orthopedic surgeries and is considered a useful practice in the postoperative period, but the use of drains remains controversial [2]. A systematic review of 30 studies on TKA [2] did not find significant advantages associated with the use of wound drainage after arthroplasty. In terms of pain, blood loss, swelling, postoperative range of motion, wound complications, deep infection, and hospital stay, there were no benefits of drainage.

In our study, the comparative analysis of the postoperative course in the early period after knee arthroplasty revealed a shorter hospital stay in the group without joint drainage. Patients in the study group were shown to mobilize faster due to reduced pain levels, as there was no fear of pulling the drainage tube while walking. The presence of a drain bottle psychologically limited the movement of patients in the comparison group (as reported by the majority). The refusal to use drainage after the postoperative wound, under conditions of stable hemostasis, helped achieve better recovery dynamics in terms of hemoglobin and erythrocyte levels in patients. Changes in ESR and CRP levels indicated a trend toward faster reduction of inflammation in patients without wound drainage. The postoperative management approach did not show differences in wound healing times between the groups. The lower intensity of postoperative pain in the study group, according to the VAS, allowed for a reduction in the use of analgesics and shortened the hospital stay by 2 days.

Our study aimed to clarify the issue of wound drainage after knee arthroplasty. Based on the results presented, knee arthroplasty without postoperative wound drainage can be considered a preferred method for postoperative management. Indeed, some patients with coagulation disorders or infection risks may still require drainage. However, we generally refrain from using wound drainage after TKA.

Conclusion

Knee arthroplasty without the use of wound drainage after surgery did not lead to an increase in post-

Table 8

Maximum body temperature after surgery in patients of both groups

Indicator	Maximum body temperature (°C)
Mean ± standard error (M ± m): – Without drainage; – With drainage	 37.12 ± 0.40 37.47 ± 0.58
Mann-Whitney U test (p)	p < 0.05 (p = 0.00000002692225707)

Table 9

Duration of hospital stay after surgery

Indicator	Time (day)
Mean ± standard error (M ± m): – Without drainage; – With drainage	 2.89 ± 0.16 4.69 ± 0.13
Mann-Whitney U test (p)	p < 0.05 (p = 0.0000000)

operative complications in our series of operations, reduced pain syndrome, and, according to laboratory data, lowered markers of the inflammatory process.

Conflict of Interest. The authors declare no conflict of interest.

Prospects for Further Research. Identifying methods to shorten the period of early medical rehabilitation with full weight-bearing on the operated limb.

Funding Information. The study was carried out independently and did not receive external funding.

Authors' Contributions. Holovakha M. L. — development of the study's purpose and objectives, drafting the article; Orliansky V. — analysis of primary findings; Belykh Ye. O. — collection of primary findings and statistical analysis; Agayev E. — manuscript review and editing prior to submission to the journal.

References

1. Bondarenko S., & Parvizi J. Recommendations of the world congress of experts on joint endoprosthesis. (2025). Kharkiv: FOP Ruban V. V.
2. Basilico, M., Vitiello, R., Liuzza, F., Minutillo, F., Ruberto, P., Matrangolo, M. R., Palmacci, O., Maccauro, G., & Malerba, G. (2020). Efficacy of postoperative drainage in total knee arthroplasty: Review of the literature. *Orthopedic Reviews.* https://doi.org/10.4081/or.2020.8663
3. Cooper, C., Antle, O., Lowerison, J., Dersch-Mills, D., & Kenny, A. (2021). Impact of weight-band dosing of Tinzaparin for venous thromboembolism prophylaxis on persistent wound drainage in adult patients undergoing hip and knee arthroplasty. *Annals of pharmacotherapy, 56*(3), 290–296. https://doi.org/10.1177/10600280211024294
4. Fu, T., Ren, S., & Nie, Y. (2024). The effects of drainage tube on pain and functional recovery after unicompartmental knee arthroplasty. *Acta ortopédica Brasileira, 32*(1). https://doi.org/10.1590/1413-785220243201e266853
5. Golovakha, M., Kirichenko, V., Gritsenko, A., Belykh, E., Titarchuk, R., Kudin, S., & Didenko, I. (2020). Wound drainage after total hip arthroplasty. *Orthopaedics traumatology and prosthetics*, (4), 5–11. https://doi.org/10.15674/0030-5987201945-11
6. Hellums, E. K., Lin, M. G., & Ramsey, P. S. (2007). Prophylactic subcutaneous drainage for prevention of wound complications after cesarean delivery—a metaanalysis. *American journal of obstetrics and gynecology, 197*(3), 229–235. https://doi.org/10.1016/j.ajog.2007.05.023
7. Hong, K., Pan, J., Yang, W., Luo, M., Xu, S., & Liu, J. (2016). Comparison between autologous blood transfusion drainage and closed-suction drainage/no drainage in total knee arthroplasty: A meta-analysis. *BMC musculoskeletal disorders, 17*(1). https://doi.org/10.1186/s12891-016-0993-z
8. Jones H. W, Savage L., White C., Goddard R., Lumley H., Kashif F., & Gurusany K. (2004). Postoperative autologous blood salvage drains--are they useful in primary uncemented hip and knee arthroplasty? A prospective study of 186 cases. *Acta orthopaedica Belgica, 70*(5):466–73
9. Kosins, A. M., Scholz, T., Cetinkaya, M., & Evans, G. R. (2013). Evidence-based value of subcutaneous surgical wound drainage. *Plastic and reconstructive surgery, 132*(2), 443–450. https://doi.org/10.1097/prs.0b013e3182958945
10. Lachance, A., Shahsavarani, S., Sogard, O., McDonald, J., Stilwell, M., & Lutton, J. (2024). Suction drain usage has no benefit following revision total hip and knee arthroplasty. *Archives of orthopaedic and trauma surgery, 144*(8), 3565–3571. https://doi.org/10.1007/s00402-024-05474-4
11. Li, T., Zhuang, Q., Weng, X., Zhou, L., & Bian, Y. (2013). Non-continuous versus continuous wound drainage after total knee arthroplasty: A meta-analysis. *International orthopaedics, 38*(2), 361–371. https://doi.org/10.1007/s00264-013-2105-0
12. Maliarov, A., Newman, N., Sabouret, P., Al-Shakfa, F., Chergui, S., & Lavoie, F. (2023). Suction drainage in total knee replacement does not influence early functional outcomes or blood loss: A randomized control trial. *Arthroplasty, 5*(1). https://doi.org/10.1186/s42836-022-00158-z
13. Maniar, R. N., Pradhan, P., Bhatnagar, N., Maniar, A., Bidwai, R., & Bindal, P. (2019). Role of suction drain after knee arthroplasty in the Tranexamic acid era: A randomized controlled study. *Clinics in orthopedic surgery, 11*(1), 73. https://doi.org/10.4055/cios.2019.11.1.73
14. Märdian, S., Perka, C., & Matziolis, G. (2013). Wound drainage in primary knee arthroplasty - a prospective randomized study. *Acta chirurgiae orthopaedicae et traumatologiae Cechoslovaca, 80*(2), 114–117. https://doi.org/10.55095/achot2013/017
15. So-Osman, C., Nelissen, R. G., Koopman-van Gemert, A. W., Kluyver, E., Pöll, R. G., Onstenk, R., Van Hilten, J. A., Jansen-Werkhoven, T. M., Van den Hout, W. B., Brand, R., & Brand, A. (2014). Patient blood management in elective total hip- and knee-replacement surgery (Part 2). *Anesthesiology, 120*(4), 852–860. https://doi.org/10.1097/aln.0000000000000135
16. Zhou, K., Wang, H., Li, J., Wang, D., Zhou, Z., & Pei, F. (2017). Non-drainage versus drainage in tourniquet-free knee arthroplasty: A prospective trial. *ANZ Journal of surgery, 87*(12), 1048–1052. https://doi.org/10.1111/ans.14183

The article has been sent to the editors	Received after review	Accepted for printing
10.06.2025	08.10.2025	10.10.2025

WOUND DRAINAGE AFTER TOTAL KNEE ARTHROPLASTY, COMPARATIVE ANALYSIS

M. L. Golovakha [1], W. Orljanski [2], E. O. Belykh [1], E. Agayev [3]

[1] Zaporizhzhya State Medical and Pharmaceutical University. Zaporizhzhia, Ukraine
[2] Department of Orthopedic Surgery, Vienna Private Clinic, Pelikangasse 15, 1090, Vienna, Austria
[3] Research Centre, Lindenhofgruppe AG, Bern, Switzerland

✉ Maxim Golovakha, MD, Prof. in Traumatology and Orthopaedics: golovahaml@gmail.com; https://orcid.org/0000-0003-2835-9333
✉ Weniamin Orljanski, MD, Prof. in Traumatology and Orthopaedics: orljanski@hotmail.com
✉ Yevhen Bilykh , MD: dr.bilykh@gmail.com; https://orcid.org/0000-0002-4332-529X
✉ Emin Aghayev, MD, MSc, PD: aghayev@eurospine.org

УДК 616.728.3-089.843:612.76](045)

DOI: http://dx.doi.org/10.15674/0030-59872026119-26

Definition of the knee phenotype in the ukrainian population based on the CPAK classification

M. D. Moroz [1], R. A. Kozak [1], O. A. Kostogryz [1], Y. O. Kostogryz [1], M. Yu. Kyrylenko [2]

[1] Diagnostic Center «M24», Kyiv. Ukraine
[2] SI «Institute of Traumatology and Orthopedics of the NAMS of Ukraine», Kyiv

Native coronal alignment of the knee joint demonstrates marked individual variability, which influences total knee arthroplasty planning and functional outcomes. The CPAK classification allows systematization of these anatomical variations based on the parameters aHKA and JLO. Although CPAK phenotypes have been described in several populations, data regarding the Ukrainian population have so far been lacking. Objective. To determine the characteristics of native lower-limb alignment and CPAK phenotypes of the knee joint in the Ukrainian population. Methods. A total of 500 full-length standing radiographs of the lower limbs were analyzed: 300 in the healthy group and 200 in the group with Kellgren-Lawrence grade III–IV osteoarthritis. LDFA and MPTA were measured, aHKA and JLO were calculated in accordance with CPAK principles, and knees were subsequently classified within the 3×3 CPAK matrix. Results. In the healthy group, the most common CPAK phenotypes were type II (24.7 %), type I (21.7 %), and type V (21.0 %). Neutral aHKA was observed in 47.3 %, varus in 39.3 %, and valgus in 13.3 %. The most frequent JLO orientation was apex distal (50.3 %). In sex-specific subgroups, type II predominated in males (28 %) and type V in females (25 %). In the osteoarthritis group, varus aHKA values predominated (58 %), with CPAK phenotypes I (35.5 %), IV (22 %), and II (19.5 %) being most common. Conclusions. This study describes for the first time the distribution of CPAK phenotypes of the knee joint in the Ukrainian population. Among healthy individuals, CPAK phenotypes I, II, and V were most prevalent, with neutral alignment observed in 47 %. In patients with grade III–IV osteoarthritis, a marked shift toward varus alignment was noted, with varus phenotypes accounting for 58 %, whereas neutral phenotypes were observed in only 34 %. These findings reflect population-specific patterns of native coronal knee alignment and may serve as a basis for further research into the clinical relevance of CPAK phenotypes and their impact on outcomes of total knee arthroplasty.

Нативне вирівнювання колінного суглоба має виражену індивідуальну варіабельність, що впливає на планування тотального ендопротезування та кінцевий функціональний результат. Класифікація «Coronal Plane Alignment of the Knee» (CPAK) дозволяє систематизувати ці анатомічні варіанти на основі параметрів aHKA та JLO. Мета. Визначити особливості нативного вирівнювання нижньої кінцівки та CPAK-фенотипів колінного суглоба в українській популяції. Методи. Проаналізовано 500 панорамних рентгенограм нижніх кінцівок, які розподілено на 2 групи: 300 — група 1 — умовно здорові, 200 — 2 (остеоартроз III–IV ст. за Kellgren-Lawrence). Вимірювали mLDFA та mMPTA, розраховували aHKA та JLO згідно з принципами CPAK-класифікації, після чого виконували розподіл фенотипів у матриці CPAK 3 × 3. Результати. У здоровій групі найпоширенішими CPAK-фенотипами були тип II (24,7 %), I (21,7 %) та тип V (21,0 %). Нейтральний тип aHKA визначався у 47,3, варусний — у 39,3, вальгусний — у 13,3 %. Найчастіший варіант JLO — apex distal (50,3 %). У статевих підгрупах домінував тип II у чоловіків (28 %) та V у жінок (25 %). У групі остеоартрозу відзначалося переважання варусних значень aHKA (58 %) із домінуванням фенотипів I (35,5 %) та IV (22 %). Висновок. На основі нашого дослідження описано розподіл CPAK-фенотипів колінного суглоба в українській популяції. У групі 1 найпоширенішими були I, II та V типи з переважанням нейтрального вирівнювання у 47 %, а у 2 — I, II та IV типи, проте спостерігалося виразне зміщення в бік варусних варіантів: їхня частка була до 58 %, тоді як частота нейтральних фенотипів склала лише 34 %. Отримані результати відображають особливості нативного фронтального вирівнювання нижньої кінцівки й можуть слугувати основою для подальших досліджень, спрямованих на вивчення клінічного значення CPAK-фенотипів та їхнього впливу на результати тотального ендопротезування колінного суглоба. Ключові слова. Колінний суглоб, вирівнювання, CPAK, aHKA, JLO, фенотипи колінного суглоба.

Keywords. Knee joint, alignment, CPAK, aHKA, JLO, knee joint phenotypes

Introduction

A key principle in knee joint arthroplasty has long been to create a stable joint with a neutral lower limb axis. This approach was long considered universal for achieving predictable clinical outcomes. Despite the high effectiveness of this method, up to 20 % of patients remain dissatisfied with the treatment results. The most frequent complaints in the postoperative period include persistent pain, limited range of motion, and a lack of anticipated functional recovery [1, 2]. A potential reason for these symptoms is not considering the patient's unique anatomical characteristics.

Recent studies have shown that neutral alignment of the lower limb is not typical for all patients [3, 4], so attempting to bring the limb axis to a neutral position during surgery may require excessive bone resections or additional soft tissue releases. These conditions disrupt joint biomechanics, leading to a longer, more complex post-surgical recovery.

Over the past decade, a significant number of studies have been assessed native alignment of the KJ. Their results convincingly show that such alignment is highly variable, and a notable proportion of healthy individuals have a natural varus or valgus axis of the lower limb [3–7]. Some studies have also focused on examining population and gender differences in KJ phenotypes. M. T. Hirschmann et al., E. Sappey-Marinier, T. Kobayashi et al. have shown that the frequency of varus, valgus, and neutral phenotypes differs significantly based on ethnic group and gender, which may determine characteristic biomechanical features of the KJ [8–12].

The need to consider this anatomical variability has contributed to the development of personalized approaches to implant positioning, based on the consideration of morphological phenotypes of the lower limb as an important element of preoperative planning. The task is complicated by the fact that as osteoarthritis progresses, the native alignment of the lower limb changes, typically towards an increase in the existing deformity, making it extremely difficult to determine the initial anatomical axis.

One of the most promising modern methods for systematically assessing individual frontal alignment of the knee joint is the "Coronal Plane Alignment of the Knee" (CPAK) classification, which emphasizes the arithmetic angle "hip-knee-ankle" (aHKA) and the joint line orientation (JLO) [13]. In 2020, S. J. MacDessi et al. proposed the aHKA concept and demonstrated that this measure is a reliable marker of constitutional alignment of the knee joint, regardless of the presence of arthritic changes [14]. In 2021, the concept of JLO was introduced, categorizing it into three distinct types: "proximal peak", "distal peak", and "neutral". This distinction helped clarify the difference between limb frontal alignment and the inclination of the joint surface.

The combination of aHKA and JLO made it possible to form the CPAK classification, which is presented in the form of a 3 × 3 matrix and encompasses 9 morphological phenotypes of the knee joint. This system allows for a more precise characterization of individual alignment variations and can serve as a guide for personalized strategies.

Despite the significant number of publications on the morphological phenotype of the knee joint in different populations, there is currently no information regarding the features of frontal alignment among the Ukrainian population. This limits the ability to correctly compare anatomical indicators and increases the potential impact of phenotype-specific features of the knee joint on surgical treatment outcomes.

In recent years, clinical interest in the individualization of surgical tactics in Ukraine has been growing, as evidenced by national studies related to the restoration of native kinematics, optimization of implant positioning, and comparison of different alignment concepts during total joint replacement [16–19].

In light of this, it is appropriate to study the distribution of CPAK phenotypes in the domestic population as an anatomical foundation for justified individualized surgical planning, with further comparison of the obtained results with data from European studies.

Purpose: To identify the features of native alignment of the lower limb and CPAK phenotypes of the knee joint in the Ukrainian population.

Materials and Methods

The study was conducted at the State Institution "National Institute of Traumatology and Orthopedics of the National Academy of Medical Sciences of Ukraine" and the diagnostic center "M24" from August 2024 to October 2025.

A total of 500 knee joint X-rays of patients from the Ukrainian population were selected, divided into two groups according to the radiological state of the joint. Group 1 (n = 300) included X-rays of individuals aged 18 years and older, who had no complaints regarding the knee joint, no signs of deformities, no history of trauma, and no previous surgeries on the lower limbs. A mandatory condition was the complete absence of radiologi-

cal signs of knee impairment. The group consisted of 166 men and 134 women, with an average age of (44.95 ± 13.17) years (M ± SD).

Group 2 (n = 200) included X-rays of patients with osteoarthritis stages III–IV according to the Kellgren-Lawrence classification. This group excluded individuals with post-traumatic osteoarthritis, previous septic arthritis, or a history of any surgical intervention. Also excluded were those with significant bone defects in the femoral or tibial condyles, frontal deformities, and contractures greater than 20°, as such changes could influence the accuracy of radiological measurements. Demographically, the group consisted of 89 men and 111 women, with an average age of (58.98 ± 11.34) years (M ± SD). Given that after the completion of skeletal growth, the main anatomical parameters of the lower limb bones remain relatively stable, the age difference observed between the groups was not considered a decisive factor affecting the results of radiological analysis.

All participants in the study underwent axial X-rays in a standing position with even load on both lower limbs, with maximum knee extension and patellar orientation forward. The rotation of the lower limbs was controlled by assessing the symmetry of anatomical landmarks, including the contour of the femoral head and the position of the patella.

In all cases, standardized construction of anatomical and mechanical axes and measurement of main reference angles were performed according to the Paley protocol (Figure 1) [20].

Radiological parameters in the healthy group were evaluated by a radiologist using the QxLink (v3.3.12) software according to the standardized protocol. Radiological assessments in the osteoarthritis patient group were carried out as part of preoperative planning using the mediCAD (v7.0) software. Only panoramic radiographic images that were technically correct and suitable according to commonly accepted criteria for assessing the quality of axial X-rays [21] were included in the analysis.

For determining the mechanical and anatomical axes of the lower limb, the following reference points were used (Figure 2):

– The center of the femur was determined by the Mose method [20];

– The center of the knee joint was defined as the midpoint between the tibial eminences;

– The center of the ankle joint was defined as the midpoint of the talus bone.

After constructing these axes, the main reference angles characterizing the alignment of the knee joint in the frontal plane were calculated:

– Mechanical Lateral Distal Femoral Angle (mLDFA) — the mechanical lateral distal angle of the femur was determined as the angle between the mechanical axis of the femur and the line of the distal femoral joint surface, which was drawn through the most distal points of the medial and lateral femoral condyles;

– Mechanical Medial Proximal Tibial Angle (mMPTA) — the mechanical medial proximal angle of the tibia was defined as the angle between the mechanical axis of the tibia and the line of its proximal joint surface, which was drawn through the deepest points of the medial and lateral tibial plateaus.

In Group 1, the mean value of the mLDFA was 89.11° ± 2.05°. In Group 2, this value was 89.53° ± 1.96°. The average values of the mMPTA were 87.98° ± 2.28° in Group 1 and 86.93° ± 2.25° in Group 2.

According to the current recommendations for the use of the CPAK classification, two additional derived parameters, aHKA and JLO, were also calculated based on the obtained radiological measurements [13]. They were computed using the following formulas:

$$aHKA = MPTA - LDFA, \quad (1)$$

$$JLO = MPTA + LDFA. \quad (2)$$

Negative values of the arithmetic angle aHKA were interpreted as varus constitutional alignment (*varus*) of the lower limb, while positive values indicated valgus alignment (*valgus*); values close to zero corresponded to neutral alignment (*neutral*). The joint line orientation (JLO) parameter was determined as the angle between the joint surface line of the KJ and the horizontal line: JLO values < 180° indicated an *apex distal* orientation, JLO ≈ 180° indicated an *apex neutral* orientation, and JLO > 180° indicated an *apex proximal* orientation.

Based on the obtained values of aHKA and JLO for each KJ, a classification according to the CPAK system was performed, presented as a 3 × 3 matrix (Figure 3). This matrix combines 3 categories of constitutional alignment (varus, neutral, valgus) with 3 variants of joint line orientation, forming 9 possible morphological phenotypes. The obtained phenotypes were recorded for further comparison between groups and statistical analysis.

All obtained values were entered into a unified database, followed by analytical and statistical processing.

The study was conducted in strict accordance with the principles of bioethics, legislative requirements, and established norms for biomedical research, as outlined in the Declaration of Helsinki of the World Medical Association, the Constitution of Ukraine, the Civil Code of Ukraine, the basic laws of Ukraine on health protection, and the Law of Ukraine on Information. Radiological studies were carried out within the framework of standard clinical diagnostic and treatment processes with written informed consent obtained from patients for examination and processing of medical data. The retrospective analysis of clinical and radiological data was approved by the bioethics committee of the State Institution "Institute of Traumatology and Orthopedics of the National Academy of Medical Sciences of Ukraine" (protocol No. 8 dated 25 November 2025).

Statistical data processing was performed using Microsoft Excel and Statistica 8.0 software. The Mann-Whitney U test was used to compare independent samples, and the Wilcoxon signed-rank test was used for paired samples.

To evaluate the relationship between individual radiometric parameters of frontal alignment, a Spearman correlation analysis was used. The data were analyzed using standard descriptive statistics methods, which included calculation of sample size (n), arithmetic mean (M), and standard deviation (SD). The level of statistical significance was set at $p < 0.05$.

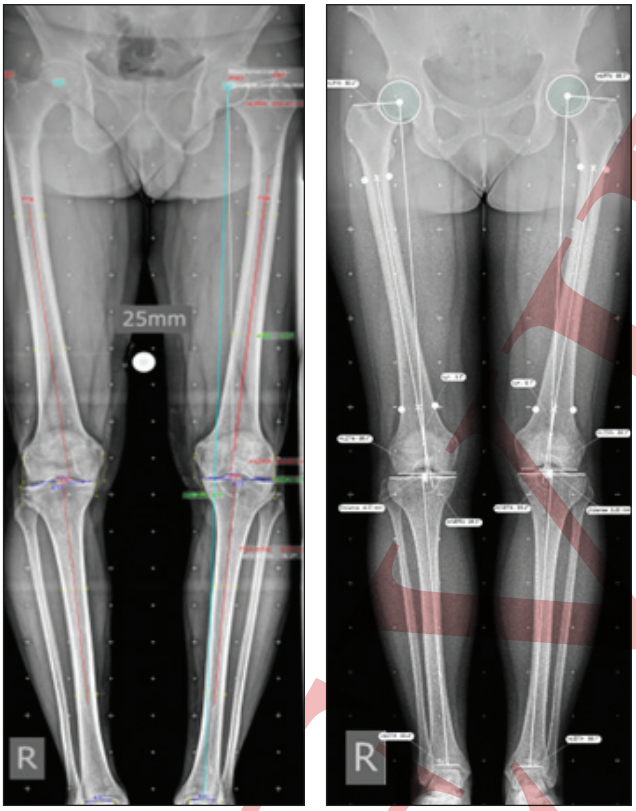

Fig. 1. Example of using software for radiometric analysis: QxLink for healthy knee joints and mediCAD for knee joints with signs of osteoarthritis

Results

To evaluate the internal consistency of the radiometric indicators, a Spearman correlation analysis was performed on the entire study cohort. A statistically significant correlation was found between mLDFA and aHKA ($\rho = -0.65$; $p < 0.001$), as well as between mMPTA and aHKA ($\rho = 0.74$; $p < 0.001$), confirming the anatomical relationship between the indicators of frontal alignment in the femoral and tibial segments and the internal consistency of the measured parameters.

To determine the typical phenotype of frontal alignment of the lower limb, the analysis was carried out based on data from the conditionally healthy population group, as this cohort reflects the native anatomical variability of the knee joint without secondary changes related to degenerative-dystrophic processes.

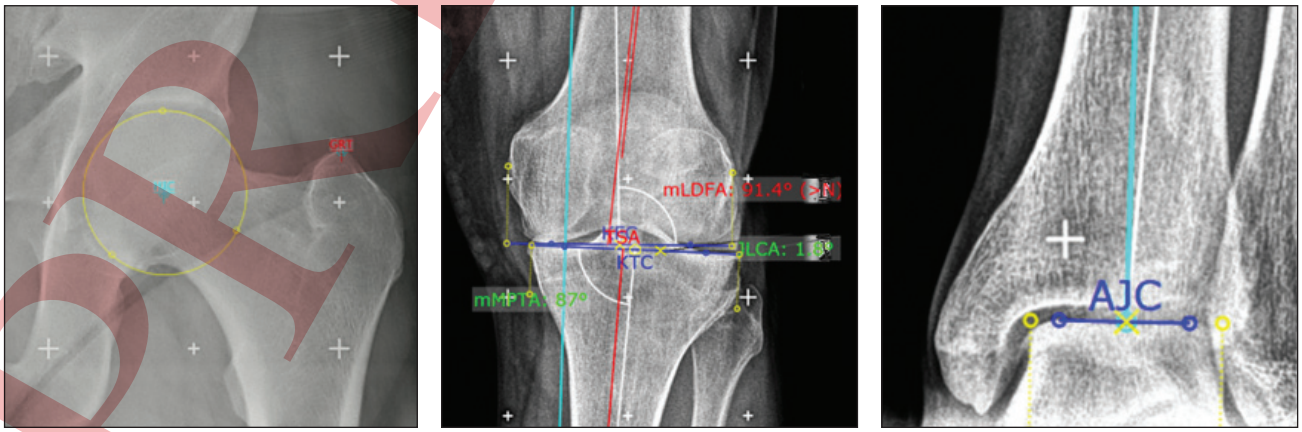

Fig. 2. Example of defining reference points according to the Paley method

A total of 9 possible combinations of the aHKA and JLO parameters were identified. Analysis of aHKA showed that in the conditionally healthy patients, neutral alignment was the most prevalent, found in 142 cases (≈ 47.3 %). Varus alignment was observed in 118 cases (≈ 39.3 %), while valgus alignment was present in 40 cases (≈ 13.3 %).

The JLO parameter highlighted that in 151 cases (≈ 50.3 %), the joint line had an *apex distal* orientation. Neutral JLO orientation was observed in 139 patients (≈ 46.3 %). The *apex proximal* orientation of the joint line was the rarest, occurring in only 10 cases (≈ 3.3 %).

Thus, the most common CPAK phenotypes in the conditionally healthy group were Type II — 74 cases (≈ 24.7 %), Type I — 65 cases (≈ 21.7%), and Type V — 63 cases (≈ 21.0 %).

The distribution of phenotypes according to the CPAK classification in the conditionally healthy group (n = 300) is shown in Table 1.

To identify potential characteristics of native frontal alignment, a separate analysis of the CPAK phenotypic distribution by gender was conducted.

In the male subgroup, the most frequent CPAK phenotype was Type II (28 %), followed by Types I (24 %) and IV (19 %). In the female subgroup, the distribution was slightly different: Type V was the leading phenotype (25 %), followed by Type II (20 %) and Type I (19 %).

In the group of patients with osteoarthritis of stage III–IV (Kellgren-Lawrence classification), during the analysis of aHKA, a significant predominance of varus alignment was noted, observed in 116 cases (58 %). Neutral values were observed in 68 patients (34 %), while valgus alignment was the least common — 16 cases (8 %).

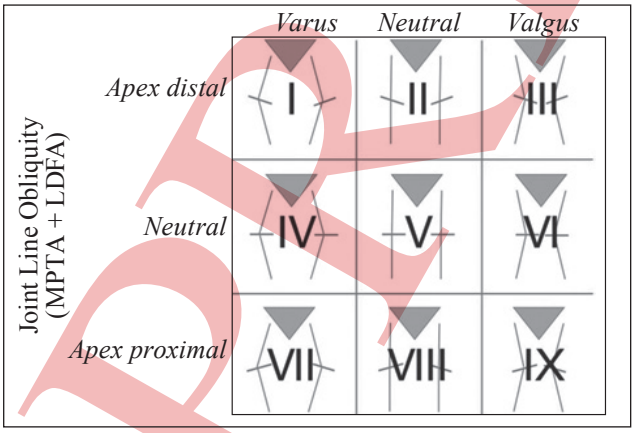

Fig. 3. Combinations of aHKA and JLO that form the CPAK phenotype matrix [13]

As for joint line orientation (JLO), the most common variant was *apex distal* — 118 cases (59 %). Neutral JLO was observed in 78 cases (39 %), while *apex proximal* was rare, occurring in 4 cases (2 %).

According to the CPAK classification, the most frequent phenotype was Type I — 71 cases (35.5 %). The next most common were Type IV — 44 cases (22 %) and Type II — 39 cases (19.5 %). The distribution of phenotypes in patients with osteoarthritis is shown in Table 2.

An analysis of the distribution of CPAK phenotypes in patients from Group 2, taking gender into account, revealed that in both subgroups, phenotypes associated with varus frontal alignment and *apex distal* joint line orientation predominated.

In the male subgroup, the most common were CPAK phenotypes I (≈ 48.3 %), IV, and II (≈ 21.3 %), reflecting a marked shift in the distribution towards varus variants of frontal alignment.

In the female subgroup, the leading phenotype was also CPAK Type I (≈ 25.2 %), followed by phenotypes II (≈ 22.5%) and V (≈ 18.9 %), indicating a more even distribution of CPAK phenotypes, with a relatively higher proportion of neutral variants compared to the males.

Among the valgus variants of frontal alignment, phenotype III was more common, with an overall frequency of about 6 % in the female population and about 3 % in the male population.

Study Limitations

This study has several limitations that should be considered when interpreting the results. It is a retrospective descriptive study, which does not allow establishing causal relationships between frontal alignment and the development of osteoarthritis.

Assessment of torsional deformities of the femur and tibia was not part of the objectives of this observation; the analysis of angular radiometric parameters was based solely on panoramic radiographs of the lower limbs, which is a widely accepted and sufficient method for evaluating frontal alignment and determining phenotypes according to the CPAK classification. Since the study had a descriptive nature and did not involve statistical comparison between cohorts, a formal assessment of measurement variability was not performed. Anthropometric and demographic factors that may significantly influence the clinical course of osteoarthritis were not analyzed in this work, as they are not decisive for determining the anatomical angular radiometric parameters of frontal alignment of the lower limb, which were the main subject of the study.

Table 1

Distribution of phenotypes according to the CPAK classification in Group 1

Parameter		aHKA			
		Varus	*Neutral*	*Valgus*	Усього
JLO	*Apex distal*	65	74	12	151
	Neutral	51	63	25	139
	Apex proximal	2	5	3	10
	Total	118	142	40	300

Table 2

Distribution of phenotypes according to the CPAK classification in Group 2

Parameter		aHKA			
		Varus	*Neutral*	*Valgus*	Усього
JLO	*Apex distal*	71	39	8	118
	Neutral	44	27	7	78
	Apex proximal	1	2	1	4
	Total	116	68	16	200

Although there are certain limitations, the findings from this study make it possible to identify the distinct characteristics of CPAK phenotype distribution within the sample examined, and establish a basis for future prospective investigations.

Discussion

This study analyzed the features of frontal alignment of the knee joint based on the CPAK classification, which uses two key radiological parameters, namely the arithmetic angle aHKA and JLO. These parameters are considered relatively stable in the absence of significant bone deformities and predominantly reflect native (constitutional) alignment, even in patients with existing osteoarthritis. Therefore, the analysis of CPAK phenotypes in the osteoarthritis group allows for interpreting frontal alignment not only as a result of degenerative changes but also as a possible reflection of the initial anatomy of the lower limb.

The results confirm the presence of significant native variability in the frontal alignment of the knee joint. The most common CPAK phenotypes were II, I, and V, which generally align with data published by other European researchers, who also note the predominance of variants with neutral or mildly varus frontal alignment and joint line orientation of the *apex distal* type [3–5].

In the group of patients with osteoarthritis stage III–IV, the distribution of CPAK phenotypes was characterized by a pronounced shift toward varus variants of frontal alignment, with the most common being I, IV, and II. The predominance of varus phenotypes may be associated with the biomechanical characteristics of load distribution on the medial compartment of the knee joint and the role of initial frontal alignment in the formation of degenerative changes. However, it is impossible to establish a causal relationship within the scope of this study, as its design did not involve prospective observation or evaluation of native alignment prior to the development of the degenerative process.

According to the meta-analysis by G. Giurazza et al. [22], for the European population, the predominance of CPAK phenotypes I and II in healthy individuals and the increase in the proportion of varus phenotypes in patients with osteoarthritis have been described. Meanwhile, a significant feature of the distribution of CPAK phenotypes in our national cohort is the significantly lower frequency of phenotype III, particularly among the female population, compared to the aggregated European data. This difference may reflect population-specific anatomical features and underscores the need for further multicenter studies on CPAK phenotypes with a larger sample of patients.

The data obtained may have practical significance in the context of individualized planning for total knee arthroplasty. Knowledge of the distribution of CPAK phenotypes in a specific population allows for a better interpretation of native frontal alignment and helps avoid a universal approach to restoring the mechanical axis, which is particularly relevant in light of the development of personalized alignment strategies.

Conclusions

The predominance of CPAK phenotypes I, II, and V in the conditionally healthy group indicates a higher prevalence of neutral and moderately varus frontal alignment variants in the lower limbs. The observed distribution of CPAK phenotypes in patients with osteoarthritis, particularly the shift toward varus alignment, underscores the potential role of initial anatomy in the formation of degenerative changes. The results support the importance of considering the CPAK phenotype and native frontal alignment when planning personalized total knee arthroplasty.

Conflict of Interest. The authors declare no conflict of interest.

Perspectives for Future Research. Further studies, particularly prospective cohort observations, are needed to determine whether the initial phenotype is a risk factor for degeneration, or if the observed distribution merely reflects the inherent anatomical features of the population.

Funding Information. The article is funded by the authors' own resources.

Author Contributions. Moroz M. D. — Conceptualization of the study, collection of clinical material, statistical analysis and interpretation of findings, drafting the main text of the article; Kozak R. A. — Participation in manuscript preparation, analysis and generalization of research findings, editing the text; Kostohryz O. A. — Scientific supervision of the study, methodological consultation, critical review of the manuscript, and approval of the final version of the article; Kostohryz Yu. O. — Collection of clinical material, systematization, and primary processing of data; Kyrylenko M. Yu. — Performing radiometric measurements, analyzing and comparing clinical and radiological parameters.

References

1. Bourne, R. B., Chesworth, B. M., Davis, A. M., Mahomed, N.N., & Charron, K. D. (2010). Patient satisfaction after total knee arthroplasty: Who is satisfied and who is not? *Clinical orthopaedics & related research, 468*(1), 57–63. https://doi.org/10.1007/s11999-009-1119-9
2. Kahlenberg, C. A., Nwachukwu, B. U., McLawhorn, A. S., Cross, M. B., Cornell, C. N., & Padgett, D. E. (2018). Patient satisfaction after total knee replacement: A systematic review. *HSS Journal®: the musculoskeletal journal of hospital for special surgery, 14*(2), 192–201. https://doi.org/10.1007/s11420-018-9614-8
3. Hirschmann, M. T., Khan, Z. A., Sava, M. P., Von Eisenhart-Rothe, R., Graichen, H., Vendittoli, P., Riviere, C., Chen, A. F., Leclercq, V., Amsler, F., Lustig, S., & Bonnin, M. (2024). Definition of normal, neutral, deviant and aberrant coronal knee alignment for total knee arthroplasty. *Knee surgery, sports traumatology, arthroscopy, 32*(2), 473–489. https://doi.org/10.1002/ksa.12066
4. Bellemans, J., Colyn, W., Vandenneucker, H., & Victor, J. (2012). The Chitranjan Ranawat award: Is neutral mechanical alignment normal for all patients? The concept of constitutional Varus. *Clinical orthopaedics & related research, 470*(1), 45–53. https://doi.org/10.1007/s11999-011-1936-5
5. Moser, L. B., Hess, S., Amsler, F., Behrend, H., & Hirschmann, M. T. (2019). Native non-osteoarthritic knees have a highly variable coronal alignment: A systematic review. *Knee surgery, sports traumatology, arthroscopy, 27*(5), 1359–1367. https://doi.org/10.1007/s00167-019-05417-2
6. Thienpont, E., Schwab, P. E., Cornu, O., Bellemans, J., & Victor, J. (2017). Bone morphotypes of the Varus and valgus knee. *Archives of orthopaedic and trauma surgery, 137*(3), 393–400. https://doi.org/10.1007/s00402-017-2626-x
7. Cooke, D., Scudamore, A., Li, J., Wyss, U., Bryant, T., & Costigan, P. (1997). Axial lower-limb alignment: Comparison of knee geometry in normal volunteers and osteoarthritis patients. *Osteoarthritis and cartilage, 5*(1), 39–47. https://doi.org/10.1016/s1063-4584(97)80030-1
8. Shetty, G. M., Mullaji, A., Bhayde, S., Nha, K. W., & Oh, H. K. (2014). Factors contributing to inherent Varus alignment of lower limb in normal Asian adults: Role of tibial plateau inclination. *The knee, 21*(2), 544–548. https://doi.org/10.1016/j.knee.2013.09.008
9. Huan, W., Mochizuki, T., Tanifuji, O., & Kawashima, H. (2022). Variability of functional knee phenotype for coronal alignment in advanced Varus knee osteoarthritis in the Japanese population. *Knee surgery, sports traumatology, arthroscopy, 31*(4), 1451–1461. https://doi.org/10.1007/s00167-022-07248-0
10. Hess, S., Moser, L. B., Amsler, F., Behrend, H., & Hirschmann, M. T. (2019). Highly variable coronal tibial and femoral alignment in osteoarthritic knees: A systematic review. *Knee surgery, sports traumatology, arthroscopy, 27*(5), 1368–1377. https://doi.org/10.1007/s00167-019-05506-2
11. Hwang, D., Wook Choi, M., Kim, S., Han, H., Bum Chang, C., Chul Lee, M., Lee, N., & Hyun Ro, D. (2023). Age and sex differences in coronal lower extremity alignment in a healthy Asian population. *The knee,* 45, 198–206. https://doi.org/10.1016/j.knee.2023.09.009
12. Moser, L. B., Hess, S., De Villeneuve Bargemon, J., Faizan, A., LiArno, S., Amsler, F., Hirschmann, M. T., & Ollivier, M. (2022). Ethnical differences in knee phenotypes indicate the need for a more individualized approach in knee arthroplasty: A comparison of 80 Asian knees with 308 Caucasian knees. *Journal of personalized medicine, 12*(1), 121. https://doi.org/10.3390/jpm12010121
13. MacDessi, S. J., Griffiths-Jones, W., Harris, I. A., Bellemans, J., & Chen, D. B. (2021). Coronal plane alignment of the knee (CPAK) classification. *The bone & joint journal, 103-B*(2), 329–337. https://doi.org/10.1302/0301-620x.103b2.bjj-2020-1050.r1
14. MacDessi, S. J., Griffiths-Jones, W., Harris, I. A., Bellemans, J., & Chen, D. B. (2020). The arithmetic HKA (aHKA) predicts the constitutional alignment of the arthritic knee compared to the normal contralateral knee. *Bone & joint open, 1*(7), 339–345. https://doi.org/10.1302/2633-1462.17.bjo-2020-0037.r1
15. Hirschmann, M. T., Hess, S., Moser, L. B., Robertson, E. L., & Leclercq, V. (2022). Phenotypes of the knee and limb: Rationale for transitioning toward personalized alignment in total knee arthroplasty. *Calipered kinematically aligned total knee arthroplasty*, 6–12. https://doi.org/10.1016/b978-0-323-75626-6.00002-0
16. Golovakha, M., & Bondarenko, S. (2023). Use of an individual tool for kinematic alignment of the limb axis during knee arthroplasty (clinical case). *Orthopaedics traumatology and prosthetics,* (1), 80–85. https://doi.org/10.15674/0030-59872023180-85
17. Zazirnyi, I. (2024). Computer navigation and robotic surgery during total knee arthroplasty. *Orthopaedics traumatology and prosthetics*, (1), 64–69. https://doi.org/10.15674/0030-59872024164-69
18. Golovakha, M., & Bondarenko, S. (2025). Assessment of the accuracy of reproduction of the lower limb axis using an individual instrument during endoprosthetics with kinematic alignment of the knee joint. *Orthopaedics traumatology and prosthetics,* (2), 52–57. https://doi.org/10.15674/0030-59872025252-57
19. Moroz, M., Kozak, R., Kostogryz, O., & Bondar, V. (2025). Evaluation of the efficacy of kinematic and mechanical alignment in primary total knee arthroplasty during the early postoperative period. *Orthopaedics traumatology and prosthetics,* (3), 53–60. https://doi.org/10.15674/0030-59872025353-60
20. Paley, D. (2002). *Normal Lower Limb Alignment and Joint Orientation. In: Principles of Deformity Correction.* Springer, Berlin, Heidelberg. https://doi.org/10.1007/978-3-642-59373-4_1
21. Marques Luís, N., & Varatojo, R. (2021). Radiological assessment of lower limb alignment. EFORT *Open reviews, 6*(6), 487–494. https://doi.org/10.1302/2058-5241.6.210015
22. Giurazza, G., Tanzilli, A., Franceschetti, E., Campi, S., Gregori, P., Parisi, F. R., Paciotti, M., Perricone, G., Zampogna, B., & Papalia, R. (2025). Coronal plane alignment of the knee phenotypes distribution varies significantly as a function of geographic, osteoarthritic and sex-related factors: A systematic review and meta-analysis. *Knee surgery, sports traumatology, arthroscopy, 33*(10), 3592–3605. https://doi.org/10.1002/ksa.12704

ISSN 0030-5987. Orthopaedics, traumatology and prosthetics. 2026. № 1

The article has been sent to the editors	Received after review	Accepted for printing
03.12.2025	02.02.2026	10.02.2026

DEFINITION OF THE KNEE PHENOTYPE IN THE UKRAINIAN POPULATION BASED ON THE CPAK CLASSIFICATION

M. D. Moroz [1], R. A. Kozak [1], O. A. Kostogryz [1], Y. O. Kostogryz [1], M. Yu. Kyrylenko [2]

[1] Diagnostic Center «M24», Kyiv. Ukraine
[2] SI «Institute of Traumatology and Orthopedics of the NAMS of Ukraine», Kyiv

✉ Mykola Moroz: morozn d@ukr.net; https://orcid.org/0000-0003-4134-1322
✉ Roman Kozak: ra.kozak@gmail.com; https://orcid.org/0000-0002-5132-027X
✉ Oleg Kostogryz, MD, DMedSci: arztkostogryz@ukr.net; https://orcid.org/0000-0002-9533-9247
✉ Yurij Kostogryz, MD, PhD: Arzt@i.ua; https://orcid.org/0000-0001-7187-298X
✉ Mykola Kyrylenko: nikolakyrylenko@gmail.com; https://orcid.org/0009-0008-0872-6638

УДК 616.727.2-002-073.763.5(045)

DOI: http://dx.doi.org/10.15674/0030-59872026127-32

MRI classification of rotator cuff arthropathy

S. S. Strafun [1], S. V. Bohdan [1], S. O. Strafun [1], R. O. Sergienko [2]

[1] SI «Institute of Traumatology and Orthopedics of the National Academy of Medical Sciences of Ukraine», Kyiv
[2] National University of Ukraine on Physical Education and Sport, Kyiv

There are several classifications of rotator cuff arthropathy, which are predominantly based on the X-ray examination of patients. The aim of the study was to develop an MRI classification of rotator cuff arthropathy of the shoulder joint. Methods. We included to the study MRI examinations of 91 patients with rotator cuff arthropathy. Presence of acromion acetabularization, deterioration of the shoulder joint articular cartilage, fatty degeneration of the rotator cuff muscles (except teres minor muscle) according to the Goutallier classification, global fatty degeneration index (GFDI) were determined on MRI. Results. After analyzing the above-mentioned criteria, we divided all patients into 4 groups depending on the stage of the disease. We compared the distribution of patients into groups according to the Hamada X-ray classification and according to the proposed MRI classification and made sure of the reproducibility of the data. Conclusion: After comparing Hamada's classification and our classification, we found that the first stage according to Hamada's classification corresponds to the first stage of our MRI classification, the second stage corresponds to the second and third stages of MRI classification, the third, fourth and fifth stages according to Hamada's classification correspond to the fourth stage of our MRI classification. The MRI classification of rotator arthropathy of the shoulder joint presented by us has advantages over the Hamada classification and other radiological classifications, since it takes into account not only the migration of the humeral head and the presence of omarthrosis, but also answers the question of the condition of the rotator cuff muscles, which allows us to determine the rational tactics of surgical treatment in this group of patients.

На сьогодні існує кілька класифікацій ротаторної артропатії, які переважним чином ґрунтуються на рентгенологічному обстеженні хворих. Мета. Розробити класифікацію, засновану на даних манітно-резонансної томографії (МРТ) ротаторної артропатії плечового суглоба. Методи. До дослідження включено МРТ-обстеження 91 хворого. Визначали наявність ацетабуляризації акроміона, зменшення величини суглобового хряща плечового суглоба, жирову дегенерацію м'язів ротаторної манжети плеча (окрім малого круглого м'яза) за класифікацією Goutallier на сагітальних зрізах у Y-проєкції, глобальний індекс жирової дегенерації (GFDI), ушкодження інших м'якотканинних структур ПС (суглобова губа, зв'язки, які утримують сухожилок довгої головки біцепса тощо). Результати. Ураховуючи зазначені критерії ми розділили всіх хворих на 4 групи залежно від стадії захворювання. Порівнюючи розподіл хворих за групами згідно з класифікацією Hamada та запропонованою нами, ще раз переконалися у відтворюваності даних. Висновки. Під час порівняння ступеней за класифікацією Hamada та МРТ, з'ясували, що 1 відповідає 1; 2 — 2 та 3; 3, 4 та 5 — 4 ступеню МРТ класифікації. Наведена нами МРТ класифікація ротаторної артропатії плечового суглоба має переваги над Hamada й іншими рентгенологічними класифікаціями, оскільки вона враховує не лише міграцію головки плечової кістки та наявність омартрозу, а й відповідає на питання про стан м'язів ротаторної манжети плеча, що дозволяє визначитися з раціональною тактикою хірургічного лікування цієї групи хворих. Ключові слова. Ротаторна манжета плеча, ротаторна артропатія, сухожилок надостьового м'яза, плечовий суглоб.

Key words. Shoulder rotator cuff, rotator cuff arthropathy, massive rotator cuff tear, shoulder joint

Introduction

Rotator cuff arthropathy (RCA) is a pathological condition of the shoulder joint (SJ) that develops as a result of massive (two or more) rotator cuff tendon ruptures, degenerative changes in the SJ, and cranial or ventrocranial displacement of the humeral head [1–4].

There are several classifications of rotator cuff arthropathy, which are primarily based on radiological examinations of patients [1, 4–6]. One of the main classifications is the radiological classification by Hamada [1, 6, 7], where the primary criterion for evaluation is the measurement of the acromio-humeral distance. Other criteria include the reduction of the distance between the scapula and humeral head due to cartilage damage in the SJ and the deformation (collapse) of the humeral head. Other well-known classifications are by Seebauer [6] and Favard [1, 7], which are also based on radiological research. The main criteria in these are the reduction of the acromio-humeral and scapulo-humeral distances and the deformation of the humeral head [7, 8]. However, all of these classifications fail to account for the condition of the rotator cuff muscles, the presence of concurrent disorders of the shoulder joint (SJ), and as a result, they do not assist clinicians in determining the appropriate surgical approach. Furthermore, when a rotator cuff tendon rupture is suspected, most patients are only referred for MRI examinations. X-ray imaging of the SJ is generally not performed regularly, nor is it done in the specific projections or angles recommended by the authors of these classifications. A review of the global literature revealed that no MRI-based classification of rotator cuff arthropathy has been developed that integrates established radiological classifications, takes into account the state of the rotator cuff muscles, and provides physicians with a comprehensive framework for guiding treatment decisions.

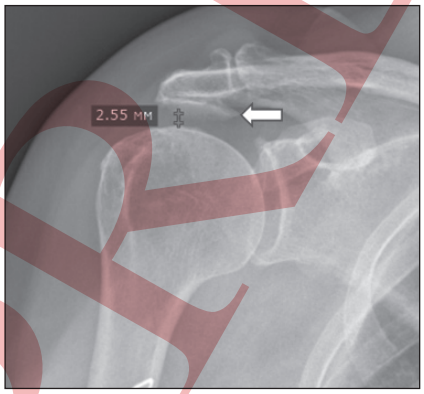

Fig. 1. X-ray of the right shoulder joint in the anteroposterior projection, showing grade 3 rotator cuff arthropathy (2.55 — the size of the subacromial space; the arrow indicates acromion acetabularization)

Purpose: To develop a classification based on MRI data of rotator cuff arthropathy of the shoulder joint.

Materials and methods

The study included MRI examinations of 91 patients who were hospitalized between 2014 and 2024 at the Clinic of Reconstructive and Restorative Surgery of the Upper Limb at the State Institution "National Institute of Traumatology and Orthopedics of the National Academy of Medical Sciences of Ukraine" (Kyiv) and had rotator cuff arthropathy of varying degrees at the time of examination. The age of the patients ranged from 35 to 80 years (mean 48.2 ± 19.8). The work was approved by the local bioethics committee (protocol No. 6 dated 14.07.2025) of the respective institution in accordance with the ICH GCP guidelines, the Helsinki Declaration on Human Rights and Biomedicine, as well as the current legislation of Ukraine. All participating patients were informed about the plan and conditions of the study and gave their written and verbal consent.

All patients underwent clinical and radiological examinations before the start of treatment. X-ray images of the SJ were performed in a standing or sitting position, with the X-ray beam perpendicular to the axis of the scapula at a craniocaudal angle of 20° (Figure 1) to determine the degree of rotator cuff arthropathy according to Hamada. The normal acromio-humeral interval was considered to be between 8–12 mm [1, 7–13].

Additionally, all patients underwent MRI examinations of the anatomical structures of the SJ, including the rotator cuff tendons and muscles, using T1, T2, Pd, and Pdfatsat imaging sequences. MRI was used to assess the following:

1. Presence of acromion acetabularization (Figure 2a);
2. Reduction in the joint cartilage thickness of the SJ (Figure 2b);
3. Fatty degeneration of rotator cuff muscles (excluding the teres minor muscle) according to the Goutallier classification on sagittal sections in the Y projection [9, 10–13] (Figure 2c);
4. Global Fatty Degeneration Index (GFDI) [7, 10];
5. Damage to other soft tissue structures of the SJ (labrum, ligaments holding the long head of the biceps tendon, etc.).

The Global Fatty Degeneration Index (GFDI) is an indicator used in orthopedics to quantitatively assess the severity of fatty degeneration, or fatty infiltration,

in the rotator cuff muscles. It is calculated as the average score based on the Goutallier scale (from 0 to 4) assigned to the supraspinatus, infraspinatus, and subscapularis muscles, which are identified via MRI. A high GFDI indicates more severe fatty infiltration and is associated with a worse prognosis, including an increased risk of re-rupture and decreased functional outcomes after rotator cuff surgery [1, 7, 10].

The study's inclusion criteria comprised the following: verified massive rotator cuff tendon rupture and rotator cuff arthropathy of the shoulder joint (SJ) irrespective of severity; availability of MRI scans conducted with a magnetic field strength of 1.5 Tesla; participant age between 35 and 80 years; and the absence of concomitant shoulder joint conditions, including arthritis, calcific tendinitis, or any bony pathology affecting the proximal epimetaphysis of the humeral bone.

Statistical data processing was carried out using the STATISTICA 12.0 software package. The Student's t-test was used for comparisons between two groups, assuming normal distribution of the data. The Mann-Whitney U test was applied for comparisons between two or more groups when the data distribution deviated from normal. The χ^2 test was used to assess the differences in distribution between two samples.

Results

Table 1 displays the SJ classification of rotator cuff arthropathy, which was developed by our team and is based on MRI results. This classification allows for dividing patients into four groups according to the severity of the disease (Table 1), which is determined by the degree of fatty degeneration in the RCMs and changes in the bony structure of the SJ, both of which can be clearly evaluated during MRI examination (Fig. 1, 2).

In no case did we observe acromion acetabularization without fatty degeneration of the RCM or a global fatty degeneration index (GFDI) > 3 in the absence of fatty degeneration of the supraspinatus muscle. Thus, all patients with rotator cuff arthropathy of the SJ were classified by severity (Table 2).

Table 1

MRI classification of rotator cuff arthropathy of the shoulder joint

Degree of rotator cuff arthropathy	MRI feature
1	Fatty degeneration of the supraspinatus muscle: < Grade 3 on the Goutallier scale GFDI < 1; No acromion acetabularization and/or arthritic changes in the shoulder joint
2	Fatty degeneration of the supraspinatus muscle: ≥ Grade 3 on the Goutallier scale GFDI = 1–1.9 No acromion acetabularization and/or arthritic changes in the shoulder joint
3	Fatty degeneration of the supraspinatus muscle: ≥ Grade 3 on the Goutallier scale GFDI > 2–2.5 No acromion acetabularization and/or arthritic changes in the shoulder joint
4	Fatty degeneration of the supraspinatus muscle: ≥ Grade 3 on the Goutallier scale GFDI > 2.5 Presence of acromion acetabularization and/or arthritic changes in the shoulder joint

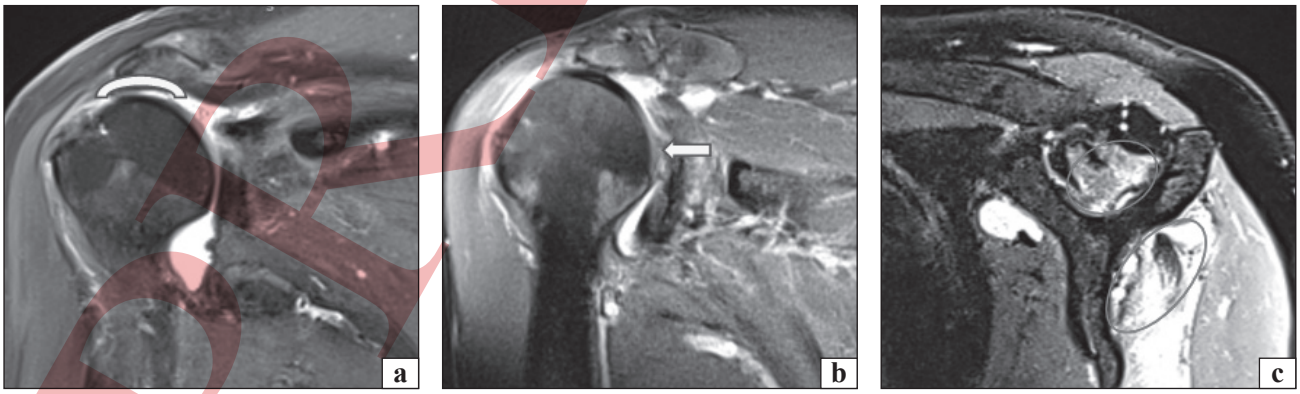

Fig. 2. MRI scan of the SJ: a) Frontal section in T2 Pdfatsat mode (yellow line indicates acromion acetabularization). b) Frontal section in T2 Pdfatsat mode (yellow arrow shows damage to the articular cartilage of the SJ). c) Sagittal section in T2 Pdfatsat mode (ellipses indicate remnants of the supraspinatus and infraspinatus muscles). Grade 3 fatty degeneration of the supraspinatus and grade 4 fatty degeneration of the infraspinatus muscles according to Goutallier

The majority of patients — 35 (38.5 %)—had grade 2 rotator cuff arthropathy according to the MRI findings (p = 0.031). The number of patients with grade 1 and grade 3 was comparatively low, accounting for 21 (23.1 %) and 20 (21.9 %) individuals, respectively. The smallest cohort comprised grade 4 patients, totaling 15 (16.5 %). In no case were signs of disease progression observed simultaneously in two groups.

Table 3 shows the distribution of patients according to the Hamada classification. It should be noted that the majority of patients had grades 1 and 2 rotator cuff arthropathy, i.e., they exhibited only soft tissue changes in the RCM, which were indirectly indicated on X-ray by a reduction in the subacromial space. Only patients with grades 3–5 rotator cuff arthropathy displayed radiological changes such as omarthrosis and acromion acetabularization.

By comparing Tables 2 and 3, we found that patients with grade 1 rotator cuff arthropathy according to the Hamada classification significantly corresponded to grade 1 in our MRI-based classification (p = 0.03); patients with grade 2 were categorized as grades 2 and 3 in the MRI classification (p = 0.67), while those with grades 3, 4, and 5 in the Hamada classification corresponded to grade 4 in the MRI classification (p = 0.041).

Table 2

Distribution of patients by grades of rotator cuff arthropathy according to MRI findings

Grade	Number of patients, (%)
1	21 (23.1)
2	35 (38.5)
3	20 (21.9)
4	15 (16.5)

Table 3

Distribution of patients by degree of rotator cuff arthropathy according to radiographic examination

Grade	Number of patients, (%)
1	21 (23.1)
2	55 (60.4)
3	8 (8.8)
4	4 (4.4)
5	3 (3.3)

Table 4 presents the treatment options for each grade of rotator cuff arthropathy of the SJ.

Thus, reverse shoulder arthroplasty is indicated for patients over 60 years of age with grade 3 rotator cuff arthropathy or grade 4 according to the MRI classification. In certain instances, reconstructive procedures involving the SJ are considered the optimal approach.

Discussion

The MRI classification of rotator cuff arthropathy of the SJ, as developed by our team, offers clinicians a dependable framework for selecting optimal treatment strategies for patients across all stages of rotator cuff arthropathy. This classification has been invaluable in our clinical practice for the past 10 years, allowing us to compare treatment outcomes using different methods.

In fact, our classification is a combination of the Hamada and Goutallier scales [1, 7, 10], which considers only the gross changes in the SJ, significantly reducing the likelihood of errors. For instance, when evaluating the acromio-humeral index (AHI) — the distance between the inferior surface of the acromion and the humeral head — 5 mm is considered grade 2 rotator cuff arthropathy according to Hamada, while 6 mm is considered grade 1. An error of 1 mm is highly probable and depends on the physician's experience, the quality, and the accuracy of the X-ray. Failure to properly position the X-ray beam at a 20° angle relative to the horizontal axis (top-to-bottom) and perpendicular to the axis of the scapula will prevent correct diagnosis (Figure 1). In our classification, the AHI is disregarded; the key factor is the presence of acromion acetabularization, which assigns the patient to grade 4 RCA with corresponding surgical treatment options. The dual evaluation of fatty degeneration according to Goutal-

Table 4

Treatment of rotator cuff arthropathy of the shoulder joint based on MRI findings

Grade	Surgical treatment
1	Rotator cuff tendon repair (open or arthroscopic)
2	Restoration of the superior capsule of the shoulder joint (open or arthroscopic).
3	In patients under 60 years of age — tendon transfer of the latissimus dorsi to the position of the external rotators, or the upper portion of the pectoralis major to the position of the internal rotators. In patients over 60 years of age — reverse shoulder arthroplasty
4	Reverse shoulder arthroplasty

lier, first for the supraspinatus and then for other muscles, along with the determination of the GFDI, also significantly reduces the risk of error.

Upon reviewing the English-language literature, we found no publications that combine the Hamada and Goutallier classifications. The vast majority of studies aimed to compare radiographic and MRI findings, particularly focusing on AHI and how factors like upper limb positioning, tendon tear size, and the time since injury affect the AHI [12–17, 20]. R. Mirzayan et al. noted that for early-stage rotator cuff arthropathy (grades 1–2), AHI values measured on radiographs did not correlate with MRI findings. Therefore, in the early stages of the disease, it is not possible to diagnose rotator cuff arthropathy using MRI. However, in the later stages (grades 3–5), there is no significant difference in AHI values [18]. C. M. Werner et al. also highlighted that AHI values for patients with rotator cuff arthropathy obtained from MRI and CT scans differed significantly from those obtained by X-ray. In their study, the authors found that AHI values during MRI correlated well with fatty degeneration of the RCM and proposed a formula to convert these MRI-based values into those obtained from radiographs [19].

Interesting findings by P. N. Chalmers et al. demonstrated that the AHI value was not dependent on the size of the rotator cuff tendon tear, and its progression over time did not influence the AHI value [5].

We believe that our proposed MRI-based classification has significant advantages over the Hamada scale and other classifications that rely solely on radiological changes in the SJ. This is because our classification takes into account not only the caudal displacement of the humeral head and the presence of articular cartilage damage in the SJ but also provides insight into the condition of the rotator cuff muscles and concomitant shoulder joint abnormalities.

Conclusions

By comparing the Hamada classification with our MRI-based classification, we found that: Grade 1 on the Hamada scale corresponds to grade 1 in our MRI classification. Grade 2 on the Hamada scale corresponds to grades 2 and 3 in our MRI classification. Grades 3, 4, and 5 on the Hamada scale correspond to grade 4 in our MRI classification.

The proposed MRI classification of rotator cuff arthropathy of the shoulder joint has advantages over the Hamada classification and other radiological classifications, as it not only considers the migration of the humeral head and the presence of omarthrosis but also addresses the condition of the rotator cuff muscles. This allows for a more rational approach to determining the appropriate surgical treatment strategy for this group of patients.

Conflict of interest. The authors declare that there is no conflict of interest.

Future research prospects. A promising direction for our upcoming research is the study of other significant pathological changes in the shoulder joint to further enhance our classification. However, adding more factors may make it more cumbersome and harder to understand for practicing orthopedic surgeons.

Funding information. The authors declare that there is no financial interest in the writing of this article. This study did not receive external funding.

Authors' contribution. Strafun S. S. — concept and design of the study; Bogdan S. V. — collection and processing of materials, writing the text; Strafun O. S. — Systematic analysis of the data; Serhienko R. O. — Systematic analysis of the data.

References

1. Matsen, F. A., Cordasco, F. A., Sperling, J. W., & Lippitt, S. B. (2021). Rockwood and Matsen's the shoulder E-book: Rockwood and Matsen's the shoulder E-book. Elsevier Health Sciences.
2. Mizuki, Y., Tamai, M., Senjyu, T., & Takagishi, K. (2022). Arthroscopic extreme Medialized repair for massive rotator cuff tear: Resection of cartilage and Subchondral bone over the top of the humeral head. *Arthroscopy techniques, 11*(6), e965–e970. https://doi.org/10.1016/j.eats.2022.01.017
3. Clifford, A. L., Hurley, E., Anakwenze, O., & Klifto, C. S. (2024). Rotator cuff arthropathy: A comprehensive review. *Journal of hand surgery global online, 6*(4), 458–462. https://doi.org/10.1016/j.jhsg.2023.12.014
4. Furuhata, R., Matsumura, N., Oki, S., Nishikawa, T., Kimura, H., Suzuki, T., Nakamura, M., & Iwamoto, T. (2022). Risk factors of radiographic severity of massive rotator cuff tear. *Scientific reports, 12*(1). https://doi.org/10.1038/s41598-022-17624-y
5. Chalmers, P. N., Salazar, D. H., Steger-May, K., Chamberlain, A. M., Stobbs-Cucchi, G., Yamaguchi, K., & Keener, J. D. (2016). Radiographic progression of arthritic changes in shoulders with degenerative rotator cuff tears. *Journal of shoulder and elbow surgery, 25*(11), 1749–1755. https://doi.org/10.1016/j.jse.2016.07.022
6. Brolin, T. J., Updegrove, G. F., & Horneff, J. G. (2017). Classifications in brief: Hamada classification of massive rotator cuff tears. *Clinical orthopaedics & related research, 475*(11), 2819–2823. https://doi.org/10.1007/s11999-017-5340-7
7. Habermeyer P. (2006). Classifications and scores of the sholder. Springer, Berlin
8. Stanborough, R. O., Bestic, J. M., & Peterson, J. J. (2022). Shoulder osteoarthritis. *Radiologic clinics of North America, 60*(4), 593–603. https://doi.org/10.1016/j.rcl.2022.03.003
9. Eajazi, A., Kussman, S., LeBedis, C., Guermazi, A., Kompel, A., Jawa, A., & Murakami, A. M. (2015). Rotator cuff tear arthropathy: Pathophysiology, imaging characteristics, and treatment options. *American journal of roentgenology, 205*(5), W502–W511. https://doi.org/10.2214/ajr.14.13815
10. Wallenberg, R. B., Belzer, M. L., Ramsey, D. C., Opel, D. M., Berkson, M. D., Gundle, K. R., Nagy, M. L., Boucher, R. J., & McCarron, J. A. (2022). MRI-based 3-dimensional volumetric assessment of fatty infiltration and muscle atrophy in rotator cuff tears. *Journal of shoulder and elbow surgery, 31*(6), 1272–1281. https://doi.org/10.1016/j.jse.2021.12.037
11. Ki, S., Lee, Y., Kim, J., Lho, T., & Chung, S. W. (2021). Relationship between fatty infiltration and gene expression in

patients with medium rotator cuff tear. *Journal of shoulder and elbow surgery, 30*(2), 387–395. https://doi.org/10.1016/j.jse.2020.06.003
12. McCrum, E. (2020). MR imaging of the rotator cuff. Magnetic Resonance *Imaging clinics of North America, 28*(2), 165–179. https://doi.org/10.1016/j.mric.2019.12.002
13. Clifford, A. L., Hurley, E., Anakwenze, O., & Klifto, C. S. (2024). Rotator cuff arthropathy: A comprehensive review. *Journal of hand surgery global online, 6*(4), 458–462. https://doi.org/10.1016/j.jhsg.2023.12.014
14. Cvetanovich, G. L., Waterman, B. R., Verma, N. N., & Romeo, A. A. (2019). Management of the irreparable rotator cuff tear. *Journal of the American academy of orthopaedic surgeons, 27*(24), 909–917. https://doi.org/10.5435/jaaos-d-18-00199
15. Verhaegen, F., Meynen, A., Plessers, K., Scheys, L., & Debeer, P. (2021). Quantitative SSM-based analysis of humeral head migration in rotator cuff tear arthropathy patients. *Journal of orthopaedic research, 40*(7), 1707–1714. https://doi.org/10.1002/jor.25195
16. Rugg, C. M., Gallo, R. A., Craig, E. V., & Feeley, B. T. (2018). The pathogenesis and management of cuff tear arthropathy. *Journal of shoulder and elbow surgery, 27*(12), 2271–2283. https://doi.org/10.1016/j.jse.2018.07.020
17. Kwong, C. A., Ono, Y., Carroll, M. J., Fruson, L. W., More, K. D., Thornton, G. M., & Lo, I. K. (2019). Full-thickness rotator cuff tears: What is the rate of tear progression? A systematic review. *Arthroscopy: the journal of arthroscopic & related surgery, 35*(1), 228–234. https://doi.org/10.1016/j.arthro.2018.07.031.
18. Mirzayan, R., Donohoe, S., Batech, M., Suh, B. D., Acevedo, D. C., & Singh, A. (2020). Is there a difference in the acromiohumeral distances measured on radiographic and magnetic resonance images of the same shoulder with a massive rotator cuff tear? *Journal of shoulder and elbow surgery, 29*(6), 1145–1151. https://doi.org/10.1016/j.jse.2019.10.020
19. Werner, C. M., Conrad, S. J., Meyer, D. C., Keller, A., Hodler, J., & Gerber, C. (2008). Intermethod agreement and interobserver correlation of radiologic acromiohumeral distance measurements. *Journal of shoulder and elbow surgery, 17*(2), 237–240. https://doi.org/10.1016/j.jse.2007.06.002
20. Furuhata, R., Matsumura, N., Oki, S., Nishikawa, T., Kimura, H., Suzuki, T., Nakamura, M., & Iwamoto, T. (2022). Risk factors of radiographic severity of massive rotator cuff tear. *Scientific reports, 12*(1). https://doi.org/10.1038/s41598-022-17624-y

The article has been sent to the editors	Received after review	Accepted for printing
07.11.2025	17..12.2025	24.12.2025

MRI CLASSIFICATION OF ROTATOR CUFF ARTHROPATHY

S. S. Strafun [1], S. V. Bohdan [1], S. O. Strafun [1], R. O. Sergienko [2]

[1] SI «Institute of Traumatology and Orthopedics of the National Academy of Medical Sciences of Ukraine», Kyiv
[2] National University of Ukraine on Physical Education and Sport, Kyiv

✉ Sergiy Strafun, MD, Prof.: strafun-s@ukr.net; https://orcid.org/0000-0001-8178-9290
✉ Sergiy Bohdan, MD, PhD: sergey-mena@ukr.net; https://orcid.org/0000-0001-6681-9615
✉ Olexandr Strafun, MD, DMSci: o_strafun@ukr.net; https://orcid.org/0000-0003-2726-5589
✉ Ruslan Sergienko, MD: anna.vovchenko.md@gmail.com; https://orcid.org/0000-0002-0497-3518

УДК 616.717.4-001.5:616.727.2-089.843](045)

DOI: http://dx.doi.org/10.15674/0030-59872026133-42

Functional outcomes of reverse total shoulder arthroplasty in acute proximal humeral fractures versus post-traumatic sequelae

Ahmed Adel Abdelaty Abdo [1], Tarek Abdelaziz [1], Mohamed Omar Soliman [2], Mohamed Ibrahim Rakha [1], Asser Abdelhay Sallam [3]

[1] Department of Orthopedic Surgery and Trauma, Suez Canal University, Ismailia. Egypt
[2] Department of Orthopedic Surgery and Trauma, Cairo University. Egypt
[3] Department of Orthopedic Surgery and Trauma, Suez University. Egypt

Proximal humeral fractures account for 4–6 % of all fractures and are the third most prevalent fracture pattern in the elderly. Reverse total shoulder arthroplasty (RTSA) is a frequently utilized surgical procedure for treating this fracture. Aim. To improve the functional outcome and quality of life of patients with acute proximal humeral fractures and post-traumatic sequelae using reverse total shoulder arthroplasty. Subjects and Methods. This comparative study was conducted on a total of 20 patients with 3- or 4-part proximal humeral fractures aged more than 55 years, 10 patients were suffering from acute fractures (group I) and 10 patients with post-traumatic sequelae (group II). All patients were evaluated preoperatively and followed up postoperatively at 6 weeks, 3 months, 6 months and one year for functional outcomes. Radiological, clinical and functional outcomes were assessed by a goniometric range of motion (ROM), Constant-Murley score, and the Arabic version of the Quick DASH score. The rate of postoperative complications and the need for revision surgery were also reported. Results. In group I, the DASH and VAS score declined from 88.30 (± 8.23) and 5.90 (± 1.28) in the 6th weeks after surgery down to 34.30 (± 11.55) and 0.70 (± 0.48), respectively after 1 year. The Constant score increased from 14.70 (± 5.67) to 67.30 (± 14.98). All scores showed almost similar improvements in all three parameters in group II. Moreover, similar improvements in the deltoid muscle power, function and ranges of motion were reported in patients of both groups. Conclusion. Reverse shoulder arthroplasty provides favorable post-operative outcomes among elderly patients with 3-part and 4-part fractures of the proximal humerus. Indication for RTSA will not be affected by whether patients are presenting with acute or post-traumatic sequelae fractures. Level of evidence: Therapeutic study level III.

Травми проксимального відділу плечової кістки становлять 4–6 % усіх переломів і посідають третє місце за поширеністю серед ушкоджень у людей похилого віку. Реверсивне тотальне ендопротезування плечової кістки (RTSA) є часто використовуваною хірургічною процедурою для їхнього лікування. Мета. Покращити функціональний результат та якість життя пацієнтів із переломами проксимального відділу плечової кістки та посттравматичними наслідками за допомогою RTSA. Методи. Це порівняльне дослідження проведене за участю 20 пацієнтів з 3- або 4-уламковими переломами проксимального відділу плечової кістки віком понад 55 років. Хворих розподілили на 2 групи: I — перелом, 10 осіб, II — посттравматичні наслідки (10 випадків). Усі пацієнти були обстежені до втручання та спостерігалися після операції через 6 тижнів, 3 і 6 місяців та один рік. Радіологічні, клінічні та функціональні результати оцінювалися за допомогою гоніометричного діапазона рухів (ROM), шкали Constant-Murley та арабської версії шкали Quick DASH. Також повідомлялося про частоту післяопераційних ускладнень та необхідність повторної операції. Результати. У групі I бал за шкалами DASH та VAS знизився з 88,30 (±8,23) та 5,90 (±1,28) через 6 тижнів після операції до 34,30 (±11,55) та 0,70 (±0,48) відповідно через рік. Бал за шкалою Constant збільшився з 14,70 (± 5,67) до 67,30 (± 14,98). Усі показники майже однаково покращилися за всіма трьома параметрами в групі II. Окрім того, у пацієнтів обох груп виявлено зростання функції та діапазону рухів дельтоподібного м'яза. Висновок. Реверсивне ендопротезування плечового суглоба забезпечує сприятливі післяопераційні результати в пацієнтів похилого віку з 3- та 4-уламковими переломами проксимального відділу плечової кістки. Показання до RTSA не залежатимуть від того, чи мають пацієнти гострі чи посттравматичні наслідки переломів. Ключові слова. Переломи проксимального відділу плечової кістки; посттравматичний; реверсивне ендопротезування плечового суглоба.

Keywords. Proximal humeral fractures; post-traumatic; acute; reverse shoulder arthroplasty

Introduction

Proximal humerus fractures (PHFs) are the third most prevalent form of fracture in individuals over 65 years of age, accounting for 4–6 % of all fractures in that population. Furthermore, PHFs are the third most prevalent form of osteoporotic fractures, with a lifetime risk of 13 % for women aged 50 and more [1].

The majority of proximal humerus fractures (stable, minimally displaced fractures) are treated nonoperatively, most typically with sling immobilization followed by early and gradual physical therapy and rehabilitation [2].

On the other hand, one of the most commonly used surgical techniques is reverse total shoulder arthroplasty, which has become the preferred treatment for older patients with non-reconstructable PHFs because the patient can achieve excellent motion even with unhealed tuberosities or an incompetent rotator cuff. It can also be used for non-surgical therapy of fracture sequelae and revision of failed HA operations [3].

In addition, reverse total shoulder arthroplasty (RTSA) has become more popular globally in treating different traumatic and degenerative glenohumeral disorders and irreversible rotator cuff arthropathies [4].

RTSA can be utilized for acute and post-traumatic PHFs. Nevertheless, the functional effects of RTSA in these fractures remain debatable.

Therefore, in our study, we compared the functional outcomes of reverse total shoulder arthroplasty in patients with recent traumatic proximal humerus fractures and posttraumatic sequelae.

Patients and methods

This comparative prospective study was conducted at the orthopedic emergency department, or the orthopedic outpatient clinic, Suez Canal and Cairo University hospitals following the approval of our Institutional Research Board on 17th May 2022 (Approval #ORT/4918). It was conducted on a total of 20 patients aging more than 55 years of age and presenting with proximal humeral fractures: 10 patients having three and four-part proximal humeral fractures (group I) and 10 patients with post-traumatic sequelae in the form of non-union or malunion of the anatomical neck of humerus with minimal calcar hinge, arthritis, or failed hemiarthroplasty (group II). Patients of both groups were managed by Reverse Shoulder System.

Patients with signs of infection around the shoulder, axillary nerve injury, acromial and scapular fractures, paralytic or neurologic disorders that affect prosthesis stability or pathological fractures were excluded from the study.

All study patients were subjected to preoperative evaluation through full history taking and clinical examination. The Modified British Medical Research Council (MRC) Scale was used for assessment of the deltoid muscle power [5]. Painless active range of motion and painless resting position of the limb were tested.

Plain shoulder radiographs (anteroposterior and lateral views) were ordered for all patients. In true AP views, the superior-inferior glenoid bone loss was assessed using the Favard classification which classifies the glenoid bone erosion into five types: from E0 to E4 [6]. The inferior glenoid tilt [7] was assessed using the Habermeyer classification. In the axillary lateral view, the posterior glenoid wear was assessed using Walch classification, which classifies the posterior wear as follows: A1, mild concentric glenoid wear; A2, marked concentric glenoid wear; B1, eccentric posterior glenoid erosion; B2, with a biconcave glenoid; C, greater than 25° retroversion [6]. Our spectrum and focus for group II patients were post-traumatic sequelae of the proximal humerus. Therefore, only glenoid arthritis patients who didn't need any augments or biografting were included, such as patients with Walch types A1 and B1. Patients with types A2, B2 and C were excluded from the study.

Computerized tomography and 3D-CT were ordered to evaluate the glenoid retroversion angle by the Friedman method. An axial computed tomography slice was taken at the level of the tip of the coracoid and a line is drawn from the medial scapula border through the middle of the glenoid. The retroversion was calculated by the angle between the glenoid joint line and the perpendicular of Friedman's line. Glenoid vault depth was measured as follows: Axial slice was used to assess the vault depth (a minimum of 10 mm is required for central peg accommodation) [8–11]. MRI was ordered routinely for all patients to assess the condition of the rotator cuff tendons. Splinting was applied, and analgesics were continued till the time of surgery.

Surgical technique

Under general anesthesia with interscalene block, the patient was placed on a beach chair position at the edge of the table to allow free shoulder movement. A third-generation cephalosporin was given preoperatively. *For the acute fracture group*, a deltopectoral approach was adopted. An 8–10 cm incision was performed starting from the coracoid process to the deltoid insertion and then through the clavipectoral

facia. Subscapularis bursae were removed, the bicipital groove was identified then biceps tenotomy was done with tenodesis. Greater tuberosity was identified and stay sutures were placed. The rotator interval was identified and opened to the glenoid. Lesser tuberosity was identified and a stay suture in the subscapularis tendon was placed. The biceps tendon is excised down to the glenoid. Four suture loops are passed through the posterosuperior cuff, flush with the tendon insertions onto the greater tuberosity; the needles are removed from two of the loops, which are passed from medial to lateral through the infraspinatus and teres minor, respectively; and the other two loops are passed from lateral to medial through the same tendons. Traction sutures are used to pull the tuberosities apart. The anterior capsule is excised to expose the anterior glenoid rim. Two retractors are placed at the anterior and posterior borders of the glenoid, respectively.

Tuberosities were pulled apart and the labrum was excised to expose the glenoid. Dissecting the capsule from the anterior glenoid down to and around the inferior pole so the upper axillary scapular border could be easily palpated and seen. After removal of the capsule and labrum, a guide wire was drilled 13 mm anterior to the posterior rim and 19 mm above the inferior glenoid rim with 10 degrees inferior tilt. The baseplate of the delta prosthesis was then placed over the guide wire to verify the right position of the central wire. Then we reamed the glenoid to remove only enough bone to make it flat.

The central hole was drilled then we inserted the central peg into the central hole. By using a 2 mm drill bit, a drill was done for the inferior screw after baseplate rotation adjustment to the axillary scapular border. After inferior screw placement, we drilled and then inserted the superior screw into the base of the coracoid process using a similar technique. A trial glenosphere was then inserted over the baseplate and any bone that abuts against the humeral polyethylene was removed.

The conical-shaped cemented trabecular metal reverse humeral stem was implanted in all patients of group I. We gradually increased the size of broaches for the proximal humerus until rotational stability was achieved provided that any cortical contact was avoided. Then a drill hole was made in the humerus for fixation of the tuberosities. Finally, the polyethylene insert was applied, and the wound was irrigated and closed in layers.

For the post-traumatic sequelae group, a similar surgical technique was utilized, but specific technical difficulties were encountered as follows: when a revision of hemiarthroplasty was planned, an extensile deltopectoral approach was adopted. Scar tissue is excised. Close attention was paid to the attachments of the latissimus dorsi, teres major, and pectoralis major tendons. Deltoid muscle was preserved. These should be spared and marked to ensure optimal function following surgery. When dissecting the glenoid capsule, the axillary nerve and its branches were identified and preserved. Complete glenoid visualization required peri-glenoid capsular resection. To expose the base of the coracoid and the anterior glenoid neck, which measured about 3 cm, the subscapularis was peeled off the glenoid neck. The head was hammered and then removed. The humeral stem was loose and was easily removed with an impactor from below without the need for osteotomy. The cement was extracted with a cement removal set. Yet, some blowout of the lateral cortex occurred in one patient. The plug and the distal cement to the tip of hemiarthroplasty left inside the medullary canal. A classical approach for the glenoid reaming and baseplate fixation and glenoshphere was adopted. The conical-shaped cemented trabecular metal reverse humeral stem was also inserted in all the patients of both groups. Stability was evaluated following the implantation of the humeral component and joint reduction. Adequate tension was checked by assessing the tension of the soft tissues, such as the conjoint tendon, which is a key stabilizer of the shoulder girdle.

In patients where there was an old anatomical neck fracture malunion or nonunion that was internally fixed, the PHILOS plate was removed and the anatomical neck and tuberosities were osteotomized. Tuberosities were then reattached to the implant and humeral shaft as closely as possible to its anatomic side. The same conical-shaped cemented trabecular metal reverse humeral stem was implanted in those patients.

In patients with arthritis, through a deltopectoral approach, adducting and externally rotating the arm while pushing the elbow forward and upward helped the humeral head to dislocate. To determine the level of humeral resection and the anatomical neck, anterior and inferior osteophytes were excised from the proximal humerus. Typically, the humeral head was removed at a retroversion angle of approximately 30 degrees. The humeral canal was reamed using different reamer sizes and then prepared by humeral stem broaches. A version rod was attached to the broach handle to monitor the version during humerus preparation. A conical-shaped cemented trabecular metal reverse humeral stem was inserted. The steps of glenoid exposure and preparation were similar to patients of group one.

Post-operative Follow-up

Follow-up visits were planned at 2 weeks, 6 weeks, 3 months, 6 months and one year post-operatively. The sutures were removed two weeks after surgery. An arm sling was applied for the first 6 weeks, during which no active ROM or weightlifting was allowed. Immediate postoperative active motion of the cervical spine, elbow, wrist, and hand were encouraged. Passive extension, elevation, external rotation and internal rotation were postponed till the 6th week. Between the 6th to 12th week, the passive range of motion was continued, and patients started a protected gradual active ROM. After the 12th week, strengthening of the muscles around the shoulder was allowed.

Post-operative Outcome Measures

Radiological outcomes (stability, radiolucency, scapular notching, heterotopic ossifications and other possible complications) were assessed by plain radiography at 2 weeks, 6 weeks, 3 months, 6 months and one-year intervals 9 (example of pre-operative versus post-operative radiological findings after 1 year is presented in Figs. 1 and 2 of patients from group I and Figs. 3, 4, and 5 of patients from group II). Clinical and functional outcomes were assessed by a goniometric range of motion (ROM), Constant-Murley score 10, and the Arabic version of the Quick DASH score 11. The rate of postoperative complications and the need for revision surgery were also reported.

Statistical analysis

Collected data were coded, entered, and analyzed using Microsoft Excel program software. Data analysis was done by Statistical Package for Social Science (SPSS) version 26.

We conducted the Shapiro-Wilk test and found that our numeric data were normally distributed, accordingly they were represented as mean (± SD). Categorical data were expressed as proportions. Demographic characteristics were compared using the Fisher exact test and the Chi-square test, while the T-test was used for mean differences of the clinical scores. The level of significance using the p-value was statistically significant if it was < 0.05.

Results

The patients' demographics are presented in Table 1. Both groups in our study had a comparable age distribution, with Group I having a mean age of 69.40 ± 10.57 years (range: 56–86) and Group II having a mean age of 70.80 ± 7.89 years (range: 56–81). Additionally, we included both males and females. Regarding comorbidities, 4 patients in Group I had no chronic illnesses, while most of the remaining patients suffered from hypertension (3/10). In Group II, half of the patients were diabetic, and 3 patients had both diabetes and hypertension. Concerning the type of fractures in Group I, 40 % of the patients had 3-part fractures, while 60 % had 4-part fractures, with no head-splitting fractures. Figure 1 represents patient with acute proximal humeral fracture who restored satisfactory function after RTSA. Figure 2 represents another example of acute proximal humeral fracture that is 73-year-old female patient who presented with a 4-part fracture and history of old humeral shaft fixation.

As for post-traumatic sequelae in group II, 40 % of the cases had arthritis, 50 % had malunion, and only 10 % had hemiarthroplasty. The patient with hemiarthroplasty underwent revision surgery by RTSA due to aseptic loosening. The patient had the first surgery 5 years ago and presented with progressive pain and limitation of movement (Fig. 3). Another example is a female patient with secondary advanced shoulder arthritis after reduced shoulder dislocation 5 years ago and underwent RTSA (Fig. 4). Furthermore, a 55-year-old patient presented with a fracture malunion. Radiographs revealed a malunited fracture of the anatomical neck of his right humerus. The malunited anatomical neck was osteomatized and a classic RTSA was performed (Fig. 5).

Table 1

Distribution of the demographic and clinical characteristics in both groups

	Group I (n=10)	Group II (n=10)
Age, years:		
Mean+SD	69.40 ±10.57	70.80 ±7.89
Range	(56-86)	(56-81)
Gender:		
Male	4 (40%)	5 (50%)
Female	6 (60%)	5 (50%)
Chronic illnesses:		
Diabetes	2 (20%)	5 (50%)
Hypertension	3 (30%)	1 (10%)
Diabetes and Hypertension	1 (10%)	3 (30%)
No chronic illness	4 (40%)	1 (10%)
Fracture Type:		
3-part fractures	4 (40%)	—
4-part fractures	6 (60%)	
Head-splitting fractures	0 (0%)	
Post-traumatic squelae:		
Malunion	—	5 (50%)
Arthritis		4 (40%)
Hemiarthroplasty		1 (10%)

Notes: * Quantitative data are expressed in mean+SD, and range. Qualitative data are presented as numbers (percentage). Group I includes patients with acute proximal humeral fractures. Group II includes patients with post-traumatic sequelae.

There was a marked improvement among the patients in both study groups when we compared their DASH scores at 6, 12, 24, and 48 weeks. However, upon examining the presence of any differences in the DASH score between both groups at each follow-up period, we found no significant difference (table 2).

The VAS score also declined markedly across the follow-up period, however, this improvement didn't vary significantly between both groups, since similar improvements were noted among the patients in both study groups (table 2).

The results of the Constant-Murley score showed that the patients' total score improved markedly over time. However, this improvement did not vary significantly across both groups (table 2).

The mean range of motions of all patients increased significantly by one year in both groups.

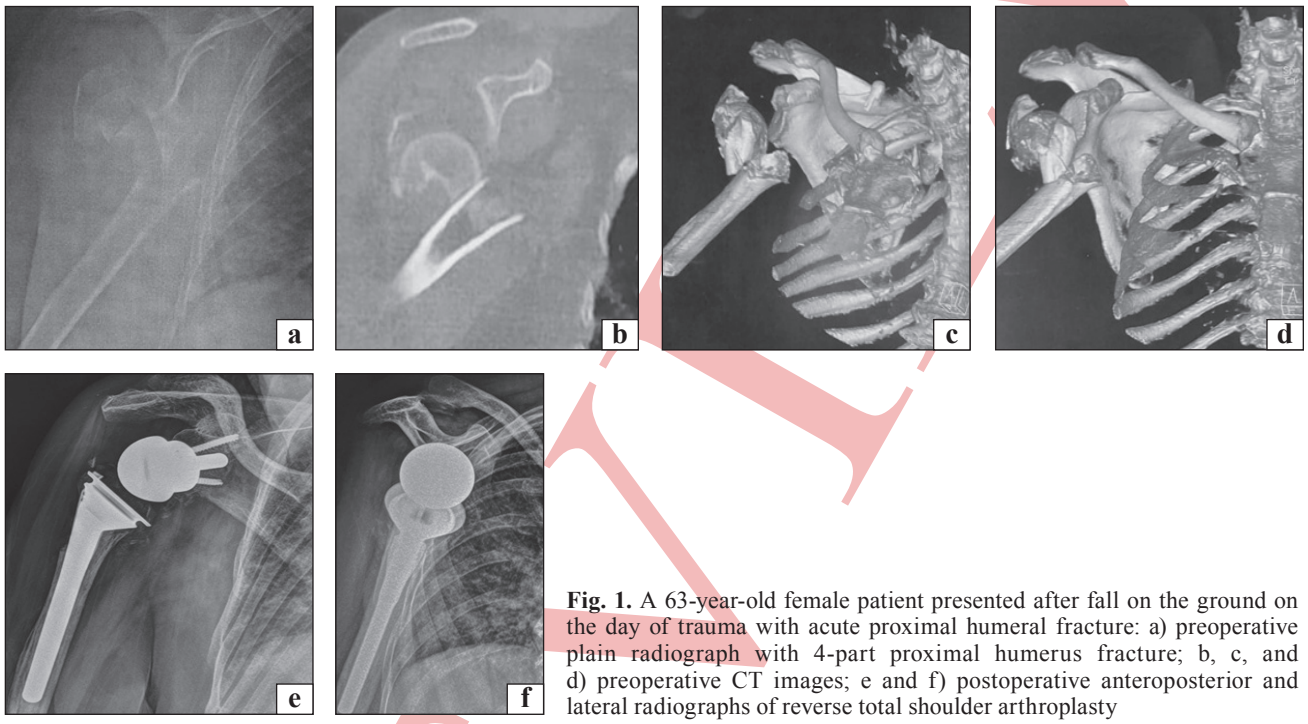

Fig. 1. A 63-year-old female patient presented after fall on the ground on the day of trauma with acute proximal humeral fracture: a) preoperative plain radiograph with 4-part proximal humerus fracture; b, c, and d) preoperative CT images; e and f) postoperative anteroposterior and lateral radiographs of reverse total shoulder arthroplasty

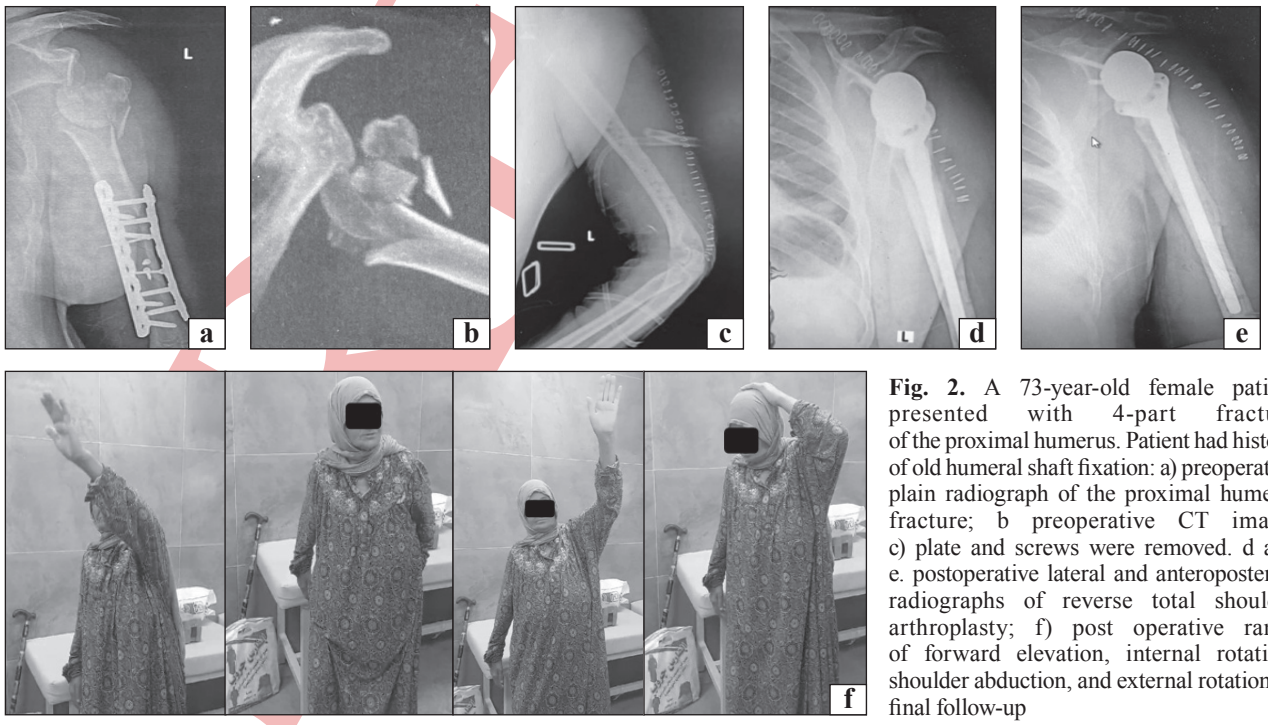

Fig. 2. A 73-year-old female patient presented with 4-part fracture of the proximal humerus. Patient had history of old humeral shaft fixation: a) preoperative plain radiograph of the proximal humeral fracture; b preoperative CT image; c) plate and screws were removed. d and e. postoperative lateral and anteroposterior radiographs of reverse total shoulder arthroplasty; f) post operative range of forward elevation, internal rotation, shoulder abduction, and external rotation at final follow-up

However, the improvement was slightly and statistically insignificantly higher among patients in group II regarding Abduction and Flexion, while patients in group I had better external rotation and internal rotation ranges (table 3).

Table 2

Distribution of the functional outcome scores at 6, 12 24, and 48 weeks after surgery in both groups

	Group I (n = 10)	Group II (n = 10)	P value
	Mean (±SD) Range		
DASH			
6 weeks	88.30 (± 8.23) (73–98)	91.00 (± 3.52) (84–95)	0.359
12 weeks	61.40 (± 11.80) (40–76)	61.30 (± 8.38) (46–70)	0.983
24 weeks	37.20 (± 13.16) (19–56)	39.00 (± 8.27) (23–46)	0.719
48 weeks	34.30 (± 11.55) (19–52)	35.80 (± 7.14) (21–42)	0.732
VAS			
6 weeks	5.90 (± 1.28) (4–8)	5.80 (± 0.78) (5–7)	0.837
12 weeks	3.50 (± 1.17) (2–5)	3.70 (± 0.82) (3–5)	0.665
24 weeks	1.20 (± 0.78) (0–2)	1.20 (± 0.42) (1–2)	1.000
48 weeks	0.70 (± 0.48) (0–1)	0.60 (± 0.51) (0–1)	0.660
CS			
6 weeks	14.70 (± 5.67) (6–25)	16.00 (± 3.39) (12–21)	0.544
12 weeks	37.90 (± 9.93) (25–55)	35.30 (±3 .94) (30–41)	0.457
24 weeks	65.60 (± 16.57) (40–90)	61.10 (± 6.36) (51–72)	0.439
48 weeks	67.30 (± 14.98) (45–90)	62.70 (± 5.92) (54–72)	0.389

Notes: DASH: Disabilities of the Arm Shoulder and Hand; VAS: Visual analogue score; CS: Constant-Murley score. Quantitative data are expressed in mean+SD and range. * p-value. < 0.05: statistically significant.

Table 3

Distribution of the mean range of motion at 6, 12 24, and 48 weeks after surgery in both groups

	Group I (n = 10)	Group II (n = 10)	P value
	Mean (±SD) Range		
Abduction			
6 weeks	37.80 (± 14.69) (23–72)	36.20 (± 11.25) (26–65)	0.788
12 weeks	(89.10 (± 34.95) (40–147)	98.50 (± 22.34) (60–131)	0.484
24 weeks	142.70 (± 30.96) (89–175)	146.50 (± 15.33) (110–164)	0.734
48 weeks	145.50 (± 28.42) (97–175)	149.30 (± 13.88) (115–166)	0.710
Flexion			
6 weeks	51.10 (± 29.49) (26–110)	41.60 (± 10.98) (29–56)	0.360
12 weeks	92.50 (± 31.92) (58–155)	92.40 (± 13.62) (73–119)	0.993
24 weeks	149.20 (± 27.08) (105–180)	149.10 (± 16.14) (114–167)	0.992
48 weeks	152.90 (± 25.54) (113–180)	156.80 (± 9.31) (145–170)	0.659
External rotation			
6 weeks	12.90 (± 4.55) (6–20)	11.60 (± 3.53) (8–18)	0.486
12 weeks	26.80 (± 11.38) (12–45)	22.60 (± 4.69) (17–32)	0.302
24 weeks	43.90 (± 15.87) (23–73)	40.30 (± 10.36) (27–55)	0.557
48 weeks	44.90 (± 15.82) (24–73)	41.70 (± 10.07) (28–55)	0.597
Internal rotation			
6 weeks	27.40 (± 5.89) (21–40)	24.60 (± 4.64) (18–32)	0.254
12 weeks	39.70 (± 6.91) (31–55)	38.10 (± 3.90) (32–43)	0.534
24 weeks	52.60 (± 11.84) (41–77)	51.60 (± 6.81) (42–65)	0.820
48 weeks	55.10 (± 10.58) (44–77)	53.70 (± 6.91) (45–69)	0.731

Notes: Quantitative data are expressed in mean+SD and range. * p < 0.05: statistically significant.

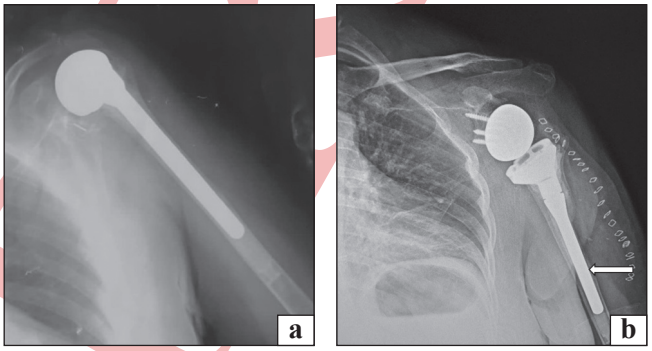

Fig. 3. A 58-year-old male patient presented with aseptic loosening of shoulder hemiarthroplasty: a) preoperative plain radiograph of the hemiarthroplasty; b) postoperative radiographs of reverse total shoulder arthroplasty (arrow indicates lateral cortex blowout during cement extraction)

A significant increase in power and function was noted when comparing the 6-week follow-up results with the one-year follow-up results. Nevertheless, there was no statistically significant difference between both groups in terms of this improvement (table 4).

The improvement in the power and function was higher in group II compared to group I in the 12-, 24-, and 1-year follow-up. On the other hand, the 6-week follow-up results showed patients in group I had more power and function (table 4).

Few intraoperative and postoperative complications occurred. Intraoperatively, in the hemiarthroplasty revision patient, a lateral cortex blow-out occurred while removing the stem. Another patient developed a superficial infection 3 weeks after surgery. Surgical debridement was done. The other two patients in the posttraumatic sequelae group got axillary nerve palsy as proved by postoperative electrophysiological studies. During regular outpatient follow-up visits, one of them regained axillary nerve functions 2 months after surgery without any further interventions. The other patient needed axillary neurotization from the radial nerve branch to the medial head of the triceps. He regained satisfactory functional outcomes 6 months later.

Discussion

We successfully improved the postoperative outcomes of all our recruited patients regarding the range of movement, pain, and functional scores following RTSA. Nevertheless, we found no statistically significant difference in the outcomes of patients in terms of the onset of injury (acute fracture versus post-traumatic sequelae).

Treatment for acute proximal humeral fractures has been extensively described in the literature, and RSA has been proposed as a surgical option for acute

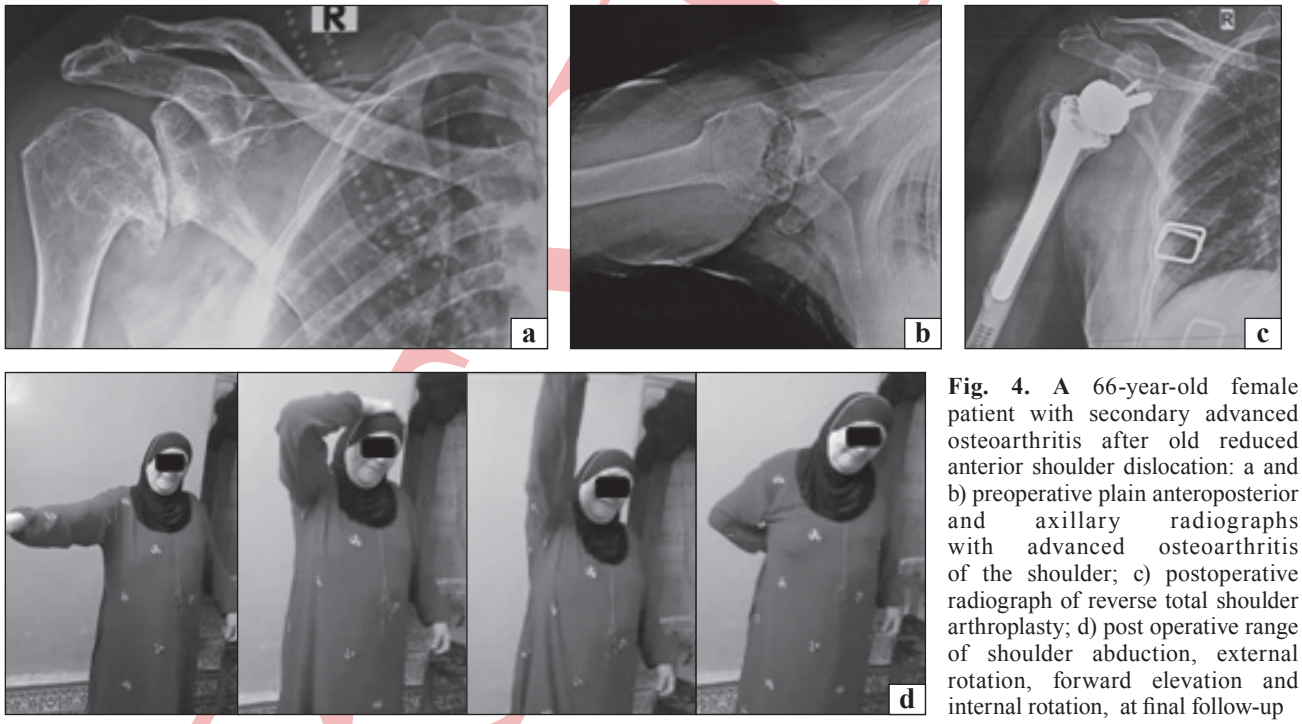

Fig. 4. A 66-year-old female patient with secondary advanced osteoarthritis after old reduced anterior shoulder dislocation: a and b) preoperative plain anteroposterior and axillary radiographs with advanced osteoarthritis of the shoulder; c) postoperative radiograph of reverse total shoulder arthroplasty; d) post operative range of shoulder abduction, external rotation, forward elevation and internal rotation, at final follow-up

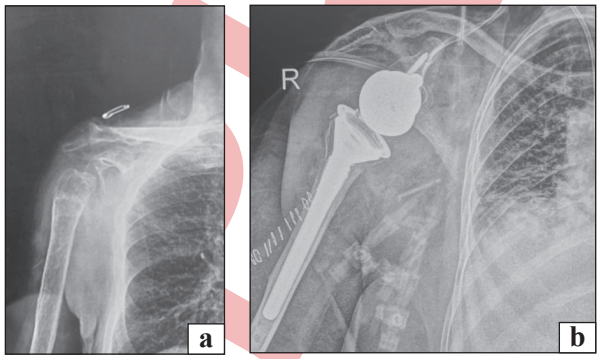

Fig. 5. A 55-year-old male patient with a fracture malunion of the anatomical neck of his right humerus: a) preoperative plain radiograph of the fracture; b) postoperative radiograph of reverse total shoulder arthroplasty

Table 4

Distribution of the deltoid muscle power and function domains of the Constant score at 6, 12 24, and 48 weeks after surgery in both groups

	Group I (n = 10)	Group II (n = 10)	P value
	Mean (±SD) Range		
Power			
6 weeks	0.60 (± 0.69) (0–2)	0.20 (± 0.42) (0–1)	0.142
12 weeks	5.70 (± 3.05) (2–11)	6.10 (± 2.60) (2–10)	0.756
24 weeks	16.20 (± 6.54) (4–22)	16.50 (± 5.23) (7–23)	0.911
48 weeks	17.00 (± 5.61) (7–22)	17.40 (± 4.62) (9–23)	0.864
Function			
6 weeks	1.30 (± 1.15) (0–4)	1.00 (± 0.47) (0–2)	0.463
12 weeks	7.20 (± 2.14) (0–4)	7.20 (± 1.31) (5–9)	1.000
24 weeks	13.40 (± 3.13) (8–18)	13.70 (± 2.54) (10–17)	0.817
48 weeks	14.50 (± 2.71) (10–18)	14.80 (± 2.25) (11–18)	0.791

Notes: Quantitative data are expressed in mean+SD and range. * $p < 0.05$: statistically significant.

complex fractures in elderly patients 1, 2, 12, 13. However, the treatment of the post-traumatic sequelae is a challenge for the surgeon and the literature on this topic is limited.

Sebastia-Forcada conducted a matched case-control study designed to investigate the outcomes of secondary RSA after failed internal fixation for proximal humeral fractures. They found that at the 2-year follow-up, the mean clinical scores in the sequelae group were significantly lower than in the acute group although the differences were not clinically relevant. This was similar to our findings but at the 6-week follow-up, because in the following periods in our study, the post-traumatic group showed better scores and clinical outcomes.

In the sequelae group in Sebastia-Forcada's study, the Constant and DASH scores significantly improved from preoperative to postoperative. At the 2-year follow-up, all the patients except one achieved improvement in the range of motion. While one patient had anterior forward and abduction less than 90 degrees. At the last follow-up, 28 patients (93.3 %) were satisfied with the results of their RSA, and 2 were dissatisfied. They also reported that there were no significant differences in postoperative pain, motion, or ability for activities of daily living in the subgroup of patients younger than 70 years in comparison to those older than [14].

Paszicsnyek et al carried out a matched cohort analysis study which included a group of patients suffering from acute and post-traumatic sequelae. In that study, they performed a subgroup analysis of the fracture group to examine the difference in range of motion and outcome scores. Like our results, they found no significant difference, despite detecting a general tendency towards superior outcome scores for the acute fracture [15].

Although previous studies reported worse outcomes and higher complication rates have been reported after arthroplasties for fracture sequelae compared with arthroplasties for acute fractures like the study by Nikola et al who included 40 patients in their study, who were treated with reverse shoulder arthroplasty for sequelae of proximal humeral fracture and acute fracture [16].

As our results, Nikola et al results showed that a group of patients treated with RSA without previous surgery in comparison with patients treated with RSA after previous surgery had better functional results. Where the external rotation was 24°, active elevation was 102°, and internal rotation was up to L4 in all patients. In patients without previous surgery treated with RSA, elevation was 116°, external rotation 24°, internal rotation up to L3. In patients with previous surgery treated with RSA, elevation was 84°, external rotation 19°, internal rotation up to L4. These findings are not statistically significant [16].

In their patients with acute fracture treated with RSA elevation was 124°, external rotation 28°, internal rotation up to L4. In patients with chronic or sequelae of the fractures treated with RSA elevation was 114°, external rotation 28°, internal rotation up to L3. They also reported that the differences between these two groups are not significant. Our patients too had an external rotation of 26.80° and internal rotation of 39.70° after 12 weeks in the acute fracture group, while in group II, we found decreased ranges, where the mean external rotation was 22.6° and the mean internal rotation was 38.1°.

The constant score in all their patients was 54. The constant score in patients without previous surgery treated with RSA was 68 and with previous surgery was 42. This was similar to our findings, where the mean constant score in group II was 62.70 after 1 year, but in group I our patients had a better score than that reported by Nikola et al [16].

Despite the differences in the functional and clinical outcomes between both groups, whether in our study or previous studies, are statistically insignifi-

cant, the better outcome in the acute fracture group could be attributed to the bone quality and muscle balance of the patients in the post-traumatic sequelae. Previously surgically treated patients had scar tissue, shortening of the soft tissue and malunion bone abnormalities. Furthermore, it is elaborated that functional results are better if tuberosities of the humerus are preserved [12–16].

This study was a prospective comparative study which represented a strength along with using objective and subjective measures for assessment of patients' outcomes. Additionally, no patients were lost to follow-up. The equal distribution of males and females across both our study groups represented a major strength by reducing the possible bias that could be attributed to the influence of gender on postoperative outcomes.

Nevertheless, our study used a small sample size which represents a limitation. Therefore, future research including larger sample sizes and extended follow-up periods is necessary to better define the indications for surgery and RTSA in PHFs.

Conclusion

Reverse shoulder arthroplasty provides favorable post-operative outcomes among elderly patients suffering from acute 3-part, and 4-part fractures of the proximal humerus. Furthermore, the indication for RTSA will not be affected by whether patients are suffering from acute or post-traumatic sequelae fractures.

All ranges of motion were similarly improved in both groups. The mean DASH score dropped from 88.3 and 91 preoperatively to 34.3 and 35.8 at final follow-up, in groups I and II, respectively. The VAS score decreased from 5.9 and 5.8 in groups I and II, respectively, to less than one, indicating improvement in pain after surgery. The Constant-Murley score increased from 14.7 and 16 to 67.3 and 62.7 in groups I and II, respectively, indicating similar restoration of satisfactory function. A few complications occurred in 4 patients of group II including superficial infection, axillary nerve palsy and lateral cortex blow-out.

Conflict of interest. All authors, their immediate family, and any research foundation with which they are affiliated did not receive any financial payments or other benefits from any commercial entity related to the subject of this article.

References

1. Kim, M., Smolev, E., Al-Humadi, S., Tantone, R. P., Park, H., Ling, K., … Wang, E. D. (2024). Predictors of extended length of stay following open reduction and internal fixation for proximal humerus fractures. *Journal of hand surgery global online, 6*(2), 195–199. https://doi.org/10.1016/j.jhsg.2023.11.013
2. Baker, H. P., Gutbrod, J., Strelzow, J. A., Maassen, N. H., & Shi, L. (2022). Management of proximal humerus fractures in adults — A scoping review. *Journal of clinical medicine, 11*(20), 6140. https://doi.org/10.3390/jcm11206140
3. Orman, S., Mohamadi, A., Serino, J., Murphy, J., Hanna, P., Weaver, M. J., … Keudell, A. V. (2019). Comparison of surgical and non-surgical treatments for 3- and 4-part proximal humerus fractures: A network meta-analysis. *Shoulder & Elbow, 12*(2), 99–108. https://doi.org/10.1177/1758573219831506
4. Best, M. J., Aziz, K. T., Wilckens, J. H., McFarland, E. G., & Srikumaran, U. (2021). Increasing incidence of primary reverse and anatomic total shoulder arthroplasty in the United States. *Journal of shoulder and elbow surgery, 30*(5), 1159–1166. https://doi.org/10.1016/j.jse.2020.08.010
5. Kiper, P., Rimini, D., Falla, D., Baba, A., Rutkowski, S., Maistrello, L., & Turolla, A. (2021). Does the score on the MRC strength scale reflect instrumented measures of maximal torque and muscle activity in post-stroke survivors? *Sensors, 21*(24), 8175. https://doi.org/10.3390/s21248175
6. Walch, G., Collotte, P., Raiss, P., Athwal, G. S., & Gauci, M. O. (2020). The characteristics of the Favard E4 glenoid morphology in cuff tear arthropathy: A CT study. *Journal of clinical medicine, 9*(11), 3704. https://doi.org/10.3390/jcm9113704
7. Walter, N., Szymski, D., Kurtz, S. M., Lowenberg, D. W., Alt, V., Lau, E., & Rupp, M. (2023). Proximal humerus fractures – epidemiology, comparison of mortality rates after surgical versus non-surgical treatment, and analysis of risk factors based on Medicare registry data. *Bone & joint research, 12*(2), 103–112. https://doi.org/10.1302/2046-3758.122.bjr-2022-0275.r1
8. Makki, D., Balbisi, B., Arshad, M. S., Monga, P., Bale, S., Trail, I., & Walton, M. (2021). Assessing the required glenoid peg penetration in native scapula when bone Graft is used during primary and revision shoulder arthroplasty. *Shoulder & Elbow, 14*(3), 268–276. https://doi.org/10.1177/1758573220987557
9. Keller, D. M., Saad, B. N., Hong, I. S., Gencarelli, P., Tang, A., Jankowski, J. M., Liporace, F. A., & Yoon, R. S. (2023). Comparison of outcomes after reverse total shoulder arthroplasty in patients with proximal humerus fractures versus rotator cuff arthropathy. *JAAOS: Global Research and Reviews, 7*(10). https://doi.org/10.5435/jaaosglobal-d-23-00160
10. Lu, V., Jegatheesan, V., Patel, D., & Domos, P. (2023). Outcomes of acute vs. delayed reverse shoulder arthroplasty for proximal humerus fractures in the elderly: A systematic review and meta-analysis. *Journal of shoulder and elbow surgery, 32*(8), 1728–1739. https://doi.org/10.1016/j.jse.2023.03.006
11. Barger, J., Stenquist, D. S., Mohamadi, A., Weaver, M. J., Dyer, G. S., & Von Keudell, A. (2021). Acute versus delayed reverse total shoulder arthroplasty for the management of proximal humerus fractures. *Injury, 52*(8), 2272–2278. https://doi.org/10.1016/j.injury.2021.05.040
12. Mayfield, C. K., Liu, K. C., Hwang, N. M., Bolia, I. K., Gamradt, S. C., Weber, A. E., Liu, J. N., & Petrigliano, F. A. (2024). Reverse total shoulder arthroplasty for proximal humerus fracture: A complex episode of care associated with increased surgical and medical complications. *Seminars in arthroplasty: JSES, 34*(2), 313–320. https://doi.org/10.1053/j.sart.2023.12.002
13. Bolam, S. M., Wells, Z., Tay, M. L., Frampton, C. M., Coleman, B., & Dalgleish, A. (2024). Reverse total shoulder arthroplasty for acute proximal humeral fracture has comparable 10-year outcomes to elective indications: Results from the New Zealand joint registry. *Journal of shoulder and elbow surgery, 33*(9), 1946–1954. https://doi.org/10.1016/j.jse.2024.01.024
14. Sebastia-Forcada, E., Lizaur-Utrilla, A., Cebrian-Gomez, R., Miralles-Muñoz, F. A., & Lopez-Prats, F. A. (2017). Outcomes

of reverse total shoulder arthroplasty for proximal humeral fractures: Primary arthroplasty versus secondary arthroplasty after failed proximal humeral locking plate fixation. *Journal of orthopaedic trauma, 31*(8), e236–e240. https://doi.org/10.1097/bot.0000000000000858

15. Paszicsnyek, A., Kriechling, P., Razaeian, S., Ernstbrunner, L., Wieser, K., & Borbas, P. (2023). Reverse total shoulder arthroplasty for proximal humeral fractures and Sequalae compared to non-fracture indications: A matched cohort analysis of outcome and complications. *Journal of clinical medicine, 12*(6), 2097. https://doi.org/10.3390/jcm12062097
16. Nikola, C., Hrvoje, K., & Nenad, M. (2014). Reverse shoulder arthroplasty in acute fractures provides better results than in revision procedures for fracture sequelae. *International orthopaedics, 39*(2), 343–348. https://doi.org/10.1007/s00264-014-2649-7

The article has been sent to the editors	Received after review	Accepted for printing
17.07.2024	15.10.2024	27.11.2025

FUNCTIONAL OUTCOMES OF REVERSE TOTAL SHOULDER ARTHROPLASTY IN ACUTE PROXIMAL HUMERAL FRACTURES VERSUS POST-TRAUMATIC SEQUELAE

Ahmed Adel Abdelaty Abdo [1], Tarek Abdelaziz [1], Mohamed Omar Soliman [2], Mohamed Ibrahim Rakha [1], Asser Abdelhay Sallam [3]

[1] Department of Orthopedic Surgery and Trauma, Suez Canal University, Ismailia. Egypt
[2] Department of Orthopedic Surgery and Trauma, Cairo University. Egypt
[3] Department of Orthopedic Surgery and Trauma, Suez University. Egypt

✉ Ahmed Adel Abdelaty Abdo, MSC: ahmedozadeloz2013@gmail.com; https://orcid.org/0000-0003-0407-0340
✉ Tarek Abdelaziz, MD: tareksh64@yahoo.com; https://orcid.org/0009-0001-3230-0791
✉ Mohamed Omar Soliman, MD: omarsoli@hotmail.com; https://orcid.org/0009-0006-0797-0255
✉ Mohamed Ibrahim Rakha, MD: mohrakha2005@gmail.com; https://orcid.org/0000-0002-9225-7393
✉ Asser Abdelhay Sallam, MD, PhD: assersallam@hotmail.com; https://orcid.org/0000-0002-0936-8296

УДК 616.711-001.5-073.763.5(045)

DOI: http://dx.doi.org/10.15674/0030-59872026143-52

Radiographic morphometric prediction of new vertebral compression fractures after vertebroplasty

A. I. Popov [1], M. V. Moloduk [1], V. O. Kutsenko [1], R. V. Zlatnik [1], M. M. Nessonova [2]

[1] Sytenko Institute of Spine and Joint Pathology National Academy of Medical Sciences of Ukraine, Kharkiv
[2] Private higher educational institution «Kharkiv International Medical University». Ukraine

New vertebral compression fractures (NVCF) following percutaneous vertebroplasty (PVP) remain a clinical challenge. Methods. A retrospective cohort study (2023–2025) was conducted at the Institute of Spine and Joint Pathology, Ukraine, involving 26 patients (24 females, 2 males; mean age (69.04 ± 2.04) years) with osteoporotic vertebral compression fractures treated with PVP. Morphometric parameters of 99 vertebrae were assessed on digital radiographs (frontal/sagittal, RadiAnt DICOM Viewer, precision 0.1 mm / 0.1°): anterior (h_a), middle (h_m), posterior (h_p) heights, relative compression (%), wedge index, local kyphotic angle, thoracic kyphosis, lumbar lordosis, and scoliosis. Results. NVCF occurred in 46.2 % of cases (45 fractures in 12 patients). Significant differences between NVCF and non-NVCF groups were observed for ha compression (20.69 ± 1.16 mm vs. 23.89 ± 0.78 mm, p = 0.0338), h_m (17.84 ± 1 mm vs. 21.31 ± 0.61 mm, p = 0.0021), h_p (26.97 ± 0.81 mm vs. 29.61 ± 0.51 mm, p = 0.0073), lumbar lordosis (44,4° ± 1,52° vs. 38.28° ± 1.46°, p = 0.01), and scoliosis (7.53° ± 0.56° vs. 5.90° ± 0.48°, p = 0.022). The linear discriminant functions model, based on h_m (canonical correlation = –0.863) and relative H_a compression (canonical correlation = 0.139), achieved Wilks' Λ = 0.8 (χ^2 = 15.77, p = 0.000376), classification accuracy of 76.25 % (sensitivity 76.9 %, specificity 75.9 %), and AUC = 0,754 ± 0,058. Adjusted function: F = 6,07 – 0,28×h_m (mm) –0,035×H_a (%); F > 0 indicates NVCF risk. Other parameters were excluded due to low discriminatory power or collinearity. Conclusion. This two-parameter model, using hm and relative Ha compression, offers moderate predictive accuracy for NVCF post-PVP. Its simplicity suits resource-limited Ukrainian clinics. External validation and inclusion of confounders (e. g., BMD, therapy) are required for broader adoption.

Нові компресійні переломи хребців (НКПХ) після пункційної вертебропластики (ПВП) є серйозною проблемою вертебрології. Методи. У ретроспективне когортне дослідження (2022–2023 р.) включено 26 пацієнтів (24 жінки, 2 чоловіки; середній вік (69,04 ± 2,04) роки) з остеопоротичними компресійними переломами хребців, яким виконувалася ПВП. Вивчено морфометричні параметри 99 хребців на цифрових рентгенограмах: висоти h_a (передня), h_m (середня), h_p (задня), відносна компресія H_a, H_m, H_p (%), ІК, локальний кіфотичний кут, грудний кіфоз, поперековий лордоз, сколіоз. Результати. Частота НКПХ склала 46,2 % (45 переломів у 12 пацієнтів). Значущі відмінності між групами з/без НКПХ виявлено для висоти h_a (20,69 ± 1,16 проти (23,89 ± 0,78) мм, p = 0,0338), h_m (17,84 ± 1 проти (21,31 ± 0,61) мм, p = 0,0021), h_p (26,97 ± 0,81 проти (29,61 ± 0,51) мм, p = 0,0073), поперекового лордозу (44,4° ± 1,52° проти 38,28° ± 1,46°, p = 0,01) та сколіозу (7,53° ± 0,56° проти 5,90° ± 0,48°, p = 0,022). Дискримінантна модель, яка базується на h_m (канонічна кореляція = –0,863) та відносній компресії H_a (канонічна кореляція = 0,139), мала Λ Уїлкса = 0,8 (χ^2 = 15,77, p = 0,000376), точність класифікації 76,25 % (чутливість 76,9 %, специфічність 75,9 %), AUC = 0,754 ± 0,058. Спрощена функція: F = 6,07–0,28×h_m (мм)–0,035×H_a (%); F > 0 свідчить про ризик НКПХ. Інші параметри виключено через низьку дискримінаційну цінність або колінеарність. Розроблено веб застосунок для прогнозування НКПХ. Висновки. Двопараметрична модель на основі висоти h_m та відносної компресії H_a забезпечує помірну прогностичну точність для виявлення ризику НКПХ після ПВП. Простота моделі робить її придатною для клінік із обмеженими ресурсами. Для впровадження потрібна зовнішня валідація та врахування додаткових чинників (мінеральна щільність кісткової тканини, терапія). Ключові слова. Пункційна вертебропластика, нові компресійні переломи, рентгеноморфометрія, дискримінантний аналіз, остеопороз.

Keywords. Percutaneous vertebroplasty, new vertebral compression fractures, radiographic morphometry, discriminant functions analysis, osteoporosis

Introduction

Percutaneous vertebroplasty (PVP) is the gold standard for minimally invasive treatment of osteoporotic vertebral compression fractures (VCFs), providing rapid pain relief, stabilization of the affected segment, and early restoration of functional activity in patients [1]. According to data from the U.S. and European registries, more than 300,000 PVP procedures are performed annually, with clinical effectiveness reaching 85-95% in the short term [2, 3].

However, the long-term outcomes of PVP are complicated by the development of new compression fractures (NCFs), which poses a significant clinical problem in modern vertebrology. Recent data from 2024-2025 shows that the frequency of symptomatic re-interventions after PVP ranges from 14.6 % to 22.2 % within 1-2 years of follow-up [4, 5]. A large cohort study of over 30,000 patients demonstrated that 15.5 % of cases required re-intervention within 24 months after the primary PVP procedure [4].

Radiomorphometric analysis remains the foundational method for assessing radiomorphometric parameters (RMP) of vertebrae and the degree of compression. Classical parameters proposed by H.K. Genant et al. include absolute and relative compression, wedge index, and the ratio of the anterior and posterior heights of the vertebrae [5]. The advantages of this approach include accessibility for hospitals with limited resources and the standardization of measurements [6].

Modern automated morphometric analysis systems based on artificial intelligence allow for the generalization of measurements and reduce inter-operator variability to less than 5% [7]. Y. Yang and colleagues demonstrated that MRI texture analysis combined with morphometric parameters achieves an AUC ≈ 0.80 for predicting the risk of fractures in patients with osteoporosis [8].

Multivariate discriminant analysis (MDA) is a classical statistical method for classification and prediction, widely used in medical research. Unlike complex machine learning algorithms, it provides transparency in mathematical calculations and ease of interpretation of results [9]. This method is especially effective when working with small samples and a limited number of parameters, making it useful in clinical practice [10].

Despite progress in the development of prognostic models for NCFs, most existing approaches are complex and require significant resources for implementation. It is important to note that there is little information regarding research on Ukrainian patients.

The development of a simple yet effective predictive model based on RMP that can be easily integrated into routine clinical practice in Ukrainian medical institutions is a relevant task.

Purpose. To identify the prognostic radiomorphometric parameters of vertebrae after percutaneous vertebroplasty that may be associated with the risk of developing new vertebral compression fractures and to develop a model for predicting these fractures.

Materials and methods

The study was reviewed and approved by the Ethics and Deontology Committee of the Professor M. I. Sytenko Institute of Spine and Joint Pathology of the National Academy of Medical Sciences of Ukraine (protocol No. 260 dated 23.02.2026). All patients provided written consent for examination, treatment, and the use of medical data for scientific research.

This was a retrospective cohort study conducted at the Vertebrology Department of the Professor M. I. Sytenko Institute of Spine and Joint Pathology of the National Academy of Medical Sciences of Ukraine, from 2022 to 2023. The sample size consisted of 26 patients (24 women, 2 men; mean age (69.04 ± 2.04) years, range 46–85) who underwent PVP due to VCFs as a result of osteoporosis. The diagnosis of "osteoporosis" was confirmed using dual-energy X-ray absorptiometry on the bone densitometer Explorer QDR W. The average follow-up period was 12 months, with NCFs diagnosed during follow-up visits at 1, 3, 6, and 12 months after PVP. In the studied cohort, 12 (46.2 ± 9.8) % of cases were verified with a total of 45 NCFs in the thoracic and lumbar regions of the spine.

Radiomorphometric parameters (RMP) of 99 treated vertebrae in the thoracic and lumbar spine were studied. Inclusion criteria: patients who underwent PVP for VCFs due to osteoporosis. Exclusion criteria: PVP due to malignant or traumatic fractures.

In a previous publication, we established that low bone mineral density (BMD), lack of anti-osteoporotic therapy, and advanced age increased the risk of developing NCFs by two times, and cement leakage almost tripled the risk [11]. Given this, these factors were not included in the study.

Radiomorphometric study

The analysis of RMP was based on digital radiographs of the thoracic and lumbar spine obtained in two standard projections: frontal and sagittal. Radiographs were taken in a standing position (or lying down for patients with limited mobility). Radiographs

were obtained at three stages: before PVP, immediately after the procedure, and during follow-up visits (1, 3, 6, and 12 months). Only radiographs after PVP were included in the analysis. The image resolution met clinical standards (0.1–0.2 mm/pixel), ensuring the accuracy of measurements.

Image quality criteria: clear visualization of the endplate contours; symmetrical depiction of spinous processes (deviation < 5 mm); absence of rib overlap artifacts on vertebral bodies and motion artifacts; contrast allowing differentiation of cortical and trabecular bone structures.

RMP measurements were performed using RadiAnt DICOM Viewer software (version 2023.1), which allowed for linear and angular measurements with an accuracy of up to 0.1 mm and 0.1°. Below is a detailed description of the measured parameters.

Vertebral height (h_a, h_m, h_p). Measurements were performed on both the vertebrae after PVP and the intact ones. The latter were used as reference values for calculating the percentage of compression according to the method of H. K. Genant et al., which allowed standardization of measurements across patients [5].

The upper and lower endplates of the vertebra were identified on the sagittal radiograph. Heights were measured as vertical distances between the corresponding points:

– h_a (anterior height) — from the anterior edge of the cranial endplate to the anterior edge of the caudal endplate;

– h_m (middle height) — in the middle of the vertebra (medial part);

– h_p (posterior height) — from the posterior edge of the cranial endplate to the posterior edge of the caudal endplate.

To normalize the height, it was compared with the corresponding values of the neighboring intact vertebra.

Relative compression (%) was determined as the percentage of height loss relative to the reference.

$$H_a(\%) = \left(\frac{h_{a\{\text{сусіднього}\}} - h_{a\{\text{ушкодженого}\}}}{h_{a\{\text{сусіднього}\}}}\right) \times 100, \quad (1)$$

For example, the relative compression of ha was calculated using the formula (1):
where h_a(neighboring) — anterior height of the intact vertebra body (mm); h_a(injured) — anterior height of the vertebral body after PVP (mm).

Similarly, the percentage of relative compression was determined for H_m and H_p.

Wedge index (WI) (%). To determine the wedge shape of the vertebrae, radiographs in the sagittal

$$IK = \frac{h_a}{h_p} \times 100. \quad (2)$$

projection were used. The height ha and hp were measured. The WI was calculated using the formula (2):

The results are expressed as percentages, where WI < 80 % indicates a wedge-shaped deformation.

The *local kyphotic angle* was measured as the Cobb angle formed between the line perpendicular to the cranial endplate of the neighboring proximal vertebra and the line perpendicular to the caudal endplate of the neighboring distal vertebra on the sagittal radiograph.

Thoracic kyphosis was evaluated as the Cobb angle between the cranial endplate of T_{IV} and the caudal endplate of T_{XII} on the sagittal projection.

Lumbar lordosis was measured between the cranial endplate of L_I and the caudal endplate of L_V.

Scoliosis was defined as the Cobb angle between the perpendicular lines to the cranial and caudal endplates of the most tilted vertebrae in the curve on the frontal projection.

Statistical data analysis was performed using the Statistica 13 software. The Shapiro-Wilk test was used to check the normality of the distribution of the variables. For paired comparisons of groups, depending on the presence of a new fracture, the Mann-Whitney non-parametric test was applied. Differences were considered statistically significant at a significance level of $p < 0.05$.

DA was employed in the development of a mathematical model for predicting NCFs. The quality of the constructed model was evaluated using ROC analysis through the web tool easyROC 1.3.1.

For the practical application of the developed NCF prediction model, a web application “Fracture Risk Calculator” has been created. The application is implemented using HTML, CSS, and JavaScript technologies and is available as a standalone web page, which can be integrated into medical institutions' systems. The user interface includes fields for entering values of hm and Ha, a button to calculate, and a section to display the results.

Results

The study of the distribution law of indicators using the Shapiro-Wilk test showed that only half of them were correct. Since the most clinically significant data, such as WI, as well as h_a, h_m, and h_p, had a normal distribution, for descriptive statistics, in addition to medians (Me) and interquartile intervals ([LQ; UQ]), mean values (M) and standard errors of the means (m) were also used (Table 1).

Statistically significant differences between groups were observed only for the vertebral height indicators, which were higher in the group without NCF, and for the Cobb angles, which were used to assess scoliosis and lumbar lordosis. In patients with NCF, significantly higher angles of scoliosis and lumbar lordosis were recorded compared to those without NCF (Table 1, Figure 1).

During the construction of the NCF prediction model, RMP data after PVP for 80 observations were considered. The development of the NCF prediction model was carried out using DA. Since there were only two groups in the data (NCF present/absent), DA was reduced to obtaining a single discriminant function (DF) and two classification functions (CF).

All 12 indicators after PVP were selected for analysis. Then, through stepwise removal (Backward stepwise), only significant indicators for classification were retained. As a result, only two values — vertebral height h_m and relative compression H_a — showed a statistically significant contribution to classifying the groups with or without NCF. The remaining

Table 1

Descriptive statistics for the compared groups with and without new compression fractures

Indicator	NCFs						p (Mann-Whitney test)
	absent			present			
	n	Me [LQ; UQ]	M ± m	n	Me [LQ; UQ]	M ± m	
1	2	3	4	5	6	7	8
Age, years	14	67.5 [59.0; 76.0]	67.7 ± 3.2	12	74.0 [63.0;78.5]	70.60 ± 2.50	0.462000
Thoracic kyphosis, degrees	21	52.50 [26.20; 64.00]	44.62 ± 5.01	21	45.00 [44.90;56.00]	50.00 ± 3.02	0.900980
*Lumbar lordosis, degrees	33	38.70 [34.90; 43.20]	38.28 ± 1.46	40	43.00 [40.00;45.30]	44.4 ± 1.52	0.009467
*Scoliosis, degrees (all data)	49	5.50 [2.90; 7.40]	5.90 ± 0.48	41	7.50 [5.50;10.70]	7.53 ± 0.56	0.0219400
– thoracic spine,	21	5.30 [4.00; 6.00]	5.49 ± 0.60	23	7,00 [4.50;8.60]	6.69 ± 0.71	0.111589
– lumbar spine,	28	5.75 [2.80; 8.40]	6.21 ± 0.70	18	9.10 [5.60;12.70]	8.61 ± 0.85	0.073117
Local kyphotic angle, degrees (all data)	53	14.30 [8.90; 20.70]	14.71 ± 1.07	17	18.35 [8.80;26.80]	18.00 ± 1.74	0.156685
– *thoracic spine,	22	16.20 [7.90; 19.30]	15.69 ± 1.76	22	20.50 [13.80;27.10]	20.75 ± 1.86	0.035627
– lumbar spine,	31	13.60 [8.90; 20.70]	14.02 ± 1.35	18	12.25 [3.40;25.90]	14.66 ± 3.01	0.787415
Wedge index, % (all data)	54	81.5 [69.0; 93.0]	80.5 ± 2.18	41	75.0 [62.0;90.0]	74.98 ± 3.15	0.155460
– thoracic spine,	22	79.0 [67.0; 85.0]	76.55 ± 3.08	23	72.0 [59.0;79.0]	69.00 ± 0.04	0.059404
– lumbar spine,	32	86.0 [69.5; 96.5]	83.22 ± 2.95	18	86.0 [72.0;97.0]	82.61 ± 0.045	0.935539
*Height h_a, mm (all data)	54	24.75 [19.00; 28.10]	23.89 ± 0.78	41	20.60 [16.50;25.90]	20.69 ± 1.16	0.033767
– *h_a (thoracic spine),	22	21.30 [17.90; 24.10]	21.00 ± 1.03	23	17.70 [15.30;22.00]	17.31 ± 1.19	0.030085
– h_a (lumbar spine),	32	27.20 [20.75; 29.85]	25.87 ± 0.98	18	26.10 [19.80;30.70]	25.01 ± 1.72	0.959696
*Height h_m, mm (all data)	54	21.35 [17.90; 24.50]	21.31 ± 0.61	41	17.90 [13.80;21.40]	17.84 ± 0.99	0.002063
– h_m (thoracic spine),	22	18.50 [17.30; 21.60]	18.97 ± 0.87	23	17.40 [13.30;19.10]	15.67 ± 0.99	0.035650
– h_m (lumbar spine),	32	22.65 [20.35;25.35]	22.92 ± 0.71	18	20.80 [15.20;25.20]	20.62 ± 1.67	0.959696

Continuation of table 1

1	2	3	4	5	6	7	8
*Height h_p, mm (all data)	54	30.50 [27.60; 32.30]	29.61 ± 0.51	41	27.70 [23.00;30.60]	26.97 ± 0.81	0.007302
– h_p (thoracic spine),	22	28.20 [24.60; 29.90]	27.33 ± 0.70	23	24.40 [21.80;28.00]	24.77 ± 1.05	0.044426
– h_p (lumbar spine),	32	31.50 [30.25; 33.35]	31.175 ± 0.58	18	30.00 [28.10;31.30]	29.78 ± 0.93	0.101509
Relative compression H_a, % (all data)	54	14.13 [5.00; 27.83]	17.46 ± 2.34	28	20.64 [7.65;35.48]	26.18 ± 5.55	0.275572
– H_a (thoracic spine),	22	6.96 [2.17; 23.75]	11.59 ± 3.69	20	20.64 [5.68;29.09]	22.38 ± 6.10	0.186093
– H_a (lumbar spine),	32	15.54 [11.09; 33.05]	21.49 ± 2.85	8	23.98 [10.43;54.78]	35.67 ± 12.09	0.576908
Relative compression H_m, % (all data)	54	30.00 [20.83; 41.32]	30.91 ± 1.96	28	35.38 [26.74;50.84]	40.72 ± 4.52	0.105574
– H_m (thoracic spine),	22	25.625 [18.85; 44.17]	27.56 ± 3.48	20	34.32 [28.03;46.66]	37.40 ± 5.04	0.137297
– H_m (lumbar spine),	32	34.08 25.07; 40.80]	33.21 ± 2.25	8	44.91 [25.72;63.16]	49.03 ± 9.48	0.170852
Relative compression H_p, % (all data)	54	9.37 [4.78; 18.42]	11.75 ± 1.26	28	7.04 [3.27;17.28]	16.65 ± 4.86	0.567286
– H_p (thoracic spine),	22	6.49 [2.11; 9.60]	7.05 ± 1.44	20	4.91 [2.35;13.86]	11.98 ± 4.94	0.969866
– H_p (lumbar spine),	32	15.78 [7.12; 20.27]	14.99 ± 1.68	8	19.095 [7.22;35.15]	28.30 ± 11.20	0.370213

Notes: n — number of observations (age data, vertebral fractures in relation to other indicators); * — statistically significant differences between groups depending on the presence of NCFs.

indicators were excluded from the model due to insufficient discriminatory ability, which may be caused, for example, by either the lack of significant variability of the indicator between groups or a high level of correlation with other variables.

When evaluating the statistical significance of the obtained DF using the approximation of the distribution by the χ^2 function from the Wilks' Λ-statistic, a p-value of 0.000376 was obtained for $\Lambda = 0.8$ and $\chi^2 = 15.77$, indicating its significance.

The contribution of each of the two indicators to the classification can be judged by the magnitude of the factor structure coefficients (Table 2): the largest is hm, with a canonical correlation between the indicator and DF of –0.863.

For classifying observations into groups (NCF present/absent after PVP), the following CFs were obtained:

$$F_{absent} = -23.22 + 1.83 \times h_m + 0.32 \times H_a, \quad (3)$$

$$F_{present} = -17.05 + 1.55 \times h_m + 0.28 \times H_a. \quad (4)$$

According to the classical scheme of using DA models, observations are assigned to the group for which the larger value of CF is obtained. However, in the case of only two classes, it is obviously more appropriate to consider the difference between the two CFs.

In our case:

$$\Delta F = F_{present} - F_{absent} = 6.17 - 0.28 \times h_m - 0.035 \times H_a. \quad (5)$$

If ΔF is greater than 0, a new compression fracture is likely to occur; if ΔF is less than 0, it is unlikely to happen. The results of the posterior classification (Table 3) indicate a fairly good adequacy of the developed model, which is also confirmed by the corresponding estimates of the area under its ROC curve: AUC = 0.754 with a 95 % CI ranging from 0.640 to 0.867 (Figure 2).

The optimal threshold value obtained from the ROC analysis for the developed model allowed increasing the overall accuracy of prediction from 73.75 % to 76.25 %, by increasing its specificity (accuracy of determining the absence of a new compression fracture) to 75.9 % (95 % CI from 62.4 to 86.5 %), without changing the sufficiently high sensitivity, which remained at 76.9 % with a 95 % CI from 56.4 to 91.0 % (Figure 2). Therefore, the formula for

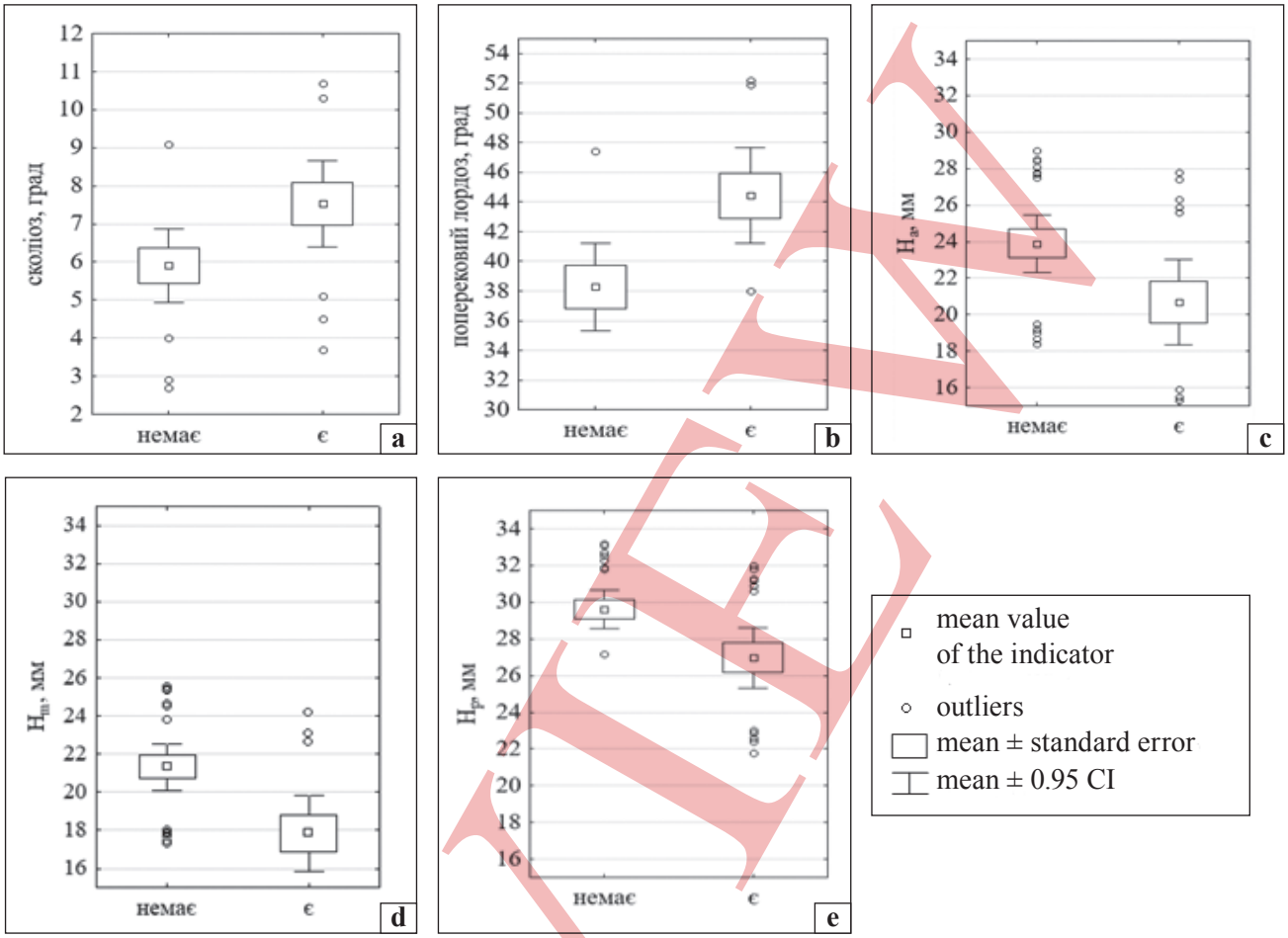

Fig. 1. Box plots of some indicators after PVP (NCF)

Table 2

Factor structure coefficients for the built discriminant analysis model of predicting NCFs

Indicator	Canonical correlation between the indicator and DF
Height h_m, мм	–0.863
Relative compression H_a, %	0.139

predicting a new compression fracture, adjusted for the optimal cutoff threshold, looks as follows:

$$\Delta F = 6.07 - 0.28 \times h_m - 0.035 \times H_a. \quad (6).$$

As before, the absence of an NCPF corresponds to $\Delta F < 0$, and its presence corresponds to $\Delta F > 0$.

Since in our study only two groups were classified using two explanatory variables, it is quite easy to visualize the discrimination of observations on a two-dimensional scatter plot (Figure 3), where the line corresponds to the discriminant function.

The developed web application "Fracture Risk Calculator" successfully implements the discriminant model for predicting NCPF using the RMPs h_m and H_a (Figure 4). Testing the application on a sample of 80 observations showed that it correctly reproduces the results of the discriminant analysis, providing a classification accuracy of 76.25 %. A $\Delta F > 0$ indicates the risk of NCPF, while $\Delta F \leq 0$ indicates its absence.

Discussion

This study is the first attempt to develop a predictive model for the risk of NCPF after PVF in the Ukrainian population based on RMPs. The obtained results demonstrate both the potential and the limitations of the simplified two-parameter approach to predicting NCPF.

Within the conducted analysis, statistically significant differences in the RMPs of vertebrae after PVF were found between patients with and without the development of NCPF. At the same time, it is crucial to emphasize that morphometric characteristics are not the direct cause of new compression fractures of the vertebrae; they reflect the systemic properties of the bone tissue and the biomechanical state of the spine, which determine the individual risk

Table 3

Posterior classification matrix for the DF model for predicting NCFs

Studies sample	Percentage of the correct (%)	Predicted by the model (n)	
		NCF absent	NCF present
NCF absent (n = 54)	72.20	39	15
NCF present (n = 26)	76.90	6	20
Total (n = 80)	73.75	47	33

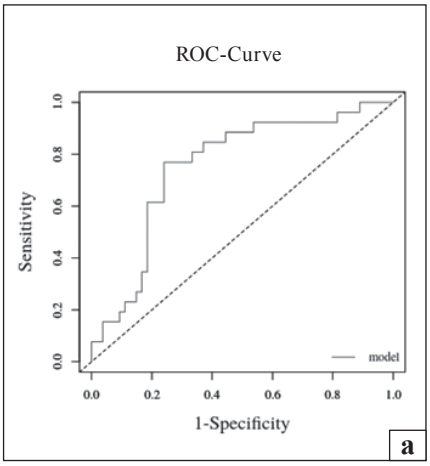

Table 1. Cut-off Results

Optimal cut-off method	: MaxSpSe
Optimal cut-off point	: 0.09944667
Optimal criterion	: 0.7592593

Table 2. Performance Measures

		Value	Lower Limit	Upper Limit
Sensitivity	:	0.769	0.564	0.910
Specificity	:	0.759	0.624	0.865
Positive Predictive Value	:	0.606	0.447	0.824
Negative Predictive Value	:	0.872	0.726	0.933
Positive Likelihood Ratio	:	3.195	1.903	5.366
Negative Likelihood Ratio	:	0.304	0.148	0.623

b

Marker	AUC	SE.AUC	LowerLimit	UpperLimit (*)	z	p-value
model2	0.7535613	0.05796304	0.6399558	0.8671667	4.374533	1.216927e-05

c

Fig. 2. Results of ROC analysis for the developed DF model for predicting NCF: (a) ROC curve plot; (b) results of determining the optimal cutoff threshold; (c) area under the ROC curve evaluations.

of new compression fractures. In essence, this concept is analogous to the use of the BMD indicator, which itself does not "cause" fractures but serves as a reliable marker of the risk of their occurrence by reflecting the quality of bone tissue.

This position is supported by numerous experimental and clinical studies.

Thus, H. K. Genant et al. demonstrated a strong negative correlation between the degree of vertebral body compression and BMD ($r = -0.68$; $p < 0.001$) [5]. In turn, S. Boutroy et al. using quantitative computed tomography showed that in patients with compression over 40 %, the volumetric density of trabecular bone is 35 % lower, and the cortical layer porosity is 28 % higher compared to those with compression less than 25 % [12]. Therefore, pronounced vertebral deformity is a marker of more severe systemic osteoporosis and poorer bone quality not only in the affected segment but also throughout the spine, which pathophysiologically justifies the increased susceptibility of such patients to the development of NCPFs.

Beyond systemic factors, local biomechanical alterations following PVP are also significant contributors. Specifically, J. Luo et al. in a study using finite element analysis showed that after PVP of vertebrae with compression over 33 %, the load on adjacent segments increases by 18–24 %, while with compression less than 25 %, it increases only by 8–12 % [13]. Clinical observations are consistent with these data.

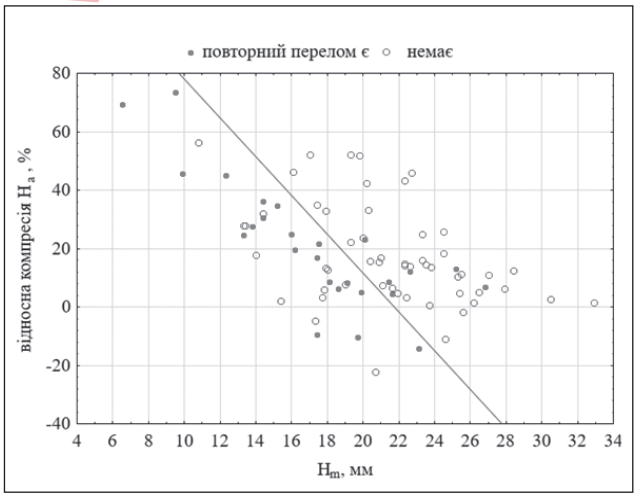

Fig. 3. Scatter plot of the indicators h^m and relative compression H_a.

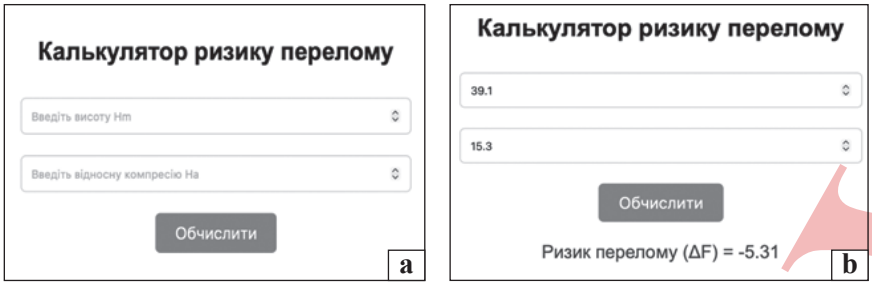

Fig. 4. Web application "Fracture Risk Calculator": (a) interface; (b) results of the work

R. Lindsay et al. found that compression over 40 % is associated with a 92 % increase in the risk of NCPF within one year, while for compression less than 25–38 %, the increase is 45 % [14]. In a long-term prospective study by J. A. Cauley et al. (15 years, n = 9,704), it was shown that the degree of vertebral deformity is an independent risk factor for NCPF (HR = 2.8; 95 % CI: 1.9–4.2) [15].

The results obtained in our study are consistent with the above data and suggest that the morphometric parameters hm and Ha can be considered accessible markers for identifying the risk of NCPF after PVP in clinical practice. At the same time, it should be noted that the frequency of NCPF in our sample (46.2 %) significantly exceeds the values reported in most current publications. A meta-analysis by A. J. Láinez Ramos-Bossini et al., which included 14 randomized controlled trials (n = 1,413), did not find a statistically significant increase in the risk of NCPF after vertebroplasty compared to conservative treatment (RR = 1.05) [16]. However, in the Optum cohort study of individuals after PVP, the frequency of new interventions was shown to be 15.5 % over 24 months of observation [4]. The observed discrepancies are likely due to the specific patient selection criteria in our study, which is confirmed by previous data: in a cohort of 520 patients who underwent PVP, the frequency of NCPF was 12.31 % [17].

The last decade has been characterized by intensive development of predictive models for individual risk assessment of NCPF. Traditional statistical approaches include multifactorial regression models and nomograms. For example, Q. Li et al. proposed a 12-parameter nomogram that integrates clinical, radiological, and technical variables, with an area under the ROC curve (AUC) of 0.85 [18]. Y. Qian et al. developed a simplified 8-parameter model with an AUC of 0.83, but even such tools remain relatively complex for routine clinical use [19].

The further development of this direction is linked to the implementation of artificial intelligence (AI) and machine learning methods. H. Wu et al. demonstrated that the support vector machine method provides the highest accuracy in predicting NCPF after PVP among the compared algorithms based on a sample of 863 patients [20]. S. Kim et al. applied a Vision Transformer-based model for analyzing MRI images, achieving a statistically significant improvement in AUC compared to classical neural networks [21]. Y. Yeh et al. demonstrated the high predictive value of the Vertebral Bone Quality Score (VBQ) as a predictor of NCPF (AUC = 0.74) [22].

Our model achieved an accuracy of 76.25 %, which corresponds to moderate discriminatory ability by the criteria of J. A. Swets [23]. Although these figures are lower than those of more complex multi-parameter and AI-based models [20–22], they are comparable to the results of simpler statistical approaches presented in the literature.

The key advantage of the proposed model is its practical applicability. The use of only two variables, which can be measured using standard radiography, makes this tool potentially suitable for widespread implementation, especially in the context of limited resources in Ukraine's healthcare system.

The statistical significance of the Ha and hm parameters has a clear biomechanical basis. For example, C. Zhou et al., in studies using the finite element method, showed that vertebrae with an initial compression of the anterior vertebral edge exceeding 25 % have 35-45 % higher stress in adjacent segments after the introduction of bone cement [24]. The mean value of Ha in the group of patients with NCPF in our study (20.64) is consistent with these data. The reduction in the absolute height of the anterior vertebral edge (> 17.2 mm) reflects not only the degree of local compression but also its overall architectural degradation. In this context, it is noteworthy that Y. Yeh et al. demonstrated the independent prognostic value of the Vertebral Bone Quality Score, which correlates with morphometric parameters (MP), regarding the risk of NCPF [22].

An important point is that a systematic review by S. R. Namireddy et al. showed that simpler statistical models often demonstrate better generalizability compared to complex artificial intelligence algo-

rithms in the context of external validation [25]. This emphasizes the appropriateness of developing simple, interpretable, and reproducible tools for routine clinical practice.

Thus, at the present stage, the proposed model can be considered a promising auxiliary tool for the primary assessment of the risk of NCPF after PVP. However, it requires further refinement and external validation before being implemented in widespread clinical practice.

Conclusion

The developed model for predicting new compression fractures of the vertebrae after percutaneous vertebroplasty is promising and is based on the morphometric parameters of vertebral height (hm) and relative compression (Ha) after PVP. The model demonstrates moderate accuracy in posterior classification (76.25 %) and statistical significance ($p = 0.000376$). The application of the model may aid in the early identification of patients at high risk for NCPF, allowing for the optimization of preventive strategies.

Conflict of interest. The authors declare no conflict of interest.

Future research directions. Future research should focus on the external validation of the developed model in other medical institutions and on independent patient cohorts, as well as its prospective clinical testing. Further work should aim at enhancing the model by integrating additional clinical and instrumental indicators.

Funding information. The study was conducted within the framework of the planned scientific research at the State Institution Professor M. I. Sytenko Institute of Spine and Joint Pathology of the National Academy of Medical Sciences of Ukraine. No additional funding was received.

Authors' contribution. Popov A. I. — study concept, patient treatment, article editing; Molodyuk M. V. — data collection, drafting the article, patient treatment; Kutsenko V. O. — study concept, literature review, drafting the article; Zlatnik R. V. — radiological diagnosis, morphometric measurements; Nessonova M. M. — statistical analysis, interpretation of findings, article editing.

References

1. Rho, Y., Choe, W. J., & Chun, Y. I. (2011). Risk factors predicting the new symptomatic vertebral compression fractures after percutaneous vertebroplasty or kyphoplasty. *European Spine Journal, 21*(5), 905–911. https://doi.org/10.1007/s00586-011-2099-5
2. Sahota, A., Vass, C., Marshall, L., & Sahota, O. (2024). Fragility fracture and fear of falling in middle aged adults-a prevalence study. *Osteoporosis International, 35*(12), 2237–2238. https://doi.org/10.1007/s00198-024-07166-6
3. Hernlund, E., Svedbom, A., Ivergård, M., Compston, J., Cooper, C., Stenmark, J., McCloskey, E. V., Jönsson, B., & Kanis, J. A. (2013). Osteoporosis in the European Union: Medical management, epidemiology and economic burden. *Archives of Osteoporosis, 8*(1–2). https://doi.org/10.1007/s11657-013-0136-1
4. Hirsch, J. A., Gilligan, C., Chandra, R. V., Brook, A., Gasquet, N. C., Ricker, C. N., & Wu, C. (2024). Real-world rates and risk factors for subsequent treatment with vertebroplasty or balloon kyphoplasty after initial vertebral augmentation: A retrospective cohort study. *Osteoporosis International, 36*(1), 129–140. https://doi.org/10.1007/s00198-024-07294-z
5. Genant, H. K., Wu, C. Y., Van Kuijk, C., & Nevitt, M. C. (1993). Vertebral fracture assessment using a semiquantitative technique. *Journal of Bone and Mineral Research, 8*(9), 1137–1148. https://doi.org/10.1002/jbmr.5650080915
6. Kuo, C. (2024). Commentary on "Deep learning-assisted quantitative measurement of thoracolumbar fracture features on lateral radiographs". *Neurospine, 21*(1), 44–45. https://doi.org/10.14245/ns.2448202.101
7. Thrall, J. H. (2024). Challenges of implementing artificial intelligence–enabled programs in the clinical practice of radiology. *Radiology: Artificial Intelligence, 6*(5). https://doi.org/10.1148/ryai.240411
8. Yang, Y., Peng, J., Deng, K., Zhang, Z., Qiu, Q., & Zhang, X. (n. d.). Prediction of vertebral fracture risk in patients with osteopenia based on MRI texture analysis. *ISMRM Annual Meeting*. https://doi.org/10.58530/2024/1553
9. Tabachnick, B. G., & Fidell, L. S. (2019). *Using multivariate statistics* (7th ed.). Pearson.
10. Izenman, A. J. (2013). *Modern multivariate statistical techniques*. Springer. https://doi.org/10.1007/978-0-387-78189-1
11. Popov, A., Moloduk, M., Kutsenko, V., & Nessonova, M. (2025). Risk factors for recurrent vertebral compression fractures after percutaneous vertebroplasty in osteoporotic patients: A systematic review and meta-analysis. *ORTHOPAEDICS TRAUMATOLOGY and PROSTHETICS,* (3), 91–102. https://doi.org/10.15674/0030-59872025391-102
12. Boutroy, S., Bouxsein, M. L., Munoz, F., & Delmas, P. D. (2005). In VivoAssessment of Trabecular Bone Microarchitecture by High-Resolution Peripheral Quantitative Computed Tomography. *The Journal of Clinical Endocrinology & Metabolism, 90*(12), 6508–6515. https://doi.org/10.1210/jc.2005-1258
13. Luo, J., Skrzypiec, D. M., Pollintine, P., Adams, M. A., Annesley-Williams, D. J., & Dolan, P. (2007). Mechanical efficacy of vertebroplasty: Influence of cement type, BMD, fracture severity, and disc degeneration. *Bone, 40*(4), 1110–1119. https://doi.org/10.1016/j.bone.2006.11.021
14. Lindsay, R. (2001). Risk of New Vertebral Fracture in the Year Following a Fracture. *JAMA, 285*(3), 320. https://doi.org/10.1001/jama.285.3.320
15. Cauley, J. A., Hochberg, M. C., Lui, L.-Y., Palermo, L., Ensrud, K. E., Hillier, T. A., Nevitt, M. C., & Cummings, S. R. (2007). Long-term Risk of Incident Vertebral Fractures. *JAMA, 298*(23), 2761. https://doi.org/10.1001/jama.298.23.2761
16. Láinez Ramos-Bossini, A. J., Jiménez Gutiérrez, P. M., Moraleda Cabrera, B., Bueno Caravaca, L., González Díez, M., & Ruiz Santiago, F. (2024). Risk of new vertebral compression fractures and serious adverse effects after vertebroplasty: A systematic, critical review and meta-analysis of randomized controlled trials. *Quantitative Imaging in Medicine and Surgery, 14*(11), 7848–7861. https://doi.org/10.21037/qims-24-396
17. Popov, A., & Moloduk, M. (2024). Prediction of repeated osteoporotic fractures of the thoracic and lumbar vertebrae (experimental study). *Orthopaedics, Traumatology and Prosthetics,* (3), 5–12. https://doi.org/10.15674/0030-5987202435-12
18. Li, Q., Long, X., Wang, Y., Fang, X., Guo, D., Lv, J., Hu, X., & Cai, L. (2021). Development and validation of a nomogram for predicting the probability of new vertebral compression fractures after vertebral augmentation of osteoporotic vertebral compression fractures. *BMC Musculoskeletal Disorders, 22*(1). https://doi.org/10.1186/s12891-021-04845-x
19. Qian, Y., Hu, X., Li, C., Zhao, J., Zhu, Y., Yu, Y., Xie, N., Ma, B., Zeng, Z., & Cheng, L. (2023). Development of a nomogram

model for prediction of new adjacent vertebral compression fractures after vertebroplasty. *BMC Surgery, 23*(1). https://doi.org/10.1186/s12893-023-02068-6
20. Wu, H., Li, C., Song, J., & Zhou, J. (2024). Developing predictive models for residual back pain after percutaneous vertebral augmentation treatment for osteoporotic thoracolumbar compression fractures based on machine learning technique. *Journal of Orthopaedic Surgery and Research, 19*(1). https://doi.org/10.1186/s13018-024-05271-0
21. Kim, S., Kim, I., Yuh, W. T., Han, S., Kim, C., Ko, Y. S., Cho, W., & Park, S. B. (2024). Augmented prediction of vertebral collapse after osteoporotic vertebral compression fractures through parameter-efficient fine-tuning of biomedical Foundation models. *Scientific Reports, 14*(1). https://doi.org/10.1038/s41598-024-82902-w
22. Yeh, Y., Chen, M., Hu, Y., Chiu, P., Kao, F., Hsieh, M., Yu, C., Tsai, T., Niu, C., Chen, L., Chen, W., & Lai, P. (2024). Vertebral bone quality score as a predictor of subsequent fractures after cement augmentation for Osteoporotic vertebral compression fracture. *Neurosurgery, 96*(6), 1410–1418. https://doi.org/10.1227/neu.0000000000003282
23. Swets, J. A. (1988). Measuring the accuracy of diagnostic systems. *Science, 240*(4857), 1285-1293. https://doi.org/10.1126/science.3287615
24. Zhou, C., Meng, X., Huang, S., Chen, H., Zhou, H., Liao, Y., Tang, Z., Zhang, X., Li, H., Sun, W., & Wang, Y. (2024). Biomechanical study of different bone cement distribution on osteoporotic vertebral compression Fracture-A finite element analysis. *Heliyon, 10*(5), e26726. https://doi.org/10.1016/j.heliyon.2024.e26726
25. Namireddy, S. R., Gill, S. S., Peerbhai, A., Kamath, A. G., Ramsay, D. S., Ponniah, H. S., Salih, A., Jankovic, D., Kalasauskas, D., Neuhoff, J., Kramer, A., Russo, S., & Thavarajasingam, S. G. (2024). Artificial intelligence in risk prediction and diagnosis of vertebral fractures. *Scientific Reports, 14*(1). https://doi.org/10.1038/s41598-024-75628-2

The article has been sent to the editors	Received after review	Accepted for printing
21.10.2025	28.11.2025	09.12.2025

RADIOGRAPHIC MORPHOMETRIC PREDICTION OF NEW VERTEBRAL COMPRESSION FRACTURES AFTER VERTEBROPLASTY

A. I. Popov [1], M. V. Moloduk [1], V. O. Kutsenko [1], R. V. Zlatnik [1], M. M. Nessonova [2]

[1] Sytenko Institute of Spine and Joint Pathology National Academy of Medical Sciences of Ukraine, Kharkiv
[2] Private higher educational institution «Kharkiv International Medical University». Ukraine

✉ Andrii Popov, MD, DSci in Orthopaedics and Traumatology: aipopovdoc@gmail.com; https://orcid.org/0000-0002-9006-7721
✉ Mykyta Moloduk, MD: NikitaMoloduk@gmail.com; https://orcid.org/0009-0005-0058-424X
✉ Volodymyr Kutsenko, MD, DSci in Orthopaedics and Traumatology: kutsvlad1956@gmail.com; https://orcid.org/0000-0001-7924-6553
✉ Ruslan Zlatnik, MD: ruslan.zlatnik@gmail.com; https://orcid.org/0009-0005-7621-9118
✉ Maryna Nessonova, PhD in Technology: m.nessonova@khimu.edu.ua; https://orcid.org/0000-0001-7729-317X

УДК 616.711-089.881-089-06(045)

DOI: http://dx.doi.org/10.15674/0030-59872026153-60

Recommendations for preventing postoperative complications of transpedicular screw fixation in patients with spinal disorders

S. Ye. Bondarenko, O. O. Barkov, V. O. Tuljakov

Sytenko Institute of Spine and Joint Pathology National Academy of Medical Sciences of Ukraine, Kharkiv

Innovations in spinal surgery have improved technical precision and perioperative efficiency, however, the issue of postoperative complications arising from the use of transpedicular screw fixation (TF) remains a concern. Objective. To develop an algorithmic protocol for reducing the likelihood of postoperative complications in patients undergoing transpedicular screw fixation. Methods. An analysis was conducted of the surgical outcomes of 2,760 patients with degenerative diseases, injuries and deformities of the spine, with radiographic assessment of transpedicular screw (TS) placement, both with and without the use of a 3D navigation system. The patients' laboratory parameters and the results of 62 intraoperative neurophysiological monitoring sessions were studied. Results. An algorithmic scheme was developed to prevent the development of TS complications and improve the quality of care for patients with spinal disorders: preoperative strategic comprehensive planning, intraoperative monitoring and techniques for precise TS placement, postoperative follow-up, prevention complications. An algorithm for action has been defined in cases of suspicion of an incorrectly placed screw or deterioration in neurological status. The core of the prediction and assessment of the likelihood of postoperative complications is an algorithmized scheme for laboratory examination of patients. Its suitability was verified during the surgical treatment of 30 patients. Conclusions. The algorithm-based protocol developed enables a structured assessment of the risk of complications, the planning of surgical treatment taking into account modern technologies, the monitoring of all critical points, the implementation of an individualized approach for each patient, and the integration of spinal navigation and neuromonitoring of the surgical process, which will minimize complications and have a positive impact on patients' condition, the length of their hospital stay, and the quality of treatment outcomes.

Інновації в хірургії хребта підвищили технічну точність і періопераційну ефективність, проте проблема післяопераційних ускладнень через застосування транспедикулярної фіксації (ТФ) залишається актуальною. Мета. Розробити алгоритмізовану схему зниження вірогідності розвитку післяопераційних ускладнень у пацієнтів із використанням транспедикулярної фіксації. Методи. Проведено аналіз результатів операцій 2 760 пацієнтів із дегенеративними захворюваннями, травмами та деформаціями хребта з рентгенологічною оцінкою введення транспедикулярних гвинтів (ТГ), без та з допомогою 3D-навігаційної системи. Вивчено лабораторні показники пацієнтів і результати 62 інтраопераційних нейрофізіологічних моніторингів. Результати. Складено алгоритмізовану схему для попередження розвитку ускладнень ТФ і підвищення якості лікування хворих із захворюваннями хребта: передопераційне стратегічне комплексне планування, інтраопераційний контроль і техніка точного встановлення ТГ, післяопераційне спостереження та профілактика ускладнень. Визначено алгоритм дії за підозри на неправильно встановлений гвинт або погіршення неврологічного статусу. Ядром предикції й оцінки вірогідності розвитку післяопераційних ускладнень є алгоритмізована схема лабораторного обстеження пацієнтів. Її придатність перевірено під час хірургічного лікуванняі 30 хворих. Висновки. Розроблена алгоритмізована схема дозволяє структуровано оцінити ризик ускладнень, запланувати хірургічне лікування з урахуваннях сучасних технологій, проконтролювати усі критичні точки, здійснити індивідуальний підхід до кожного пацієнта й інтеграцію спінальної навігації, нейромоніторинг операційного процесу, що дозволить мінімізувати ускладнення та позитивно впливатиме на стан пацієнтів, тривалість їхнього перебування в стаціонарі, покращення якості результатів лікування. Ключові слова. Хребет, грудний відділ, поперековий відділ, транспедикулярна фіксація, ускладнення, лабораторні показники.

Key words. Spine, thoracic section, lumbar section, transpedicular fixation, complication, prevention, biochemistry, immunology

Introduction

Spinal fusion with transpedicular fixation (TPF) is considered the most frequently performed procedure in orthopedic practice, although it may be accompanied by complications that require re-intervention [1, 2].

Incorrect placement of transpedicular screws (TPS) is a major cause of neurological, vascular, visceral complications, as well as cerebrospinal fluid leakage. The average frequency of incorrect TPS placement in various studies ranges from 0–2 % to 25–95 % in patients with scoliosis and about 4.2% of cases in patients with degenerative spine diseases [1–3].

Among patients experiencing complications, body mass index (BMI) frequently exceeds 25 kg/m², reflecting a lower initial health status as measured by the SF-36 scale and a disrupted lumbopelvic balance. These factors contribute to extended hospital stays, an increased number of TPS levels, and consequently, less optimal postoperative frontal and sagittal correction [5]. H. E. Goheer et al. noted that with each unit increase in a patient's BMI, the time required for posterior lumbar spinal fusion increased by 0.84 minutes. At the same time, the likelihood of complications related to the surgical wound increased by 19.7% after posterior spinal fusion at one level [6].

The presence of the upper instrumented vertebra at the apex of the kyphosis, preoperative sagittal lumbopelvic imbalance, and osteoporosis have been identified as significant risk factors for complications in patients with degenerative lumbar scoliosis and concomitant thoracolumbar kyphosis. Surgical planning for this condition should account for spinal morphology to avoid positioning the upper instrumented vertebra at the kyphosis apex [4–6].

Advances in spinal surgery have increased precision and efficiency, yet complications with TPF procedures remain a significant concern and are the focus of this study. We believe it is important to analyze the data from the State Institution Professor M. I. Sytenko Institute of Spine and Joint Pathology of the NAS of Ukraine regarding surgeries performed with transpedicular fixation, as well as to investigate the causes of complications and adverse outcomes, and to systematize the results of clinical and laboratory findings.

Purpose: To develop an algorithmic method to reduce the likelihood of postoperative complications in patients undergoing spinal transpedicular fixation.

Material and Methods

The study was conducted at the Spine Pathology Clinic of the State Institution Professor M. I. Sytenko Institute of Spine and Joint Pathology of the NAS of Ukraine. It was approved by the local bioethics committee of this institution (protocol No. 257 dated 22.12.2025) and carried out in compliance with the principles of good clinical practice (ICH GCP), the Helsinki Declaration on Human Rights and Biomedicine (1977 edition), as well as the requirements of current Ukrainian legislation. All patients involved in the study were properly informed about the purpose, plan, and conditions of the study and provided written informed consent for participation.

A retrospective and prospective analysis was conducted on the results of surgical interventions in 2,760 patients between 2004 and 2018, due to degenerative diseases, traumatic injuries, and deformities of the thoracic and lumbar spine, all of whom underwent transpedicular fixation of the vertebrae at these locations. Revision surgeries were carried out on 268 patients. Among these, complications associated with transpedicular constructions (TPC), including those caused by transpedicular screws (TPS), rods, or combined systems, were examined in 143 cases. The accuracy of TPS placement in vertebrae was compared using radiological examinations (frontal, sagittal), computed tomography (CT), and magnetic resonance imaging (MRI). The number of revision surgeries directly linked to improper screw placement was analyzed between Group I, using the standard screw placement technique (free-hand technique) (2,128 patients, 12,879 screws), and Group II, which utilized a 3D navigation system based on preoperative CT (632 patients, 3,203 screws). Additionally, 62 results of intraoperative neurophysiological monitoring (IONM) were analyzed.

At the same time, clinical-laboratory, biochemical, and immunological blood tests of these patients were studied prior to treatment, and their diagnostic sensitivity was determined. Among these, the following were evaluated: hemoglobin content, total bilirubin (TB), total glycoproteins (GP), haptoglobin (HP), C-reactive protein (CRP), alkaline and acid phosphatase activities (ALP and ACP), alanine aminotransferase (ALT), aspartate aminotransferase (AST), fibrinogen (FG), D-dimers, soluble fibrin-monomer complexes (SFMC), circulating immune complexes (CIC), activated partial thromboplastin time (APTT), fibrinolytic activity (FA), leukocyte count, erythrocyte sedimentation rate (ESR), and the content and spontaneous migration of lymphocytes (LIF).

Results

The algorithmic approach developed (see Figure 1) facilitated the application of a well-considered protocol to minimize the risk of postoperative and intraopera-

tive complications in patients undergoing decompression-stabilization spinal surgeries.

Preoperative strategic comprehensive planning involves determining indicators before performing decompression-stabilizing surgical interventions using TPF and clarifying risk factors for each specific patient:

– Clinical-diagnostic study — patient history (degenerative diseases, trauma, spinal deformities, tumors, inflammation, osteoporosis, previous surgeries); laboratory (biochemical) examination according to an algorithmized scheme; assessment of comorbid conditions (diabetes, obesity, cardiovascular diseases, hormone therapy);

– Instrumental diagnosis — spinal radiography (frontal, sagittal projections) to determine structure, degree of deformation and its mobility, displacement, instability of vertebrae, and the height of vertebral bodies and intervertebral discs; CT of the spine (individual anatomy of vertebral arches, length, and diameter), identification of intracanalar and other congenital anomalies (diastematomyelia, spondylolysis, defects in vertebral formation and integrity); MRI (study of nerve structures and their compression, intervertebral discs, muscles); densitometry (detection of osteoporosis for correction of intervention tactics);

– Surgical treatment planning — selecting the length of spinal fixation considering segment stability, degree and magnitude of deformation, sagittal contour of the spine, type of disease (degenerative, trauma, tumors, deformities). Extensive instrumentation of the lumbar spine requiring fixation of the L_V–S_I zone necessitates additional fixation to the iliac bones; consideration of bone mineral density (BMD); individual selection of the construction: diameter, length, and type of TPS (mono-, polyaxial, reduction), stiffness of rods, and their length.

Intraoperative Oversight and Precision in TPS Placement

During this phase, it is essential to pay close attention to several key factors:

– preparation and visualization — marking the level planned for surgery using intraoperative radiography and spinal navigation; verifying the intervention plan according to the patient's anatomy; placing electrodes and performing IONM, drawing baseline lines;

– choice of screw placement technique: "free-hand" (using predefined screw entry points based on anatomical landmarks) or under the control of a 3D navigation system, ensuring the necessary conditions to avoid navigation errors (accurate point registration, accounting for the patient's position differences during CT and on the operating table; control of patient positioning, respiratory movements, and antenna displacement on the spinous process after registration; avoiding damage to the reflective coating of the balls on the antenna or instrument);

– work on distant segments of the spine from the site of registration requires special control of the surgical wound to avoid errors in the image display on the monitor;

– TPS monitoring (radiographic control, IONM using as many muscles as possible);

– reducing complication risks (asepsis/antisepsis), monitoring blood loss, preventing neurological damage (monitoring the tools near the dura mater and spinal nerves during screw placement and rod installation, blockers).

Postoperative Monitoring, Prevention, and Rehabilitation

At the early and late postoperative stages, it is necessary to use radiographic studies or CT scans to determine the accuracy of TPS placement in the vertebrae, as well as the formation of the spinal fusion, stability of the transpedicular system, adjacent segments, loss of achieved deformation correction, and neurological status, as well as to provide rehabilitation treatment.

A general action plan in case of suspicion of improperly placed screws or deterioration of neurological status during surgery and after the intervention is shown in Figure 2.

Indications for revision surgery include improper placement of screws resulting in significant pain, neurological deficit, or the detection of an infectious process. These are technically very complex surgeries with uncertain and unguaranteed results. Preoperative, intraoperative, and postoperative monitoring of these patients is more challenging than for patients with primary surgeries. In such cases, preoperative planning is of utmost importance. The decision-making process should address the scope and type of revision surgery, the necessity and extent of spinal segment fixation, sagittal balance correction, type of osteotomy, and its location.

In cases where intraoperative concerns arise regarding the positioning of the TPS, it is imperative to promptly obtain radiographs in both frontal and sagittal projections, accompanied by neuro-monitoring. Based on the results, a decision must be made regarding screw revision. It may also be possible to reposition the screw along the cortical trajectory if it was initially placed using the transpedicular trajectory, and vice versa.

If there is concern regarding potential improper screw placement following surgery, the physician's response will be guided by when the issue becomes

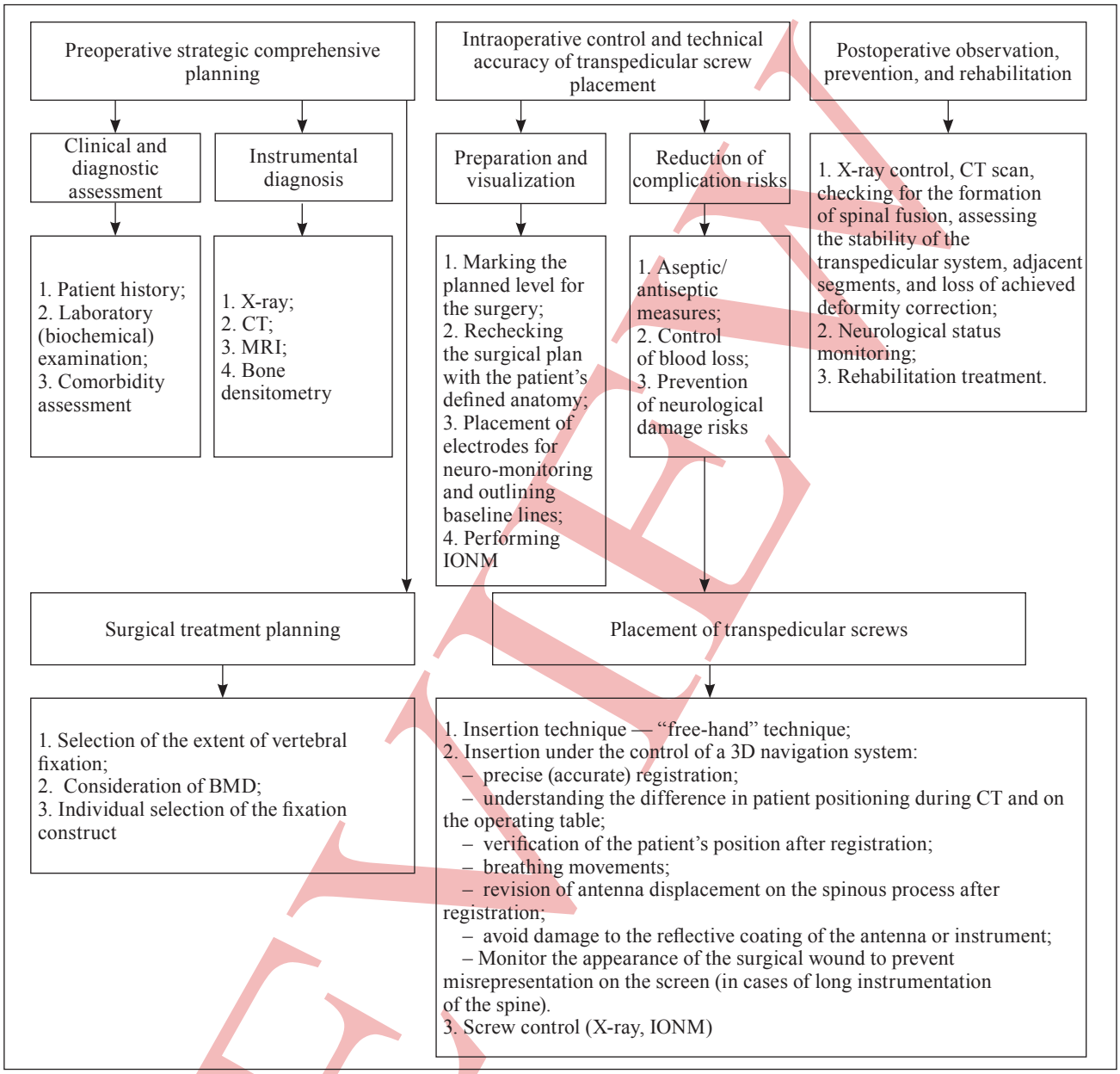

Fig. 1. Algorithmic Methodology for Preventing Postoperative Complications in Transpedicular Spinal Fixation

apparent. If a patient experiences pain or neurological changes, such as numbness in a particular dermatome, a few hours or days after surgery, these symptoms may result from local tissue swelling. In this case, the wound and adjacent tissues should be examined, their temperature and color assessed, and tenderness evaluated. Next stage involves a limited laboratory examination of the patient, namely a clinical and biochemical blood test with a focus on markers of the inflammatory process, such as acute-phase proteins, glycoprotein (GP), and C-reactive protein (CRP). Parallel to this, radiographic examination or CT scan should be performed, as well as a detailed neurological examination and IONM.

If no changes in the patient's status occur within two weeks of observation, revision surgery with screw repositioning is indicated. The presence of an infectious process also indicates the need for revision surgery, which may involve the removal of the entire transpedicular construct.

Case Study

A 64-year-old female patient presented with a diagnosis of postmenopausal osteoporosis (early surgical menopause at 42 years old) and multiple pathological fractures of the thoracic and lumbar vertebrae (Fig. 3, a).

Before undergoing surgery, which was performed on 20.02.2020, a clinical and diagnostic examination

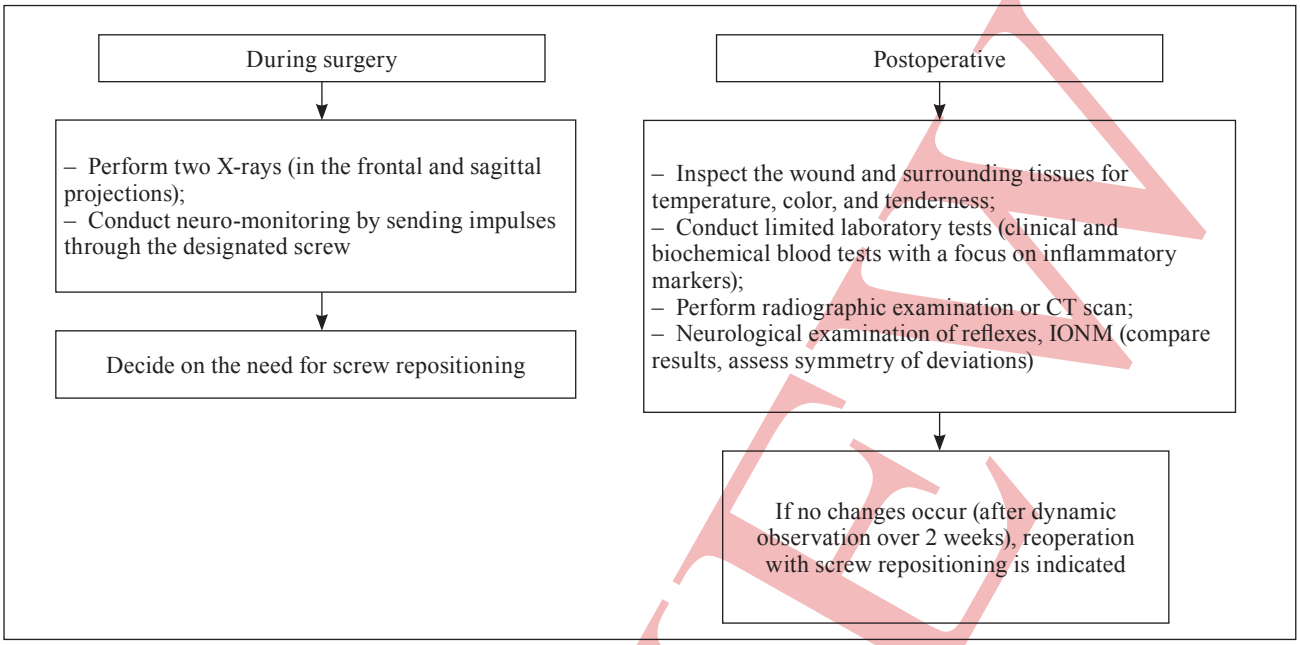

Fig. 2. Algorithm for Action in Case of Suspected Incorrect Screw Placement or Decrease in Neurological Status During Spinal TF Surgery

was conducted. Despite her comorbid status, spinal deformity correction was performed using transpedicular fixation (TPF) at the ThX–SI level, along with allograft spinal fusion.

During post-operative monitoring, one month later, instability of the TPF system and the formation of an adjacent spinal deformity were noted, as indicated by control radiographs (Fig. 3, b). A loss of deformity correction was identified, resulting in destabilization of the transpedicular system. These factors led to a revision procedure for the correct placement of the TPS, involving extension of the spinal instrumentation to the ThIII vertebra at the ThIII–SI level (Fig. 3, c).

Discussion

The scientific literature emphasizes that following spinal fusion using TPF, common complications include residual pain in the operated segment or neuropathic pain. Neuropathic pain is a potential complication of spine surgery with TPF, and it can significantly impair the patient's quality of life. Research shows that neurological issues caused by nerve compression in the lumbar spine may persist even after decompressive-stabilizing surgery, and full recovery is not always achieved [7]. Chronic neuropathic pain after spinal fusion typically does not subside with treatment; it often persists and may even worsen, caused by alterations in the anatomical relationships of the spinal motion segment [8]. This type of pain usually begins before the surgery and remains, or even intensifies, after the procedure. According to the literature, this type of pain syndrome is observed in 5 % to 30 % of patients [9]. In our study, the incidence was 23.9 %.

The torque applied during the tightening of the TPS is crucial. S. Nakamura and colleagues stress the importance of correlating the torque during the tightening of the TPS with the BMD, age, and BMI. This correlation helps predict the stiffness of the fixation and prevents the failure of instruments during lumbar spine fusion surgery. Generally, the torque should remain within specific limits: the lower side is restricted by the minimal force necessary to create the required friction, while the upper limit should not exceed the threshold beyond which bone tissue destruction begins [10–11].

In conclusion, we recommend the use of 3D navigation during the placement of TPS, particularly in complex cases involving long instrumentation for scoliosis deformity stabilization. This aligns with the conclusions of A. R. Kothari et al., who examined the placement of 259 screws in 21 scoliosis patients and found that navigation using the O-arm reduced the frequency of medial and lateral (i.e., “critical”) placement errors of TPS (> 2 mm) [12].

In cases of abnormal laboratory data, consideration should be given to the possibility of infection, either deep or superficial. S. Tummala et al. found that preoperative colonization by methicillin-resistant Staphylococcus aureus significantly increases the risk of mortality, wound complications, systemic infections, hematologic disorders, and acute renal injury following elective lumbar spine surgery [13].

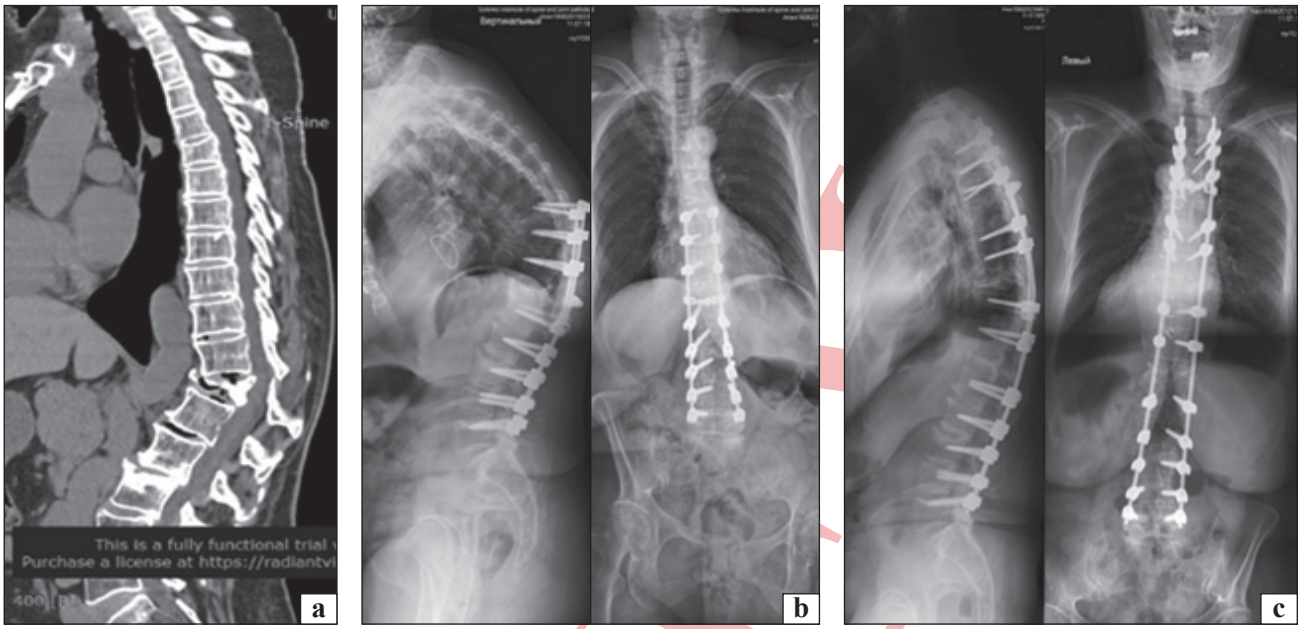

Fig. 3. X-ray Images: a) Before surgery and b) After initial surgery. One month later, c) Revision of the transpedicular system

Creating posterior bone-plastic spinal fusion using TPS provides stabilization of the affected area; however, it simultaneously disrupts the normal biomechanical relationships between the spinal motion segments. This can lead to or accelerate degenerative changes in adjacent spinal segments. Pathological changes in these adjacent areas are manifested by decreased disc height, the formation of hernias, scoliosis deformities, spondylolisthesis, or spinal canal stenosis [14]. Radiological signs of disease in adjacent segments may occur without clinical symptoms in 12.2 % to 42.6 % of cases, while radiological changes with clinical manifestations are observed in 4% to 20% of cases [15].

The surgeon must be prepared to manage accompanying complications, such as cerebrospinal fluid leakage or massive blood loss, and decide which type of TPS to use to ensure the successful completion of spinal fusion [16].

According to numerous researchers, including E. Adindu et al., patients diagnosed with metabolic syndrome tend to undergo longer surgical procedures, have extended hospital stays, and exhibit increased rates of postoperative complications such as dura mater tears, infections, and re-operations [17].

Recent innovations in lumbar spine surgery have enhanced technical accuracy and perioperative efficiency without compromising patient safety [18, 19]. A meta-analysis by G. Galieri et al. showed that intraoperative navigation improved tool precision, while augmented reality (AR) improved the ergonomics of the procedure [20].

The 2D/3D registration methodology with augmented reality visualization effectively addresses key limitations of current navigation paradigms, maintaining high accuracy standards during surgery. Augmented reality navigation with two- and three-dimensional registration is a promising technological advancement that can increase the accuracy and effectiveness of spinal instrumentation procedures [21].

Conclusions

The developed algorithmic scheme allows for a structured assessment of complication risks, planning surgical treatment based on modern technologies and knowledge, and ensuring control over all critical points, with an individualized approach to each patient. The integration of spinal navigation and neuromonitoring into the surgical process will help minimize complications during transpedicular fixation in patients with spinal diseases.

The practical use of the methods developed in this study for reducing postoperative inflammatory complications following transpedicular implantations, particularly through the registration of preoperative clinical-laboratory and biochemical deviations from normal values, may prevent complications, resulting in reduced patient severity, shorter hospital stays, and most importantly, improved treatment outcomes.

Conflict of Interest. The authors declare no conflicts of interest.

Prospects for Further Research. The authors plan to continue work in the direction of developing and implementing therapeutic and organizational measures to reduce complications in transpedicular fixation during the treatment of degenerative diseases and deformities of the thoracic and lumbar spine. Spe-

cifically, the current conceptual work needs to be confirmed under clinical conditions.

Funding Information. The study was carried out within the framework of comprehensive research topics of the State Institution Professor M. I. Sytenko Institute of Spine and Joint Pathology of the NAS of Ukraine "Study of main errors and complications of transpedicular fixation in spine surgery and the development of prevention and treatment measures" (applied), and "Improvement of surgical treatment methods for patients with degenerative-dystrophic diseases of the lumbar spine using modern technologies". Specific medical devices or pharmaceuticals were not involved in our research.

Author Contributions. Bondarenko S. E. — Justified the relevance of the study and developed its concept; Barkov O. O. — Analyzed literature sources and the results of own surgical interventions; Tulyakov V. O. — Conducted research on scientific and medical information and participated in the development of the main sections of the article.

References

1. Alshameeri, Z. A., Ahmed, E., & Jasani, V. (2020). Clinical outcome of spine surgery complicated by accidental dural tears: Meta-analysis of the literature. *Global spine journal, 11*(3), 400–409. https://doi.org/10.1177/2192568220914876
2. Alshameeri, Z. A., & Jasani, V. (2021). Risk factors for accidental dural tears in spinal surgery. *International journal of spine surgery, 15*(3), 536–548. https://doi.org/10.14444/8082
3. Sarathy, K., Dhawale, A., Rokade, S., Badve, S., Mandlecha, P., Aroojis, A., Mehta, R., Chaudhary, K., & Nene, A. (2021). Assessment of pedicle screw malposition in uniplanar versus multiplanar spinal deformities in children. *North American spine society journal (NASSJ)*, 5, 100049. https://doi.org/10.1016/j.xnsj.2021.100049
4. Pellisé, F., Bayo, M. C., Ruiz de Villa, A., Núñez-Pereira, S., Haddad, S., Barcheni, M., Pizones, J., Valencia, M. R., Obeid, I., Alanay, A., Kleinstueck, F. S., & Mannion, A. F. (2024). The impact of unplanned Reoperation following adult spinal deformity surgery. *Journal of bone and joint surgery, 106*(8), 681–689. https://doi.org/10.2106/jbjs.23.00242
5. O'Toole, J. E., Sasso, R. C., Harrop, J. S., Mariscal, G., Chaput, C. D., Arnold, P. M., Witiw, C. D., Jacobs, W. B., & Steinmetz, M. P. (2025). Adverse impact of obesity on lumbar spine fusion, patient-reported outcomes and costs. *Spine, 50*(17), 1208–1218. https://doi.org/10.1097/brs.0000000000005395
6. Goheer, H. E., Botros, M., Leggett, A. R., Ramirez, G., Haddas, R., Molinari, R. W., & Puvanesarajah, V. (2025). The impact of obesity on spine surgery operative time: A quantitative analysis. *Global spine journal, 16*(2), 975–984. https://doi.org/10.1177/21925682251369432
7. Gao, S., Li, Z., Li, X., Rudd, S., Wang, H., Gao, Z., Ding, W., & Yang, S. (2023). The treatment effect of posterior lumbar fusion surgery on patients suffering from lumbar disc herniation concurrent with peroneal nerve paralysis. *Frontiers in surgery,* 9. https://doi.org/10.3389/fsurg.2022.1063528
8. Cristea, A., Heijnen, B. F., Park, S. W., Krutko, A., Santos, C., Senker, W., Arzoglou, V., & Pereira, P. (2025). Neuropathic pain appears to be the main symptom associated with higher disease burden and lower pain alleviation in degenerative lumbar disease fusion patients. *Brain and spine,* 5, 104224. https://doi.org/10.1016/j.bas.2025.104224
9. Cannizzaro, D., Anania, C. D., Safa, A., Zaed, I., Morenghi, M., Riva, M., Tomei, M., Pessina, F., Servadei, F., Ortolina, A., & Fornari, M. (2023). Lumbar adjacent segment degeneration after spinal fusion surgery: A systematic review and meta-analysis. *Journal of neurosurgical sciences, 67*(6). https://doi.org/10.23736/s0390-5616.22.05891-x
10. Nakamura, S., Takahashi, T., Inoue, T., Minami, M., Kanematsu, R., Suda, I., Takeuchi, S., Tokunaga, S., & Hanakita, J. (2025). Measurement of Intraoperative insertional torque: Usefulness for prediction of the deviation of pedicle screw insertion in lumbar degenerative diseases. *International journal of spine surgery, 19*(4), 452–458. https://doi.org/10.14444/8785
11. Addevico, F., Morandi, M., Scaglione, M., & Solitro, G. F. (2020). Screw insertion torque as parameter to judge the fixation. Assessment of torque and pull-out strength in different bone densities and screw-pitches. *Clinical biomechanics,* 72, 130–135. https://doi.org/10.1016/j.clinbiomech.2019.12.004
12. Kothari, A. R., Katkade, S. M., Bhilare, P. D., Aiyer, S., Situt, N. V., Hadgaonkar, S. R., Shyam, A., & Sancheti, P. K. (2023). "Critical pedicle wall" breaches analysis in complex spinal deformity using O-arm navigation. *Surgical neurology international*, 14, 306. https://doi.org/10.25259/sni_437_2023
13. Tummala, S., Haslam, D., Gibbs, D., Alder, J., Chavarria, J., Avramis, I., & Rizkalla, J. (2025). Evaluating the risk of postoperative infection and complications in lumbar spine surgery patients with preoperative methicillin-resistant staphylococcus aureus (MRSA) colonization. *Archives of orthopaedic and trauma surgery, 145*(1). https://doi.org/10.1007/s00402-025-06036-y
14. Lopez, I. B., Benzakour, A., Mavrogenis, A., Benzakour, T., Ahmad, A., & Lemée, J. (2022). Robotics in spine surgery: Systematic review of literature. *International orthopaedics, 47*(2), 447–456. https://doi.org/10.1007/s00264-022-05508-9
15. Arim, O., Alshalcy, A., Shakir, M., Agha, O., & Alhamdany, H. (2024). Transpedicular screw fixation in degenerative lumbosacral spine disease surgical outcome. *Georgian medical news*, 34, 117–121. https://www.geomednews.com/Articles/2024/3_2024/117-121.pdf
16. Khan, B., Mansoor Shah, S., Khan, A., Ali, H., Ullah, A., Ullah, I., Haqqani, U., & Uliqbal, R. (2024). Revision lumbar spine surgeries: An early career neurosurgery experience. *Cureus.* https://doi.org/10.7759/cureus.57371
17. Adindu, E., Singh, D., Geck, M., Stokes, J., & Eeric Truumees. (2025). The impact of obesity on postoperative and perioperative outcomes in lumbar spine surgery: A systematic review and meta-analysis. *The spine journal, 25*(6), 1081–1095. https://doi.org/10.1016/j.spinee.2024.12.006
18. Radchenko, V., Barkov, O., & Skidanov, A. (2019). Five years of experience in using of navigation system in spine surgery. *Orthopaedics, traumatology and prosthetics, 0*(1), 5–13. https://doi.org/10.15674/0030-5987201915-13
19. Barkov, O., & Karpinska, O. (2025). Analysis of revisional surgical interventions in the thoracic and lumbar spine after transpedicular fixation. *Trauma, 26*(3), 189–196. https://doi.org/10.22141/1608-1706.3.26.2025.1019
20. Galieri, G., Orlando, V., Altieri, R., Barbarisi, M., Olivi, A., Sabatino, G., & La Rocca, G. (2025). Current trends and future directions in lumbar spine surgery: A review of emerging techniques and evolving management paradigms. *Journal of clinical medicine, 14*(10), 3390. https://doi.org/10.3390/jcm14103390
21. Castillo, J. A., Urreola, G., Kalistratova, V., Le, M., Harris, A. M., Shahzad, H., Massel, D. H., Shepard, N., Cook, C., Lim, R., Khan, S., & Price, R. L. (2025). Augmented reality–guided pedicle screw placement with 2D–3D registration: Proof-of-Concept using 151 cadaveric trajectories. *Global spine journal.* https://doi.org/10.1177/21925682251387550

ISSN 0030-5987. Orthopaedics, traumatology and prosthetics. 2026. № 1

The article has been sent to the editors	Received after review	Accepted for printing
02.01.2026	28.01.2026	02.02.2026

RECOMMENDATIONS FOR PREVENTING POSTOPERATIVE COMPLICATIONS OF TRANSPEDICULAR SCREW FIXATION IN PATIENTS WITH SPINAL DISORDERS

S. Ye. Bondarenko, O. O. Barkov, V. O. Tuljakov

Sytenko Institute of Spine and Joint Pathology National Academy of Medical Sciences of Ukraine, Kharkiv

✉ Stanislav Bondarenko, MD, DSci in Orthopaedics and Traumatology: bondarenke@gmail.com; https://orcid.org/0000-0003-2463-5919

✉ Oleksandr Barkov, MD, PhD in Traumatology and Orthopaedics: a.barkov.79@gmail.com; https://orcid.org/0000-0003-2161-416X

✉ Vladyslav Tuliakov, DSci in Pharmacy: tulakov1967v@gmail.com; https://orcid.org/0000-0002-3187-1592

УДК 616.718.4-001.5-007.23-092.9-085:615.382](045)

DOI: http://dx.doi.org/10.15674/0030-59872026161-69

Stimulation of periosteal bone formation with platelet-rich plasma in a rat model of femoral atrophic non-union

P. M. Vorontsov, V. Ye. Maltseva, Z. M. Danyshchuk, O. A. Nikolchenko, V. V. Kovtun, S. I. Laponin

Sytenko Institute of Spine and Joint Pathology National Academy of Medical Sciences of Ukraine, Kharkiv

Objective. To investigate the effect of local injection of platelet-rich plasma (PRP) on periosteal bone formation in a rat model of femoral atrophic non-union. Methods. The study was conducted on 11 rats. Atrophic non-union was modelled by performing a mid-shaft femoral osteotomy with intramedullary Kirschner wire fixation, followed by periosteal stripping (2 mm) at both ends of the osteotomized bone and their separation with a silicone spacer. On day 7 post-surgery, 5 animals received a local PRP injection into the injury zone. Radiography was performed at weeks 2 and 4. After 8 weeks, euthanasia was performed, and the operated femurs were harvested for histological analysis. Results. In the atrophic non-union model, a loose connective tissue capsule of varying thickness without signs of inflammation was found around the spacer in all rats. Acellular areas were identified within the cortex. The structure of the periosteum and endosteum near the osteotomy site was disrupted. In 5 out of 6 animals, no signs of bone formation were observed near the spacer from either the periosteal or endosteal zones. Following PRP injection, a higher density of capillary-type vessels was observed within the capsule. Areas of cartilage with hypertrophic chondrocytes were identified, indicating endochondral ossification. In 4 rats, formed bone tissue was recorded on the fragments, predominantly on one side, in both periosteal and endosteal zones. The bone tissue was cancellous in the periosteal zone and woven bone in the endosteal zone. Conclusion. Local PRP injection into the injury zone on day 7 in a rat model of femoral atrophic non-union with previously disrupted periosteum positively affects periosteal bone formation at the fragment ends.

Мета. Вивчити вплив локального введення збагаченої тромбоцитами плазми на періостальне кісткоутворення в моделі атрофічного незрощення перелому стегнової кістки щурів. Методи. Дослідження проведено з використанням 11 щурів, яким змоделювали стан атрофічного незрощення перелому шляхом виконання остеотомії в середній третині стегнової кістки з інтрамедулярною фіксацією спицею Кіршнера, руйнування періосту (2 мм) обох країв остеотомованої кістки та відокремлення їх силіконовим спейсером. На 7 добу 5 тваринам після втручання локально вводили PRP у зону ушкодження. Рентгенографію виконували на 2 та 4 тиждень. Через 8 тижнів після операції здійснили евтаназію та вилучили оперовану стегнову кістку для гістологічного аналізу. Результати. У моделі атрофічного незрощення у всіх щурів навколо спейсера виявлено сполучнотканинну капсулу різної товщини без ознак запалення. У кортексі визначали безклітинні ділянки. Структура періосту й ендосту поблизу зони остеотомії — зруйнована. У 5 з 6 тварин не виявили жодних ознак кісткоутворення поблизу місця розміщення спейсера як з боку періосту, так і ендосту. У разі введення PRP у сполучнотканинній капсулі густіше розміщувалися судини капілярного типу. Визначено ділянки хрящової тканини з гіпертрофованими хондроцитами, що свідчить про процес енхондральної осифікації. У 4 щурів зафіксовано сформовану кісткову тканину на уламках, переважно на одному як у періостальній, так і в ендостальній зонах. Кісткова тканина — губчаста в періостальній зоні та грубоволокниста — в ендостальній. Висновок. Введення PRP в зону ушкодження на 7-му добу в моделі атрофічного незрощення перелому з попередньо зруйнованим періостом стегнової кістки щурів позитивно впливає на періостальне кісткоутворення на краях уламків. Ключові слова. Щур, атрофічне незрощення, перелом стегнової кістки, збагачена тромбоцитами плазма (PRP), періостальне кісткоутворення, гістологія, енхондральна осифікація.

Keywords. Rat, atrophic non-union, femoral fracture, platelet-rich plasma (PRP), periosteal bone formation, histology, endochondral ossification

Introduction

Non-union or delayed union of long bone fractures is one of the serious complications that leads to the loss of limb functionality and/or worsens the quality of life for patients. The causes of this complication are considered to include bone defects, osteomyelitis, high-energy trauma, disruption of bone regeneration mechanisms, systemic diseases such as diabetes, etc. [1], as well as fracture treatment with metallic fixators [2]. Non-unions most commonly occur in fractures of the humerus (10–15%), femur, or tibia (up to 12.5%) [2]. As a result of military activity in Ukraine, there has been a notable increase in high-energy injuries that are often accompanied by long bone fractures and bone defects [3, 4]. This trend indicates that the number of cases of non-union among those affected may rise in the future.

The main task in the treatment of atrophic non-unions is achieving stable fixation, removal of scar tissue that hinders union, and replacing the formed defect with autografts or allografts [5]. Additionally, the use of various angiogenesis promoters and cell differentiation agents in the osteogenic direction during surgical interventions is being developed. These orthobiological methods include the use of platelet-rich plasma (PRP), autologous mesenchymal stem cells (MSCs) from bone marrow, bone morphogenetic proteins (BMPs) [1, 5], or their combinations [6]. The goal of using these methods is to accelerate fracture healing, although their effectiveness is still being researched both clinically and experimentally. This is particularly due to the lack of clinical studies with Level I evidence [5].

Platelet-rich plasma contains platelets from which several growth factors are released (platelet-derived growth factor (PDGF), transforming growth factor (TGF-β), and insulin-like growth factor (IGF-1)), which positively influence vascularization at the site of non-union and then stimulate the differentiation of MSCs in the direction needed for bone healing [7]. The periosteum plays a key role in reparative osteogenesis due to the presence of osteogenic precursor cells and a large number of blood vessels in its structure. Disruption of its structure and biological activity is considered one of the factors contributing to the formation of atrophic non-unions [8]. The growth factors present in PRP are potentially capable of stimulating periosteal cell activity, angiogenesis, and restoring its osteogenic potential, as evidenced by research combining periosteal stem cells and PRP to stimulate bone regeneration [10]. However, the exact mechanisms of PRP action in the case of non-union fractures are still unknown, and the timing of its application remains unclear [9].

A recent systematic review encompassing 24 clinical studies investigating molecular and biological disruptions in the regenerate of individuals with non-unions reported a suppression of BMP-7 expression in these cases [11]. This protein belongs to the TGF-β superfamily and induces the differentiation of MSCs into osteoblasts [12]. Additionally, signaling pathways of BMP and matrix metalloproteinases are likely involved in the development of non-unions [11]. At the tissue level, aseptic atrophic non-union leads to disturbances, the mechanisms of which are also almost unstudied. One of the main differences between atrophic non-union and hypertrophic non-union is the cell death in the cortical fragments at the site of non-union [11]. Therefore, targeting MSCs, the precursors of osteoblasts, for further bone formation, and the appearance of monocytes, precursors of osteoclasts, for resorption of the parent cortical bone in the periosteal zone, may be a promising treatment approach for non-unions. This may potentially support the use of orthobiological methods, specifically PRP.

Purpose: To study the effect of locally administered platelet-rich plasma on periosteal bone formation in a model of atrophic non-union of femoral fractures in rats.

Materials and Methods

Experimental research was conducted in accordance with the requirements for humane treatment of laboratory animals, as regulated by the Law of Ukraine “On the Protection of Animals from Cruelty” (No. 3447-IV dated 21.02.2006) and the European Convention for the Protection of Vertebrate Animals Used for Experimental and Other Scientific Purposes (1986) [13, 14]. The experimental research plan was approved by the Bioethics Committee at the State Institution Professor M. I. Sytenko Institute of Spine and Joint Pathology of the National Academy of Medical Sciences of Ukraine (protocol No. 224 dated 13.06.2022).

The study involved 11 male white rats, aged 6 months (body weight ranging from 325 to 550 g), from the experimental biological clinic of the State Institution Professor M. I. Sytenko Institute of Spine and Joint Pathology of the National Academy of Medical Sciences of Ukraine. A model of atrophic non-union of fractures was created in all animals by performing osteotomy in the middle third of the femur with intramedullary fixation using a Kirschner wire, destruction of the periosteum (2 mm) on both ends of the osteotomized bone using an electrocautery

device, and separation of the bone fragments using a silicone spacer. The rats were divided into two equal groups: 1 — model of atrophic non-union of the fracture (n = 6); 2 — model with local PRP injection in the injury zone on the 7th day after the intervention (n = 5).

Surgical interventions were performed under aseptic and antiseptic conditions, with general anesthesia (ketamine, 50 mg/kg body weight, intramuscularly). After shaving the right thigh and disinfecting the area with the antiseptic Betadine, osteotomy was performed in the middle third of the femur through a lateral approach using a circular burr (Fig. 1, a). Subsequently, the surgical area was flushed with the antiseptic agent Decasan. To destroy the periosteum on both ends of the osteotomized bone, its coagulation was performed 2 mm distal and proximal to the osteotomy site using a high-frequency electro-surgical unipolar generator HF-1760 Model DTC-03 (Fig. 1, b).

Next, the femoral bone fragments were separated, one end of the Kirschner wire was inserted into the bone marrow canal of the distal fragment, and a silicone spacer (diameter 7 mm) was placed over the wire through a pre-made hole in the center. Then, after stretching the limb muscles, the other end of the wire was inserted into the bone marrow canal of the proximal fragment, and both osteotomized bone parts were brought together with the silicone spacer in between (Fig. 1, c, d). The Kirschner wires ranged in length from 17 to 22 mm and in diameter from 1.5 to 2.0 mm; they were selected during the procedure based on the individual size and shape of the bone canal in each animal (Fig. 1, a). The wounds were treated with the antibiotic Bicillin, and the muscles and skin were sutured layer by layer with single knot sutures (MEFIL No. 2 suture material). The skin around the surgical area was treated with Betadine.

Seven days after the surgery, 6 rats were injected with 0.3 ml of PRP into the injury zone. This time point was chosen based on the stages of the reparative osteogenesis process, where the first stage is traumatic inflammation (lasting approximately 7 days) [15]. Since PRP injections can potentially intensify inflammation, the injection was done after the inflammation stage had ended. Moreover, in a previous study, we demonstrated that injecting PRP on the 7th day after implantation of a bone allograft in a critical-size femoral defect in older rats, where bone formation was suppressed, promoted the remodeling of the graft and the replacement of bone tissue [16].

To obtain PRP, 8 ml of venous blood was collected from two donor rats into an 8.5 ml vacuum tube containing anticoagulant. The blood samples were centrifuged for 10 minutes at 1500 rpm in a laboratory clinical centrifuge OPn-3.02 DASTAN, after which the plasma was collected using an automatic pipette with a sterile tip.

Four weeks after the surgical procedure, all rats were euthanized by decapitation under ether anesthesia for histological and biochemical analysis. The method of euthanasia was chosen due to the need to obtain blood for biochemical studies.

Radiological assessments were conducted on all rats at both two and four weeks following surgical intervention. The imaging was done under general anesthesia (ketamine 50 mg/kg body weight, intramuscularly). Digital radiographs were obtained using the OPERA T90cex radiological diagnostic system.

For *histological examination*, after decapitation, the operated femora were removed from the animals, cleaned of soft tissues, and fixed for 4 days in 10 % neutral formalin. After washing in running water, the femora were decalcified in a 5 % formic acid solution for 5 days and then transferred to 70 % ethyl

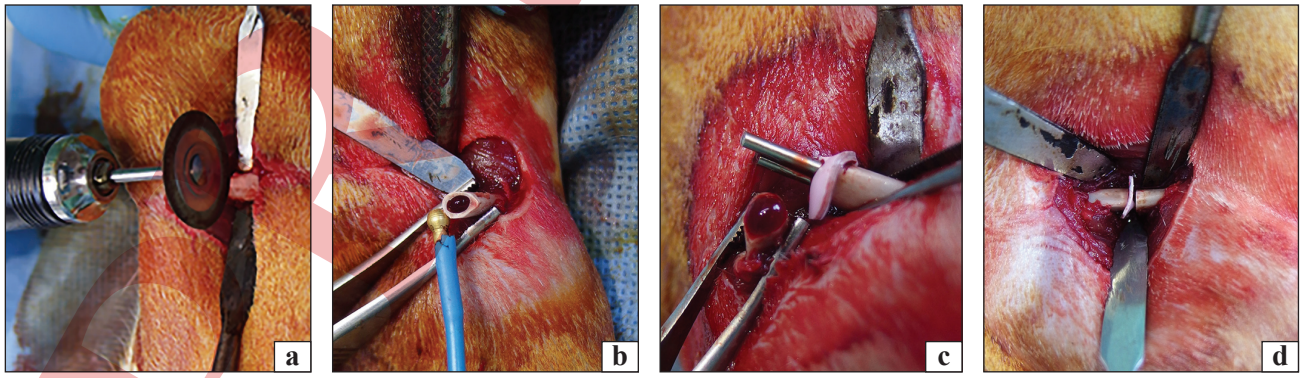

Fig. 1. Stages of surgical intervention to model atrophic non-union of the femoral fracture in rats: a) performing osteotomy of the femoral bone using a circular milling cutter; b) destruction of the periosteum of one bone fragment using a coagulator; c) insertion of the other end of the Kirschner wire with the silicone spacer into the proximal bone fragment; d) apposition of the bone fragments with the spacer between them

alcohol. The Kirschner wires were removed from the bones, and a fragment of the diaphysis with the osteotomy site was cut out. The obtained samples were dehydrated in increasing concentrations of isopropyl alcohol, then infiltrated with a mixture of isopropyl alcohol and paraffin, followed by series of paraffin baths and embedding in paraffin. Longitudinal sections were made using a Reichert sliding microtome and stained with hematoxylin and eosin. The structure of the cells and the intercellular substance in the osteotomy area and around it were analyzed using a light microscope Olympus BX63. Digital photography was performed using a DP73 Olympus digital camera, with the software Cell Sens Dimension 1.8.1.

Statistical Analysis

To assess the effect of PRP on periosteal bone formation, data from each rat were classified as either "bone formation present" or "bone formation absent", and the results were compared between the groups using the χ^2 test for categorical data. The difference between groups was considered significant if $p < 0.05$. SPSS Statistics was used for analysis.

Results

Radiographic Analysis

After modeling atrophic non-union, on the radiographs of all rats with/without PRP injection on the 7th day, the position of the intramedullary fixator (Kirschner wire) was correct at 2 weeks, providing alignment of the right limb axis. The bone fragments were adapted, and a gap was visible between them, with a radiologically transparent silicone spacer placed in the gap (Fig. 2, a, b). In the rats of the non-union model, no significant changes were observed after 4 weeks compared to the previous observation period (Fig. 2, b). In the PRP-treated group, periosteal regeneration was observed predominantly in one of the bone fragments (Fig. 3, d).

Histological Analysis. Model of Atrophic Non-Union of the Femur. Four weeks after osteotomy in the middle third of the femur diaphysis, intramedullary fixation with a Kirschner wire, and the placement of a silicone spacer between the bone fragments, microscopic examination revealed the area consisting of the spacer and fragments of the original cortex of the femur, both proximally and distally (Fig. 3, a). The spacer was not present in the histological samples due to the dissolution of silicone during the paraffin removal process in xylene before staining. Around the spacer, a connective tissue capsule of varying thickness was found in all rats, without signs of inflammation (Fig. 3, c). The capsule was widest near the bone fragments, and its thickness decreased as it moved away from the external surface of the bone. The connective tissue capsule was connected to the external surface of the bone fragments slightly away from their edges. It consisted of parallel bundles of collagen fibers with fibroblasts with basophilic

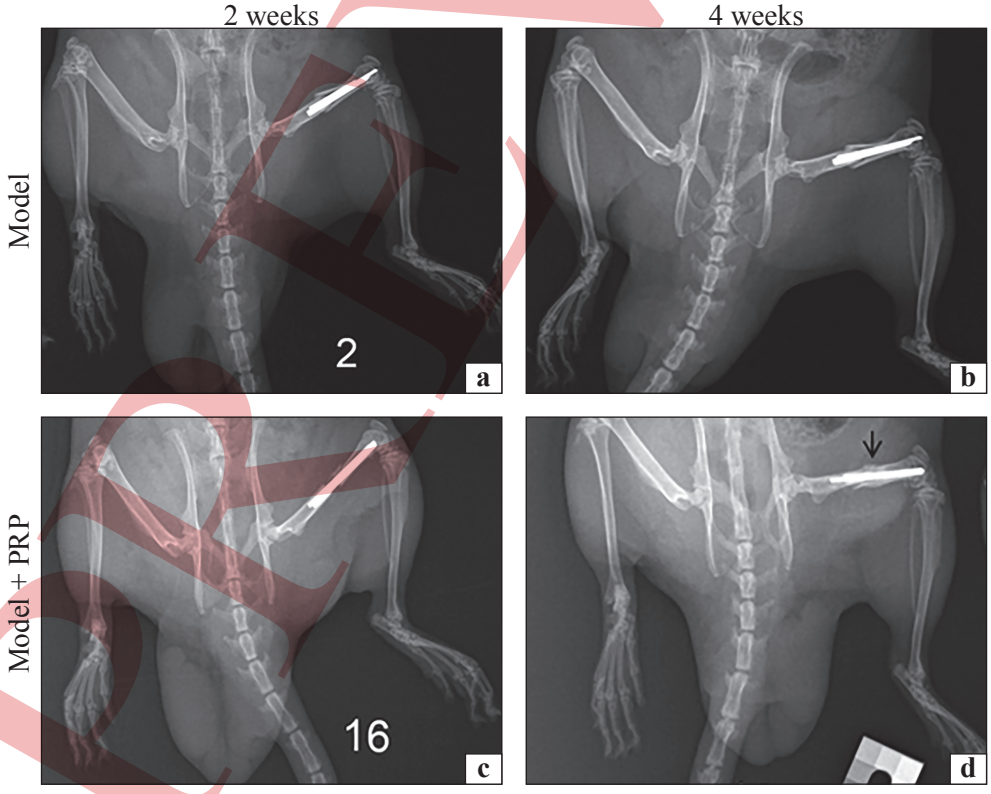

Fig. 2. X-rays of rats with atrophic non-union of the femoral bone with/without PRP injection on day 7, taken at 2 and 4 weeks post-surgery. Kirschner wires are positioned in the bone marrow canal at 2 weeks (a, c). Model: No signs of regenerate formation in the osteotomy zone at 4 weeks (b). Model+PRP: Periosteal regenerate in the distal bone fragment at 4 weeks (d)

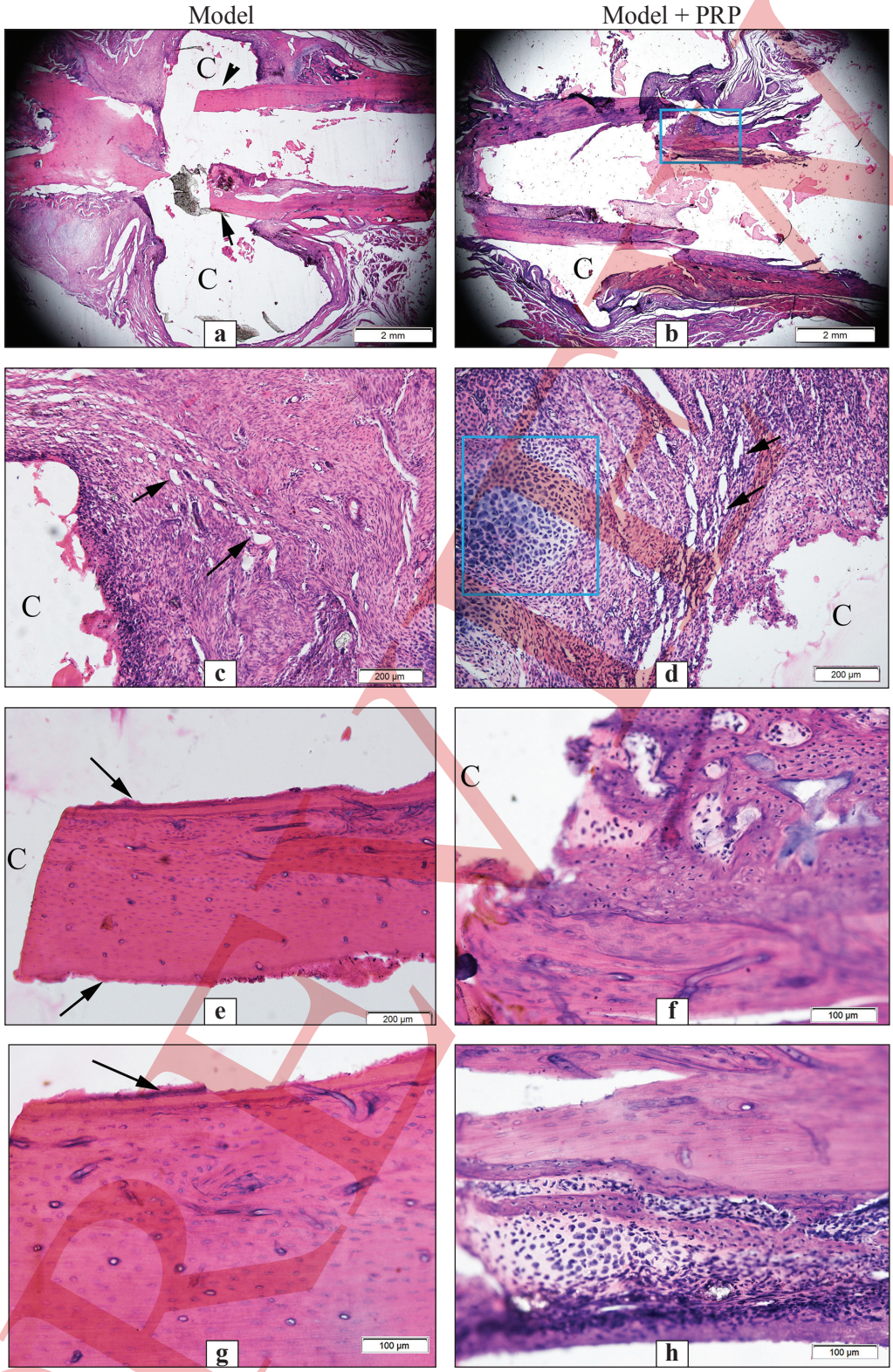

Fig. 3. Fracture sites 4 weeks after femoral osteotomy in rats with intramedullary fixation using Kirschner wire, separation of osteotomized bone fragments by a silicone spacer (S), and periosteal coagulation with/without PRP injection on the 7th day. The cavity from the spacer is surrounded by a connective tissue capsule of varying thickness (a, b). Non-union model (a, c, f, i): Fragments of the connective tissue capsule surrounding the silicone spacer with capillary-type vessels (arrows) in the thickness of the capsule (c). The ends of the osteotomized femoral bone fragments in rats with destroyed periosteum (f). Absence of newly formed tissues in the periosteal and endosteal zones (arrow) (f). Empty lacunae without osteocytes in the cortical matrix (i). Model + PRP (b, g, e, h): Capsule with signs of enchondral ossification (d). Periosteal and endosteal regenerates on one of the bone fragments (b). Newly formed trabeculae of spongy bone tissue in the periosteal zone (g). Fibrous bone tissue in the endosteal zone (k). Absence of osteocytes in lacunae in the bone matrix (g, k). Hematoxylin and eosin staining

nuclei tightly arranged between them (Fig. 3, c). In the periosteum, where the capsule was wider, areas of vascularization with capillary-type vessels of varying diameters were sometimes observed (Fig. 3, c).

In the cortical matrix near the osteotomy site, acellular areas without osteocytes were found, with a predominance of empty lacunae or debris inside them. Some areas exhibited uneven eosinophilic staining of the matrix (Fig. 3, e, i). No periosteal or endosteal structures were found near the osteotomy site where coagulation was performed during the surgical procedure (Fig. 3, e).

In one rat, bone formation was observed at the ends of the bone fragments on one side. In the remaining 5 out of 6 rats (83%), no bone formation was observed near the spacer site, neither in the periosteum nor in the endosteum.

Outside the injury zone (>2 mm from the osteotomy site), newly formed trabecular bone was found primarily in the periosteum, and in some rats, also in the endosteum. This bone consisted of fine trabeculae and osteocytes within the matrix. Osteoblasts with cuboidal shapes and basophilic nuclei were found on the surface of the bone trabeculae. In the periosteum and endosteum, where live osteocytes were absent in the cortical matrix, osteoclasts were observed.

In rats with the model of atrophic non-union of fractures, which received a PRP injection, a zone of osteotomy with two fragments and a cavity from the spacer surrounded by a connective tissue capsule was detected after 4 weeks, similar to animals without PRP injection (Fig. 3, b). In 80 % (4 out of 5) of the animals, bone tissue formation was observed on the fragments, primarily on one of the fragments (Fig. 3, b), both in the periosteum and in the endosteum. The significance of these changes compared to the model was confirmed (χ^2 (2, n = 11) = 4.41, p = 0.036). The bone tissue was spongy in the periosteal zone and coarse fibrous in the endosteal zone (Fig. 3, g, k). In two animals, the formation of bone regenerate was more intense than in others, with complete remodeling of one fragment. Just as in the model, the cortical matrix at the ends of the fragments contained empty lacunae without osteocytes, and areas without new tissue were found at the ends of the fragments in each rat. The connective tissue capsule had a similar structure as in the model (Fig. 3, d), but in animals with more pronounced tissue formation, capillary-type blood vessels were denser in the capsule, and areas of cartilage tissue with hypertrophic chondrocytes were found, indicating endochondral ossification.

Discussion

As a result of the transverse osteotomy at the mid-diaphyseal level of the femur, fixation with a Kirschner wire, periosteal coagulation, and placement of a silicone spacer, atrophic non-union of the fracture was achieved 4 weeks after surgery. At the same time, this is only a localized disturbance, meaning that normal periosteal function is preserved at a distance of 2 mm from the damage zone, confirmed by the presence of a formed periosteal regenerate of spongy bone tissue. The histological characteristics of the damage area correspond to those found in cases of atrophic non-union of fractures [11]: fibrous capsule around the spacer, absence of periosteal and endosteal regenerate, death of osteocytes in the cortical matrix of the fragments, and the absence of osteoclasts due to impaired vascularization. Radiographically, no signs of regenerative processes were observed in the damage zone.

In similar models of atrophic fracture non-union in small animals [17-23], periosteal destruction was performed, but in combination with the destruction of the endosteum [24], bone marrow [25, 26] to improve reproducibility. Another model similar to ours used latex-silicone foil [27] to isolate the fragments, but our approach uses a simpler method of fragment isolation with a silicone spacer placed on a Kirschner wire. Results have also been published using a silicone insert [28, 29] or a polysulfone plate [30], though without periosteal coagulation.

Our methodological approach in the created model resulted in atrophic non-union in 5 out of 6 rats. The worse results in one animal were likely due to insufficient periosteal coagulation, leading to new bone tissue formation at the ends of the fragments. This suggests that the proposed model can be successful in studying methods of treating atrophic non-unions.

The clinical effectiveness of PRP has not been fully proven, as indicated by an analysis of two systematic reviews [9, 31]. This is due to the heterogeneity of existing clinical data, as well as an incomplete understanding of the mechanisms of PRP action at the non-union site. In general, PRP is used in combination with bone grafts or MSCs, as well as in the form of transcutaneous local injections into the non-union fracture site. In most studies, PRP application had a positive effect on fracture healing, with only two studies finding no effect, and one showing worse results compared to recombinant BMP-7 [9, 31]. The use of PRP during surgery promoted faster bone healing and reduced pain on the visual analog scale in the PRP group (n = 16)

compared to the non-PRP group in patients with tibial diaphyseal non-unions [15]. In the case of a single transcutaneous PRP injection (n = 14) into the site of oligotrophic non-union in patients with diaphyseal fractures of long bones, healing was accelerated by approximately 3 weeks (19.07 weeks vs. 16.7 weeks), which is 13 % faster compared to using intramedullary fixation with a bone graft (n = 15) [17]. In our study, we anticipate that this effect of PRP may be due to its positive impact on the restoration of periosteal bone formation, which we experimentally verified.

The injection of PRP on day 7 in the model of atrophic non-union of femoral fractures in rats positively influenced the course of the regenerative process, which manifested in the formation of bone regenerate in the periosteal and endosteal zones at the edges of the bone fragments, where the periosteum had previously been destroyed. However, this process had an uneven character, likely related to the precision of PRP injection into the damage zone.

In a similar study on the effects of PRP in a non-union model in rabbits, where a spacer was inserted between the fragments of the tibia for 3 weeks, and after its removal, the cavity was filled with a synthetic bone implant (Coragraft) with or without PRP, it was found that such a combination ensured faster bone healing (radiologically and histologically) at 3, 7, and 11 weeks compared to using only Coragraft [32]. However, the use of PRP alone without Coragraft did not show similar results. The results of using PRP in such a non-union model under conditions of periosteal coagulation and during the acute phase of the fracture, as achieved in our study, are unknown.

The results obtained in our study are consistent with other experimental studies using PRP. For example, when PRP was injected during the formation of a tibial fracture in rabbits, the cortical regenerate was more mature at 6 and 12 weeks [33, 34]. In diabetic type I rats, an increase in cell differentiation in the periosteum was observed during femoral fracture healing with the injection of PRP starting from day 12 of the experiment, which may indicate an effect of PRP on the periosteum function or on the cells of adjacent tissues under systemic disturbances in the body [35].

Conclusions

Transverse osteotomy of the femur in rats with periosteal coagulation at 2 mm from the edges of the fragments, placement of a silicone spacer between the fragments, and intramedullary fixation with Kirschner wires, results in atrophic non-union of the fracture in 83% of cases after 4 weeks.

The injection of PRP into the damage zone on day 7 in this model has a positive effect on periosteal bone formation at the edges of the fragments with previously destroyed periosteum, but predominantly in only one of the fragments. This indicates the need for the development of a more accurate method for PRP injection into the damage zone.

Conflict of Interest. The authors declare no conflict of interest.

Prospects for Further Research. Further experimental studies on the combined use of bone morphogenetic proteins with platelet-rich plasma for stimulating periosteal bone formation in non-union fracture models.

Funding Information. The research was carried out within the framework of the scientific research project “Investigating the possibilities of biotechnology for the correction of reparative osteogenesis disorders in cases of non-unions and pseudoarthroses” (state registration No. 0123U100134).

Contributions of the Authors. Vorontsov P. M. — concept and design of the study, editing of the final version of the article; Maltseva V. Ye. — histological analysis, writing of the draft, and editing of the final version of the article; Danyshchuk Z. M. — histological analysis; Nikolenko O. A. — study design, experimental modeling in rats; Kovtun V. V. — experimental modeling in rats; Laponin S. I. — experimental modeling in rats. All authors reviewed and approved the final version of the article.

References

1. Impieri, L., Pezzi, A., Hadad, H., Peretti, G. M., Mangiavini, L., & Rossi, N. (2024). Orthobiologics in delayed union and non-union of adult long bones fractures: A systematic review. *In bone reports*, 21, 101760. https://doi.org/10.1016/j.bonr.2024.101760
2. Garnavos, C. (2017). Treatment of aseptic non-union after intramedullary nailing without removal of the nail. *Injury,* 48, S76–S81. https://doi.org/10.1016/j.injury.2017.04.022
3. Jarrassier, A., Py, N., de Rocquigny, G., Raux, M., Lasocki, S., Dubost, C., Bordier, E., Libert, N., Leclerc, T., Meaudre, É., & Pasquier, P. (2024). Lessons learned from the war in Ukraine for the anesthesiologist and intensivist: A scoping review. *Anaesthesia critical care & pain medicine, 43*(5), 101409. https://doi.org/10.1016/j.accpm.2024.101409
4. Lurin, I., Burianov, O., Yarmolyuk, Y., Klapchuk, Y., Derkach, S., Gorobeiko, M., & Dinets, A. (2024). Management of severe defects of humerus in combat patients injured in Russo-Ukrainian war. *Injury, 55*(2), 111280. https://doi.org/10.1016/j.injury.2023.111280
5. Gagnon, D., Mouallem, M., Leduc, S., Rouleau, D. M., & Chapleau, J. (2024). A systematic scoping review of the latest data on orthobiologics in the surgical treatment of non-union. *Orthopaedics and traumatology: surgery and research, 110*(6), 103896). https://doi.org/10.1016/j.otsr.2024.103896
6. Lana, J. F. S. D., da Fonseca, L. F., Macedo, R. D. R., Mosaner, T., Murrell, W., Kumar, A., Purita, J., & de sAndrade, M. A. P. (2021). Platelet-rich plasma vs bone marrow aspirate concentrate: An overview of mechanisms of action and orthobiologic synergistic effects. *World journal of stem cells, 13*(2), 155–167. https://doi.org/10.4252/wjsc.v13.i2.155
7. Bacevich, B. M., Smith, R. D. J., Reihl, A. M., Mazzocca, A. D., & Hutchinson, I. D. (2024). Advances with Platelet-Rich Plasma for Bone Healing. *Biologics: targets and therapy*, 18, 29–59. https://doi.org/10.2147/BTT.S290341
8. Wang, L., Tower, R. J., Chandra, A., Yao, L., Tong, W., Xiong, Z.,

Tang, K., Zhang, Y., Liu, X. S., Boerckel, J. D., Guo, X., Ahn, J., & Qin, L. (2019). Periosteal Mesenchymal Progenitor Dysfunction and Extraskeletally-Derived Fibrosis Contribute to Atrophic Fracture Nonunion. *Journal of bone and mineral research, 34*(3), 520–532. https://doi.org/10.1002/jbmr.3626

9. Jamal, M. S., Hurley, E. T., Asad, H., Asad, A., & Taneja, T. (2022). The role of Platelet Rich Plasma and other orthobiologics in bone healing and fracture management: A systematic review. *Journal of clinical orthopaedics and trauma*, 25, 101759. https://doi.org/10.1016/j.jcot.2021.101759
10. Dai, H., Zhang, H., Qiu, Z., & Shi, Q. (2023). Periosteum-derived skeletal stem cells encapsulated in platelet-rich plasma enhance the repair of bone defect. *Tissue and cell*, 83, 102144. https://doi.org/10.1016/j.tice.2023.102144
11. Panteli, M., Vun, J. S. H., Pountos, I., J. Howard, A., Jones, E., & Giannoudis, P. V. (2022). Biological and molecular profile of fracture non-union tissue: A systematic review and an update on current insights. *Journal of cellular and molecular medicine, 26*(3), 601–623. https://doi.org/10.1111/jcmm.17096
12. Narasimhulu, C. A., & Singla, D. K. (2020). The role of bone morphogenetic protein 7 (BMP-7) in inflammation in heart diseases. *Cells, 9* (2), 280. https://doi.org/10.3390/cells9020280
13. Law of Ukraine No. 3447-IV, article 26. On the protection of animals from cruel treatment. Kyiv, 21 February, 2006. (In Ukrainian)
14. European convention for the protection of vertebrate animalsused for experimental and other scientific purposes: Strasbourg,18 March 1986. (2000).
15. Maruyama, M., Rhee, C., Utsunomiya, T., Zhang, N., Ueno, M., Yao, Z., & Goodman, S. B. (2020). Modulation of the Inflammatory Response and Bone Healing. *Frontiers in endocrinology*, 11, 386. https://doi.org/10.3389/fendo.2020.00386
16. Vorontsov, P. M., Ashukina, N. O., Maltseva, V. Y., Danyshchuk, Z. M., Nikolchenko, O. A., & Samoylova, K. M. (2023). Histological evaluation of reparative osteogenesis in critical size femoral bone defects in rats of different ages after introduction of allografts saturated with blood plasma growth factors. *Orthopaedics, Traumatology and Prosthetics, 2023*(2), 25–32. https://doi.org/10.15674/0030-59872023225-32
17. Oktaş, B., Orhan, Z., Erbil, B., Değirmenci, E., & Ustündağ, N. (2014). Effect of extracorporeal shock wave therapy on fracture healing in rat femural fractures with intact and excised periosteum. *Eklem hastaliklari ve cerrahisi = joint diseases & related surgery, 25*(3), 158–162. https://doi.org/10.5606/ehc.2014.33
18. Wu, X.-Q., Wang, D., Liu, Y., & Zhou, J.-L. (2021). Development of a tibial experimental non-union model in rats. *Journal of orthopaedic surgery and research, 16*(1), 261. https://doi.org/10.1186/s13018-021-02408-3
19. Eckardt, H., Ding, M., Lind, M., Hansen, E. S., Christensen, K. S., & Hvid, I. (2005). Recombinant human vascular endothelial growth factor enhances bone healing in an experimental nonunion model. *The journal of bone and joint surgery. British Volume, 87*(10), 1434–1438. https://doi.org/10.1302/0301-620X.87B10.16226
20. Brownlow, H. C., Reed, A., & Simpson, A. H. R. W. (2002). The vascularity of atrophic non-unions. *Injury, 33*(2), 145–150. https://doi.org/10.1016/s0020-1383(01)00153-x
21. Reed, A. A. C., Joyner, C. J., Isefuku, S., Brownlow, H. C., & Simpson, A. H. R. W. (2003). Vascularity in a new model of atrophic nonunion. *The journal of bone and joint surgery. British Volume, 85*(4), 604–610. https://doi.org/10.1302/0301-620x.85b4.12944
22. Sharun, K., Pawde, A. M., Banu S, A., Manjusha, K. M., Kalaiselvan, E., Kumar, R., Kinjavdekar, P., & Amarpal. (2021). Development of a novel atrophic non-union model in rabbits: A preliminary study. *Annals of medicine and surgery,* 68. https://doi.org/10.1016/j.amsu.2021.102558
23. Chaubey, A., Grawe, B., Meganck, J. A., Dyment, N., Inzana, J., Jiang, X., Connolley, C., Awad, H., Rowe, D., Kenter, K., Goldstein, S. A., & Butler, D. (2013). Structural and biomechanical responses of osseous healing: a novel murine nonunion model. *Journal of orthopaedics and traumatology : official journal of the italian society of orthopaedics and traumatology, 14*(4), 247–257. https://doi.org/10.1007/s10195-013-0269-4
24. Tawonsawatruk, T., Kelly, M., & Simpson, H. (2014). Evaluation of native mesenchymal stem cells from bone marrow and local tissue in an atrophic nonunion model. *Tissue engineering. part C, methods, 20*(6), 524–532. https://doi.org/10.1089/ten.TEC.2013.0465
25. Shimizu, T., Akahane, M., Morita, Y., Omokawa, S., Nakano, K., Kira, T., Onishi, T., Inagaki, Y., Okuda, A., Kawate, K., & Tanaka, Y. (2015). The regeneration and augmentation of bone with injectable osteogenic cell sheet in a rat critical fracture healing model. *Injury, 46*(8), 1457–1464. https://doi.org/10.1016/j.injury.2015.04.031
26. Onishi, T., Shimizu, T., Akahane, M., Okuda, A., Kira, T., Omokawa, S., & Tanaka, Y. (2020). Robust method to create a standardized and reproducible atrophic non-union model in a rat femur. *Journal of orthopaedics*, 21, 223–227. https://doi.org/10.1016/j.jor.2020.03.040
27. Schmidhammer, R., Zandieh, S., Mittermayr, R., Pelinka, L. E., Leixnering, M., Hopf, R., Kroepfl, A., & Redl, H. (2006). Assessment of bone union/nonunion in an experimental model using microcomputed technology. *The journal of trauma, 61*(1), 199–205. https://doi.org/10.1097/01.ta.0000195987.57939.7e
28. Schützenberger, S., Kaipel, M., Schultz, A., Nau, T., Redl, H., & Hausner, T. (2014). Non-union site debridement increased the efficacy of rhBMP-2 in a rodent model. *Injury, 45*(8), 1165–1170. https://doi.org/10.1016/j.injury.2014.05.004
29. Skaliczki, G., Weszl, M., Schandl, K., Major, T., Kovács, M., Skaliczki, J., Redl, H., Szendrői, M., Szigeti, K., Máté, D., Dobó-Nagy, C., & Lacza, Z. (2012). Compromised bone healing following spacer removal in a rat femoral defect model. *Acta physiologica Hungarica, 99*(2), 223–232. https://doi.org/10.1556/APhysiol.99.2012.2.16
30. Cheng, A., Krishnan, L., Pradhan, P., Weinstock, L. D., Wood, L. B., Roy, K., & Guldberg, R. E. (2019). Impaired bone healing following treatment of established nonunion correlates with serum cytokine expression. *Journal of orthopaedic research : official publication of the orthopaedic research society, 37*(2), 299–307. https://doi.org/10.1002/jor.24186
31. Roffi, A., Di Matteo, B., Krishnakumar, G. S., Kon, E., & Filardo, G. (2017). Platelet-rich plasma for the treatment of bone defects: from pre-clinical rational to evidence in the clinical practice. A systematic review. *International orthopaedics, 41*(2), 221–237. https://doi.org/10.1007/s00264-016-3342-9
32. Kanthan, S. R., Kavitha, G., Addi, S., Choon, D. S. K., & Kamarul, T. (2011). Platelet-rich plasma (PRP) enhances bone healing in non-united critical-sized defects: a preliminary study involving rabbit models. *Injury, 42*(8), 782–789. https://doi.org/10.1016/j.injury.2011.01.015
33. Canbeyli, İ. D., Akgun, R. C., Sahin, O., Terzi, A., & Tuncay, İ. C. (2018). Platelet-rich plasma decreases fibroblastic activity and woven bone formation with no significant immunohistochemical effect on long-bone healing: An experimental animal study with radiological outcomes. *Journal of orthopaedic surgery, 26*(3). https://doi.org/10.1177/2309499018802491
34. Atik, A., Sargin, S., Meriç, G., & Ceylan, C. (2021). Immunohistological Effects of Transforming Growth Factor-ß via Platelet-Rich Plasma On Segmental Bone Defects: An Animal Study. *Turkish journal of veterinary and animal sciences, 45*(2), 363–371. https://doi.org/10.3906/vet-2010-1
35. Gandhi, A., Doumas, C., O'Connor, J. P., Parsons, J. R., & Lin, S. S. (2006). The effects of local platelet rich plasma delivery on diabetic fracture healing. *Bone, 38*(4), 540–546. https://doi.org/10.1016/j.bone.2005.10.019

The article has been sent to the editors	Received after review	Accepted for printing
11.11.2025	28.01.2026	02.02.2026

STIMULATION OF PERIOSTEAL BONE FORMATION WITH PLATELET-RICH PLASMA IN A RAT MODEL OF FEMORAL ATROPHIC NON-UNION

P. M. Vorontsov, V. Ye. Maltseva, Z. M. Danyshchuk, O. A. Nikolchenko, V. V. Kovtun, S. I. Laponin

Sytenko Institute of Spine and Joint Pathology National Academy of Medical Sciences of Ukraine, Kharkiv

✉ Petro Vorontsov, MD, PhD in Traumatology and Orthopaedics: vorontsov64@ukr.net

✉ Valentyna Maltseva, Phd in Biol. Sci.: maltseva.val.evg@gmail.com; https://orcid.org/0000-0002-9184-0536

✉ Zinayda Danyshchuk, MD: zinada1962@gmail.com; https://orcid.org/0000-0003-2968-3821

✉ Olga Nikolchenko, PhD in Biol. Sci.: o_nicolchenko@ukr.net; https://orcid.org/0000-0001-9808-9485

✉ Volodymyr Kovtun: vladimir.kovtin@gmail.com; https://orcid.org/0009-0008-6693-3897

✉ Stanislav Laponin, MD: laponin.st@gmail.com

ISSN 0030-5987. Orthopaedics, traumatology and prosthetics. 2026. № 1

УДК 616.727.2-089.5-089.168:616.831-005(045)

DOI: http://dx.doi.org/10.15674/0030-59872026170-75

Changes in cerebral oxygenation at different beach chair position angles as a predictor of early postoperative neurocognitive disorders

K. I. Lyzohub, M. V. Lyzohub, Z. A. Arutiunian

Sytenko Institute of Spine and Joint Pathology National Academy of Medical Sciences of Ukraine, Kharkiv

The beach chair position during shoulder surgery may lead to reduced cerebral oxygenation due to the hydrostatic gradient and anesthesia-induced vasodilation. Increasing the tilt angle potentially elevates the risk of cerebral hypoxia and early postoperative cognitive impairment. Objective. To investigate the effect of body tilt angle in the beach chair position on cerebral oxygenation parameters and the risk of early postoperative cognitive impairment. Methods. In this prospective randomized study, 75 ASA I–II patients undergoing shoulder surgery were assigned to a beach chair position at either 80° (n = 35) or 60° (n = 40). Regional cerebral oxygen saturation (rSO_2) was monitored using near-infrared spectroscopy (NIRS), along with hemodynamic parameters and BIS. Cognitive function was assessed using the MMSE preoperatively and 24 hours postoperatively. Quality of recovery was evaluated using the QoR-15 questionnaire, and discharge readiness using the Modified Aldrete score. Statistical analysis was performed using Student's t-test. Results. After positioning, mean rSO_2 was lower in the 80° group (71.9 ± 6.6 %) compared with the 60° group (83.3 ± 5.3 %; p < 0.001), with no significant differences in mean arterial pressure. At 24 hours, MMSE scores were lower in the 80° group (25.1 ± 1.5 vs 28.1 ± 1.3; p < 0.001). This group also demonstrated poorer QoR-15 scores and longer extubation time (p <0.001). Conclusions. A tilt angle of 80° is associated with greater reductions in rSO_2 and worse early cognitive outcomes.

Напівсидяче положення (НСП) пацієнта («пляжне крісло») під час операцій на плечовому суглобі може спричинити зниження церебральної оксигенації внаслідок гідростатичного градієнта й анестезіологічної вазодилатації. Збільшення кута нахилу потенційно підвищує ризик мозкової гіпоксії та ранніх післяопераційних когнітивних порушень. Мета. Дослідити вплив кута нахилу тіла в НСП на показники церебральної оксигенації та ризик розвитку ранніх післяопераційних когнітивних порушень. Методи. У проспективне рандомізоване дослідження включено 75 пацієнтів (ASA I–II), яких розподілили на 2 групи: 1 — оперували в НСП під кутом 80° (n = 35), 2 — втручання виконано за 60° (n = 40). Проводили моніторинг rSO_2 (NIRS), гемодинаміки. Когнітивний статус оцінювали за шкалою MMSE до операції та через 24 години. Якість відновлення визначали за QoR-15, швидкість пробудження — за шкалою Альдрете. Результати. Після позиціювання в НСП середній показник rSO_2 нижчий у групі 80° ((71,9 ± 6,6) % порівняно з 60° (83,3 ± 5,3) %; p < 0,001) за відсутності достовірних відмінностей середнього артеріального тиску. Через 24 год значення MMSE нижче у групі 80° (25,1 ± 1,5 проти 28,1 ± 1,3; p < 0,001). У цій групі також відзначено гірші показники QoR-15 та більшу тривалість екстубації (p < 0,001). Висновки. Збільшення кута нахилу тіла до 80° порівняно з 60° асоціюється з вираженим зниженням rSO_2 та гіршими ранніми когнітивними результатами. Ключові слова. Напівсидяче положення, мозкова оксигенація, кут нахилу тіла.

Keywords. Beach chair position, cerebral oxygenation, body tilt angle

Introduction

The "beach chair" position (semi-sitting, SSP) utilized during shoulder joint surgeries has been linked to documented occurrences of cerebral desaturation episodes, with a reported incidence as high as 17.5 % according to published literature [1].

The use of near-infrared spectroscopy (NIRS) technology provides continuous real-time monitoring of cerebral oxygenation and is considered an effective tool for reducing the incidence of cerebral desaturation. Assessment of brain function during general anesthesia, along with monitoring of hemodynamics and appropriate levels of anesthesia, is one of the main tasks of anesthesiologic monitoring. This is attributed to the fact that hypoxic brain injuries are still among the most frequent and serious anesthesiologic complications [2]. Non-invasive monitoring of cerebral oximetry is a key method for controlling and protecting brain perfusion, especially in situations where there is a risk of iatrogenic brain ischemia. Numerous clinical studies suggest that, despite certain limitations, such monitoring is an important neuroprotective tool, especially in clinical situations associated with the risk of this impairment.

The SSP is routinely used during shoulder arthroplasty (SA) and arthroscopy; however, it is associated with the development of arterial hypotension, which can lead to reduced cerebral perfusion and, consequently, increase the risk of neurological injuries. Moreover, SA procedures are usually characterized by longer durations, which potentially increases the risk of brain hypoperfusion during the perioperative period. Cases of ischemic brain injury have been reported in healthy patients following surgery in the SSP due to hypoperfusion. Near-infrared spectroscopy is described as a non-invasive, continuous method for monitoring cerebral oxygen saturation; however, its impact on neurobehavioral outcomes remains underexplored [3]. Despite the existence of studies describing cerebral desaturation during surgeries, high-quality data on this topic remain limited. Analyzing 10 publications with a total sample of 24,701 patients, only one case of postoperative neurocognitive deficit was recorded, constituting 0.004 % of all observations. Additionally, 4 clinical reports, not included in the main studies, described 6 patients with catastrophic neurocognitive complications after SA in the SSP. The incidence of registered intraoperative cerebral desaturation cases varied from 0 to 100 %, with the average value being 41.1 % [4]. Monitoring and preventing intraoperative brain ischemia are crucial since a patient under anesthesia in the operating room cannot be neurologically assessed [5]. Most existing studies focus either on the frequency of cerebral desaturation or on hemodynamic parameters, without paying sufficient attention to the role of the specific angle of positioning as a modified risk factor. Data on threshold values of decreased rSO_2, which may be clinically significant for the development of cognitive impairments, also remain limited.

Purpose: To investigate the impact of body tilt angle in the "beach chair" position on cerebral oxygenation indicators and the risk of developing early postoperative cognitive impairments.

Materials and Methods

The study was carried out at the State Institution Professor M. I. Sytenko Institute of Spine and Joint Pathology of the National Academy of Medical Sciences of Ukraine. The study was approved by the local bioethics committee of the institution (protocol No. 257 dated 22.12.2025), conducted in compliance with the principles of Good Clinical Practice (ICH GCP), the Helsinki Declaration on Human Rights and Biomedicine (1977 edition), and the requirements of the current legislation of Ukraine. All patients involved in the study were properly informed about the purpose, plan, and conditions of the study and provided written informed consent to participate.

A prospective randomized study included 75 patients, who were divided into 2 groups: Group I (n = 35) — surgical intervention was performed in SSP at a tilt angle of 80°, and Group II (n = 40) — patients in SSP with a tilt angle of 60°. The average age of patients in Group I was (45.02 ± 13.55) years, and in Group II (44.87 ± 11.50).

Exclusion criteria: patients with arrhythmia, angina pectoris, respiratory failure, a history of acute cerebrovascular disorders, traumatic brain injury, transient ischemic attacks, or refusal to participate in the study.

The physical status of patients in the preoperative period was assessed using the American Society of Anesthesiologists (ASA) scale, with all patients being classified as ASA I–II. Initial patient positioning in both groups was in the standard position, i. e. lying on their back. After securing venous access, 12 ml/kg of volume loading was performed [6], and premedication included 75 mg pregabalin, 40 mg omeprazole before induction, and 10 mg diazepam. Induction consisted of 2 mg/kg of 1 % propofol solution, 0.2 mg of 0.005 % fentanyl solution, and muscle relaxation during tracheal intubation was ensured by administering 0.1 mg/kg of succinylcholine and,

thereafter, maintaining muscle relaxation with 0.3 mg/kg of atracurium besylate. After securing the airway and transitioning the patient to mechanical ventilation with the Drager Atlan A300 (pressure support mode), general anesthesia was maintained with 1 % propofol based on the bispectral index (BIS) values (propofol dosage ranged from 4.5 to 6.5 mg/kg/h). Analgesia was provided with a 0.005 % fentanyl solution. Ten minutes after induction, patients were positioned in SSP. Peripheral blood oxygen saturation (SpO2), non-invasive systolic arterial pressure (SAP), diastolic arterial pressure (DAP), and mean arterial pressure (MAP) were measured using the Mediana YM 6000 monitor. The first measurement was taken immediately upon arrival in the operating room and then every 5 minutes thereafter. BIS monitoring (COVIDEN) was used to control sedation depth and adjust the propofol infusion; according to the manufacturer's recommendations, the target BIS value for general anesthesia was between 40 and 60. The manufacturer indicates that the BIS has a processing delay of 5-10 seconds [7]. Given that CO_2 concentration affects cerebral vascular tone [8], end-tidal carbon dioxide ($ETCO_2$) was continuously measured in both groups and maintained within the range of 35–45 mm Hg. Cerebral oxygenation (rSO_2) was monitored using the INVOS 5100 Regional Oximeter. The speed of awakening was assessed using the Aldrete scale [9], extubation time, and Quality of Recovery-15 (QoR-15) were assessed 24 hours later. Cognitive impairments were evaluated preoperatively and 24 hours postoperatively using the Mini Mental State Examination. Early postoperative hemodynamic responses to position changes were analyzed.

Statistical Analysis

The obtained data were analyzed using IBM SPSS 9.0 software. Normal distribution of the samples was checked using the Kolmogorov-Smirnov test. The mean values and standard deviations were calculated. Differences between groups were evaluated using the Student's t-test.

Results

Patients in both groups were comparable in terms of age, duration of surgery, and blood loss (Table 1).

Assessment of changes in the main hemodynamic parameters of SBP, DBP, pulse, as well as non-invasive cerebral oxygenation monitoring (NIRS) showed no significant differences before positioning. After positioning, there was a statistically significant difference between the groups in terms of hemodynamic parameters and rSO_2: the average rSO_2 value in Group I was 71.97 ± 6.59, while in Group II it was 83.3 ± 5.26 ($p < 0.001$). No statistically significant differences were found in arterial pressure indicators; specifically, the average SAP in Group I was 102.91 ± 13.13, and in Group II it was 108.35 ± 12.57 ($p = 0.07$), while the DAP in Group I was 65.2 ± 10.90 and in Group II it was 68.97 ± 11.02 ($p = 0.14$). However, a significant difference was found in pulse rate, with the average pulse in Group I being 87.05 ± 11.79, while in Group II it was 80.9 ± 14.9 ($p < 0.001$). In Group I, two patients had minimal rSO_2 levels: a 81-year-old man had an rSO_2 of 68 %, and a 49-year-old had an rSO_2 of 61 %. The data obtained are summarized in Table 2.

During the assessment of cognitive functions before surgery, no significant differences were found between the study groups. However, their analysis 24 hours postoperatively revealed a significant difference between the groups, specifically the average Mini-Mental State Examination (MMSE) score in Group I was 25.17 ± 1.50, while in Group II it was 28.17 ± 1.35 ($p < 0.001$). The clinical picture was characterized by mild short-term memory disturbances (episodic forgetting of dates), attention reduction, and slower thinking and concentration processes. At the same time, the patients remained critically aware of their condition (Table 3).

The study of extubation duration from the end of the surgery revealed statistical significance: the average extubation time in Group I was 22.75 ± 11.20 minutes, while in Group II it was 14.17 ± 7.96 minutes ($p < 0.001$). Moreover, there was a difference in the incidence of orthostatic collapse: in Group I, postural hypotension occurred in 7 patients, while in Group II it was observed in 3 cases, making it 15.5 % and 8.57 %, respectively. Regarding the safety of transferring patients to the recovery unit, no statistical difference was found ($p = 0.49$).

A statistically significant difference was found between the groups on the QoR-15 scale: the average score in Group I was 130.82 ± 3.73, while in Group II it was 141.35 ± 3.64 ($p < 0.001$).

Table 1

Comparison of age, duration of surgical intervention, blood loss, and cognitive functions in patients of the study groups

Group	Age of patients	Blood loss (ml)	Duration of surgery (min)
I	45.02 + 13.55	235.85 + 62.13	119.02 + 15.03
II	44.87 + 11.50	231.28 + 55.11	120.,08 + 18.07

Discussion

This study examined the effect of body position, particularly the perioperative tilt angle in the BCP, on cerebral oxygenation and the development of cognitive dysfunctions in the early postoperative period. At a tilt angle of 80°, a significant reduction in cerebral oxygenation was observed, with the lowest rSO_2 value being 61 %. The clinical manifestations were limited to minimal cognitive changes, including slight reduction in operational memory, attention, and cognitive processing speed. It should be noted that 15.5 % of patients experienced orthostatic collapse after verticalization, with the average age of patients being (48.71 ± 6.57) years. The maximum decrease in rSO_2 was up to 22 % from baseline values of cerebral oximetry. Furthermore, a larger tilt angle was associated with worse recovery quality scores on the QoR-15 scale and longer extubation times. This may reflect the complex impact of positional factors on cerebral oxygenation, autonomic regulation, and early functional recovery. The incidence of postural hypotension was higher in Group I, which aligns with the physiological mechanisms of blood redistribution in the upright position.

According to the data obtained by R. M. Cox et al., after examining 41 patients who were divided into 2 groups based on the use of open NIRS monitoring, 7 episodes of cerebral desaturation were recorded, with 5 cases observed in the group with open NIRS monitoring and 2 in the control group. According to the results of cognitive function assessment using the MoCA scale, no cognitive disorders were detected in the early postoperative period, as well as at 2 and 6 weeks after surgery [1]. In the study by J. Chan et al., among 25 patients in the BCP at 30º, cerebral desaturation was recorded in 19 patients, and in 42 % of cases, it occurred specifically during positioning [10]. A. Özgültekin et al. studied the incidence of cognitive disorders and episodes of arterial hypotension in individuals operated on in the BCP at 45° and 90°, considering age-related characteristics. According to the MMSE scale assessment, cognitive changes were observed in 14 % of patients. In patients under 65 years of age, rSO_2 reduction was up to 18 % of the initial level, while in those older than 65, it was 26 % [11].

At the same time, J. A. Aguirre et al. noted that during the observation of 40 patients in the beach chair position, the frequency of cerebral desaturation cases was 5 %. In all subjects, a significant decrease in arterial pressure was recorded 5 minutes after positioning in the beach chair position compared to baseline values (pressure was measured at the forearm at heart level). There was no decrease in either rSO_2 or maximum blood flow in the middle cerebral artery. However, 24 hours later, cognitive dysfunction was found in the patients. It should be noted that the perioperative systolic arterial pressure (SiAT) was ≤ 100 mm Hg [12]. Overall, the frequency of rSO_2 occurrences was 28.8 %, with a strong positive correlation observed between the development of desaturation and the height of the patient's elevation in the beach chair position (p = 0.056). The level of evidence IV suggests the possibility of stratifying patients by age, presence of hypertension, previous stroke, body mass index, diabetes, obstructive sleep apnea, and height. At the same time, the issue of determining the critical degree and duration of cerebral desaturation

Table 2

Comparison of hemodynamic indicators and rSO_2 in two groups

Parameter	Indicator						Statistical significance
	primary		after induction		after positioning		
	I	II	I	II	I	II	
SBP (mmHg)	143.88 + 22.00	138.57 + 18.77	116.25 + 17.24	111.75 + 14.66	102.91 + 13.13	108.35 + 12.57	—
DBP (mmHg)	86.05 + 13.02	84.55 + 12.61	73.85 + 10.77	71.45 + 11.06	65.2 + 10.90	68.97 + 11.02	—
Pulse, min	84.31 + 14.49	85.15 + 12.81	82.11 + 13.38	85.67 + 14.04	87.05 + 11.79	80.9 + 14.9	p < 0.001
rSO_2	97.08 + 1.42	95.78 + 1.56	85.17 + 8.59	85.50 + 6.54	71.97 + 6.59	83.3 + 5.26	p < 0.001

Table 3

Comparison of cognitive function data in two groups

Parameter	Indicator				Statistical difference
	before operation		after operation		
	I	II	I	II	
MMSE (бал)	28.12 + 1.12	27.92 + 1.15	25.17 + 1.50	28.17 + 1.35	p < 0.001

measured by the NIRS method, which is necessary for the formation of postoperative neurocognitive deficit, remains unresolved. This emphasizes the need for further research to clarify the threshold values of desaturation and assess their clinical significance for postoperative neurocognitive prognosis [13]. The data obtained confirm that the perioperative body tilt angle is a clinically significant modified factor that affects cerebral oxygenation parameters and early cognitive outcomes. However, the study has limitations: a relatively small sample size, absence of long-term cognitive observation, and a lack of direct correlational analysis between the depth of desaturation and neurocognitive indicators.

Conclusions

The perioperative body tilt angle in the semi-sitting position is a significant factor affecting cerebral oxygenation levels and is one of the factors associated with the development of postoperative cognitive disorders.

Conflict of Interest. The authors declare no conflict of interest.

Perspectives for Further Research. Future studies should focus on determining individual threshold values for cerebral desaturation and limits of autoregulation associated with the development of postoperative cognitive disorders. Additionally, the development of personalized monitoring algorithms and optimization of hemodynamics to improve neurocognitive outcomes should be explored.

Funding Information. There is no external financial support.

Authors' Contributions. Lyzohub K. I. — development of the research concept, assessment of findings; Lyzohub M. V. — supervision of the research; Arutyunyan Z. A. — statistical analysis, summarizing the conclusions.

References

1. Cox, R. M., Jamgochian, G. C., Nicholson, K., Wong, J. C., Namdari, S., & Abboud, J. A. (2018). The effectiveness of cerebral oxygenation monitoring during arthroscopic shoulder surgery in the beach chair position: A randomized blinded study. *Journal of shoulder and elbow surgery, 27*(4), 692–700. https://doi.org/10.1016/j.jse.2017.11.004
2. Vutskits, L., & Xie, Z. (2016). Lasting impact of general anaesthesia on the brain: Mechanisms and relevance. Nature reviews neuroscience, 17(11), 705–717. https://doi.org/10.1038/nrn.2016.128
3. Aguirre, J., Borgeat, A., Trachsel, T., Cobo del Prado, I., De Andrés, J., & Bühler, P. (2014). Cerebral oxygenation in patients undergoing shoulder surgery in beach chair position: Comparing general to regional anesthesia and the impact on neurobehavioral outcome. *Revista Española de anestesiología y reanimación, 61*(2), 64–72. https://doi.org/10.1016/j.redar.2013.08.002
4. Salazar, D. H., Davis, W. J., Ziroğlu, N., & Garbis, N. G. (2019). Cerebral desaturation events during shoulder arthroscopy in the beach chair position. *JAAOS: global research and reviews, 3*(8), e007. https://doi.org/10.5435/jaaosglobal-d-19-00007
5. Jin, X., Li, P., Michalski, D., Li, S., Zhang, Y., Jolkkonen, J., Cui, L., Didwischus, N., Xuan, W., & Boltze, J. (2022). Perioperative stroke: A perspective on challenges and opportunities for experimental treatment and diagnostic strategies. *CNS neuroscience & therapeutics, 28*(4), 497–509. https://doi.org/10.1111/cns.13816
6. Lyzogub, K., & Lyzogub, M. (2025). The impact of preoperative volume overload on hemodynamic parameters during shoulder arthroscopy. *Orthopaedics traumatology and prosthetics,* (1), 45–49. https://doi.org/10.15674/0030-59872025145-49
7. Ferreira, A. L., Mendes, J. G., Nunes, C. S., & Amorim, P. (2019). Evaluation of Bispectral index time delay in response to anesthesia induction: An observational study. Brazilian Journal of Anesthesiology (English Edition), 69(4), 377-382. https://doi.org/10.1016/j.bjane.2019.04.006
8. Lafave, H. C., Zouboules, S. M., James, M. A., Purdy, G. M., Rees, J. L., Steinback, C. D., Ondrus, P., Brutsaert, T. D., Nysten, H. E., Nysten, C. E., Hoiland, R. L., Sherpa, M. T., & Day, T. A. (2019). Steady-state cerebral blood flow regulation at altitude: Interaction between oxygen and carbon dioxide. *European Journal of applied physiology, 119*(11-12), 2529–2544. https://doi.org/10.1007/s00421-019-04206-6
9. S. Ishag. (2025). Aldrete Scoring System Ding Ding, StatPearls Publishing.
10. Chan, J. H., Perez, H., Lee, H., Saltzman, M., & Marra, G. (2020). Evaluation of cerebral oxygen perfusion during shoulder arthroplasty performed in the semi–beach chair position. *Journal of shoulder and elbow surgery, 29*(1), 79–85. https://doi.org/10.1016/j.jse.2019.05.022
11. Ozgultekın, A. (2023). Cerebral oxygen desaturation and postoperative cognitive effects in elderly patients operated in beach chair position. *Haydarpasa numune training and research hospital medical journal.* https://doi.org/10.14744/hnhj.2022.70446
12. Aguirre, J. A., Märzendorfer, O., Brada, M., Saporito, A., Borgeat, A., & Bühler, P. (2016). Cerebral oxygenation in the beach chair position for shoulder surgery in regional anesthesia: Impact on cerebral blood flow and neurobehavioral outcome. *Journal of clinical anesthesia,* 35, 456–464. https://doi.org/10.1016/j.jclinane.2016.08.035
13. Pant, S., Bokor, D. J., & Low, A. K. (2014). Cerebral oxygenation using near-infrared spectroscopy in the beach-chair position during shoulder arthroscopy under general anesthesia. *Arthroscopy: the journal of arthroscopic & related surgery, 30*(11), 1520–1527. https://doi.org/10.1016/j.arthro.2014.05.042

The article has been sent to the editors	Received after review	Accepted for printing
19.01.2026	10.02.2026	02.03.2026

CHANGES IN CEREBRAL OXYGENATION AT DIFFERENT BEACH CHAIR POSITION ANGLES AS A PREDICTOR OF EARLY POSTOPERATIVE NEUROCOGNITIVE DISORDERS

K. I. Lyzohub, M. V. Lyzohub, Z. A. Arutiunian

Sytenko Institute of Spine and Joint Pathology National Academy of Medical Sciences of Ukraine, Kharkiv

✉ Kseniia Lyzohub, MD, PhD: kslizogub@gmail.com; https://orcid.org/0000-0001-9149-7208

✉ Mykola Lyzohub, MD, DMSci: nlizogub@gmail.com; https://orcid.org/0000-0003-4776-1635

✉ Zorik Arutiunian, MD, PhD: zorik.dr@gmail.com; https://orcid.org/0000-0001-5918-0905

REHABILITATION

УДК 616.728.3-089.22-089.168:615.477.4](045)

DOI: http://dx.doi.org/10.15674/0030-59872026176-84

Analysis of the quality of rehabilitation of patients with patellar tendinopathy using a robotic orthosis

A. S. Gerasymenko, O. Ye. Yurik, S. I. Gerasymenko, O. V. Mayko, V. V. Hromadskyi, A. V. Hryschenko

SI «National Institute of Traumatology and Orthopedics of the NAMS of Ukraine», Kyiv

Objective. To analyze the results of treatment using a robotic orthosis during the rehabilitation of patients following arthroscopy who developed pain in the anterior compartment of the knee joint (KJ), using clinical and instrumental assessments of their condition. Methods. We reviewed the medical records of 120 patients with anterior knee pain syndrome (46 women aged (28.6 ± 7) years and 74 men aged (38.2 ± 8) years). Patients underwent rehabilitation in a robotic orthosis with various body weight support settings ranging from 65% to 10%. A multivariate analysis of clinical indicators was performed, including pain levels on the Visual Analog Scale (VAS) and the Anterior Knee Pain Scale (AKPS). Joint functional characteristics were assessed using the Knee Society Score (KSS). Results. The functional status of 60 patients was analyzed. Six weeks after surgery, the mean VAS score was 3.8 ± 0.3 in group 1 and 1.8 ± 0.4 in group 2; the difference 2.00, $t \approx 30.99$, $p < 0.001$; for KSS (part 1) in group 1 — 68 ± 6.5; in group 2 — 83 ± 2.3; difference −15.00, $t \approx -16.85$, $p < 0.001$; for KSS (part 2), the means were 72 ± 4.8 versus 80 ± 3.2; difference –8.00, $t \approx -10.74$, $p < 0.001$, indicating better function in group 2. The AKPS score was 64 ± 5.8 in group 1 and 76 ± 3.8 in group 2; difference −12.00, $t \approx -13.40$, $p < 0.001$. After 3 months, the VAS score in group 1 was 2.2 ± 0.6, and in group 2 — 1.2 ± 0.4; difference 1.00, $t \approx 10.74$, $p < 0.001$; for KSS (part 1) 78 ± 4.7 vs. 90 ± 2.2; difference −12.00, $t \approx -17.92$, $p < 0.001$; for KSS (part 2) — 80 ± 3.8 vs. 90 ± 1.8; difference −10.00, $t \approx -18.42$, $p < 0.001$; AKPS after 3 months was 76 ± 1.6 in group 1 and 89 ± 2.0 in group 2; difference −13.00, $t \approx -39.34$, $p < 0.001$. Conclusions. All confidence intervals for the differences do not include 0, so the differences are statistically significant; the effect sizes are large, indicating a clinically important advantage of using a robotic orthosis for pain reduction and improvement of upper limb function.

Мета. Проаналізувати результати лікування зі застосуванням роботичного ортезу під час реабілітації пацієнтів після артроскопії, у яких розвинувся біль у передньому відділі колінного суглоба (КС) за допомогою клінічного й інструментального оцінювання його стану. Методи. Вивчено історії хвороб 120 осіб із синдромом переднього болю в КС (46 жінок віком (28,6 ± 7) років і 74 чоловіків (38,2 ± 8) років). Пацієнтам проводилась реабілітація в роботизованому ортезі з різними налаштуваннями підтримки маси тіла від 65 до 10 %. Виконано багатофакторний аналіз клінічних показників, включаючи рівень болю за візуальною аналоговою шкалою (ВАШ) та Anterior Knee Pain Scale (AKPS). Вивчено функціональні характеристики суглоба за Knee Society Score (KSS). Результати. Проаналізовано функції пацієнтів із 60 осіб. Через 6 тижнів після операції середній ВАШ складав у групі 1 — 3,8 ± 0,3; у 2 — 1,8 ± 0,4; різниця 2,00, $t \approx 30,99$, $p < 0,001$; за KSS (част. 1) у групі 1 — 68 ± 6,5; у 2 — 83 ± 2,3; різниця −15,00, $t \approx -16,85$, $p < 0,001$; за KSS (част. 2) середні становили 72 ± 4,8 проти 80 ± 3,2; різниця –8,00, $t \approx -10,74$, $p < 0,001$, що свідчить про кращу функцію у групі 2. Показник AKPS був 64 ± 5,8 у групі 1 і 76 ± 3,8 у 2; різниця −12,00, $t \approx -13,40$, $p < 0,001$. Через 3 міс. ВАШ у групі 1 становив 2,2 ± 0,6, у 2 — 1,2 ± 0,4; різниця 1,00, $t \approx 10,74$, $p < 0,001$; за KSS (част. 1) 78 ± 4,7 проти 90 ± 2,2; різниця −12,00, $t \approx -17,92$, $p < 0,001$; за KSS (част. 2) — 80 ± 3,8 проти 90 ± 1,8; різниця −10,00, $t \approx -18,42$, $p < 0,001$; AKPS через 3 міс. становив 76 ± 1,6 у групі 1 і 89 ± 2,0 у 2; різниця −13,00, $t \approx -39,34$, $p < 0,001$. Висновки. Усі довірчі інтервали для різниць не включають 0, отже відмінності є статистично значущими; величини ефекту великі, що свідчить про клінічно важливу перевагу застосування роботичного ортезу для зниження болю та покращення функції КС. Ключові слова. Артроскопія колінного суглоба; реабілітація; роботизовані ортези; синдром «переднього болю» колінного суглоба; тендинопатія влаяної зв'язки наколінка; нейропластичність.

Key words. Knee arthroscopy; rehabilitation; robotic orthoses; Lokomat Pro; anterior knee pain syndrome; neuroplasticity

Introduction

Patellar tendinopathy is a common condition after arthroscopic procedures on the knee joint (KJ). It is associated with pain, functional limitations, and a reduction in the quality of life of patients [3]. Rehabilitation after knee arthroscopy is generally aimed at restoring mobility, muscle strength, and normal biomechanics. Its programs include controlled development of the range of motion, gradual load increase on the quadriceps, proprioceptive exercises, and work on gait and functional tasks [1, 2]. The goal is to reduce pain and swelling, restore muscle strength symmetry and coordination, as well as prevent contractures and chronic movement disorders. However, traditional rehabilitation approaches, which are based on relative rest and load management, are often lengthy and do not always ensure optimal recovery [4]. In patients diagnosed with patellar tendinopathy during the postoperative period, rehabilitation becomes more complicated and often yields unsatisfactory results. Pain during loading, a reduced range of motion, and quadriceps weakness complicate the execution of standard rehabilitation exercises, slowing progress and potentially leading to compensatory movement disorders [5–9]. These patients more often require modifications to protocols, namely slower load increments, targeted eccentric exercises, additional physiotherapeutic methods (ultrasound, laser, electrical muscle stimulation), and longer periods of activity restriction. As a result, recovery of function and return to preoperative activity levels may take considerably more time, and the risk of recurrence or chronic pain remains higher.

Currently, there is a demand for innovative methods that can accelerate and improve rehabilitation outcomes, especially for younger individuals seeking a swift return to physical activity [10]. Therefore, the use of advanced technologies, such as robotic rehabilitation, is becoming increasingly relevant in the context of optimizing recovery after arthroscopic interventions [10]. At the same time, in many cases, rehabilitation protocols are insufficiently detailed, complicating their application and objective assessment of results.

In this study, we compare the effectiveness of rehabilitation for individuals with patellar tendinopathy after knee arthroscopy using a robotic orthosis with traditional methods, focusing on objective recovery indicators and functional outcomes.

Purpose: To analyze the results of rehabilitation treatment using a robotic orthosis for patients who developed anterior knee pain after arthroscopy, through clinical and instrumental assessment of their condition, and to lay the foundation for the development of more effective and individualized rehabilitation protocols for patients with patellar tendinopathy.

Materials and Methods

We conducted a prospective study that included the following stages: patient examination before surgery, 14 days, 6 weeks, and 3 months after the operation. The study was conducted at the clinical base of the Department of Joint Diseases in Adults of the State Institution “Institute of Traumatology and Orthopedics of the National Academy of Medical Sciences of Ukraine” (Kyiv) and approved by the local ethics committee (protocol No. 1 dated 07.01.2026) in accordance with the ICH GCP amendment, the Helsinki Declaration of Human Rights and Biomedicine, and current Ukrainian legislation. All participating patients were informed about the study plan and conditions and provided written and verbal consent.

Inclusion Criteria: Age between 18 and 50 years, BMI < 30, confirmed meniscus injury (Stoller 3A-3B) on MRI, no other intra-articular structural injuries, history of arthroscopic intervention on KJ (resection of the affected part of the meniscus), development of pain in the anterior KJ area in the patellar tendon region, patellar tendinopathy confirmed by clinical and instrumental data within 14 days post-surgery.

Patients who had concomitant injuries of KJ structures (chondromalacia, injuries of the anterior/posterior cruciate ligaments, collateral ligaments, free bodies in the joint cavity) or joint dysplasia, high patella (patella alta), and degenerative changes in its ligaments on MRI were excluded.

Using simple randomization and gradual inclusion, 120 individuals with patellar tendinopathy (46 women, aged (28.6 ± 7) years, and 74 men (38.2 ± 8) years) were selected. The patients were divided into two groups:

1. Group 1 — Classical rehabilitation;
2. Group 2 — Rehabilitation using a robotic orthosis.

In Group 2, rehabilitation treatment started from the 15th day post-surgery. It consisted of 15 sessions and subsequent observation for up to 3 months after knee arthroscopy. A final examination was conducted and the patient's condition was evaluated using scales with and without the robotic orthosis [10-12].

The intervention performed on patients included arthroscopic resection of the damaged part of the medial meniscus (Stoller 3A-3B damage based on MRI results).

General principles of classical rehabilitation for group 1 [16] considering tendinopathy:

– Avoidance of early peak and rapid eccentric loads;

– Start with isometrics, gradually introduce eccentric exercises according to tolerance.

Phase 0 (0–3 days):

– Measures: ice compresses for 10–15 minutes several times a day, leg elevation, compression / elastic bandage, light movements in the ankle joint, isometric quadriceps contractions (10–20 seconds hold, 8–10 times/hour);

– Load: partial weight-bearing / walking with crutches as instructed by the surgeon.

Phase 1 (3–14 days):

– ROM: passive and active-passive exercises within the pain limit; avoid deep flexion if painful;

– Muscle work: isometric quadriceps, isometric adductors, light isometric exercises for the calf; 3–5 sets of 8–12 reps (holding for 10–20 seconds);

– Balance/proprioception: standing on both legs, gradual transition to single leg stance if possible;

– Tendinopathy prevention: isometric exercises to reduce pain (5–6 times a day, 30–45 seconds).

Phase 2 (2–6 weeks):

– ROM: full, slow ROM to tolerated limits; joint mobilization;

– Strength: isolation exercises (direct integration of quadriceps): partial squats to 45°, leg extension in sitting position (without pain), gradual load exercises; 3 sets of 10–15 reps;

– Tendinopathy: initial controlled eccentric exercises (e.g., slow eccentric squats/single-leg lowering or on a sloped plane) starting with low intensity twice a day, progression gradually; during exacerbations — return to isometrics;

– Cardio: low-resistance cycling, walking — gradually increasing duration;

– Frequency: 3–4 physiotherapy sessions per week plus home program.

Group 2 rehabilitation involved a robotic orthosis, with patients moving in it with various body weight support settings, from 65 % to 10 %. The duration of each session was 1 to 1.5 hours, 3–4 times per week.

Main rehabilitation stages using robotic orthosis:

1. Assessment of the patient's physical parameters — determining the physical condition and capabilities before starting the training;

2. Patient adaptation. Before the first session, patients were introduced to the device, placed in gloves, pants, or straps for smooth movement;

3. Individual device adjustment according to the patient's medical condition:

– Body weight support (BWS) level;

– Walking speed;

– Range of motion;

– Load according to the patient's specific needs.

4. Conducting the training:

– Automatic walking: Under the control of the robotic orthosis, the patient begins to walk with a natural or adapted gait;

– Symmetrical or asymmetrical program depending on the condition (training of both or one lower limb);

– Speed and load: The initial walking speed was set by the patient at a comfortable pace, usually 1.5 km/h, gradually increasing to 3.0 km/h. Load on the lower limbs was modeled by BWS, ranging dynamically from 100 % (full body weight support) to 10–20 %;

– Mobilization: Using the movement system of the device and the active participation of the patient, which contributes to the recovery of muscle tone, coordination, and motor skills.

5. Monitoring and adjustment:

– During the training session, activity, movement coordination, load, and walking speed of the patient are monitored.

6. Conclusion and results analysis:

– At the end of the session, progress is assessed, and parameters are recorded (session duration, distance, range of motion (L-ROM) in the lower limb, muscle strength (L-Force) in the lower limbs, level of stiffness or resistance to movement (L-Stiff)).

– Based on the results and the patient's condition, further rehabilitation strategies are planned.

Initial sessions are performed in a passive or moderately assisted walking mode with moderate weight support (BWS 30–50 %), low speed (approximately 0.3–0.6 m/s), and limited L-ROM to avoid deep flexion during early stages; the duration of active walking at the beginning is approximately 10–20 minutes, with the overall session lasting 30–45 minutes.

Progression occurs gradually: reduction in weight support to 10–30 %, increase in walking duration and speed, decrease in BWS, and extension of L-ROM as tolerance improves and pain decreases; L-Force is monitored to prevent peak loads during active extension in case of muscle weakness.

Among the subjective pain assessment methods used in the study, the Visual Analog Scale (VAS) [20] was used, allowing patients to self-assess pain level from 0 (no pain) to 10 (maximum pain), as well as

the Knee Society Score (KSS) and Kujala/Anterior Knee Pain Score (AKPS).

– KSS Scale includes the assessment of pain and function in the knee joint. The knee assessment allocates up to 100 points for indicators of range of motion (1 point for 5°, maximum 125°), stability (medial/lateral (15 points) and anterior/posterior (10 points)), and pain (50 points), subtracting points for lag in extension, presence of flexion contracture, and deformity (if the axis of the lower limb is < 5° or > 10° on radiological examination). The maximum score of 100 points indicates a well-aligned knee joint with a range of motion of 125°, almost complete absence of anterior-posterior or medial-lateral instability, and no pain. The functional score includes the walking distance (50 points) and stair climbing (50 points), taking into account the use of walking aids. A patient who can walk without restrictions and has no problems with stair climbing receives the maximum score in the Function Score subscale — 100.

– Anterior Knee Pain Scale (AKPS, Kujala Scale) is a 13-item self-reported questionnaire that evaluates subjective responses to specific activities and symptoms known to correlate with anterior knee pain syndrome. AKPS is scored from 0 to 100, with 100 being the highest possible score. Lower scores reflect greater pain and disability.

Pain in the anterior compartment of the KJ frequently leads to dysfunctions that cause difficulties during activities that load the KJ (running, squats, and stair climbing), and the AKPS assesses these types of activities. This index has high reliability for retesting and is a valuable tool for evaluating the patient's condition over time [13, 14]. It has been found that the four formats of the AKPS scale have acceptable standard measurement errors (from 0.82 to 3.00), high internal consistency (acoef = 0.83–0.91), equivalency between the short and long forms (r = 0.98), and moderate to high criterion validity, as determined by the physician's diagnosis: 0.92 (13-item form), 0.90 (long form), and 0.90 (short form) (6-item form). The AKPS questionnaire is an effective tool for epidemiological screening with valid and reliable assessment of anterior knee pain [15].

Dynamic analysis was used to assess changes in pain levels, joint functionality, and muscle strength throughout the observation period (pre-surgery examination, 14 days, 6 weeks, and 3 months after surgery).

Muscle strength in both patient groups was studied using the robotic orthosis at the indicated time intervals.

Clinical analysis is the most appropriate tool and standard criterion for diagnosing tendinopathy of the patellar tendon.

The first clinical task is to determine if the tendon is the source of the patient's symptoms. The most common finding in manual examination is tenderness at a focal point [21, 22]. While this may be observed along the entire length of the patellar tendon, it most commonly occurs at the lower portion and the distal attachment to the tibial tuberosity. Pain intensifies during loading on the knee extensors.

Functional tests for patients with patellar tendinopathy include jumping and landing after jumping [23].

The main differential diagnosis of patellar tendinopathy is patellofemoral pain syndrome, which is defined as a form of nonspecific, nonstructural knee pain around or behind the patella. This pain syndrome is characterized by crepitus or "grinding" under the patella during knee flexion and tenderness along the facets [24].

Statistical analysis was conducted using standard approaches. The analysis used averaged values of patient indicators. Quantitative data (mean (M) and standard deviation (SD)) in the study groups were compared both within groups and over the observation period.

Relative reduction in symptom severity (% reduction in pain intensity and functional improvement) was calculated. A comparative analysis of the groups was performed using the Welch-test.

Results

Main demographic and diagnostic characteristics of participants: The average age was (28.6 ± 7) years for women (18 %) and (38.2 ± 8) years for men (82 %). The average body mass index (BMI) of the subjects was (28.6 ± 6.0) kg/m². The most common type of procedure performed on the patients was arthroscopic resection of the damaged part of the medial meniscus (74 %) and debridement of fibrous growths causing impingement with joint structures (26 %). Table 1 presents data on the dynamics of pain level changes on pain and functional scales over the observation period.

Comparative analysis of the effectiveness of rehabilitation measures in both groups was conducted after the rehabilitation course (15 sessions), corresponding to the 6-week and 3-month post-intervention periods.

In the study, which included 60 patients in each group, the rehabilitation used in Group 2 showed consistently better clinical outcomes compared to Group 1 at both the early (6 weeks) and mid-term

(3 months) stages of recovery. By the 6th week, patients in Group 2 experienced significantly less pain: their average VAS was about half that of Group 1 (1.8 vs 3.8; 95 % CI 1.87–2.13, $p < 0.001$). Functional scales also showed noticeable improvement: for KSS (parts 1 and 2) and AKPS, the difference between groups ranged from 8 to 15 points in favor of Group 2, which was both statistically significant and clinically relevant.

In 3 months, Group 2 continued to show better results and even increased functional indicators: the VAS remained lower (1.2 vs 2.2; 95% CI 0.82–1.19, $p < 0.001$), and the KSS and AKPS showed significant improvement in knee joint function in Group 2 (differences ranging from 10 to 13 points, all 95 % CI excluding 0, $p < 0.001$). These data indicate that treatment in Group 2 not only reduces pain symptoms more quickly but also provides better recovery of knee joint function, which is important for returning to everyday activities and professional duties.

The overall effect sizes and confidence intervals confirm the stability and reliability of the observed differences: the intervals for mean differences are narrow and exclude 0, meaning the estimates are precise, and the large Cohen's d values suggest a clinically meaningful effect. From a practical perspective, this means that the approach used in Group 2 contributes to a faster reduction in pain, improved walking ability, and better functional outcomes in the postoperative period.

Study Limitations. The study has several limitations that should be considered when interpreting the results. In particular, the analysis did not include patients with cartilage damage, capsular-ligamentous damage of the knee joint, osteoarthritis stages II–IV according to Kellgren-Lawrence, or knee joint dysplasia, which limits the ability to generalize the results to severe forms of the disease. The selected age range (18–50 years) analyzed also does not allow definitive conclusions about the effectiveness of the therapy in older patients. It is worth noting that the study describes a relatively short follow-up period, which did not exceed 3 months. This does not allow for an objective evaluation of the long-term effectiveness and stability of functional results in the distant period. Therefore, large-scale prospective studies with standardized treatment approaches, clear evaluation criteria, and long-term follow-up periods are necessary.

Discussion

The obtained results allowed for a comprehensive analysis of the impact of robotic rehabilitation on functional recovery, pain levels, and quali ty of life of patients after knee arthroscopy. Our study revealed statistically significant improvements in the recovery of range of motion and functional indicators of the knee joint in Group 2, compared to the traditional rehabilitation group.

Specifically, as early as 4 weeks after the start of the rehabilitation course, patients in Group 2 showed significant improvement in physical functioning, pain reduction, and by 3 months, the physical functioning level in this group reached (90 ± 1.8) points, surpassing the traditional rehabilitation group with (80 ± 3.8), indicating near-complete recovery to the preoperative state. Statistically significant differences and large effect sizes that exclude 0 in the 95 % confidence intervals indicate a clinically important advantage of using robotic orthosis

Table 1

Dynamics of changes in the studied indicators before and after classical rehabilitation

Indicator	VAS	KSS		AKPS
		part 1	part 2	
Group 1: – before intervention;	6.9 ± 1.0	74 ± 5.2	62 ± 4.4	68 ± 4.3
after intervention: – 2 weeks; – 6 weeks; – 3 months	 5.2 ± 1.2 3.8 ± 0.3 2.2 ± 0.6	 38 ± 8.6 68 ± 6.5 78 ± 4.7	 32 ± 7.2 72 ± 4.8 80 ± 3.8	 28 ± 8.8 64 ± 5.8 76 ± 1.6
Group 2: – before intervention;	7.0 ± 1.2	78 ± 6.2	60 ± 5.3	68 ± 4.3
after intervention: – 2 weeks; – 6 weeks; – 3 months	 5.6 ± 1.0 1.8 ± 0.4 1.2 ± 0.4	 40 ± 7.4 83 ± 2.3 90 ± 2.2	 30 ± 6.8 80 ± 3.2 90 ± 1.8	 32 ± 8.4 76 ± 3.8 89 ± 2.0

Notes: VAS— Visual Analog Scale; KSS — Knee Society Score; AKPS — Anterior knee pain score.

Table 3

Comparison of changes in the studied indicators after rehabilitation in both groups

Indicators	Group 1	Group 2	CI	Welch	P
6 weeks after intervention:					
– VAS;	3.8 ± 0.3	1.8 ± 0.4	1.872; 2.128	$t \approx 31.0$	$p < 0.001$
– KSS Part 1;	68.0 ± 6.5	83.0 ± 2.3	−16.770; −13.230	$t \approx -16.8$	$p < 0.001$
– KSS Part 2;	72.0 ± 4.8	80.0 ± 3.2	−9.480; −6.520	$t \approx -10.7$	$p < 0.001$
– AKPS	64.0 ± 5.8	76.0 ± 3.8	−13.780; −10.220	$t \approx -13.4$	$p < 0.001$
3 months after intervention:					
– VAS;	2.2 ± 0.6	1.2 ± 0.4	0.815; 1.185	$t \approx 10.74$	$p < 0.001$
– KSS Part 1;	78.0 ± 4.7	90.0 ± 2.2	−13.330; −10.670	$t \approx -17.92$	$p < 0.001$
– KSS Part 2;	80.0 ± 3.8	90.0 ± 1.8	−11.080; −8.920	$t \approx -18.42$	$p < 0.001$
– AKPS	76.0 ± 1.6	89.0 ± 2.0	−13.655; −12.345	$t \approx -39.30$	$p < 0.001$

in pain reduction and improvement of joint function. This aligns with the results of previous studies, such as by S. Sancenzi et al., confirming the effectiveness of robotic systems in accelerating lower extremity function recovery after injuries and surgical interventions [25].

We demonstrated the high potential of using robotic orthosis in the rehabilitation process of patients with anterior knee pain syndrome after arthroscopy. The main outcomes are significant improvement in functional indicators, manifested by increased values in KSS and AKPS, which correspond to rapid recovery of movement functions and pain reduction.

The KSS values, which reflect the overall functional status of the knee joint, decreased in the first 2 weeks after the procedure, which suggests acute symptoms and limited motor activity during the acute period. However, by 6 weeks, the indicators had increased to levels almost comparable to the initial values (83 ± 2.3 and 80 ± 3.2, respectively) and stabilized above 90 by 3 months, corresponding to full functional recovery. Similarly, the AKPS scale values indicate significant improvement in both subjective and objective aspects of the knee joint condition.

These results align with numerous studies. T. M. Rossi et al., in their systematic review, noted that robotic rehabilitation contributes to faster functional recovery of the knee joint in patients with various pathologies [26]. A. C. Brito et al., in their meta-analysis, emphasized that the use of robotic systems positively affects joint range of motion, muscle strength, and the ability to move independently [27]. Additionally, S. Sancenzi et al. in their pilot study found that robotic devices help reduce pain and accelerate recovery after knee surgeries [28].

Furthermore, contemporary rehabilitation practice has concluded that robotic systems have advantages in stimulating neuromuscular pathways and creating conditions for more natural movements, which positively influence neuromuscular plasticity processes and contribute to more effective reintegration after injuries and surgeries. This confirms the potential of robotic devices not only for functional recovery but also for preventing complications due to muscle hypotrophy and weakness, which is especially important for patients with injuries or in the postoperative period, where early and adequate loading is a critical factor for preventing complications and ensuring faster recovery.

Although conservative methods for treating patellar tendinopathy, such as progressive loading of tendons and eccentric exercises, demonstrate effectiveness [26, 31], our study points to the potential benefits of integrating robotic systems. It was found that robotic walking training allows the lower limbs to perform alternative and circular movements (effectively correcting their movement after ACL reconstruction and improving walking ability and muscle strength) [32]. Systems that provide resistance during walking can have significant biomechanical effects (which transfer to normal walking), making them a useful approach for improving locomotor functions [34].

In the context of robotic rehabilitation effectiveness, the research by C. Klampt et al. is of great importance, as it demonstrated that robotic walking training can significantly improve functional abilities in patients with various knee joint conditions, including osteoarthritis [29]. The authors emphasized that automated systems provide precise load adjustment and movement repetition, which promotes faster functional recovery, pain reduction, and increased patient motivation for active rehabilitation. Considering our results, which show significant improvements in functional status just a few weeks after starting rehabilitation, we can conclude that the use of robotic systems can be an effective tool for accelerating the recovery process and improving the quality of life for patients with various knee joint conditions. All of this emphasizes the need for widespread implementation

of robotic methodologies into modern rehabilitation protocols, especially when traditional approaches are insufficient or require a long time to achieve desired results.

Moreover, in the systematic review by S. Hesse et al., although the focus was on the use of robotic walking during rehabilitation after stroke, the findings are highly relevant for individuals with knee joint injuries. Their findings underscore that robotic therapy not only aids in the restoration of walking skills but also improves muscle strength, stability, and coordination of lower limb movements [30]. These data demonstrate that such systems have universal potential for recovering damaged lower limb and knee structures across a wide range of neurological and orthopedic diseases. Our study shows that significant improvements in the functional state of the knee joint in patients with anterior knee pain syndrome after just a few weeks are facilitated by the use of robotic orthoses. This supports the idea that the neuromuscular plasticity mechanisms and improvements in motor skills described by S. Hesse et al. are relevant for orthopedic abnormalities as well.

It is also worth noting that Verheyden et al. have demonstrated that the use of robotic systems reduces fear of physical activity and improves emotional well-being, which plays an important role in boosting motivation and the long-term success of rehabilitation measures [33–35].

Thus, the use of robotic systems in rehabilitation appears to be promising, especially in combination with traditional approaches, allowing for improved speed and quality of patient recovery.

Conclusions

The use of a robotic orthosis in the rehabilitation process of patients with anterior knee pain syndrome after arthroscopy resulted in better outcomes. Compared to Group 1, Group 2 showed a significant relative improvement across all indicators: at the 6th week, the pain intensity on the VAS decreased by almost 52.6% (3.8 → 1.8), KSS part 1 increased by approximately 22.1% (68 → 83), KSS part 2 by approximately 11.1% (72 → 80), and AKPS by approximately 18.8% (64 → 76). After 3 months, significant improvement was maintained: VAS decreased by approximately 45.5% (2.2 → 1.2), KSS part 1 increased by approximately 15.4% (78 → 90), KSS part 2 by approximately 12.5% (80 → 90), and AKPS by approximately 17.1% (76 → 89).

Compared to traditional rehabilitation, the use of such a system provides stable and high results, which are consistent with modern developments in neuromuscular plasticity and the technological capabilities of robotic therapy.

However, certain limitations should be noted, namely the small sample size and the lack of long-term follow-up. A crucial factor is also the individual characteristics of the patients, which may influence the speed and degree of recovery. Additionally, the application of robotics requires significant resources, which may limit its use.

Overall, the results confirm the promise of robotic systems in rehabilitation practice to improve the speed and quality of recovery, as well as to reduce the risk of complications and improve the quality of life for individuals with orthopedic and traumatic knee joint injuries.

Conflict of Interest. The authors declare no conflict of interest.

Future Research Prospects. Further studies should focus on optimizing protocols and evaluating the long-term effectiveness of such technologies, as well as analyzing the broader use of robotic techniques within comprehensive rehabilitation and recovery of lower limb functions after orthopedic and traumatic injuries.

Funding Information. The authors declare no financial interests during the study and article writing process.

Authors' Contribution. Herasymenko S. I., Polulyakh D. M., Herasymenko A. S. — concept and design of the study, analysis of findings, text revision; Babko A. M. — statistical processing and analysis of findings; Hromadskyi V. V. — selection of patients, conducting the rehabilitation program, literature review; Yuryk O. Ye. — development of the rehabilitation program.

References

1. O'Donnell, K., Freedman, K. B., & Tjoumakaris, F. P. (2016). Rehabilitation protocols after isolated Meniscal repair: A systematic review. *The American journal of sports medicine, 45*(7), 1687–1697. https://doi.org/10.1177/0363546516667578
2. Spang III, R. C., Nasr, M. C., Mohamadi, A., DeAngelis, J. P., Nazarian, A., & Ramappa, A. J. (2018). Rehabilitation following meniscal repair: A systematic review. *BMJ open sport & exercise medicine, 4*(1), e000212. https://doi.org/10.1136/bmjsem-2016-000212
3. Moreira, J., Miguel, S., Delgado, B., & Boto, P. (2024). Patient-reported outcome measures in rehabilitation after knee surgery: a rapid systematic review. *Journal of public health*. https://doi.org/10.1007/s10389-024-02283-2
4. Stepanenko, O. S. (2022). Профілактика пателофеморального больового синдрому та тендінопатії колінного суглобу у спортсменів. *Physical education sport and health culture in modern society*, 62. https://doi.org/10.29038/2220-7481-2022-03-62-68
5. Malliaras, P., Cook, J., Purdam, C., & Rio, E. (2015). Patellar tendinopathy: Clinical diagnosis, load management, and advice for challenging case presentations. *Journal of orthopaedic & sports physical therapy, 45*(11), 887–898. https://doi.org/10.2519/jospt.2015.5987
6. Theodorou, A., Komnos, G., & Hantes, M. (2023). Patellar tendinopathy: An overview of prevalence, risk factors, screening, diagnosis, treatment and prevention. *Archives of orthopaedic and trauma surgery, 143*(11), 6695–6705. https://doi.org/10.1007/s00402-023-04998-5
7. Amestoy, J., Pérez-Prieto, D., Torres-Claramunt, R., Sánchez-Soler, J. F., Leal-Blanquet, J., Ares-Vidal, J., Hinarejos, P., &

Monllau, J. C. (2021). Patellofemoral pain after arthroscopy: Muscle atrophy is not everything. *Orthopaedic journal of sports medicine, 9*(6). https://doi.org/10.1177/23259671211013000
8. Culvenor, A., Øiestad, B., Holm, I., Gunderson, R., Crossley, K., & Risberg, M. (2017). Anterior knee pain following anterior cruciate ligament reconstruction does not increase the risk of patellofemoral osteoarthritis at 15- and 20-year follow-UPS. *Osteoarthritis and cartilage, 25*(1), 30–33. https://doi.org/10.1016/j.joca.2016.09.012
9. Ghisi, J., Megey, P., & Maquirriain, J. (2012). Patellar tendinopathy after Arthroscopic meniscectomy: A case report. *Journal of knee surgery, 26*(S 01), S063–S066. https://doi.org/10.1055/s-0032-1313740
10. Wen, Y., Wang, X., Mao, Y., Sun, X., Xu, N., & Han, X. (2025). Effectiveness of an intelligent weight-bearing rehabilitation robot in enhancing recovery following anterior cruciate ligament reconstruction. *Frontiers in public health*, 13. https://doi.org/10.3389/fpubh.2025.1526105
11. Vu, N. V., Nazari, M. A., Dang, T., Muralev, Y., Mohanraj, M., Tran, T., & Quoc, H. A. (2025). Type of the Paper: Article. *SSRN Electronic Journal*. https://doi.org/10.2139/ssrn.5384374
12. Li, W., Chen, X., Deng, Q., You, M., Xu, Y., Liu, D., Lin, Y., Li, P., & Li, J. (2023). Effectiveness of a digital rehabilitation program based on computer vision and augmented reality for isolated meniscus injury: protocol for a prospective randomized controlled trial. *Journal of orthopaedic surgery and research, 18*(1). https://doi.org/10.1186/s13018-023-04367-3
13. Crossley, K. M., Bennell, K. L., Cowan, S. M., & Green, S. (2004). Analysis of outcome measures for persons with patellofemoral pain: Which are reliable and valid?11No commercial party having a direct financial interest in the results of the research supporting this article has or will confer a benefit upon the author(s) or upon any organization with which the author(s) is/are associated. *Archives of physical medicine and rehabilitation, 85*(5), 815–822. https://doi.org/10.1016/s0003-9993(03)00613-0
14. Watson, C. J., Propps, M., Ratner, J., Zeigler, D. L., Horton, P., & Smith, S. S. (2005). Reliability and responsiveness of the lower extremity functional scale and the anterior knee pain scale in patients with anterior knee pain. *Journal of orthopaedic & sports physical therapy, 35*(3), 136–146. https://doi.org/10.2519/jospt.2005.35.3.136
15. Ittenbach, R. F., Huang, G., Barber Foss, K. D., Hewett, T. E., & Myer, G. D. (2016). Reliability and validity of the anterior knee pain scale: Applications for use as an epidemiologic screener. *PLOS ONE, 11*(7), e0159204. https://doi.org/10.1371/journal.pone.0159204
16. Pujol, N., Giordano, A. O., Wong, S. E., Beaufils, P., Monllau, J. C., Arhos, E. K., Becker, R., Della Villa, F., Brett Goodloe, J., Irrgang, J. J., Klugarova, J., Klosterman, E. L., Królikowska, A., Krych, A. J., LaPrade, R. F., Manske, R., Van Melick, N., Monson, J. K., Ostojic, M., . . . Prill, R. (2025). The formal EU-US meniscus rehabilitation 2024 consensus: An ESSKA-AOSSM-AASPT initiative. Part I—Rehabilitation management after meniscus surgery (meniscectomy, repair and reconstruction). *Knee surgery, sports traumatology, arthroscopy, 33*(8), 3002–3013. https://doi.org/10.1002/ksa.12674
17. Riener, R., Lünenburger, L., Maier, I. C., Colombo, G., & Dietz, V. (2010). Locomotor training in subjects with sensori-motor deficits: An overview of the robotic gait orthosis Lokomat. *Journal of healthcare engineering, 1*(2), 197–216. https://doi.org/10.1260/2040-2295.1.2.197
18. Duschau-Wicke, A., Caprez, A., & Riener, R. (2010). Patient-cooperative control increases active participation of individuals with SCI during robot-aided gait training. *Journal of neuroengineering and rehabilitation, 7*(1). https://doi.org/10.1186/1743-0003-7-43
19. Hussain, S., Xie, S. Q., & Liu, G. (2011). Robot assisted treadmill training: Mechanisms and training strategies. *Medical engineering & physics, 33*(5), 527–533. https://doi.org/10.1016/j.medengphy.2010.12.010
20. Heller, G. Z., Manuguerra, M., & Chow, R. (2016). How to analyze the visual analogue scale: Myths, truths and clinical relevance. *Scandinavian journal of pain, 13*(1), 67–75. https://doi.org/10.1016/j.sjpain.2016.06.012
21. Cook, J. L., Khan, K. M., Kiss, Z. S., Purdam, C. R., & Griffiths, L. (2001). Reproducibility and clinical utility of tendon palpation to detect patellar tendinopathy in young basketball players. *British journal of sports medicine, 35*(1), 65–69. https://doi.org/10.1136/bjsm.35.1.65
22. Coombes, B. K., Mendis, M. D., & Hides, J. A. (2020). Evaluation of patellar tendinopathy using the single leg decline squat test: Is pain location important? *Physical therapy in sport,* 46, 254–259. https://doi.org/10.1016/j.ptsp.2020.10.002.
23. Sprague, A. L., Smith, A. H., Knox, P., Pohlig, R. T., & Grävare Silbernagel, K. (2018). Modifiable risk factors for patellar tendinopathy in athletes: A systematic review and meta-analysis. *British journal of sports medicine, 52*(24), 1575–1585. https://doi.org/10.1136/bjsports-2017-099000
24. Crossley, K. M., Stefanik, J. J., Selfe, J., Collins, N. J., Davis, I. S., Powers, C. M., McConnell, J., Vicenzino, B., Bazett-Jones, D. M., Esculier, J., Morrissey, D., & Callaghan, M. J. (2016). 2016 Patellofemoral pain consensus statement from the 4th international Patellofemoral pain research retreat, Manchester. Part 1: Terminology, definitions, clinical examination, natural history, patellofemoral osteoarthritis and patient-reported outcome measures. *British journal of sports medicine, 50*(14), 839–843. https://doi.org/10.1136/bjsports-2016-096384
25. Şendir, M., Büyükyılmaz, F., & Muñovi, D. (2013). Patients' discharge information needs after total hip and knee arthroplasty: A quasi-qualitative pilot study. *Rehabilitation nursing, 38*(5), 264–271. https://doi.org/10.1002/rnj.103
26. Breda, S. J., Oei, E. H. G., Zwerver, J., Visser, E., Waarsing, E., Krestin, G. P., & Vos, R. de. (2020). Effectiveness of progressive tendon-loading exercise therapy in patients with patellar tendinopathy: a randomised clinical trial. *British journal of sports medicine, 55*(9), 501. https://doi.org/10.1136/bjsports-2020-103403
27. Brito A. C., & da Rosa C. (2017). «Efficacy of robotic gait training in patients with knee pathologies.» https://doi.org/10.1519/JPT.0000000000000100
28. Sancenzi S., et al. (2020). «Rehabilitation using Lokomat in patients after knee surgery: a pilot study.» https://doi.org/10.13140/RG.2.2.25074.17607
29. Klampt C., Smith J., & Williams R. (2014). Robotic-assisted gait training improves walking ability in patients with knee osteoarthritis. *Journal of rehabilitation research and development, 51*(8), 1079–1090. https://doi.org/10.1682/JRRD.2014.01.0001
30. Hesse S. (2003). Robotic-assisted gait training after stroke: a systematic review. *NeuroRehabilitation, 18*(4), 229–238. https://doi.org/10.1023/A:1025609404710
31. Čobec, J., & Kozinc, Ž. (2022). Conservative Treatments for Patellar Tendinopathy: A Review of Recent High-Quality Evidence [Review of conservative treatments for patellar tendinopathy: a review of recent high-quality evidence]. *BioMed, 2*(4), 359. https://doi.org/10.3390/biomed2040028
32. Hu, C., Huang, Q., Yu, L., & Ye, M. (2016). The immediate intervention effects of robotic training in patients after anterior cruciate ligament reconstruction. *Journal of physical therapy science, 28*(7), 2031. https://doi.org/10.1589/jpts.28.2031
33. Verheyden G., et al. (2015). Patients' experiences with robot-assisted gait training after stroke. *Disability and rehabilitation: assistive technology, 10*(2), 151–156. https://doi.org/10.3109/17483107.2014.921516
34. Washabaugh, E. P., & Krishnan, C. (2018). A wearable

resistive robot facilitates locomotor adaptations during gait. *Restorative neurology and neuroscience, 36*(2), 215. https://doi.org/10.3233/rnn-170782

35. Kuroda, Y., Young, M., Shoman, H., Punnoose, A., Norrish, A., & Khanduja, V. (2020). Advanced rehabilitation technology in orthopaedics—a narrative review [Review of Advanced rehabilitation technology in orthopaedics — a narrative review]. *International orthopaedics, 45*(8), 1933. Springer Science+Business Media. https://doi.org/10.1007/s00264-020-04814-4

The article has been sent to the editors	Received after review	Accepted for printing
12.11.2025	20.02.2026	23.02.2026

ANALYSIS OF THE QUALITY OF REHABILITATION OF PATIENTS WITH PATELLAR TENDINOPATHY USING A ROBOTIC ORTHOSIS

A. S. Gerasymenko, O. Ye. Yurik, S. I. Gerasymenko, O. V. Mayko, V. V. Hromadskyi, A. V. Hryschenko

SI «National Institute of Traumatology and Orthopedics of the NAMS of Ukraine», Kyiv

✉ Andrii Gerasymenko, MD, DMSci: corado734@ukr.net; https://orcid.org/0000-0002-6378-1196
✉ Olha Yurik, MD, DMSci: olhayuryk01@gmail.com; https://orcid.org/0000-0003-2245-9333
✉ Sergii Gerasymenko, MD, DMSci, Prof.: kievorto3@gmail.com; https://orcid.org/0000-0002-6378-1196
✉ Olena Mayko, PhD: drmaiko146@ukr.net; https://orcid.org/0000-0002-4399-4741
✉ Vadym Hromadskyi, MD: gromadsky94@gmail.com; https://orcid.org/0000-0002-4399-4741
✉ Andrii Hryschenko, MD: gryna000s@gmail.com; https://orcid.org/0000-0002-4399-4741

ISSN 0030-5987. Orthopaedics, traumatology and prosthetics. 2026. № 1

УДК 616.717-001.45-036.82:004.946](045)

DOI: http://dx.doi.org/10.15674/0030-59872026185-90

Use of virtual reality eyeglasses as an additional method in rehabilitation after upper limb injury

N. Prytula [1], V. Staude [1, 2], O. Zemlyana [3], I. Subbota [1], O. Kuznetsov [1, 2]

[1] Sytenko Institute of Spine and Joint Pathology National Academy of Medical Sciences of Ukraine, Kharkiv
[2] Stepan Gzhytskyi Lviv National University of Veterinary Medicine and Biotechnologies
[3] Kharkiv National Medical University. Ukraine

Over the past two decades, there has been a significant increase in the use of immersive technologies in rehabilitation. VR technologies allow for the simulation of motor tasks in a safe gaming digital environment, which contributes to better integration of the patient into the rehabilitation process, activates the neuromuscular system and reduces psychoemotional stress during the restoration of motor functions. While traditional methods involving simple, repetitive movements can be exhausting for patients and make them less motivated to continue treatment. Objective. Examined the effectiveness of using VR technology as an auxiliary method of rehabilitation in patients with traumatic injuries of the upper limbs after a blast injury. Materials. The effectiveness of using VR technology as an auxiliary rehabilitation method in patients with traumatic injuries of the upper extremities after a blast injury was analyzed. Results. The study included a case series of 4 military personnel with traumatic injuries of the upper limbs resulting from a blast injury. The rehabilitation program included standard physical therapy and physiotherapy methods in combination with training in a virtual environment using virtual reality glasses with the VR Vitalis program. Patients performed tasks aimed at improving coordination, strength and amplitude of movements in the shoulder, elbow and radiocarpal joints, considering the need for movement restoration. The dynamics of the range of motion was assessed using goniometry, muscle strength using dynamometry, and the level of motivation for classes was assessed using a survey. Conclusion. It was found that the use of VR technologies as an additional method to traditional rehabilitation contributed to a noticeable improvement in the indicators of functional recovery of upper limb movements. Positive dynamics were recorded not only in physical indicators, but also in the psycho-emotional state. All participants reported increased motivation and better involvement in the treatment process.

Протягом останніх років спостерігається значне зростання використання імерсивних технологій в реабілітації. VR-технології дозволяють моделювати рухові завдання в безпечному ігровому цифровому середовищі, що сприяє кращому інтегруванню пацієнта в процес реабілітації, активують нервово-м'язову систему та знижують психоемоційне навантаження під час відновлення рухових функцій, тоді як традиційні методи, які включають прості, повторювані рухи, можуть бути виснажливими для хворих і зменшувати мотивацію до лікування. Мета. Оцінити ефективність використання VR-технології як допоміжного методу реабілітації у пацієнтів із травматичними ушкодженнями верхніх кінцівок після вибухової травми. Матеріали. Проаналізовано ефективність використання VR-технології як допоміжного методу реабілітації в пацієнтів із травматичними ушкодженнями верхніх кінцівок після вибухової травми. Результати. У дослідження включено історії хвороб 4 військовослужбовців із травматичними ушкодженнями верхніх кінцівок. Реабілітаційна програма складалася зі стандартних методів фізичної терапії в поєднанні з тренуванням у віртуальному середовищі з використанням окулярів віртуальної реальності з програмою VR Vitalis. Пацієнти виконували завдання, спрямовані на покращення координації, сили й амплітуди рухів у плечовому, ліктьовому та променево-зап'ястковому суглобах. Аналіз динаміки обсягу рухів здійснювали за допомогою гоніометрії, сили м'язів — динамометрії та рівень мотивації до занять методом опитування. Висновок. Виявлено, що застосування VR-технологій як додаткового інструмента до традиційної реабілітації сприяло помітному покращенню показників функціонального відновлення рухів верхньої кінцівки. Зафіксовано позитивну динаміку не лише у фізичних показниках, а й у психоемоційному стані. Усі учасники повідомляли про зростання мотивації та кращу залученість у процес лікування. Ключові слова. Віртуальна реальність, ураження верхніх кінцівок, вибухова травма, реабілітація.

Keywords. Virtual reality, upper limb injury, blast injury, rehabilitation

Introduction

Over the past two decades, there has been a significant increase in the use of immersive technologies in rehabilitation. These technologies include Virtual Reality (VR), Augmented Reality (AR), and Mixed Reality (MR), collectively referred to as Extended Reality (XR) [1]. Among these, VR technologies are the most popular today, as they allow the patient to be immersed in a fully controlled three-dimensional environment, while AR technologies overlay VR elements onto the real-world environment in the form of real-time video displayed on an electronic device screen [2]. Therefore, AR is useful for training doctors on a virtual patient, detailed planning of medical interventions, and even enhancing intraoperative navigation [3]. VR technologies allow the simulation of movement tasks in a safe, game-like digital environment, promoting better integration of the patient into the rehabilitation process [4], activating the neuromuscular system, and reducing emotional stress during the recovery of motor functions [5]. In contrast, traditional methods that involve simple repetitive movements may be exhausting for patients and reduce motivation to continue treatment [6].

In the context of an increase in explosive and mine-related trauma (EMT) among both military personnel and civilians [7], the issue of effective rehabilitation after injuries to the upper limbs becomes especially important. Chronic pain, peripheral nerve damage, and functional limitations are the primary barriers to optimal recovery for patients following traumatic injuries to this area [8]. Traditional physical exercises require significant time and focus from the patient, which can reduce their motivation to engage in rehabilitation. The use of VR technology as an adjunctive method makes the rehabilitation process more interactive and psychologically comfortable, enhancing the effectiveness of restoring motor function [9].

Purpose: To assess the effectiveness of using VR technology as an adjunctive method in the rehabilitation of patients with traumatic injuries to the upper limbs following blast trauma.

Materials and methods

The study included 4 cases of rehabilitation treatment for military personnel with traumatic injuries to the upper limbs resulting from blast trauma. The rehabilitation program combined standard physical therapy methods with training in a virtual environment using VR headsets (VR glasses) and the VR Vitalis software. Patients performed tasks aimed at improving coordination, strength, and range of motion in the shoulder, elbow, and wrist joints. The dynamics of range of motion were analyzed using goniometry, muscle strength was measured using a dynamometer, and motivation levels were assessed through surveys.

The study was conducted in accordance with bioethical principles, legislative requirements, and the Helsinki Declaration, the Constitution of Ukraine, and the fundamentals of Ukrainian legislation. It was carried out as part of the standard rehabilitation process with written informed consent obtained from the patients and approved by the bioethics committee of the State Institution Professor M. I. Sytenko Institute of Spine and Joint Pathology of the National Academy of Medical Sciences of Ukraine, Kharkiv (Protocol No. 259 dated 29.01.2026).

Results

After two weeks of training with VR headsets, all patients showed improvement in range of motion and muscle strength. Virtual tasks designed to simulate daily activities (e.g., grasping objects, rotational movements, etc.) stimulated the activation of fine motor skills, coordination, and proprioception. Over time, there was noticeable restoration of movement control and reduction in rigidity of the affected segments.

Case study No. 1

A 28-year-old patient D. Diagnosis: consequences of blast injury (May 2022), post-traumatic osteoarthritis of the left shoulder joint. Severe pain syndrome. Deformation of the II-III fingers of the left hand. Impaired hand function. Median nerve neuropathy on the left (Table 1). Moderate but stable improvement in the range of motion of the left shoulder joint was observed. Flexion increased by 12°, extension by 3°, abduction by 2°, indicating a positive impact of therapy on the capsular-ligamentous and muscle apparatus of the shoulder girdle. More significant changes were recorded in strength parameters (%): flexor muscle strength increased by 32.9 %, extensor strength by 53.6 %, adductor strength by 21.3 %, and abductor strength by 24.5 %. A similar positive dynamics was noted in the radiocarpal joint, where the maximum increase in the range of motion was observed during dorsal flexion (+18°).

Case study No. 2

A 36-year-old patient A. Diagnosis: consequences of a gunshot fragment injury (03.10.2024): multiple blind fragment injuries of both upper and lower limbs with foreign bodies (metal fragments); consolidated fracture of the II metacarpal bone of the right hand with mixed contracture of the 2-5 metacarpoph-

alangeal joints of the right radiocarpal joint with moderate dysfunction; post-traumatic neuropathy of the right radial and ulnar nerves, left ulnar nerve with moderate sensorimotor disorders; post-operative hardened skin scars with minor functional impairment (Table 2). Due to severe neurological and structural limitations, improvement in the range of motion was minimal. However, dynamometric parameters showed functionally significant improvement. The greatest strength increase was recorded in the finger flexors (+45.5%) and the muscles responsible for wrist flexion (+25.0%).

Case study No. 3

A 33-year-old patient Y. Diagnosis: consequences of a gunshot fragment injury (18.03.2024): consolidated fractures of both bones of the left forearm, fixed with metal constructs in the middle third. Combined contracture of the left elbow and radiocarpal joints. Post-traumatic ulnar nerve neuropathy (Table 3). The patient showed improvement in both range of motion and muscle strength. In the elbow joint, there was a reduction in extension deficit by 6° and an increase in flexion by 5°. In the radiocarpal joint, significant improvement was observed in palmar flexion (+13°). Dynamometry revealed a significant increase in strength: elbow flexors increased by 70.6 %, extensors by 46.3 %. The most notable result was the doubling of finger flexor strength (+100 %), which has high clinical significance for the recovery of self-care functions.

Case study No. 4

A 30-year-old patient B. Diagnosis: consequences of a gunshot fragment injury (28.03.2025) to the left hand: weakly consolidated gunshot fracture of the II metacarpal bone, pseudoarthrosis and gunshot bone defect of the III metacarpal bone with displacement. Post-operative stage after left hand surgical treatment: revision of the fracture zone of the III metacarpal bone, installation of a rod (19.08.2025), resection of the upper third of the right fibula, autoplasty of the fibula bone defect in the III metacarpal bone, removal of the rod, and MOS of the III metacarpal bone with a plate and screws (02.09.2025). Combined contracture of the left hand.

Table 1

Functional evaluation of the joints in the left upper limb of patient D.

Indicator	Initial value	Final value
Goniometry – Shoulder joint; – Radiocarpal joint	Extension/Flexion: 47°/0°/135°, Abduction/Adduction: 123°/0°/44° Dorsal/Palmar flexion: 60°/0°/73°, Elbow/Radial flexion: 23°/0°/52°	Extension/Flexion: 50°/0°/147°, Abduction/Adduction: 125°/0°/44° Dorsal/Palmar flexion: 78°/0°/83°, Elbow/Radial flexion: 25°/0°/54°
Dynamometry, kg (Shoulder joint):	Flexors —14.0; Extensors — 8.4; Adductors — 10.8; Abductors — 11.0	Flexors — 18.6; Extensors — 12.9; Adductors — 13.1; Abductors — 13.7

Table 2

Functional evaluation of the right radiocarpal joint of patient A.

Indicator	Initial value	Final value
Goniometry (right radiocarpal joint)	Dorsal/Palmar flexion: 0°/23°/65°; Ulnar/Radial flexion: 0°/10°/18°	Dorsal/Palmar flexion: 0°/17°/65°; Ulnar/Radial flexion: 2°/0°/17°
Dynamometry, kg (right radiocarpal joint)	Dorsal flexion: 0.4; Palmar flexion: 8.3; Ulnar flexion: 6.6; Radial flexion: 3.2; Finger flexors: 11.0	Dorsal flexion: 1.0; Palmar flexion: 8.6; Ulnar flexion: 6.6; Radial flexion: 4.0; Finger flexors: 16.0

Table 3

Functional assessment of left upper limb joints of patient E.

Indicator	Initial value	Final value
Goniometry – Elbow joint: – Radiocarpal joint:	Flexion/Extension: 0°/21°/138° Dorsal/Palmar flexion 36°/0°/37°; Ulnar/Radial flexion: 21°/0°/21°	Flexion/Extension: 0°/15°/143° Dorsal/Palmar flexion: 45°/0°/50° Ulnar/Radial flexion: 22°/0°/25°
Dynamometry (kg) – Radiocarpal joint; – Elbow joint	Dorsal flexion: 1.9; Palmar flexion: 2.7 Ulnar flexion: 2.2; Radial flexion: 2.7 Finger flexors: 5.0 Flexors: 3.4; Extensors: 4.1	Dorsal flexion: 2.4; Palmar flexion: 4.3 Ulnar flexion: 5.6; Radial flexion: 3.2 Finger flexors: 10.0; Elbow joint: Flexors: 5.8; Extensors: 6.0

Temporary loss of function of the left upper limb (Table 4). The patient showed moderate improvement in the range of motion of the radiocarpal joint, mainly due to palmar (+8°) and elbow flexion (+3°). At the same time, there was a significant increase in muscle strength, especially in the hand flexors, whose strength increased threefold (+200 %). The strength of the muscles responsible for dorsal (+59.4 %) and elbow flexion (+44.2 %) also increased significantly, indicating a substantial improvement in the functional endurance of the hand.

Discussion

Although the use of VR technology is more widespread in the rehabilitation of stroke patients [10, 11], in recent years, attention has also been paid to its use as an adjunctive method in the orthopedic profile [12, 13].

A systematic review by A. M. AlHossan et al. [14] included observations involving patients who had undergone rotator cuff repair and compared rehabilitation based on virtual reality with standard physical therapy (6 studies (n ≈ 332 patients) met the inclusion criteria). The authors did not find a statistically significant difference between VR-based rehabilitation and traditional rehabilitation in terms of reducing perceived pain and improving functional outcomes reported by the patients. Nevertheless, their findings showed that VR therapy resulted in a notable enhancement in the overall range of shoulder abduction when compared to conventional rehabilitation methods. However, improvement in shoulder flexion and external rotation did not differ significantly between the groups. Based on the results obtained, it can be concluded that digital rehabilitation can improve patient adherence to the treatment regimen due to greater engagement and accessibility. However, for maximum effectiveness, periodic interaction with clinicians may be necessary. Thus, these results confirm the possibility of incorporating digital health technologies into postoperative rehabilitation protocols for the shoulder, tailored to the individual needs of the patient.

In 2025, several randomized controlled trials were conducted regarding the use of virtual reality in the rehabilitation of individuals with upper limb injuries. S. Prahm et al. [15] conducted a single-center randomized controlled trial with 150 inpatient medical histories, who underwent rehabilitation after traumatic hand injuries using the StableHandVR application (n = 75 intervention group, n = 75 control group). During the assessment, the active range of motion (ROM) of the hand, thumb opposition (Kapanji test), hand flexor strength, upper limb function (DASH), pain (NRS), quality of life (SF-36), usability (SUS), intrinsic motivation (IMI), and training adherence were evaluated. As a result, the intervention group showed a significantly greater improvement in wrist rotation (+27.8° vs. +17.3; $p < 0.001$) and thumb opposition ($p = 0.04$). Pain during movement decreased in both groups. Patients who used StableHandVR voluntarily exceeded the prescribed training volume by 63 %, reporting better perceived effort ($p < 0.001$), usefulness ($p = 0.018$), and excellent usability (SUS = 85.3). Thus, the application of the VR intervention StableHandVR improved motor function recovery, patient engagement in therapy, and adherence to the training regimen, proving its potential for integration into clinical rehabilitation pathways.

S. Kablanoğlu et al. [16] studied the impact of VR-based motor therapy on pain, sensation, quality of life, activity participation, and upper limb function in patients with peripheral nerve injuries of the hand. The study involved 42 individuals (n = 21 intervention group, n = 21 control group). Both groups underwent 30 therapeutic sessions over 6 weeks, consisting of 5 sessions per week, each lasting 60 minutes. In addition to their usual upper limb rehabilitation programs, participants in the intervention group received 30 sessions of VR-based motor therapy (6 weeks, 5 days a week, 20 minutes each). Pain in the upper limbs was assessed using the visual analog scale (VAS), sensory threshold was measured using the Semmes-Weinstein Monofilament Test (5-thread version), hand grip strength was assessed using the Jamar Dynamometer, activity participation was measured using the Quick Disabilities of the Arm,

Table 4

Functional assessment of the left radiocarpal joint of patient B.

Indicator	Initial value	Final value
Goniometry (radiocarpal joint)	Dorsal/palmar flexion: 71°/0°/60°; Ulnar/radial deviation: 29°/0°/43°	Dorsal/palmar flexion: 70°/0°/68°; Ulnar/radial deviation: 32°/0°/44°
Dynamometry, kg (radiocarpal joint)	Dorsal flexion: 6.9; Palmar flexion: 11.0; Ulnar flexion: 8.6; Radial flexion: 7.2; Wrist flexors: 8.0	Dorsal flexion: 11.0; Palmar flexion: 13.8; Ulnar flexion: 12.4; Radial flexion: 11.2; Wrist flexors: 24.0

Shoulder, and Hand scale and Duruoz Hand Index, and upper limb functionality was tested using the Jebsen-Taylor Hand Function Test. Quality of life was assessed using the 5-level European Quality of Life (EQ-5D-3L) scale. Statistically significant differences were found between the groups for VAS ($p = 0.001$), Jamar ($p = 0.004$), Quick Disabilities of the Arm, Shoulder, and Hand ($p = 0.015$), and the Duruoz Hand Index ($p < 0.001$) in favor of the intervention group. VR technologies demonstrated a positive effect on reducing pain, improving quality of life, increasing activity levels, and enhancing upper limb function in patients with peripheral nerve injuries of the hand.

The case series presented underscores that the use of VR technologies as an adjunct to traditional rehabilitation significantly improves functional recovery indicators of upper limb movements. Patients not only show positive dynamics in physical measures but also in their psychological and emotional state: they display a high level of engagement in the process, actively collaborate with specialists, and demonstrate consistent motivation for regular sessions. Importantly, after several sessions with VR headsets, patients noted an increase in interest even during the performance of standard physical exercises, which they had previously perceived as monotonous or exhausting. It is worth noting that explaining the VR system to the patient can improve their expectations from rehabilitation [17]. The elements of game-based interaction and the ability to see their own progress in a virtual environment significantly enhance self-esteem and contribute to maintaining a positive mood during treatment [18].

Thus, the results support the effectiveness of VR-based rehabilitation methods in improving upper limb recovery outcomes and can be considered a valuable tool in enhancing patient adherence and motivation during rehabilitation [18].

Conclusions

The use of virtual reality in the rehabilitation of patients with traumatic upper limb injuries following explosive trauma is an effective adjunctive method. The effectiveness is driven by improved activation of neuromuscular connections, repetitive motor stimuli, and visual feedback provided by the VR environment. The technology enhances motivation, facilitates the execution of exercises, and promotes faster recovery of motor functions. It is important to note that case series studies are a valuable tool for generating knowledge and forming hypotheses but are not suitable for justifying the effectiveness of treatment within the framework of evidence-based medicine. Therefore, further research is needed to study in more detail the effectiveness and optimization of VR technologies in the rehabilitation process. However, the obtained results suggest the feasibility of further integrating VR technologies into clinical rehabilitation practice and developing specialized programs using virtual environments.

Conflict of interest. The authors declare no conflict of interest.

Prospects for further research. It can be expected that the use of VR headsets as an additional method to standard rehabilitation interventions will be appropriate for increasing motivation for exercise, improving the psychological state, and enhancing patient engagement in the treatment process.

Information on funding. No benefits in any form have been or will be received from manufacturers of medical devices involved in our research.

Authors' contributions. Prutula N. Yu., Staude V. A. — justified the relevance of the study, developed the methodology, and selected patients; Subota I. A. — conducted biomechanical studies and analyzed the results; Kuznetsov O. O. — conducted practical sessions with patients; Zemlyana O. V. — literature review and drafting the corresponding section of the text.

Acknowledgements. Equipment was provided with the support of the Technology Agency of the Czech Republic and the Ministry of Industry and Trade within the TREND program.

References

1. Azini, P., Estejab, H., Raisali, F., Jafari, N., & Hedayat, D. (2026). Leveraging extended reality technologies to enhance the architectural design of healthcare environments: A Systematic Review. *Applied ergonomics,* 131, 104656. https://doi.org/10.1016/j.apergo.2025.104656
2. Yeung, A. W. K., Tosevska, A., Klager, E., Eibensteiner, F., Laxar, D., Stoyanov, J., Glisic, M., Zeiner, S., Kulnik, S. T., Crutzen, R., Kimberger, O., Kletecka-Pulker, M., Atanasov, A. G., & Willschke, H. (2021). Virtual and Augmented Reality Applications in Medicine: Analysis of the Scientific Literature. *Journal of medical Internet research, 23*(2), e25499. https://doi.org/10.2196/25499
3. van Doormaal, J. A. M., & van Doormaal, T. P. C. (2024). Augmented Reality in Neurosurgery. *Advances in experimental medicine and biology,* 1462, 351–374. https://doi.org/10.1007/978-3-031-64892-2_21
4. Lim, D. Y., Hwang, D. M., Cho, K. H., Moon, C. W., & Ahn, S. Y. (2025). Correction: A Fully Immersive Virtual Reality Method for Upper Limb Rehabilitation in Spinal Cord Injury. *Annals of rehabilitation medicine, 49*(1), 60. https://doi.org/10.5535/arm.19181.e
5. Tao, G., Garrett, B., Taverner, T., Cordingley, E., & Sun, C. (2021). Immersive virtual reality health games: a narrative review of game design. *Journal of neuroengineering and rehabilitation, 18*(1), 31. https://doi.org/10.1186/s12984-020-00801-3
6. Donati, D., Pinotti, E., Mantovani, M., Casarotti, S., Fini, A., Tedeschi, R., & Caselli, S. (2025). The Role of Immersive Virtual Reality in Upper Limb Rehabilitation for Subacute Stroke: A Review. *Journal of clinical medicine, 14*(6), 1903. https://doi.org/10.3390/jcm14061903
7. Harrington, C. J., Dearden, M. E., McGlone, P., Potter, B. K., Tintle, S. M., & Souza, J. M. (2025). The scope and distribution of upper extremity nerve injuries associated with combat-related extremity limb salvage. *The journal of hand surgery, 50*(3), 384.e1–384.e5. https://doi.org/10.1016/j.jhsa.2023.09.008
8. Leal, J. A., Hayda, R., Biliavskyi, V., Klapchuk, Y., Gomez, A., & Whiting, P. (2025). 2024 international trauma care forum guest nation symposium: gunshot injuries. *OTA international: the open access journal of orthopaedic trauma, 8*(6 Suppl),

e444. https://doi.org/10.1097/OI9.0000000000000444
9. Valmaggia, L. R., Latif, L., Kempton, M. J., & Rus-Calafell, M. (2016). Virtual reality in the psychological treatment for mental health problems: An systematic review of recent evidence. *Psychiatry research*, 236, 189–195. https://doi.org/10.1016/j.psychres.2016.01.015
10. Zhang, J., Yang, J., Xu, Q., Xiao, Y., Zuo, L., & Cai, E. (2024). Effectiveness of virtual reality-based rehabilitation on the upper extremity motor function of stroke patients: A protocol for systematic review and meta-analysis. *PloS one, 19*(11), e0313296. https://doi.org/10.1371/journal.pone.0313296
11. Xie, Q., Zhang, Q., Zhang, Y., Sheng, B., Wang, X., Luo, J., & Huang, J. (2025). Research on upper limb motor function evaluation and rehabilitation training system of stroke patients based on artificial intelligence: A usability and feasibility study from therapist and patient perspectives. *Digital health,* 11, 20552076251386665. https://doi.org/10.1177/20552076251386665
12. Lattré, T., Decramer, A., Vanhaecke, J., Van der Linden, D., & Goubau, J. (2024). Immersive virtual reality in orthopedic hand therapy. *Hand surgery & rehabilitation, 43*(4), 101750. https://doi.org/10.1016/j.hansur.2024.101750
13. Jha, C. K., Shukla, Y., Mukherjee, R., Rathva, P., Joshi, M., & Jain, D. (2024). A glove-based virtual hand rehabilitation system for patients with post-traumatic hand injuries. *IEEE transactions on bio-medical engineering, 71*(7), 2033–2041. https://doi.org/10.1109/TBME.2024.3360888
14. AlHossan, A. M., Jahhaf, R. H., Alharbi, A. S., Alqahtani, L. M., Alshahrani, R. M., Alowaidah, L. T., Alshangiti, H. Y., & Degen, R. M. (2025). Digital and virtual reality-based rehabilitation versus conventional therapy for rotator cuff tears and post-repair recovery: a systematic review and meta-analysis. *JSES reviews, reports, and techniques, 6*(1), 100584. https://doi.org/10.1016/j.xrrt.2025.09.003
15. Prahm, C., Bressler, M., Gohlke, T., Hönning, A., Harhaus-Wähner, L., Daigeler, A., & Kolbenschlag, J. (2025). Immersive virtual reality for functional hand and finger rehabilitation: results from a randomized controlled trial in 150 patients after traumatic hand injuries. *NPJ digital medicine, 8*(1), 792. https://doi.org/10.1038/s41746-025-02206-9
16. Kablanoğlu, S., & Sade, S. I. (2025). Effectiveness of virtual reality-based movement therapy in peripheral nerve injuries of the hand. *Journal of hand therap: official journal of the American Society of Hand Therapists, 38*(2), 370–377. https://doi.org/10.1016/j.jht.2025.04.010
17. Slatman, S., van Lankveld, W., Staal, J. B., van Goor, H., Ostelo, R., Westendorp, J., & Knoop, J. (2025). The effect of physiotherapists' explanation of therapeutic virtual reality on treatment expectations in healthy people and people with chronic musculoskeletal pain: Two online RCTs. *PEC innovation,* 8, 100443. https://doi.org/10.1016/j.pecinn.2025.100443
18. Tao, G., Garrett, B., Taverner, T., Cordingley, E., & Sun, C. (2021). Immersive virtual reality health games: a narrative review of game design. *Journal of neuroengineering and rehabilitation, 18*(1), 31. https://doi.org/10.1186/s12984-020-00801-3

The article has been sent to the editors	Received after review	Accepted for printing
11.01.2026	16.02.2026	23.02.2026

USE OF VIRTUAL REALITY EYEGLASSES AS AN ADDITIONAL METHOD IN REHABILITATION AFTER UPPER LIMB INJURY

N. Prytula [1], V. Staude [1, 2], O. Zemlyana [3], I. Subbota [1], O. Kuznetsov [1, 2]

[1] Sytenko Institute of Spine and Joint Pathology National Academy of Medical Sciences of Ukraine, Kharkiv

[2] Stepan Gzhytskyi Lviv National University of Veterinary Medicine and Biotechnologies

[3] Kharkiv National Medical University. Ukraine

✉ Nataliia Prytula: natpryt@ukr.net

✉ Volodymyr Staude, MD, DMSci: staudevl@gmail.com; https://orcid.org/0000-0003-2959-9208

✉ Olga Zemlyana, MD, PhD: earthhaz2022@gmail.com

✉ Igor Subbota: igorsublabor@gmail.com

✉ Oleksandr Kuznetsov: sash.kuznetso@gmail.com

ISSN 0030-5987. Orthopaedics, traumatology and prosthetics. 2026. № 1

SHORT REPORTS AND NOTES FROM PRACTIC

УДК 616-006.33-003.8-089.2:[615.277.3546.17-14]](045)

DOI: http://dx.doi.org/10.15674/0030-59872026191-95

Cryosurgical Management of Extraskeletal Myxoid Chondrosarcoma: A Case Report with Long-term Functional Outcomes

Mohammad Faza Anggito Widagdo [1, 2], Muhammad Hardian Basuki [1, 2]

[1] Soetomo General Academic Hospital, Surabaya, Jawa. Indonesia

[2] Faculty of Medicine, Airlangga University, Surabaya, Jawa. Indonesia

Introduction. Extraskeletal myxoid chondrosarcoma (EMC) is a rare soft-tissue sarcoma with a substantial risk of local recurrence and distant metastasis. Liquid-nitrogen cryosurgery may serve as an adjunct during limb-salvage procedures, including bone recycling. Objective. To report a juxta-articular EMC of the knee treated with wide excision, liquid-nitrogen cryosurgery of resected bone segments, and reconstruction with total knee replacement (TKR), and to present functional follow-up outcomes. Methods. A wide excision was performed via a medial parapatellar approach with osteotomy of the patella and proximal tibia. Resected bone was treated with liquid nitrogen (15 minutes) followed by stepwise thawing, then reattached; reconstruction included TKR and internal fixation. Follow-up assessed union, recurrence/metastasis (MRI/CT), and function (MSTS). Results. Surgical margins were negative. Union was achieved within 1 year. No local recurrence or progression of lung lesions was detected during 1–3 years of follow-up. Function was preserved (ROM 0–90°) with MSTS 90 % (1 year), 97 % (2 years), and 93 % (3 years), without reported complications. Conclusions. Cryosurgery with bone recycling can be a useful adjunct for limb-salvage surgery in knee EMC, enabling reconstruction with favorable functional outcomes in early to mid-term follow-up.

Позаскелетна міксоїдна хондросаркома (extraskeletal myxoid chondrosarcoma, EMC) є рідкісною саркомою м'яких тканин, для якої характерні часті місцеві рецидиви та метастазування. Кріохірургія з використанням рідкого азоту потенційно може бути корисним ад'ювантом під час органозбережних втручань. Мета. Описати клінічний випадок EMC колінного суглоба з ураженням кісткових структур, пролікований широким висіченням, кріообробкою резектованих сегментів і реконструкцією з ендопротезуванням, і навести функціональні результати спостереження. Методи. Проведено широке видалення пухлини через медіальний парапателярний доступ з остеотомією проксимальної великогомілкової кістки та наколінка. Резектовані кісткові фрагменти обробляли рідким азотом (15 хв) із послідовним відтаванням; виконано реімплантацію фрагментів, тотальне ендопротезування коліна та внутрішню фіксацію. Оцінювали зрощення, рецидив/метастази (МРТ, КТ) та функцію (MSTS). Результати. Резекційні краї були негативні. Зрощення досягнуто протягом року. Ознак місцевого рецидиву чи прогресування метастатичних легеневих вогнищ упродовж 1–3 років не виявлено. Функція збережена: ROM 0–90°, MSTS 90 % (1 рік), 97 % (2 роки), 93 % (3 роки). Ускладнень не відзначено. Висновки. Кріохірургія з реконструкцією кістки може бути ефективним ад'ювантом під час органозбережної хірургії за EMC навколо коліна з добрими ранніми та середньостроковими функціональними результатами. Ключові слова. Кріохірургія; позаскелетна міксоїдна хондросаркома; клінічний випадок; рідкий азот; рециклінг кістки; тотальне ендопротезування колінного суглоба; функціональний результат.

Keywords. Cryosurgery; extraskeletal myxoid chondrosarcoma; case report; liquid nitrogen; bone recycling; total knee replacement; functional outcome

Introdution

Extraskeletal myxoid chondrosarcoma (EMC) is a rare and generally indolent soft-tissue sarcoma that nevertheless demonstrates a substantial risk of local recurrence and distant metastasis [1]. Although historically grouped with cartilaginous neoplasms because of its chondroid-like morphology, EMC lacks true cartilaginous differentiation and is classified by the World Health Organization as a tumor of uncertain differentiation [4]. Clinically, EMC may behave as a low-grade malignancy but is associated with reported local recurrence rates of approximately 30–50 % and distant metastasis rates up to 50 %, most commonly to the lungs [3, 4]. Wide local excision with negative margins remains the cornerstone of treatment; adjuvant radiotherapy may be considered for large tumors, although EMC is often described as relatively radioresistant [5]. Cryosurgery using liquid nitrogen has been proposed as an adjunctive method for local tumor control and for recycling resected bone segments during limb-salvage reconstruction [6, 7].

Purpose. To report a juxta-articular EMC of the knee treated with wide excision, liquid-nitrogen cryosurgery of resected bone segments (bone recycling), and reconstruction with total knee replacement, and to describe early to mid-term oncologic and functional outcomes.

Materials and methods

Expert opinion for regarding the possibility of publishing the material of 01.26.2026.

Study design: Case report.

Patient and setting: A 37-year-old woman presented with a slowly enlarging anterior mass of the left knee for approximately five years, with intermittent pain and activity-related worsening.

Diagnostic work-up: Plain radiographs demonstrated a soft-tissue mass. Contrast-enhanced MRI showed a large septated solid–cystic intra-articular lesion (82.1 × 47.5 × 103.1 mm) involving the femorotibial and patellofemoral compartments, extending to subcutaneous fat and invading the patella and proximal tibia, while major neurovascular structures were spared. High-resolution thoracic CT demonstrated multiple bilateral pulmonary nodules suspicious for metastasis. Core needle biopsy with immunohistochemistry supported the diagnosis of extraskeletal myxoid chondrosarcoma.

Laboratory tests showed mildly elevated erythrocyte sedimentation rate and C-reactive protein; hepatitis B and HIV serologies were non-reactive.

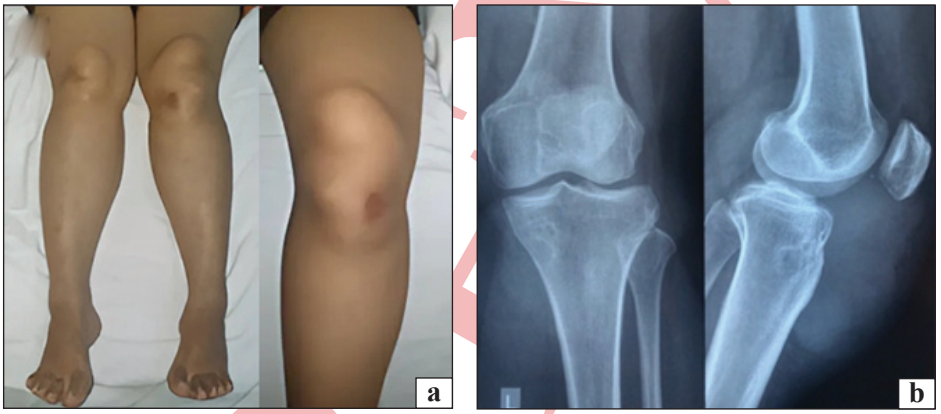

Fig. 1. Clinical Picture of both lower leg and Right Knee from anterior (a), and X-Ray findings of the left knee lateral (b)

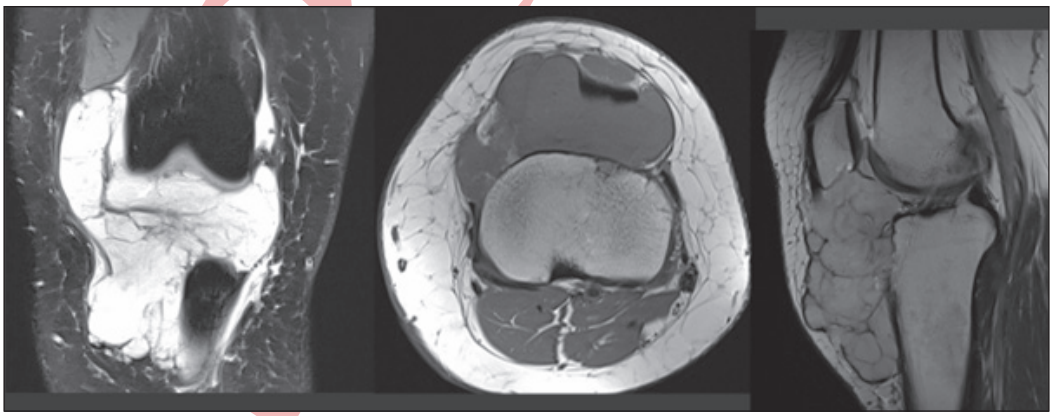

Fig. 2. MRI of The Left Knee With Contrast

Surgical technique: Through a medial parapatellar approach, wide local excision was performed with osteotomy of the proximal tibia and patella. Resected bone segments were treated with liquid nitrogen for 15 minutes, followed by sequential thawing in 0.9 % NaCl solution and at room temperature. Reconstruction included reattachment of the recycled bone segments, total knee replacement, and internal fixation of the proximal tibia and patella. Perioperative prophylactic antibiotics were administered.

Follow-up and outcomes: Follow-up occurred every 6 months during the first year and annually thereafter. Outcomes included margin status, radiologic union, evidence of recurrence/metastasis (contrast MRI of the extremity and thoracic CT), knee range of motion, extensor mechanism function, and Musculoskeletal Tumor Society (MSTS) score.

Ethics and consent: Written informed consent for publication and images was obtained from the patient.

Results

Postoperative histopathology demonstrated negative resection margins. During follow-up at 1, 2, and 3 years, contrast MRI of the operated extremity showed no local recurrence, and thoracic CT showed no progression of pulmonary lesions. Radiographic union of the recycled bone segments was achieved at 1 year. Functional outcomes were favorable: knee range of motion was 0–90 degrees without extension lag, and MSTS scores were 90 % (1 year), 97 % (2 years), and 93 % (3 years). No perioperative or late complications were recorded.

Discussion

EMC is an ultra-rare soft-tissue sarcoma with an indolent course but a meaningful propensity for local recurrence and pulmonary metastasis [1, 3, 4]. In cases where the tumor is juxta-articular and involves critical bony and soft-tissue structures, achieving local control while preserving function can be challenging. Liquid-nitrogen cryosurgery is an adjunctive technique that may enhance local tumor control and enable recycling of resected bone segments for reconstruction [6, 7]. Cryoablation causes cell death through direct cellular injury, osmotic shifts during freezing- thawing, and intracellular ice crystal formation, which together

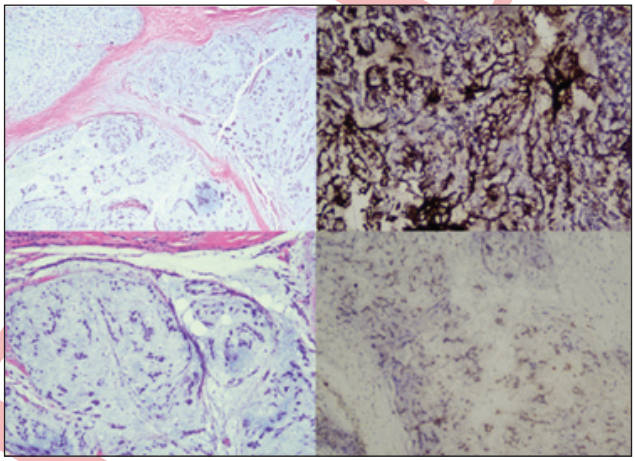

Fig. 3. Immunohistology Examination of The Core Biopsy

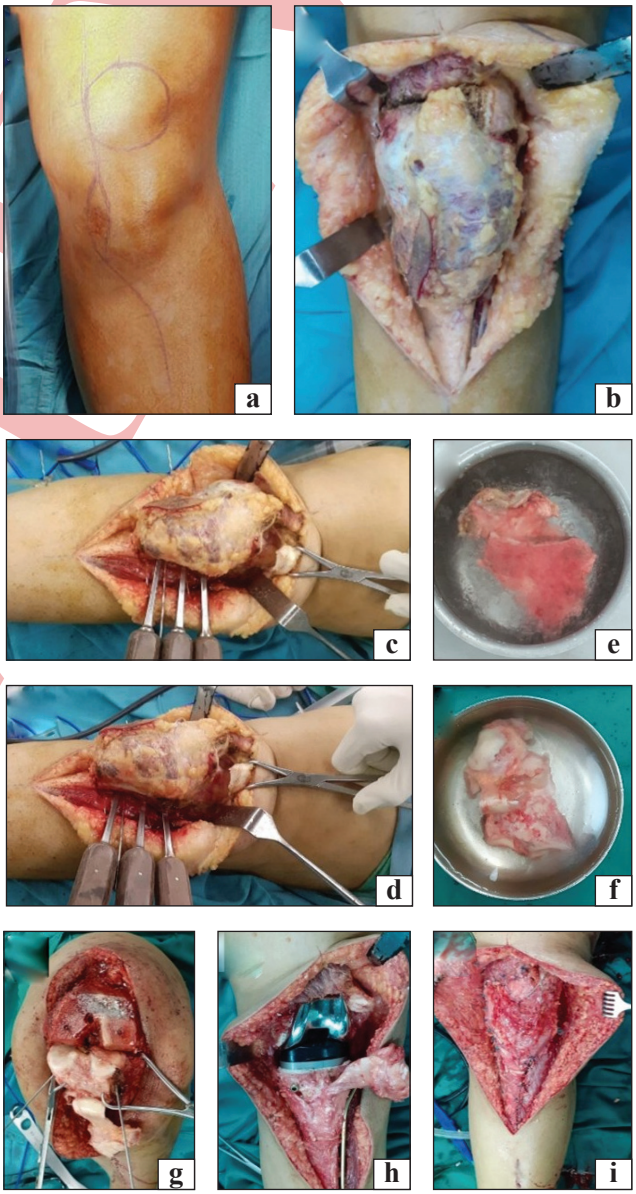

Fig. 4. Surgical Procedure. Incision according to the medial parapatellar approach (a); Tissue dissection and tumor margins identification (b); Tumor tissue resection a fas as proximal osteotomy of the tibia and patella (c, d); The resected tibia and patella immersed in liquid nitrogen (e) for 15 minutes and thawing process in 0.9 % NaCl solution for 10 minutes (f); Reattachment of tissue after cryosurgery resection (g), total knee replacement and internal fixation of the proximal tibia and patella (h), and soft tissue closure (i)

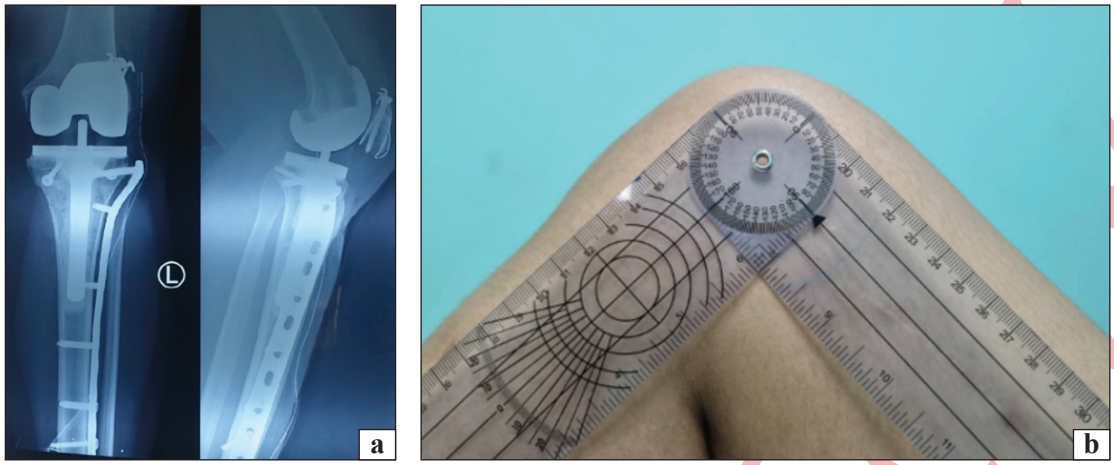

Fig. 5. Two-year follow-up of the patient. Knee radiograph (a) and knee ROM flexion (b)

Table 1

Patient timeline

Date	Event
05/01/2022	Initial presentation with knee mass
12/01/2022	Imaging (MRI, CT) supporting EMC
15/01/2022	Wide excision, cryosurgery (liquid nitrogen), and TKR
15/01/2023	1-year follow-up (MSTS 90 %)
17/01/2024	2-year follow-up (MSTS 97 %)
10/01/2025	3-year follow-up (MSTS 93 %)

can disrupt membranes and organelles [6]. In our case, cryosurgery facilitated limb salvage combined with total knee replacement and internal fixation, with negative margins, radiographic union at 1 year, and favorable functional outcomes up to 3 years. The absence of local recurrence on serial MRI and stable pulmonary findings on thoracic CT are encouraging, although oncologic conclusions are limited by the single-case design and the inherent variability in the natural history of EMC. Limitations include the single-patient nature of the report and limited generalizability; longer follow-up and larger series are required to better define indications, oncologic safety, complication profiles, and functional outcomes of cryosurgery-assisted reconstruction in EMC.

Conclusions

Cryosurgery with bone recycling may be a useful adjunct for limb-salvage management of juxta-articular EMC of the knee, enabling reconstruction with favorable functional outcomes and no observed local recurrence during early to mid- term follow-up.

Conflict of interest. The authors declare no conflicts of interest related to this work.

References

1. Chiusole, B., Le Cesne, A., Rastrelli, M., Maruzzo, M., Lorenzi, M., Cappellesso, R., et al. (2020). Extraskeletal myxoid chondrosarcoma: Clinical and molecular characteristics and outcomes of patients treated at two institutions. *Frontiers in Oncology,* 10, 828. https://doi.org/10.3389/fonc.2020.00828
2. Fice, M. P., Lee, L., Kottamasu, P., Almajnooni, A., Cohn, M. R., Gusho, C. A., et al. (2022). Extraskeletal myxoid chondrosarcoma: A case series and review of the literature. *Rare Tumors*, 14, 20363613221079754. https://doi.org/10.1177/20363613221079754
3. Brown, J. M., Rakoczy, K., & Pretell-Mazzini, J. (2022). Extraskeletal myxoid chondrosarcoma: Clinical features and overall survival. *Cancer Treatment and Research Communications*, 31, 100530. https://doi.org/10.1016/j.ctarc.2022.100530
4. Hisaoka, M., & Hashimoto, H. (2005). Extraskeletal myxoid chondrosarcoma: Updated clinicopathological and molecular genetic characteristics. *Pathology International, 55*(8), 453-463. https://doi.org/10.1111/j.1440- 1827.2005.01853.x
5. Stacchiotti, S., Baldi, G. G., Morosi, C., Gronchi, A., & Maestro, R. (2020). Extraskeletal myxoid chondrosarcoma: State of the art and current research on biology and clinical management. *Cancers, 12*(9), 2703. https://doi.org/10.3390/cancers12092703
6. Yiu, W.-K., Basco, M. T., Aruny, J. E., Cheng, S. W. K., & Sumpio, B. E. (2007). Cryosurgery: A review. *International Journal of Angiology, 16*(1), 1-6. https://doi.org/10.1055/s-0031-1278235
7. Tsuchiya, H., Wan, S. L., Sakayama, K., Yamamoto, N., Nishida, H., & Tomita, K. (2005). Reconstruction using an autograft containing tumour treated by liquid nitrogen. *The Journal of Bone and Joint Surgery. British Volume, 87*(2), 218-225. https://doi.org/10.1302/0301-620X.87B2.15325

ISSN 0030-5987. Orthopaedics, traumatology and prosthetics. 2026. № 1

The article has been sent to the editors	Received after review	Accepted for printing
26.01.2026	10.02.2026	12.02.2026

CRYOSURGICAL MANAGEMENT OF EXTRASKELETAL MYXOID CHONDROSARCOMA: A CASE REPORT WITH LONG-TERM FUNCTIONAL OUTCOMES

Mohammad Faza Anggito Widagdo [1, 2], Muhammad Hardian Basuki [1, 2]

[1] Soetomo General Academic Hospital, Surabaya, Jawa. Indonesia
[2] Faculty of Medicine, Airlangga University, Surabaya, Jawa. Indonesia

✉ Mohammad Faza Anggito Widagdo, MD: fazawidagdo@gmail.com; https://orcid.org/0000-0002-4960-1611
✉ Muhammad Hardian Basuki, MD: basukimh@gmail.com; https://orcid.org/0000-0003-2845-965X

УДК 616.728.2-089.22:546.41.135

DOI: http://dx.doi.org/10.15674/0030-59872026196-100

Clinical case of using tricalcium phosphate-based bone cement reinforced with hydroxyapatite

V. A. Filipenko [1], K. S. Ivanchuk [2]

[1] Sytenko Institute of Spine and Joint Pathology National Academy of Medical Sciences of Ukraine, Kharkiv
[2] SI «National Institute of Traumatology and Orthopedics of the NAMS of Ukraine», Kyiv

The study and implementation of biomaterials for reconstructive orthopedic interventions remain a key focus of modern biomaterials science. Calcium phosphate ceramics are notable for their high biocompatibility, osteoconductive properties, and biodegradability. Developing materials capable of adapting to the shape of bone defects is particularly relevant. Objective. To evaluate the effectiveness of a metastable tricalcium phosphate cement reinforced with needle-shaped hydroxyapatite crystals for filling cavity defects in the acetabulum during total hip arthroplasty. Methods. A clinical case of a 52-year-old patient with stage IV coxarthrosis and acetabular cystic defects is presented. Following marginal cyst resection, the cement was applied to the cavity prior to implantation of an uncemented acetabular cup. Postoperative follow-up was performed on days 7 and 30 using radiography and multislice CT. Results. The postoperative course was uneventful. On day 7, the cavity was fully filled with cement; by day 30, multiple bone trabeculae had formed within the material, with density similar to native bone. Prosthesis fixation remained stable, without cement migration or aseptic demarcation. Conclusions. The use of calcium phosphate cement with a paste-like consistency reinforced with needle-shaped hydroxyapatite crystals allows complete defect filling, promotes bone-cement complex formation, and provides stable prosthesis fixation in the early postoperative period. Further studies with longer follow-up are required to assess long-term outcomes and material resorption.

Дослідження біоматеріалів для реконструктивно-відновних втручань в ортопедії залишається актуальним напрямом сучасного біоматеріалознавства. Особливу увагу привертають кальцій-фосфатні кераміки, які мають високу біосумісність, остеокондуктивні властивості та здатність до біодеградації. Актуальною є розробка матеріалів, здатних адаптуватися до форми порожнинних дефектів кісток. Мета. Оцінити ефективність метастабільного цементу на основі трикальційфосфату, посиленого голчастими кристалами гідроксилапатиту, для заповнення порожнинних дефектів кульшової западини під час тотального ендопротезування. Методи. Наведено клінічний приклад 52-річного пацієнта з коксартрозом IV ст. і кістами, локалізованими в кульшовій западині. Після пристінкової резекції кіст цемент пломбували в порожнину перед установкою безцементної чашки ендопротеза. Динамічне спостереження проводили на 7-му та 30-ту добу післяопераційного періоду зі застосуванням рентгенографії та МСКТ. Результати. Післяопераційний період проходив без ускладнень. На 7-му добу порожнина була заповнена цементом, на 30-ту добу візуалізували численні кісткові балки, що проростали в матеріал, із щільністю, подібною до кісткової тканини. Фіксація ендопротеза залишалася стабільною, ознак міграції цементу чи асептичного розмежування не зафіксовано. Висновки. Використання кальцій-фосфатного цементу з пастоподібною консистенцією та голчастими кристалами гідроксилапатиту забезпечує повноцінне заповнення дефекту, сприяє формуванню кістково-цементного комплексу та створює умови для стабільної фіксації компонентів ендопротеза в ранньому післяопераційному періоді. Подальші дослідження з тривалішим спостереженням дозволять оцінити віддалені результати та резорбцію матеріалу. Ключові слова. Кульшовий суглоб, дефекти кісткової тканини, кістковий цемент.

Keywords. Hip joint, bone defects, bone cement

Introduction

The study and implementation of biomaterials for reconstructive and restorative interventions in the field of orthopedics remains one of the key directions of modern biomaterials science [1, 2]. Special attention is drawn to calcium phosphate ceramics, which are characterized by high biocompatibility, chemical affinity with bone tissue, biodegradability, and pronounced osteoconductive and osteointegrative properties. Given the variety of configurations and sizes of cavitary bone defects that occur as a result of disease or surgery, the search for materials capable of adapting to the shape of the formed defect is highly relevant [3, 4]. At the same time, the optimal composition of ceramic materials that would ensure necessary mechanical properties without compromising their bioresorbable characteristics has yet to be determined. This paper presents a clinical case of using a calcium-phosphate biomaterial developed at the Department of Physics, Karazin Kharkiv National University [5], for filling a cavitary defect of the acetabulum during hip joint arthroplasty. The clinical testing followed thorough experimental studies on rats, the results of which indicate the promising application of this biomaterial in orthopedic practice [26].

Purpose: To investigate the possibility of using metastable cement based on tricalcium phosphate, reinforced with hydroxyapatite needles, as a material for filling cavitary defects in bone tissue.

Materials and methods

The study was approved by the local bioethics committee (protocol of the meeting at the State Institution Professor M. I. Sytenko Institute of Spine and Joint Pathology of the National Academy of Medical Sciences of Ukraine, dated 03.08.2023, No. 234).

A 52-year-old male patient, referred to as Patient V., presented with pain, discomfort during walking and at rest, limping, and restricted range of motion in the hip joint. The patient had been suffering for at least 5 years, having undergone conservative treatment with short-term improvements. The pain syndrome exacerbated 2–3 times a year. Clinical and radiological examination revealed signs of stage IV coxarthrosis. A massive cyst was detected on the upper-anterior wall of the acetabulum (Figure 1). No related pathological changes were detected.

In targeted radiographs of the right hip joint in both the anteroposterior and lateral projections, subchondral changes were observed, mainly on the roof of the acetabulum and the upper part of the femoral head. Bone resorption was noted in the subchondral zone (the maximum diameter of the cyst in the acetabular roof area was up to 13 mm, and in the femoral head up to 8 mm; at some levels, the endplate bone was significantly thinned). Radiographic signs of right-sided coxarthrosis stage IV with pronounced cyst-like bone remodeling were diagnosed.

A total hip arthroplasty surgery using a cementless construct was planned. The identified bone tissue defects could potentially affect the secondary stability of the acetabular cup of the prosthesis, which occurs through the ingrowth of bone trabeculae into the pores of the outer surface. To achieve full secondary stability of the cup, it was decided to perform a wall resection of the cyst on the upper-anterior wall of the acetabulum and to replace the formed defect.

For the defect replacement, synthetic calcium-phosphate bioceramics — hydroxyapatite (HA $Ca_{10}(PO_4)_6(OH)_2$) and tricalcium phosphate (TCP $Ca_3(PO_4)_2$) — were selected for their safety and efficacy [7]. The bone cement based on TCP was reinforced with needle-like crystals of HA.

The study of the dependency of the changes in compressive strength of the cement on the amount of needle-like hydroxyapatite crystals revealed that the strength increases proportionally with the number of these crystals. At 4 % weight/weight, it reaches the maximum values with an average of 5.5 MPa [25]. The full setting time of the calcium phosphate cement (CPC) usually takes several tens of minutes. A 2.5 % sodium hydrogen phosphate (Na2HPO4) solution was used as the liquid phase for preparing the cement, which was added to the portion of the α′-TCP powder, ensuring a solid/liquid phase ratio of 1/1.25. Just before use, 4 % weight/weight of needle-like hydroxyapatite crystals were added to the liquid phase. These crystals were obtained by hydrothermal synthesis

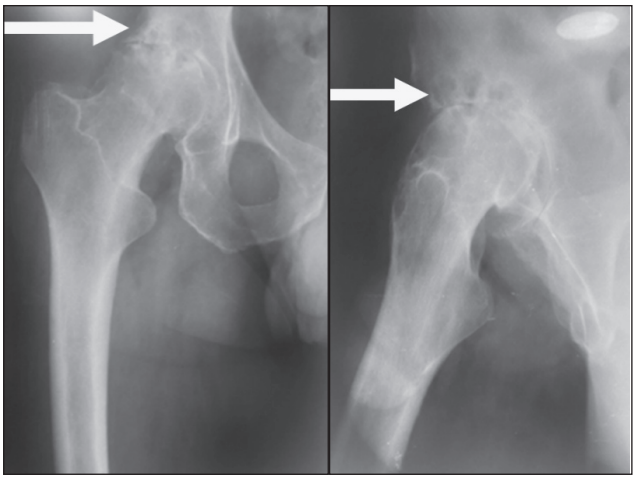

Fig. 1. X-ray images of the right hip joint (noting cysts in the acetabulum)

using an original technology (T = 235 °C, P = 20 atm, t = 1 hour) [8].

The mass was then carefully mixed with a spatula until a homogeneous paste was obtained, and it was allowed to rest for 3–5 minutes [5]. Two minutes after the mixing started, a paste-like consistency formed, which gradually hardened and took shape over time. The resulting paste was used to fill the bone defect, compacting each new portion with a spatula until the defect was fully filled.

After preparing the acetabulum with reamers to the required size, the cyst on the upper-anterior wall was visualized (Figure 2). Using a curette, the wall resection was performed, creating a cavity of dimensions 2×2.5×3 cm. After careful hemostasis, a portion of cement was prepared sufficient to fill the defect: 15 grams of cement and the corresponding amount of liquid, reinforced with HA needles, were used. After the bone cavity was filled with cement, the acetabular cup and other components of the prosthesis were installed.

Results and discussion

No complications were observed in the postoperative period. The patient was examined on the 7th and 30th day after the surgery.

Medications in the postoperative period followed the standard protocol for primary hip arthroplasty patients: prevention of thromboembolic complications and antibiotic therapy for infection prevention. The first three days of dressing changes were performed daily. On the second day, the drain was removed. The postoperative wound healed with primary tension. The patient's mobilization followed a standard process: the patient was taught to walk the day after surgery with a controlled load (40 % of body weight), using crutches as additional support. Therapeutic exercises targeting the lower limb musculature were prescribed, and a structured postoperative rehabilitation program was conducted under the supervision of a rehabilitation specialist.

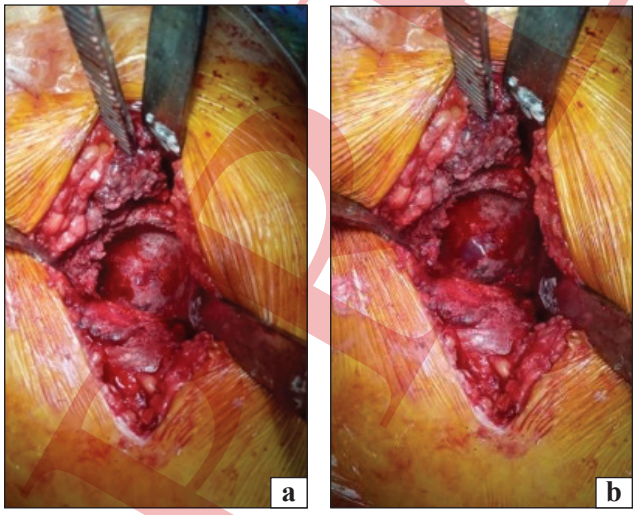

Fig. 2. Intraoperative photo. Cyst in the upper wall of the acetabulum: a) before and b) after the filling

7th day post-surgery. Radiographic signs of the state after right hip joint arthroplasty were observed. The cyst in the lateral part of the subchondral zone of the acetabular roof was filled with a plastic material (calcium phosphate cement) (Figure 3).

30th day post-surgery: Bone growth along the edge of the acetabulum was noted, extending up to 8 mm, with some sclerosis in the subchondral zone. In this region, a single cyst with a diameter of 13 mm was found, filled with material in which numerous bone trabeculae were identified, with density identical to that of bone tissue (Figure 4).

Compared to the radiographic images taken on the 7th day after surgery, many bone trabeculae were observed between the acetabular endplate and the outer surface of the prosthetic acetabular cup.

Additionally, a multi-slice computed tomography (MSCT) scan of the right hip joint was performed on the 30th day (Figure 5). The results indicated that bone growth had formed along the edge of the acetabulum, extending up to 9 mm. The subchondral zone in this area was unevenly sclerosed, and the cyst was filled with a dense material (likely cement). In one of the cysts, between its walls and the substance, numerous bone trabeculae could be traced, which blurred the boundary between the bone and the material [9].

The clinical and radiological data obtained confirm the appropriateness and potential of using calcium phosphate cement based on TCP, reinforced with needle-like HA crystals, to fill cavitary defects in the acetabulum during total hip arthroplasty. The distinctive feature of this clinical case is the presence of a significant irregularly shaped defect in the acetabular roof zone, which could potentially affect the secondary stability of the uncemented acetabular cup.

The use of calcium phosphate cement with a paste-like consistency enabled the complete filling of the complex-shaped defect and ensured a tight contact between the material and the walls of the bone cavity. This created favorable conditions for the further ingrowth of bone trabeculae into the implanted material. The radiological and MSCT signs observed on the 30th postoperative day, indicating the formation of bone trabeculae in the cemented area, are consistent with experimental data on the bioresorption

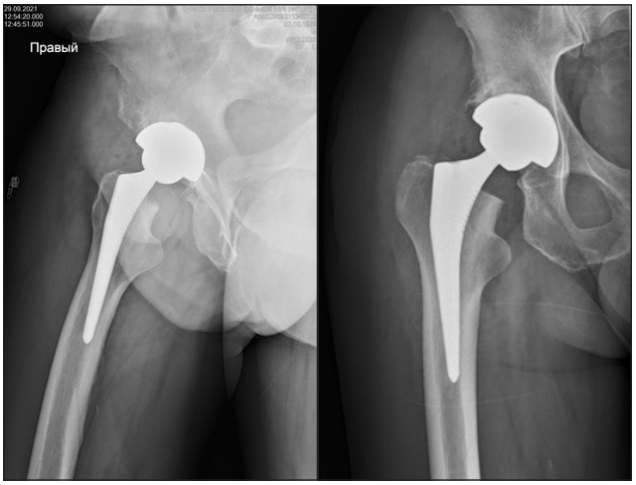

Fig. 3. X-ray images of the joint on the 7th day after hip replacement surgery and bone defect reconstruction

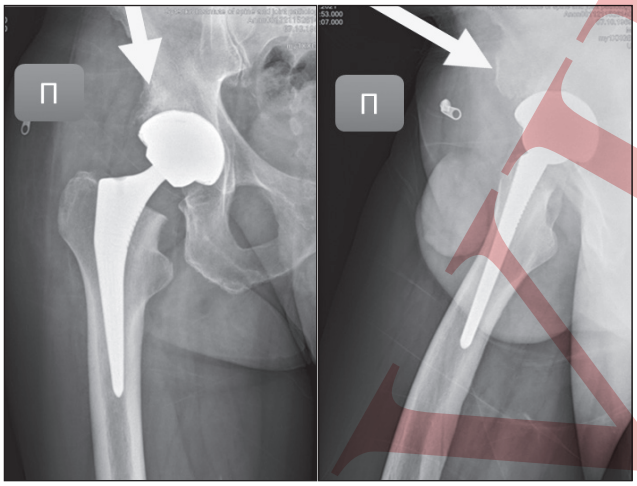

Fig. 4. X-ray images of the right hip joint on the 30th day after hip replacement surgery and bone defect reconstruction

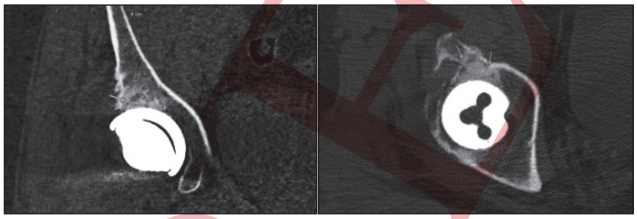

Fig. 5. Multi-slice computed tomography of the right hip joint

and osteointegration of materials based on TCP and HA [10].

The reinforcement of the cement with needle-like HA crystals at a concentration of 4 % w/w allowed for an increase in its compressive strength to a level sufficient for use in load-bearing zones, without compromising the biological activity of the material. The balance between mechanical stability and controlled resorption is known to be a critical factor for the successful reconstruction of bone defects in the hip joint region [11–14]. In the presented clinical case, no signs of cement migration, formation of an aseptic boundary zone, or disruption of prosthesis fixation were observed in the early postoperative period.

The results obtained also indicate that the use of this biomaterial may improve the conditions for secondary stability of the prosthetic cup by restoring the integrity of the subchondral bone and forming a bone-cement complex capable of gradual remodeling [15–16]. Further studies with a larger number of clinical observations and a longer period of dynamic monitoring will allow for a more objective assessment of the long-term effectiveness, resorption rates, and the impact of the reinforced calcium phosphate cement on the survivability of the hip prosthesis components.

Conclusion

Postoperative radiological and MSCT data indicate positive dynamics in the replacement of the cavitary bone defect with bone cement based on tricalcium phosphate, reinforced with needle-like hydroxyapatite crystals, showing signs of osteointegration. The paste-like consistency, osteoconductive and biocompatible properties of the cement ensured full filling of the defect with a complex configuration and created conditions for the stable fixation of the prosthesis components in the early postoperative period. The limited follow-up period did not allow for the assessment of long-term results, thus emphasizing the need for further clinical research.

Conflict of interest. The authors declare no conflict of interest.

Prospects for further research. Optimization of surgical outcomes in patients with cavitary bone defects.

Authors' contribution. Filipenko V. A. — performing the surgical intervention, setting the goals and objectives of the study, editing the article; Ivanchuk K. S. — analysis of primary material, conducting experimental research, drafting the article.

References

1. Filipenko, V., Vorontsov, P., Valeriia, H., Zorik, A., Samoylova, K., Slota, O., & Mezentsev, V. (2021). Allografting in the case of revision hip arthroplasty at aseptic loosening of the acetabular component. *Orthopaedics, traumatology and prosthetics,* (4), 5–11. https://doi.org/10.15674/0030-5987202045-11
2. Li, J. J., Dunstan, C. R., Entezari, A., Li, Q., Steck, R., Saifzadeh, S., Sadeghpour, A., Field, J. R., Akey, A., Vielreicher, M., Friedrich, O., Roohani-Esfahani, S., & Zreiqat, H. (2019). A novel bone substitute with high bioactivity, strength, and porosity for repairing large and load-bearing bone defects. *Advanced healthcare materials, 8*(13), e1900641. https://doi.org/10.1002/adhm.201900641
3. Baldwin, P., Li, D. J., Auston, D. A., Mir, H. S., Yoon, R. S., & Koval, K. J. (2019). Autograft, allograft, and bone graft substitutes: Clinical evidence and indications for use in orthopaedic trauma surgery. *Journal of orthopaedic trauma, 33*(4), 203–213.

https://doi.org/10.1097/BOT.0000000000001420
4. Jiang, J., Wang, J., Fan, P., Zhao, Z., Deng, H., Li, J., Wang, Y., & Wang, Y. (2025). Biomaterial-based strategies for bone cement: Modulating the bone microenvironment and promoting regeneration. *Journal of nanobiotechnology, 23*(1). https://doi.org/10.1186/s12951-025-03363-5
5. Goncharenko, A., Zyman, Z., & Epple, M. (2020). *Structure–property relationships in a reinforced calcium phosphate cement based on metastable α'-tricalcium phosphate.* In book of abstracts: joint polish-german crystallographic meeting.
6. Poplavska, K., & Ashukina, N. (2023). Bone regeneration after implantation of calcium phosphate cements based on metastable tricalcium phosphate (in vivo experimental study). *Orthopaedics, traumatology and prosthetics*, (1), 41–48. https://doi.org/10.15674/0030-59872023141-48
7. Chun, C. H., Kim, J. W., Kim, S. H., Kim, B. G., Chun, K. C., & Kim, K. M. (2014). Clinical and radiological results of femoral head structural allograft for severe bone defects in revision TKA: A minimum 8-year follow-up. *The knee, 21*(2), 420–423. https://doi.org/10.1016/j.knee.2013.04.012
8. Zyman, Z., Goncharenko, A., Khavroniuk, O., & Rokhmistrov, D. (2020). Crystallization of metastable and stable phases from hydrolyzed amorphous calcium phosphates with a Ca/P ratio of 1:1. *Journal of crystal growth,* 535, 125547. https://doi.org/10.1016/j.jcrysgro.2020.125547
9. Kumar, V., Naik, G. N., Tuteja, S., Bhasin, M. T., Chattopadhyay, D., Chowdhury, S., & Kashwani, R. (2025). Evaluation of radiographic and clinical outcomes in the use of bone substitutes in periapical surgery and periodontal regeneration. *Journal of pharmacy and bioallied sciences, 17*(Suppl. 3), S2218–S2220. https://doi.org/10.4103/jpbs.jpbs_1058_25
10. Czechowska, J. P., Dorner-Reisel, A., & Zima, A. (2024). Hybrid bone substitute containing tricalcium phosphate and silver-modified hydroxyapatite–methylcellulose granules. *Journal of functional biomaterials, 15*(7), 196. https://doi.org/10.3390/jfb15070196
11. Cerbu, C., Ursache, S., Botis, M. F., & Hadăr, A. (2021). Simulation of hybrid carbon-aramid composite materials based on mechanical characterization by digital image correlation method. *Polymers, 13*(23), 4184. https://doi.org/10.3390/polym13234184
12. Dorozhkin, S. (2013). Calcium orthophosphate-based bioceramics. *Materials, 6*(9), 3840–3942. https://doi.org/10.3390/ma6093840
13. Dziadek, M., Zima, A., Cichoń, E., Czechowska, J., & Ślósarczyk, A. (2020). Biomicroconcretes based on hybrid HAp/CTS granules, α-TCP, and pectins as novel injectable bone substitutes. *Materials letters,* 265, 127457. https://doi.org/10.1016/j.matlet.2020.127457
14. Elgali, I., Omar, O., Dahlin, C., & Thomsen, P. (2017). Guided bone regeneration: Materials and biological mechanisms revisited. *European journal of oral sciences, 125*(5), 315–337. https://doi.org/10.1111/eos.12364
15. Gu, X., Li, Y., Qi, C., & Cai, K. (2022). Biodegradable magnesium phosphates in biomedical applications. *Journal of materials chemistry B, 10*(13), 2097–2112. https://doi.org/10.1039/d1tb02836g
16. Hou, X., Zhang, L., Zhou, Z., Luo, X., Wang, T., Zhao, X., Lu, B., Chen, F., & Zheng, L. (2022). Calcium phosphate-based biomaterials for bone repair. *Journal of functional biomaterials, 13*(4), 187. https://doi.org/10.3390/jfb13040187

The article has been sent to the editors	Received after review	Accepted for printing
12.01.2026	12.02.2026	23.02.2026

CLINICAL CASE OF USING TRICALCIUM PHOSPHATE-BASED BONE CEMENT REINFORCED WITH HYDROXYAPATITE

V. A. Filipenko [1], K. S. Ivanchuk [2]

[1] Sytenko Institute of Spine and Joint Pathology National Academy of Medical Sciences of Ukraine, Kharkiv

[2] SI «National Institute of Traumatology and Orthopedics of the NAMS of Ukraine», Kyiv

✉ Volodymyr Filipenko, MD, DMSci, Prof. in Orthopaedic and Traumatology: filippenko1957@gmail.com; https://orcid.org/0000-0001-5698-2726

✉ Karolina Ivanchuk, MD, PhD: https://orcid.org/0000-0002-9838-1651

ISSN 0030-5987. Orthopaedics, traumatology and prosthetics. 2026. № 1

DIGEST AND REVIEWS

УДК 616.711-001.36-036.87(048.8)

DOI: http://dx.doi.org/10.15674/0030-598720261101-108

Risk factors of recurrence lumbar disc herniation after primary endoscopic transforaminal discectomy. Part 2

V. K. Piontkovskyi [1], V. A. Kolesnichenko [2], M. B. Holbaum [3]

[1] V. T. Zaitsev Institute of General and Emergency Surgery of the National Academy of Medical Sciences of Ukraine

[2] V. N. Karazin Kharkiv National University, Ukraine

[3] Sytenko Institute of Spine and Joint Pathology National Academy of Medical Sciences of Ukraine, Kharkiv

Recurrence of lumbar disc herniation (LDH) after primary endoscopic transforaminal discectomy (PETD) is diagnosed in 3.8–15 % of cases. Objective. To study preoperative radiographic and MRI signs that potentiate LDH recurrence after PETD. Methods The study material consisted of articles identifying radiographic and MRI risk factors for recurrent LDH after PETD between 2015 and 2025 in the PubMed, Google Scholar, and Medline databases. The study method was a systematic review of relevant literature sources. Results. The level of LDH does not influence the incidence of rLDH, although some authors consider the presence of a disc herniation in the upper lumbar spine as a risk factor for recurrence. rLDH is significantly more frequently recorded with primary disc protrusion; in cases of migrated disc herniation, the risk of rLDH significantly increases with large intracanal displacement of disc material extending beyond the inferior margin of the superior or inferior vertebral pedicle. The use of PETD for resection of central disc herniations most often results in recurrent LDH (compared to foraminal, extraforaminal, and migratory) due to technical errors. A study of disc height index dynamics in the pre- and postoperative periods and the degree of Modic type endplate degeneration showed that the less severe the degenerative processes in the prolapsed intervertebral disc, the higher the risk of herniation recurrence after PETD. Conclusions. Recurrence disc herniation after PETD is significantly more common in cases of primary protrusion and significantly increases with large annular defects (≥ 6 mm). rLDH is significantly more common in discs with moderate degenerative changes, with a disc height index of approximately 0.37 ± 0.09 and Modic type 1.

Рецидив грижі міжхребцевого диска (ГМД) поперекового відділу хребта (ПВХ) після первинної ендоскопічної трансфораміналної дискектомії (ПЕТД) діагностується в 3,8–15 % випадків. Мета. Вивчити на передопераційному етапі рентгенологічні та МРТ-ознаки, які потенціюють рецидив ГМД ПВХ після ПЕТД. Методи. Проаналізовано статті, які містять визначення рентгенологічних і МРТ-факторів ризику рецидиву грижі міжхребцевого диска (рГМД) ПВХ після ПЕТД, за період 2015–2025 р. у базах даних PubMed, Google Scholar, Medline. Здійснено систематичний огляд релевантних джерел літератури. Результати. Рівень грижі міжхребцевого диска ПВХ не впливає на частоту рГМД, хоча окремі автори розглядають її наявність у верхньопоперековому відділі як ризик рецидивування. Значущо частіше рГМД реєструється в разі первинної протрузії диска; у разі грижі, яка мігрувала, ризик рГМД достовірно зростає за умов значного інтраканального зміщення матеріалу диска, який виходить за межі нижнього краю верхньої або нижньої ніжки хребця. Використання ПЕТД для резекції центральних гриж дисків найчастіше призводить до рГМД через технічні помилки. Вивчення динаміки індексу висоти диска в перед- та післяопераційному періодах та ступеня дегенерації замикальних пластинок диска за типом Modic показало, що чим менш виражені дегенеративні процеси, тим вище ризик рецидиву грижі після ПЕТД. Висновки. рГМД після ПЕТД достовірно частіше реєструється в разі первинної протрузії і достовірно зростає за умов значних дефектів фіброзного кільця. Значимо частіше ГМД рецидивує в дисках із помірно вираженими дегенеративними змінами з індексом висоти диска приблизно 0,37 ± 0,09 та типом Modic 1. Ключові слова. Первинна ендоскопічна трансфораміналь дискектомія, рецидив грижі міжхребцевого диска поперекового відділу хребта, фактори ризику, морфометрія поперекового сегмента, дегенеративні зміни міжхребцевих дисків поперекового відділу хребта.

Keywords. Primary endoscopic transforaminal discectomy, recurrent lumbar disc herniation, risk factors, lumbar segment morphometry, degenerative changes in lumbar intervertebral disc

Introduction

Percutaneous transforaminal endoscopic discectomy (PTED) is one of the most widely used and successful modern methods of minimally invasive surgical treatment for lumbar intervertebral disc herniation (LDH). The advantages of PTED include minimal tissue trauma, reduced blood loss, a clean surgical field [1], the possibility of preserving the posterior ligamentous complex and other biomechanical structures [2], the ability to perform surgery in some cases under local anesthesia [3], relatively low surgical costs [4], and high patient satisfaction rates [5].

Despite the ongoing development and improvement of the endoscopic discectomy technique for LDH [6, 7], there are reports of unfavorable treatment outcomes [8–11]. One of the most common complications of PTED is recurrent lumbar disc herniation (rLDH), with the incidence varying significantly in the literature: 3.8–7.4 % [12], 1.4–11.4 % [13], 5–15 % [14]. It is the most frequent cause of reoperation, with an overall rate of 5.2–19 %, increasing with the length of follow-up [13, 15]. Reoperations are more commonly performed earlier in older patients [16]. Although re-surgery remains effective, it is often associated with worse functional outcomes, increases the likelihood of further reoperations, and is frequently complicated by the formation of epidural scar tissue [17, 18], which raises the risk of dural tears or nerve damage [19, 20]. Additionally, the removal of the posterior vertebral structure may increase the risk of segmental instability [21]. Both reoperation and the clinical symptoms associated with rLDH have a negative psychological impact [22] and substantial economic burden on patients [23]. Therefore, identifying risk factors for rLDH after PTED is of significant clinical importance for developing surgical protocols, selecting patients appropriately, and improving the effectiveness of endoscopic transforaminal discectomy.

Risk factors for rLDH after primary transforaminal discectomy have been reported in numerous studies, often with conflicting results [22, 24–28]. In our previous literature review on clinical risk factors for rLDH, the most likely factors identified were age > 50 years, body mass index > 25 kg/m², and the time from initial discectomy > 8 weeks after the clinical manifestation [29].

Purpose: To study the radiological and MRI signs that may predispose to recurrent lumbar disc herniation after percutaneous transforaminal endoscopic discectomy.

Material and Methods

The study material includes professional articles that define radiological and MRI signs considered as risk factors for recurrent lumbar disc herniation after primary PTED, published between 2015 and 2024, sourced from PubMed, Google Scholar, and Medline databases. These studies were selected using medical subject headings and keywords such as “recurrent lumbar disc herniation”, “minimally invasive lumbar spine surgery”, “percutaneous endoscopic lumbar discectomy”, “percutaneous endoscopic transforaminal discectomy”, “reoperation”, “re-discectomy”, “radiological risk factors for recurrent lumbar disc herniation”, “lumbar vertebral segment morphometry”, and “MRI signs of intervertebral disc degeneration”.

Recurrent lumbar disc herniation was defined as a confirmed, symptomatic recurrence of LDH at the level of the initial discectomy, detected by imaging methods (radiography/CT/MRI), with radiculalgia ipsilateral to the preoperative symptoms, leading to a repeat surgery [12].

Inclusion criteria: articles that address the results of identifying radiological and MRI risk factors for recurrent mono-segmental LDH after primary PTED.

Exclusion criteria: publications on the outcomes of open surgical treatment for LDH, open and endoscopic discectomy for polysegmental and recurrent LDH in the lumbar spine.

Research method: systematic review of relevant literature sources.

Results and discussion

Level of intervertebral disc herniation

The prevailing view in the literature is that there is no significant correlation between the level of LDH and the frequency of recurrence [22, 30–32]. More intense preoperative radiculalgia and relatively prolonged (up to 1 month) postoperative pain syndrome in patients with extraforaminal and foraminal hernias of L_{IV}–L_V discs are associated with compression or irritation of the ganglion of the posterior nerve roots by the disc material [30, 33]. Some authors consider the location of the disc herniation in the upper lumbar region as a risk factor for rLDH [34].

Type of intervertebral disc herniation:

Recurrent LDH is significantly more frequent in cases of primary disc protrusion, where the defect in the annulus fibrosus (AF) has a wider diameter due to the broad neck of the hernia [35]. Primary extrusion of the intervertebral disc, both transligamentous and subligamentous, does not increase the risk of rLDH [36]. In cases of migrated hernias, the risk increases significantly when there is considerable in-

tracanalar displacement of the disc material beyond the lower edge of the upper or lower vertebral facet [37–39].

When using traditional transforaminal access, complete resection of migrated disc material is complicated by technical difficulties in grasping the distal fragment of the disc [40]. Recently, modified surgical techniques have been proposed for such cases, including targeted puncture and foraminotomy [38], suprapedicular retrocorporeal access [41], and mobile "outside-in" techniques [42]. Most of these methods are considered more appropriate for PTED of migrating hernias of the lower lumbar intervertebral discs [38, 43]. Endoscopic discectomy for LDH in the upper lumbar segments is more often performed through an interlaminar approach [39, 44].

The risk of rLDH significantly increases in cases of large defects in the annulus fibrosus (≥ 6 mm) [45, 46], with irritation of the nerve root causing clinically significant postoperative radiculalgia [47]. Additionally, through defects in the annulus fibrosus, inflammatory mediators can come into contact with the nerve roots, potentially leading to chemical radiculitis [48].

To prevent recurrent disc material protrusion, aggressive discectomy is performed to remove as much of the gelatinous nucleus as possible [49]. However, the drawbacks of this approach include a more rapid decrease in intervertebral disc height and accelerated degeneration of the disc [48, 50].

Localization of the intervertebral disc herniation

Recurrent LDH after PTED most commonly occurs after resection of central disc herniations, with the primary cause of this complication being technical errors [51, 52]. In the past, the presence of a central disc herniation was considered a contraindication for PTED due to the location of the working zone near the posterior midline, making it difficult to position the endoscope at the correct angle and differentiate the soft tissues visually [51]. This could lead to nerve root injury and incomplete removal of the disc material [42, 51]. Over time, with the advancement of PTED techniques, resection of central disc herniations has been performed using foraminoplasty. In this case, the newly created expanded intervertebral foramen provides a full view of the central disc herniation, the adjacent compromised nerve root, and, if necessary, the contralateral spinal nerve root, following the principle of "unilateral access, bilateral decompression" [51]. The presence of intervertebral disc herniation at other locations (foraminal, extraforaminal) or migrated hernias does not affect the recurrence rate after PTED [38, 43, 53, 54].

Intervertebral disc height

The height of the intervertebral disc (IDH) is determined by both absolute and relative measurements. The absolute height is the arithmetic mean of the height of the disc in the anterior and posterior sections, or the anterior, middle, and posterior parts of the disc [55].

As a predictor for rLDH, the dynamic change in IDH during the pre- and postoperative periods is important. The IDH typically decreases by approximately 0.8 mm after disc tissue is removed during discectomy [56]. A lower IDH in the early postoperative period (compared to preoperative values) indicates a more aggressive discectomy [55]. The frequency of rLDH after limited discectomy is twice as high as that following aggressive discectomy [57, 58]. It is important to note that the optimal amount of disc herniation that should be removed for the best clinical outcomes remains unclear [55]. A decrease in IDH over time [29, 47] is often accompanied by inclination and later hyperplasia of the articular processes and their facets, which may lead to clinically significant spondyloarthrosis in the long-term postoperative period [59].

The relative measurement of IDH is the intervertebral disc height index (IDHI), which is calculated as the ratio of the disc height to the height or width of the adjacent vertebra [55]. Regardless of the calculation method, higher IDHI values at the level of surgical intervention are significantly correlated with an increased frequency of rLDH after PTED [25, 35, 36, 55]. For example, at 48 months post-surgery, the average IDHI was 0.37 ± 0.09 in the group with recurrent disc herniation and 0.29 ± 0.09 in patients without rLDH [25]; and 0.35 ± 0.007 and 0.26 ± 0.002, respectively [55]. In other words, the less pronounced the degenerative processes in the prolapsed intervertebral disc, the higher the risk of recurrent herniation after PTED.

Higher IDHI values correspond to moderate degenerative changes in the intervertebral disc. A hypointense signal from the prolapsed nucleus pulposus on T2-weighted MRI images [60] indicates the preservation of some amount of hydrophilic glycosaminoglycans in the extracellular matrix of the nucleus pulposus [61], and undamaged collagen, predominantly in the anterior part of the annulus fibrosus [62]. The structural-functional properties of the intervertebral disc are partially preserved; its tissues are capable of maintaining some oncotic pressure [63]. However, the presence of a structural defect in the disc leads to a reduction in its mechanical stiffness, resulting in excessive segmental mobility.

Discectomy in such a "latent unstable segment" [55] ("segment with micron instability" [64]) accelerates degeneration of the disc, leading to persistent chronic pain syndrome [56], rLDH [25, 35, 36, 55], and potential instability of the operated segment [65, 66].

At later stages of degeneration, structural changes in the disc tissue with herniation are characterized by an increase in the number of fibrous-cartilage and hypertrophic cells in the nucleus pulposus matrix, significant loss of disc volume, an increase in the overall thickness of the endplates, and degeneration of the annulus fibrosus layers [67]. This is visualized on MRI as a "gray/black disc" appearance [68]. As the intervertebral disc undergoes fibrotization, the segment gradually loses its motor function. Restabilization of the segment occurs when the disc collapses with a reduction in its height of more than 50 %, which correlates with an IDHI of approximately 0.15 [55]. Therefore, the relationship between IDHI and rLDH is determined by the interdependence of the processes of structural degradation in the disc tissue and their biomechanical consequences.

MRI signs of intervertebral disc degeneration

The degree of intervertebral disc degeneration is determined on MRI scans using the Modic classification [69] and the Pfirrmann classification [70]. Modic changes reflect alterations in the endplates and bone marrow of the vertebral bodies adjacent to the intervertebral disc, detected through changes in signal intensity on T1- and T2-weighted tomography scans, and correlate with histological findings [36] and disc degeneration [71].

Modic type 1 changes are associated with splitting, microfractures in the endplates, and edema in the bone marrow; type 2 indicates fatty degeneration of the bone marrow [69]; and type 3 involves sclerosis of the endplates and subchondral bone [72]. There is a consensus in the literature regarding the significant correlation between the higher frequency of rLDH and the presence of Modic type 1 changes [12, 22, 27, 36, 37, 73, 74]. This is thought to be due to the damage to the endplates and the bone marrow edema, which leads to an increase in intraosseous pressure in the vertebral body [75], resulting in increased oncotic pressure in the disc. This promotes the migration of the nucleus pulposus through the cracks in the annulus fibrosus and the endplates, thereby increasing the risk of forming rLDH [76].

The MRI classification for assessing the degree of intervertebral disc degeneration according to Pfirrmann on sagittal T2-weighted tomograms includes the following qualitative parameters: the signal intensity from the nucleus pulposus and the homogeneity of its structure; the differentiation between the images of the nucleus pulposus and the annulus fibrosus; and the height of the intervertebral disc. The classification consists of 5 stages of degeneration, where Stage I represents normal disc MRI images, and Stage V corresponds to the late stages of degeneration with a loss of structure and disc collapse [70]. The relationship between the frequency of rLDH after PTED and the degree of disc degeneration according to the Pfirrmann classification in the literature is debated. Some authors have found no significant correlation between these parameters [36, 43], while others have established a significant connection when degeneration reaches Pfirrmann Stage ≥ IV [22, 77, 78], Stage III [75], or ≥ Stage III [79]. In other words, in most reports, the frequency of rLDH, according to the Pfirrmann classification, is significantly higher in discs with advanced degeneration, while disc height, IDHI, and Modic type correlate with rLDH frequency in cases of moderate degeneration of the disc tissue. These contradictory results may be explained by the insufficient discreteness of the Pfirrmann criteria [80, 81] and their incomplete correspondence with morphological, particularly involutional, features [82, 83], which were noted by the authors of the classification themselves [70].

J. F. Griffith and colleagues developed a modified Pfirrmann classification that contains 8 stages based on the interpretation of sagittal T2-weighted tomograms using three main criteria: signal intensity from the nucleus pulposus and the internal fibers of the annulus fibrosus (Stages 1–3); differentiation between the internal and external fibers of the annulus fibrosus at the posterior edge of the disc (Stages 4 and 5); and reduction in disc height (Stages 6–8) [80]. Although the Griffith classification for disc degeneration is more detailed, it has not gained widespread use.

Conclusions

Recurrent disc herniation after PTED is significantly more frequent in cases of primary disc protrusion and increases with significant defects in the annulus fibrosus (≥ 6 mm). Most disc herniation recurrences occur after resection of central disc hernias due to technical errors. The level of disc herniation does not influence the frequency of recurrence.

rLDH after PTED is significantly more frequent in discs with moderate degenerative changes, with an IDHI of approximately 0.37 ± 0.09 and Modic type 1 changes. The data on the relationship between rLDH frequency and the degree of disc degeneration according to the Pfirrmann classification remain contradictory.

Conflict of Interest. The authors declare that there is no conflict of interest.

Future research prospects. Currently, it is important to analyze the literature regarding the impact of radiological, including radiometric, indicators on the frequency of recurrent lumbar disc herniations.

Funding information. No financial benefit, in any form, has been or will be received from any commercial party directly or indirectly associated with the subject matter of this article.

Authors' contributions. Piontkovsky V.K. — Concept and design, assessment of findings; Kolesnichenko V.A. — Concept and design, literature search; Holbaum M.B. — Data analysis, material processing, text editing.

References

1. Jarebi, M., Awaf, A., Lefranc, M., & Peltier, J. (2021). A matched comparison of outcomes between percutaneous endoscopic lumbar discectomy and open lumbar microdiscectomy for the treatment of lumbar disc herniation: A 2-year retrospective cohort study. *The spine journal, 21*(1), 114–121. https://doi.org/10.1016/j.spinee.2020.07.005
2. Jang, J. N., Song, Y., Kim, J. W., & Kim, Y. U. (2023). Comparison of ligamentum flavum thickness between central and lateral lesions in a patient with central lumbar spinal canal stenosis. *Medicine, 102*(33), e34873. https://doi.org/10.1097/md.0000000000034873
3. Mooney, J., Laskay, N., Erickson, N., Salehani, A., Mahavadi, A., Ilyas, A., Mainali, B., Nowak, B., & Godzik, J. (2022). General vs local anesthesia for percutaneous endoscopic lumbar Discectomy (PELD): A systematic review and meta-analysis. *Global spine journal, 13*(6), 1671–1688. https://doi.org/10.1177/21925682221147868
4. Droeghaag, R., Schuermans, V. N., Hermans, S. M., Smeets, A. Y., Caelers, I. J., Hiligsmann, M., Evers, S., Van Hemert, W. L., & Van Santbrink, H. (2023). Methodology of economic evaluations in spine surgery: A systematic review and qualitative assessment. *BMJ open, 13*(3), e067871. https://doi.org/10.1136/bmjopen-2022-067871
5. Dandurand, C., Mashayekhi, M. S., McIntosh, G., Singh, S., Paquet, J., Chaudhry, H., Abraham, E., Bailey, C. S., Weber, M. H., Johnson, M. G., Nataraj, A., Attabib, N., Kelly, A., Hall, H., Rampersaud, Y. R., Manson, N., Phan, P., Thomas, K., Fisher, C., … Dea, N. (2023). Cost consequence analysis of waiting for lumbar disc herniation surgery. *Scientific Reports, 13*(1). https://doi.org/10.1038/s41598-023-31029-5
6. Abdulla Hasan, G., & Hayder Qatran, M. (2023). Endoscopic spine surgery: The next golden standard technique in spinal surgeries. *Frontiers in spinal neurosurgery*. https://doi.org/10.5772/intechopen.1001469
7. Khandge, A. V., Sharma, S. B., & Kim, J. (2021). The evolution of Transforaminal endoscopic spine surgery. *World neurosurgery,* 145, 643–656. https://doi.org/10.1016/j.wneu.2020.08.096
8. Chen, Z., Zhang, L., Dong, J., Xie, P., Liu, B., Chen, R., Li, S., Liu, Z., Yang, B., Feng, F., He, L., Yang, Y., Pang, M., & Rong, L. (2022). Percutaneous Transforaminal endoscopic Discectomy versus Microendoscopic Discectomy for lumbar disk Herniation: Five-year results of a randomized controlled trial. *Spine, 48*(2), 79–88. https://doi.org/10.1097/brs.0000000000004468
9. Ju, C. I., & Lee, S. M. (2023). Complications and management of endoscopic spinal surgery. *Neurospine, 20*(1), 56–77. https://doi.org/10.14245/ns.2346226.113
10. Yang, C., Chen, C., Lin, M. H., Huang, W., Lee, M., Kim, J., & Chen, K. (2022). Complications of full-endoscopic lumbar Discectomy versus open lumbar Microdiscectomy: A systematic review and meta-analysis. *World neurosurgery*, 168, 333–348. https://doi.org/10.1016/j.wneu.2022.06.023
11. Chen, Q., Zhang, Z., Liu, B., & Liu, S. (2020). Evaluation of percutaneous Transforaminal endoscopic Discectomy in the treatment of lumbar disc Herniation: A retrospective study. *Orthopaedic surgery, 13*(2), 599–607. https://doi.org/10.1111/os.12839
12. Zileli, M., Oertel, J., Sharif, S., & Zygourakis, C. (2024). Lumbar disc herniation: Prevention and treatment of recurrence: WFNS spine committee recommendations. *World neurosurgery: X,* 22, 100275. https://doi.org/10.1016/j.wnsx.2024.100275
13. Hassan Kadri, Mohamad Shehadeh Agha, Raed Abouharb, Rostom Mackieh, Ahmad Atto, & Tim Kadri. (2024). Is spinal fusion the preferred treatment for recurrent lumbar disc herniation of the lumbar spine? *World journal of biology pharmacy and health sciences, 18*(3), 303–308. https://doi.org/10.30574/wjbphs.2024.18.3.0247
14. Gupta, A., Chhabra, H. S., Nagarjuna, D., & Arora, M. (2020). Comparison of functional outcomes between lumbar Interbody fusion surgery and Discectomy in massive lumbar disc Herniation: A retrospective analysis. *Global spine journal, 11*(5), 690–696. https://doi.org/10.1177/2192568220921829
15. Yoshihara, H., Chatterjee, D., Paulino, C. B., & Errico, T. J. (2016). Revision surgery for "Real" recurrent lumbar disk Herniation. *Clinical spine surgery: a spine publication, 29*(3), 111–118. https://doi.org/10.1097/bsd.0000000000000365
16. Siccoli, A., Schröder, M. L., & Staartjes, V. E. (2020). Association of age with incidence and timing of recurrence after microdiscectomy for lumbar disc herniation. *European spine journal, 30*(4), 893–898. https://doi.org/10.1007/s00586-020-06692-1
17. Hoang, R., Song, J., Tiao, J., Trent, S., Ngan, A., Hoang, T., Kim, J. S., Cho, S. K., Hecht, A. C., Essig, D., Virk, S., & Katz, A. D. (2024). Comparison of postoperative complications and outcomes following primary versus revision discectomy: A national database analysis. *Journal of Craniovertebral Junction and Spine, 15*(3), 303–307. https://doi.org/10.4103/jcvjs.jcvjs_97_24
18. Aihara, T., Kojima, A., Urushibara, M., Endo, K., Sawaji, Y., Suzuki, H., Nishimura, H., Murata, K., Konishi, T., & Yamamoto, K. (2022). Long-term reoperation rates and causes for reoperations following lumbar microendoscopic discectomy and decompression: 10-year follow-up. *Journal of clinical neuroscience*, 95, 123–128. https://doi.org/10.1016/j.jocn.2021.11.015
19. Luo, L., Zhao, C., Li, P., Liu, L., Zhou, Q., Luo, F., & Liang, L. (2021). Posterior dynamic stabilization with limited Rediscectomy for recurrent lumbar disc Herniation. *Pain research and management,* 2021, 1–7. https://doi.org/10.1155/2021/1288246
20. Heo, D. H., Ha, J. S., Lee, D. C., Kim, H. S., & Chung, H. J. (2020). Repair of incidental Durotomy using Sutureless Nonpenetrating clips via Biportal endoscopic surgery. *Global spine journal, 12*(3), 452–457. https://doi.org/10.1177/2192568220956606
21. Arif, S., Brady, Z., Enchev, Y., & Peev, N. (2020). Is fusion the most suitable treatment option for recurrent lumbar disc herniation? A systematic review. *Neurological research, 42*(12), 1034–1042. https://doi.org/10.1080/01616412.2020.1787661
22. Zhao, J., Zeng, L., Zhao, S., Liang, G., Sha, B., Fu, H., Yang, W., Liu, J., & Zeng, Y. (2024). Associations of recurrent lumbar disc herniation after percutaneous endoscopic lumbar discectomy with age, body mass index, modic change, disc degeneration and sacral slope: A quantitative review. *Experimental and therapeutic medicine, 27*(5). https://doi.org/10.3892/etm.2024.12483
23. Droeghaag, R., Schuermans, V. N., Hermans, S. M., Smeets, A. Y., Caelers, I. J., Hiligsmann, M., Van Hemert, W. L., Evers, S., & Van Santbrink, H. (2021). Evidence-based recommendations for economic evaluations in spine surgery: Study protocol for a Delphi consensus. *BMJ open, 11*(12), e052988. https://doi.org/10.1136/bmjopen-2021-052988
24. Park, C. H. (2019). Risk factors for early recurrence After-Transforaminal endoscopic lumbar DiscDecompression. *Pain physician, 2*(22.2), E133–E138. https://doi.org/10.36076/

ppj/2019.22.e133
25. Kim, K., Lee, D., Cho, D., Sung, J., & Kim, Y. (2015). Preoperative risk factors for recurrent lumbar disk Herniation in L5–S1. *Journal of spinal disorders & techniques, 28*(10), E571–E577. https://doi.org/10.1097/bsd.0000000000000041
26. Kandregula, S., & Guthikonda, B. (2021). Minimally invasive TLIF. *Neurology India, 69*(5), 1141. https://doi.org/10.4103/0028-3886.329539
27. Abdallah, A., & Güler Abdallah, B. (2022). Factors associated with the recurrence of lumbar disk herniation: non-biomechanical–radiological and intraoperative factors. *Neurological research, 45*(1), 11–27. https://doi.org/10.1080/01616412.2022.2116525.
28. Patgaonkar, P., Goyal, V., Agrawal, U., Marathe, N., & Patel, V. (2022). Impact of body weight, height, and obesity on selection of skin entry point for Transforaminal endoscopic lumbar Discectomy. *Asian journal of neurosurgery, 17*(02), 262–267. https://doi.org/10.1055/s-0042-1751005
29. Kolesnichenko, V., Piontkovskyi, V., Holbaum, M., Chernyshov, O., Palkin, O., & Palkin, B. (2025). Risk factors of recurrence lumbar intervertebral disc herniation after primary endoscopic transforaminal discectomy. Part 1 (Literature review). *Orthopaedics, traumatology and prosthetics*, (2), 92–98. https://doi.org/10.15674/0030-59872025292-98
30. Kang, M., Hwang, J., Park, S., Yang, J., You, K., Hong, S., Cho, S. K., & Park, H. (2024). Comparison of biportal endoscopic and microscopic tubular paraspinal approach for foraminal and extraforaminal lumbar disc herniation. *Journal of neurosurgery: spine, 41*(4), 473–482. https://doi.org/10.3171/2024.4.spine23707
31. Echt, M., Holland, R., Mowrey, W., Cezayirli, P., De la Garza Ramos, R., Hamad, M., Gelfand, Y., Longo, M., Kinon, M. D., Yanamadala, V., Chaudhary, S., Cho, S. K., & Yassari, R. (2020). Surgical outcomes for upper lumbar disc Herniations: A systematic review and meta-analysis. *Global spine journal, 11*(5), 802–813. https://doi.org/10.1177/2192568220941815
32. Kapetanakis, S., Gkantsinikoudis, N., & Apostolakis, S. (2022). Technical challenges and surgical outcomes of percutaneous transforaminal endoscopic discectomy in patients with upper lumbar disc herniation: A prospective clinical study. *Archives of orthopaedic and trauma surgery, 143*(8), 4613–4623. https://doi.org/10.1007/s00402-022-04725-6
33. Kim, H. S., Kim, J. Y., Wu, P. H., & Jang, I. (2021). Effect of dorsal root ganglion retraction in endoscopic lumbar decompressive surgery for foraminal pathology: A retrospective cohort study of interlaminar contralateral endoscopic lumbar Foraminotomy and Discectomy versus Transforaminal endoscopic lumbar Foraminotomy and Discectomy. *World neurosurgery,* 148, e101–e114. https://doi.org/10.1016/j.wneu.2020.12.176
34. Tao, H. (2018). Prevalence of recurrent Herniation Following-Percutaneous endoscopic lumbar Discectomy:A meta-analysis. *Pain physician, 1*(21;1), 337–350. https://doi.org/10.36076/ppj.2018.4.337
35. Li, Z., Yang, H., Liu, M., Lu, M., Chu, J., Hou, S., & Hou, T. (2018). Clinical characteristics and risk factors of recurrent lumbar disk Herniation. *Spine, 43*(21), 1463–1469. https://doi.org/10.1097/brs.0000000000002655
36. Brooks, M., Dower, A., Abdul Jalil, M. F., & Kohan, S. (2021). Radiological predictors of recurrent lumbar disc herniation: A systematic review and meta-analysis. *Journal of neurosurgery: spine, 34*(3), 481–491. https://doi.org/10.3171/2020.6.spine20598
37. Jia, M., Sheng, Y., Chen, G., Zhang, W., Lin, J., Lu, S., Li, F., Ying, J., & Teng, H. (2021). Development and validation of a nomogram predicting the risk of recurrent lumbar disk herniation within 6 months after percutaneous endoscopic lumbar discectomy. *Journal of orthopaedic surgery and research, 16*(1). https://doi.org/10.1186/s13018-021-02425-2
38. Shen, J., Wang, X., Cai, B., Chen, Y., Zhang, G., Xu, J., & Lian, X. (2022). Transforaminal endoscopic lumbar discectomy with targeted puncture and foraminotomy for very highly migrated disc herniation: A technique note with case series. *Heliyon, 8*(10), e11115. https://doi.org/10.1016/j.heliyon.2022.e11115
39. Yang, F., Ren, L., Ye, Q., Qi, J., Xu, K., Chen, R., & Fan, X. (2021). Endoscopic and microscopic interlaminar Discectomy for the treatment of far-migrated lumbar disc Herniation: A retrospective study with a 24-Month follow-up. *Journal of pain research,* 14, 1593–1600. https://doi.org/10.2147/jpr.s302717
40. Lew, S. M., Mehalic, T. F., & Fagone, K. L. (2001). Transforaminal percutaneous endoscopic discectomy in the treatment of far-lateral and foraminal lumbar disc herniations. *Journal of neurosurgery: spine, 94*(2), 216–220. https://doi.org/10.3171/spi.2001.94.2.0216
41. Chen, C., Lin, G., Sharma, S., Kim, H., Sun, L., Wu, H., Chang, K., & Chen, Y. (2020). Suprapedicular Retrocorporeal technique of Transforaminal full-endoscopic lumbar Discectomy for highly downward-migrated disc Herniation. *World neurosurgery,* 143, e631–e639. https://doi.org/10.1016/j.wneu.2020.08.038
42. Kim, H. S., Adsul, N., Kapoor, A., Choi, S. H., Kim, J. H., Kim, K. J., Bang, J. S., Yang, K. H., Han, S., Lim, J. H., Jang, J., Jang, I., & Oh, S. (2018). A mobile outside-in technique of Transforaminal lumbar endoscopy for lumbar disc Herniations. *Journal of visualized experiments*, (138). https://doi.org/10.3791/57999-v
43. AbdElfattah, M., Elkazaz, M., & Khedr, A. S. (2022). Transforaminal percutaneous endoscopic lumbar Discectomy (TPELD) in caudal migrated lumbar disc Herniations: A case series and literature review. *Advanced spine journal, 41*(1). https://doi.org/10.57055/2314-8969.1005
44. Huang, K., Chen, G., Lu, S., Lin, C., Wu, S., Chen, B., Ying, J., Wang, Y., Zhu, M., & Teng, H. (2021). Early clinical outcomes of percutaneous endoscopic lumbar Discectomy for L4-5 highly down-migrated disc Herniation: Interlaminar approach versus Transforaminal approach. *World neurosurgery*, 146, e413–e418. https://doi.org/10.1016/j.wneu.2020.10.105
45. Miller, L. E., McGirt, M. J., Garfin, S. R., & Bono, C. M. (2018). Association of annular defect width after lumbar Discectomy with risk of symptom recurrence and Reoperation. *Spine, 43*(5), E308–E315. https://doi.org/10.1097/brs.0000000000002501
46. Zhang, Y., Chu, J., Xia, Y., Xie, Y., Zhang, R., Chen, X., Chen, Z., & Yao, X. (2023). Research trends of percutaneous endoscopic lumbar Discectomy in the treatment of lumbar disc Herniation over the past decade: A bibliometric analysis. *Journal of pain research,* 16, 3391–3404. https://doi.org/10.2147/jpr.s421837
47. Martens, F., Lesage, G., Muir, J. M., & Stieber, J. R. (2018). Implantation of a bone-anchored annular closure device in conjunction with tubular minimally invasive discectomy for lumbar disc herniation: A retrospective study. *BMC musculoskeletal disorders, 19*(1). https://doi.org/10.1186/s12891-018-2178-4
48. Zhao, Y., Tian, B., Ma, Q., & Zhang, M. (2023). Study on the clinical effect of percutaneous transforaminal endoscopic discectomy combined with annulus fibrosus repair in the treatment of single-segment lumbar disc herniation in young and middle-aged patients. *Pakistan journal of medical sciences, 40*(3). https://doi.org/10.12669/pjms.40.3.3419
49. Kienzler, J. C., Rey, S., Wetzel, O., Atassi, H., Bäbler, S., Burn, F., & Fandino, J. (2021). Incidence and clinical impact of vertebral endplate changes after limited lumbar microdiscectomy and implantation of a bone-anchored annular closure device. *BMC surgery, 21*(1). https://doi.org/10.1186/s12893-020-01011-3
50. Wang, F., Li, J., Li, J., Sun, K., Zhang, B., Wang, D., Song, E., & Li, F. (2025). Bone anchoring annular suture technique for repairing annular defects at vertebral body edge following lumbar discectomy. *Scientific reports, 15*(1). https://doi.org/10.1038/

s41598-025-89179-7
51. Li, P., Yang, F., Chen, Y., & Song, Y. (2021). Percutaneous transforaminal endoscopic discectomy for different types of lumbar disc herniation: A retrospective study. *Journal of international medical research, 49*(10). https://doi.org/10.1177/03000605211055045
52. Yerramneni, V. K., Kanala, R. R., Kolpakawar, S., & Yerragunta, T. (2021). MITLIF operative nuances- Step by step. *Neurology India, 69*(5), 1196–1199. https://doi.org/10.4103/0028-3886.329566
53. Ahn, Y., Bae, S., Jo, D., & Yoo, B. (2025). Magnetic resonance imaging predictors of surgical difficulty in Transforaminal endoscopic lumbar Discectomy for far-lateral disc Herniation under local anesthesia. *Biomedicines, 13*(4), 778. https://doi.org/10.3390/biomedicines13040778
54. Pruttikul, P., Pluemvitayaporn, T., Bannachirakul, M., Surapuchong, S., Kittithamvongs, P., Ratanakoosakul, W., Tiracharnvut, K., Piyasakulkaew, C., & Kunakornsawat, S. (2025). Transforaminal percutaneous endoscopic Discectomy for L3/4 and L4/5 foraminal and Extraforaminal lumbar disc Herniation: Clinical outcomes and technical note. *Asian journal of neurosurgery, 20*(02), 337–343. https://doi.org/10.1055/s-0045-1805018
55. Kweon, M., Bak, K., Yi, H., Choi, K., Han, M., Na, M., & Chun, H. (2024). Changes in disc height as a prognostic factor in patients undergoing microscopic Discectomy. *Journal of Korean neurosurgical society, 67*(2), 209–216. https://doi.org/10.3340/jkns.2023.0110
56. Brinckmann, P., & Grootenboer, H. (1991). Change of disc height, radial disc bulge, and Intradiscal pressure from Discectomy an in vitro investigation on human lumbar discs. *Spine, 16*(6), 641–646. https://doi.org/10.1097/00007632-199106000-00008
57. McGirt, M. J., Ambrossi, G. L., Datoo, G., Sciubba, D. M., Witham, T. F., Wolinsky, J., Gokaslan, Z. L., & Bydon, A. (2009). Recurrent disc herniation and long-term back pain after primary lumbar discectomy. *Neurosurgery, 64*(2), 338–345. https://doi.org/10.1227/01.neu.0000337574.58662.e2
58. Zileli, M. (2014). Recurrent disc Herniation. *Textbook of surgical management of lumbar disc herniation,* 298–298. https://doi.org/10.5005/jp/books/12000_45
59. Chen, X., Sandhu, H. S., Vargas Castillo, J., & Diwan, A. D. (2021). The association between pain scores and disc height change following discectomy surgery in lumbar disc herniation patients: A systematic review and meta-analysis. *European spine journal, 30*(11), 3265–3277. https://doi.org/10.1007/s00586-021-06891-4
60. Çetin, T., Kahraman, S., Kızılgöz, V., & Aydın, S. (2023). The comparison between herniated and non-herniated disc levels regarding Intervertebral disc space height and disc degeneration, a magnetic resonance study. *Diagnostics, 13*(20), 3190. https://doi.org/10.3390/diagnostics13203190
61. Ding, Y., Liu, L., Shi, J., Zhang, X., Chen, R., & Xu, S. (2024). Biochemical changes in lumbar facet joint and disc degeneration by T2* mapping. *BMC musculoskeletal disorders, 25*(1). https://doi.org/10.1186/s12891-024-07265-9
62. Yang, L., Sun, C., Gong, T., Li, Q., Chen, X., & Zhang, X. (2022). T1ρ, T2 and T2* mapping of lumbar intervertebral disc degeneration: A comparison study. *BMC musculoskeletal disorders, 23*(1). https://doi.org/10.1186/s12891-022-06040-y
63. Zhou, M., Theologis, A. A., & O'Connell, G. D. (2023). Understanding the etiopathogenesis of lumbar intervertebral disc herniation: From clinical evidence to basic scientific research. *JOR spine, 7*(1). https://doi.org/10.1002/jsp2.1289
64. Fu, Y., Yan, Y., Ru, X., & Qu, H. (2022). Analysis of chronic low back pain caused by lumbar Microinstability after percutaneous endoscopic Transforaminal Discectomy: A retrospective study. *Journal of pain research*, 15, 2821–2831. https://doi.org/10.2147/jpr.s380060
65. Chiang, C., Hsieh, Y., Tsuang, F., Chiang, Y., & Wu, L. (2022). Assessment of spinal stability after Discectomy followed by annulus fibrosus repair and augmentation of the nucleus Pulposus: A finite element study. *Applied sciences, 12*(23), 11906. https://doi.org/10.3390/app122311906
66. Prado, M., Mascoli, C., & Giambini, H. (2022). Discectomy decreases facet joint distance and increases the instability of the spine: A finite element study. *Computers in biology and medicine*, 143, 105278. https://doi.org/10.1016/j.compbiomed.2022.105278
67. Bouhsina, N., Decante, C., Hardel, J., Rouleau, D., Abadie, J., Hamel, A., Le Visage, C., Lesoeur, J., Guicheux, J., Clouet, J., & Fusellier, M. (2022). Comparison of mri t1, t2, and T2* mapping with histology for assessment of intervertebral disc degeneration in an ovine model. *Scientific reports, 12*(1). https://doi.org/10.1038/s41598-022-09348-w
68. Han, J., Meng, X. H., Ji, Z., Niu, F., Zhu, N., Zhao, T., Shen, Z., Wang, Z., & Yang, Q. (2025). Quantitative assessment of lumbar intervertebral disc degeneration and its correlation with clinical symptoms: A study utilizing ultrashort time-of-echo and T2 mapping as biomarkers. *BMC musculoskeletal disorders, 26*(1). https://doi.org/10.1186/s12891-025-09039-3
69. Modic, M. T., Steinberg, P. M., Ross, J. S., Masaryk, T. J., & Carter, J. R. (1988). Degenerative disk disease: Assessment of changes in vertebral body marrow with MR imaging. *Radiology, 166*(1), 193–199. https://doi.org/10.1148/radiology.166.1.3336678
70. Pfirrmann, C. W., Metzdorf, A., Zanetti, M., Hodler, J., & Boos, N. (2001). Magnetic resonance classification of lumbar Intervertebral disc degeneration. *Spine, 26*(17), 1873–1878. https://doi.org/10.1097/00007632-200109010-00011
71. Rajasekaran, S., Ramachandran, K., K S, S. V., Kanna, R. M., & Shetty, A. P. (2024). From Modic to disc Endplate bone marrow complex — The natural course and clinical implication of vertebral Endplate changes. *Global spine journal, 15*(1), 196–209. https://doi.org/10.1177/21925682241271440
72. Jones, A., Clarke, A., Freeman, B. J., Lam, K. S., & Grevitt, M. P. (2005). The Modic classification. Spine, 30(16), 1867–1869. https://doi.org/10.1097/01.brs.0000173898.47585.7d
73. Li, Z., Liu, L., Liu, H., Tan, J., Li, X., Xu, Z., Ouyang, Z., Wang, C., Yan, Y., & Xue, J. (2022). Radiologic analysis of causes of early recurrence after percutaneous endoscopic Transforaminal Discectomy. *Global spine journal, 14*(1), 113–121. https://doi.org/10.1177/21925682221096061
74. Hao, L., Li, S., Liu, J., Shan, Z., Fan, S., & Zhao, F. (2020). Recurrent disc herniation following percutaneous endoscopic lumbar discectomy preferentially occurs when Modic changes are present. *Journal of orthopaedic surgery and research, 15*(1). https://doi.org/10.1186/s13018-020-01695-6
75. Yuan, F. (2023). Development and validation of a prognostic model for the risk of recurrent lumbar disc Herniation after percutaneous endoscopic Transforaminal Discectomy. *Pain physician journal, 26*(1), 81–90. https://doi.org/10.36076/ppj.2023.26.81
76. Hedman, T., & Rogers, A. (2025). Pathomechanics of early-stage lumbar Intervertebral disc degradation leading to Discogenic pain—A narrative review. *Bioengineering, 12*(4), 389. https://doi.org/10.3390/bioengineering12040389
77. He, H., Ma, J., Xiong, C., Wei, T., Tang, A., Chen, Y., & Xu, F. (2023). Development and validation of a nomogram to predict the risk of lumbar disk Reherniation within 2 years after percutaneous endoscopic lumbar Discectomy. *World neurosurgery,* 172, e349–e356. https://doi.org/10.1016/j.wneu.2023.01.026
78. Zhao, C., Zhang, H., Wang, Y., Xu, D., Han, S., Meng, S., Han, J., Liu, H., Zhou, C., & Ma, X. (2021). Nomograms for predicting recurrent Herniation in PETD with preoperative radiological factors. *Journal of pain research*, 14, 2095–2109. https://doi.org/10.2147/jpr.s312224

79. Yang, J., Liu, R., Miao, Y., Nian, L., & Meng, X. (2023). Risk factors for recurrence after percutaneous endoscopic lumbar Discectomy: A meta-analysis. *World neurosurgery*, 172, 88–93. https://doi.org/10.1016/j.wneu.2023.02.009
80. Griffith, J. F., Wang, Y. J., Antonio, G. E., Choi, K. C., Yu, A., Ahuja, A. T., & Leung, P. C. (2007). Modified Pfirrmann grading system for lumbar Intervertebral disc degeneration. *Spine, 32*(24), E708–E712. https://doi.org/10.1097/brs.0b013e31815a59a0
81. Wang, Y. X. (2022). Several concerns on grading lumbar disc degeneration on MR image with Pfirrmann criteria. *Journal of orthopaedic translation,* 32, 101–102. https://doi.org/10.1016/j.jot.2021.12.003
82. Scarcia, L., Pileggi, M., Camilli, A., Romi, A., Bartolo, A., Giubbolini, F., Valente, I., Garignano, G., D'Argento, F., Pedicelli, A., & Alexandre, A. M. (2022). Degenerative disc disease of the spine: From anatomy to pathophysiology and radiological appearance, with morphological and functional considerations. *Journal of personalized medicine, 12*(11), 1810. https://doi.org/10.3390/jpm12111810
83. Neeson, D., & Roberts, D. (2021). Imaging the spine. *Surgery (Oxford), 39*(6), 371–382. https://doi.org/10.1016/j.mpsur.2021.04.007

The article has been sent to the editors	Received after review	Accepted for printing
23.10.2025	05.12.2025	07.12.2025

RISK FACTORS OF RECURRENCE LUMBAR DISC HERNIATION AFTER PRIMARY ENDOSCOPIC TRANSFORAMINAL DISCECTOMY. PART 2

V. K. Piontkovskyi [1], V. A. Kolesnichenko [2], M. B. Holbaum [3]

[1] V. T. Zaitsev Institute of General and Emergency Surgery of the National Academy of Medical Sciences of Ukraine
[2] V. N. Karazin Kharkiv National University, Ukraine
[3] Sytenko Institute of Spine and Joint Pathology National Academy of Medical Sciences of Ukraine, Kharkiv

✉ Valentin Piontkovskyi, MD, DMSci, Prof. in Orthopaedics and Traumatology: pio_val@ukr.net; https://orcid.org/0000-0002-0967-877X

✉ Vira Kolesnichenko, MD, DMSci: vira.a.kolesnichenko@karazin.ua; https://orcid.org/0009-0007-4106-1730

✉ Maksym Holbaum, MD: golbaymplaymarket@gmail.com; https://orcid.org/0009-0004-9047-0088

ISSN 0030-5987. Orthopaedics, traumatology and prosthetics. 2026. № 1

OBITUARIES

УДК 617.3(477)(092)Анкін

DOI: http://dx.doi.org/10.15674/0030-598720261109

Lev Mykolajovych Ankin

With deep sadness, we announce that Professor, Doctor of Medical Sciences, Military Doctor, and outstanding Ukrainian orthopedist-traumatologist Lev Mykolayovych Ankin passed away on 23.01.2026.

Lev Mykolayovych Ankin was born on 12 January 1936, and graduated from Kazan Medical Institute in 1959. He joined the Armed Forces, where he progressed from a military epidemiologist in a regiment to the Chief Traumatologist of the Kyiv Military District, achieving the rank of Colonel. After moving to Kyiv, Lev Mykolayovych became the Head of the Traumatology Department at the Military Hospital (1978). Over 30 innovative proposals were made by L. M. Ankin while working as the Chief Traumatologist of the Kyiv Military District, and he devoted significant time and attention to staff training, scientific conferences, and consultations.

In 1986, Lev Mykolayovych transitioned to civilian healthcare and successfully worked as the Head of the Traumatology Clinic at Kyiv Scientific Research Institute of Traumatology and Orthopedics, the Director of the Traumatology Clinic at the Scientific Production Union of Emergency and Disaster Medicine, the Chief Traumatologist of Kyiv, and a Professor at the Department of Military Surgery at the Ukrainian Military Medical Academy. He achieved significant success in scientific research, particularly in the development of a method for treating fractures.

In 1993, L. M. Ankin suggested reorganizing the city's traumatology service by establishing four 24-hour trauma centers. He promoted the implementation of methods of minimally invasive (biological) osteosynthesis, pelvic and hip surgery, and improvements in the medical care of patients with polytrauma in Ukrainian traumatology. His books, such as "Osteosynthesis with Metal Plates", "Principles of Stable-Functional Osteosynthesis", "Practice of Osteosynthesis and Endoprosthetics", "Polytrauma", "Traumatology — European Standards", and "Injuries of the Pelvis and Fractures of the Hip Joint", are still of interest to specialists worldwide. Lev Mykolayovych was the first to introduce emergency hip fracture prosthetic procedures for elderly patients in Kyiv. Professor Ankin introduced minimally invasive biological osteosynthesis into practice, developed plates for performing the procedure with minimal (partial) contact, and launched their production. These innovations reduced complications and shortened fracture healing times. For many years, L. M. Ankin shared his knowledge with students at the Ukrainian Military Medical Academy, serving as the scientific supervisor for three doctoral dissertations and many master's theses.

Professor Lev Mykolayovych Ankin was a distinguished scholar, doctor, and educator, a person of high professional and personal qualities, and a mentor to several generations of doctors. His name will forever remain in the history of the department and Ukrainian medicine.

The life path of Lev Mykolayovych is an example of human dignity, integrity, and the ability to work with people. We extend our heartfelt condolences to his family, loved ones, students, and colleagues.

Editorial Board of the Journal "Orthopedics, Traumatology and Prosthetics"
P. L. Shupyk National University of Health Care of Ukraine